University of Alberta

Characterization of gibberellin overexpression lines in pea

by

Aruna Dushyanthe Wickramarathna

A thesis submitted to the Faculty of Graduate Studies and Research
in partial fulfillment of the requirements for the degree of

Doctor of Philosophy

in

Plant Science

Department of Agricultural, Food and Nutritional Science

Fall, 2009

Edmonton, Alberta

Examining Committee

Dr. Jocelyn Ozga; Department of Agricultural, Food and Nutritional Science

Dr. Randall Weselake; Department of Agricultural, Food and Nutritional Science

Dr. Allen Good; Department of Biological Sciences

Dr. Walter Dixon; Department of Agricultural, Food and Nutritional Science

Dr. Neil Emery; Department of Biology, Trent University.

To my dearest parents,
for showing me the value of education

Abstract

Gibberellins (GAs) are a class of plant hormones that regulate many aspects of plant growth and development including seed germination, stem elongation and fruit development. To investigate the regulation of GA biosynthesis and the impact of altered GA levels on plant growth and development, transgenic pea (*Pisum sativum* L. cv. Carneval) plants were generated to overexpress *PsGA3ox1* (codes for GA 3β-hydroxylase which converts GA_{20} to bioactive GA_1) under the control of the CaMV-35S promoter. Increased expression of the transgene *PsGA3ox1* was correlated with altered plant phenotype including longer internodes, larger stipules and tendrils, and longer pods. Transgenic lines also showed upregulation of the GA catabolic genes *PsGA2ox1* and/or *PsGA2ox2*, suggesting that GA_1 substrate-induced feedback regulation also occurs to maintain GA homeostasis. Changes in endogenous GAs, quantified using an isotope dilution method, indicated that an increased flux in GA biosynthesis occurred in the expanding internodes, stipules and tendrils of the *PsGA3ox1*-overexpressor lines. Higher bioactive GA_1 levels and growth were correlated with lower *PsGA2ox1* transcript levels in elongating internodes, and oscillation of these parameters between adjacent elongating internodes in the *PsGA3ox1*-overexpression lines suggests that coordination of bioactive GA levels and growth occurs between adjacent internodes. During germination and early seedling growth, GA gene expression studies suggested that *PsGA3ox1*-overexpression increased the flux through to bioactive GA in the cotyledons, shoots and roots of pea seedlings, resulting in longer shoots but shorter roots.

Auxins are a class of plant hormones involved in growth and differentiation of plants that can influence GA biosynthesis and action. The location and action of auxins is in part regulated by auxin carrier proteins. The expression patterns of the putative auxin efflux carrier genes *PsPIN1* and *PsPIN2* in elongating internodes were correlated with vascular re-patterning events in this tissue, and *PsGA3ox1*-overexpression appears to increase internode *PsPIN1* and *PsPIN2* transcript abundance and the formation of the vascular connections between the internode and the axillary buds. Overall, characterization of *PsGA3ox1*-overexpressor lines in pea demonstrated that bioactive GA levels are tightly regulated in pea tissues for the coordination of plant growth and development.

Acknowledgements

There are many people and organizations who contributed in many ways towards the success of my graduate program. First and foremost I would like to sincerely thank my supervisor Dr. Jocelyn Ozga for her guidance and support throughout my candidature, particularly for her time and energy directed towards reviewing this thesis. She was always available to answer my questions, give advice and share her knowledge. I wish to thank Drs. Randall Weselake, Allen Good, Michael Deyholos, and Walter Dixon for their constructive criticisms and support during my program. I am very thankful to Dr. Dennis Reinecke who was very generous with his time in sharing his experience and expertise. I am grateful to Dr. Leonid Kurepin for hormone quantifications. Many thanks to Gabe Botar for constant encouragements and help with initial writing; to Randy Mandrik for help with microscopy studies; to Szidonia Botar and Jen Becker for helping me in numerous ways during my research. I would also like to acknowledge the support given by all past and present members of the research group including Belay, Pankaj, Rose, Ashley, Courtney, Aleena, Celia and Amber and all my dear friends in the department especially Bill, Aparna, Katy, Nidhi, Sawumya, Jacob, and Bernhard for being great mates through thick and thin. There were many people in the department who extended their helping hands in many occasions including Drs. Urmila Basu, Muhammad Rahman and Joan Turchinsky and Bruce Alexander during my research, I greatly appreciate their help. I also want to thank many Sri Lankan-Canadian families who constantly supported me during my stay in Edmonton in many ways. Financial support received from Canadian Commonwealth and Scholarship and Fellowship Program and Rubber Research Institute of Sri Lanka for providing me the opportunity to do my PhD are greatly appreciated. My sincere gratitude goes to my wife Dilushika Chamari for all her support, understanding and taking entire responsibilities of our daughter Tharuli during my studies. I am very much grateful to my uncle and cousin sister for their continued support. Most importantly, my heartfelt gratitude goes to my parents for their unreserved love, inspiration, and never ending financial and emotional support throughout my life.

Table of Contents

Chapter **Page Number**

List of Tables

Table **Page Number**

List of Figures

Figure **Page Number**

List of Abbreviations

Abbreviation	Definition
2ODDs	2-oxoglutarate dependent dioxygenases
4-Cl-IAA	4-chloroindole-3-acetic acid
ANOVA	analysis of variance
ARFs	auxin response factors
AuxRE	auxin response element
bp	base pair
BSFTA	N,O,-bis(trimethylslyl)trifluoroacetamide
CaMV	Cauliflower mosaic virus
CDP	*ent*-copalyl diphosphate
cpm	counts per minute
CPS	*ent*-copalyl diphosphate synthase
Ct	cycle threshold
CTAB	cetyltrimethylammonium bromide
CV	coefficient of variation
cv	cultivar
d	days
DAI	days after imbibition
DEPC	diethylpyrocarbonate
dpm	decays per minute
DW	dry weight

EA	embryo axis
EUI	*elongated uppermost internode*
FAM	6-carboxyfluorescein
FW	fresh weight
g	grams
GA	gibberellin
GC-MS	gas chromatography-mass spectrometry
gdw	gram dry weight
GGDP	geranylgeranyl diphosphate
HPLC	high performance liquid chromatography
IAA	indole-3-acetic acid
IBA	indole-3-butyric acid
IPA	indole-3-propionic acid
KAO	encodes *ent-kaurenoic acid oxidase*
KO	encodes *ent*-kaurene oxidase
KS	encodes *ent*-kaurene synthase
LB	left border
LE	*LENGTH;* encodes *GA 3-oxidase*
LH	encodes *ent- kaurene oxidase*
LS	encodes *ent-copalyl diphosphate synthase*
LSD	least square difference
M	molar
ME	mature embryo

MeOH	methanol
MGB	minor-grove binding
min	minutes
mRNA	messenger RNA
MSD	mass selective detector
NA	encodes *ent-kaurenoic acid oxidase*
NOS	nopaline synthase
NPTII	*neomycin phosphotransferase II*
PAA	phenylacetic acid
PAT	polar auxin transport
PC	preparative column
PCIB	*p*-chlorophenoxyisobutric acid
qRT-PCR	quantitative real-time reverse transcriptase polymerase chain reaction
RB	right border
rRNA	ribosomal RNA
Rt	retention time
RWC	relative water content
s	second
SE	standard error of mean
SIM	selected ion monitoring
SLN	*SLENDER*; encodes *GA 2-oxidase*
TAMRA	tetramethylrhodamine

T-DNA	transfer-DNA
TG	transgenic line
TIBA	2, 3, 5-triidobenzoic acid
TMCS	trimethylchlorosilane
tml	*tumor morphology large*
WT	wild-type

Chapter 1

General Introduction

Motivation

Modulation of genes responsible for the GA biosynthesis pathway through transgenic approaches has been a powerful research tool in understanding flux through the pathway and the regulatory mechanisms involved with synthesis and catabolism of bioactive GA. GA 3β-hydroxylation converts biologically inactive GAs into biologically active GAs. It has been debated whether GA 3β-hydroxylation is a major step in controlling the flux through to the bioactive GA in the biosynthesis pathway and results from transgenic approaches have not consistently shown that increasing GA 3β-hydroxylase transcript levels have had a substantial effect on the level of bioactive GAs. Overexpression of the wild-type gene (*PsGA3ox1;LE*) responsible for GA 3β-hydroxylation in pea lines containing a mutation in this gene resulting in low enzyme activity (*le-1*) was used to further explore the importance of GA 3β-hydroxylation in the GA biosynthesis pathway in pea (*Pisum sativum*) which has been a valuable model species, particularly with respect to hormone related studies.

Thesis structure

Chapter 1: A review of literature pertinent to the studies in this thesis is arranged into several major sections. Literature on GA biosynthesis and catabolism and its regulation (with special emphasis to the pathway that is found in the model plant pea) provides key background information for the studies described in Chapters 2, 3 and 4. Literature on GA signal transduction and GA

action is general information that aids in understanding the events that take place after the production of bioactive GA resulting in phenotypic changes observed in the studies described in Chapters 2, 3, and 4. Literature pertinent to GA-auxin interactions, movement of auxin, auxin signal transduction and auxin efflux carriers in the plant are provided for interpretation of the putative auxin efflux carrier expression profiles presented in Chapter 3.

Chapter 2 details the molecular, biochemical and phenotypic effects of overexpression of the wild-type gene *PsGA3ox1 (LE*) responsible for GA 3β-hydroxylation in pea lines containing a mutation in this gene resulting in low enzyme activity (*le-1*), with special emphasis on vegetative development. Transcript profiling of the *PsGA3ox1* transgene along with other late GA biosynthesis and catabolism genes in both transgenic and control lines is presented and possible regulatory mechanisms of GA biosynthesis are also discussed at the transcript level. This chapter relates transcript level changes to steady state levels of GAs, and how these changes are associated with plant phenotype. Using these data, general conclusions are drawn on the role of the GA 3β-hydroxylation step in increasing the flux through to bioactive GA in the GA biosynthesis pathway in specific pea tissues.

Chapter 3, based on the GA feedback regulatory mechanisms observed in Chapter 2, presents a more comprehensive study of GA homeostasis in the internodes of the *PsGA3ox1*-overexpressor lines, and also explores possible roles of auxin efflux carriers in maintaining GA homeostasis and in internode growth and development.

Coordination and regulation of late GA biosynthesis and catabolism genes both spatially and temporally are vital for successful seedling establishment of pea. Chapter 4 focuses on the molecular and phenotypic effects of overexpression of the wild-type gene *PsGA3ox1 (LE*) in a pea line containing a mutation in this gene resulting in low enzyme activity (*le-1*) during seed germination and early seedling growth. Changes in transcript profiles of the late GA biosynthesis and catabolism genes were associated with phenotype changes in the cotyledons, roots and shoots during seed germination to 3 days after imbibition in the highest *PsGA3ox1*-overexpressor line and a transgenic null control. Possible GA-related mechanisms involved in the changes of phenotype observed in the *PsGA3ox1*-overexpressor line are discussed.

Chapter 5 summarizes the key outcomes of the thesis research and provides overall conclusions. It also addresses the shortcomings of specific procedures and protocols used and discusses possible ways of improvements. Future research directions are also discussed.

Review of Literature

Plant Hormones

Plant hormones are a group of naturally occurring small organic compounds which influence physiological processes at low concentrations. Many processes are influenced by hormones including plant growth, differentiation and development (Davies, 2004).

The term “hormone” was first used in medicine about 100 years ago for a stimulatory factor, to describe a type of chemical messenger with characteristic attributes. The word is derived from Greek, where its meaning is “*to stimulate*” or “*to set in motion*” (Davies, 2004). The mammalian concept of a hormone involves a localized site of synthesis, movement in the transport stream to a target tissue, and the control of a physiological response in the target tissue via the concentration of the hormone (Trewavas, 1981). Conceptually, plant hormones vary from the classical mammalian hormones. The synthesis of plant hormones may be localized (as occurs for animal hormones), but it may also occur in a wide range of tissues, or cells within tissues. Plant hormones can cause the effect near the site of their synthesis or they can be transported and cause the effect at a distance from the point of synthesis (Davies, 2004).

There are currently five “classical” groups of plant hormones: auxins, gibberellins, cytokinins, abscisic acid, and ethylene. More recently other compounds, namely brassinosteroids and jasmonates have been added to the list of plant hormones and some compounds (such as salicylic acid, peptides, polyamines and strigolactones) have hormone-like properties (Davies, 2004; Umehara et al., 2008). In addition to the discovery of new hormones, recent studies have shown the importance of hormone interactions or “cross-talk” and how these interactions affect hormone biosynthesis, signal transduction and physiological processes (van Huizen et al., 1997; Ross and O’Neill, 2001; Swarup et al., 2002; Ozga and Reinecke, 2003; Woodward and Bartel, 2005).

Gibberellins (GAs)

Japanese farmers witnessed the phenomenon of abnormal elongation in certain rice plants and this phenomenon was called the *"bakanae"* or "foolish seedling" disease (Hori, 1898). This disease was found to be caused by substances produced by the fungus *Gibberella fujikuroi* (the vegetative or imperfect stage was called *Fusarium moniliforme*; Phinney, 1983). Eiichi Kurosawa, in 1926, isolated a "secretion factor" from sterile filtrates of *G. fujikuroi* cultures and further isolated the "active principle" and characterized its biological properties (Phinney, 1983). In 1934, Teijiro Yabuta isolated a non-crystalline solid from a fungal culture filtrate that stimulated the growth of rice seedlings. This compound was named "gibberellin" by Yabuta in 1935 (Yabuta, 1935; Phinney, 1983).

In the mid 1950s, evidence that gibberellins were naturally occurring substances in higher plants began to appear in the literature. Using techniques that had been used to isolate gibberellins from the fungus, Margaret Radley at the Imperial Chemical Laboratories (ICI) in the UK demonstrated the presence of gibberellin-like substances in higher plants (Radley, 1956). In the US, the first reports of a gibberellin-like substance in maize came from the lab of Bernard Phinney using dwarf maize mutants to assay for activity in plant extracts (Phinney et al., 1957). This was followed by the isolation of crystalline gibberellin A_1, A_5, A_6 and A_8 from runner bean (*Phaseolus multiflorus*) (MacMillan et al. 1958, 1959, 1960, 1962).

In the 1960s, the number of gibberellins reported in the literature isolated from fungal and plant origins rapidly increased. In 1968, J. MacMillan and N.

Takahashi reached an agreement that all gibberellins should be assigned numbers as gibberellin A ($_{1\text{-}x}$), irrespective of their origin, in chronological order of their identification (MacMillan and Takahashi, 1968). To date, 136 fully characterized gibberellins (GAs), designated gibberellin A_1 (GA_1) through GA_{136} that have been identified from 128 different species of vascular plants and also from seven bacterial and seven fungal species (Mutasa-Gottgens and Hedden, 2009; also see www.plant-hormones.info).

Gibberellin biosynthesis and catabolism

The GA biosynthesis pathway has been elucidated and its key components identified (for review, see Hedden and Phillips, 2000; Olszewski et al, 2002; Yamaguchi, 2008). On the basis of the nature of the enzymes involved, and the corresponding localization in the cell, the GA biosynthesis pathway can be divided into three phases (Figure 1.1).

1. Biosynthesis from isopentenyl diphosphate to *ent*- kaurene
2. Biosynthesis from *ent*-kaurene to GA_{12}-aldehyde
3. Biosynthesis from GA_{12}-aldehyde to bioactive GA_1

For this review, GA biosynthesis from geranylgeranyl diphosphate (GGPP; produced in the latter part of phase one of the GA biosynthesis pathway) will be covered. GAs are products of the diterpenoid pathway and their cyclization is initiated from the common 20-carbon precursor GGPP. The early pathway, from GGPP to GA_{12}-aldehyde, encompasses the first two phases that are common to all species (Hedden and Phillips, 2000).

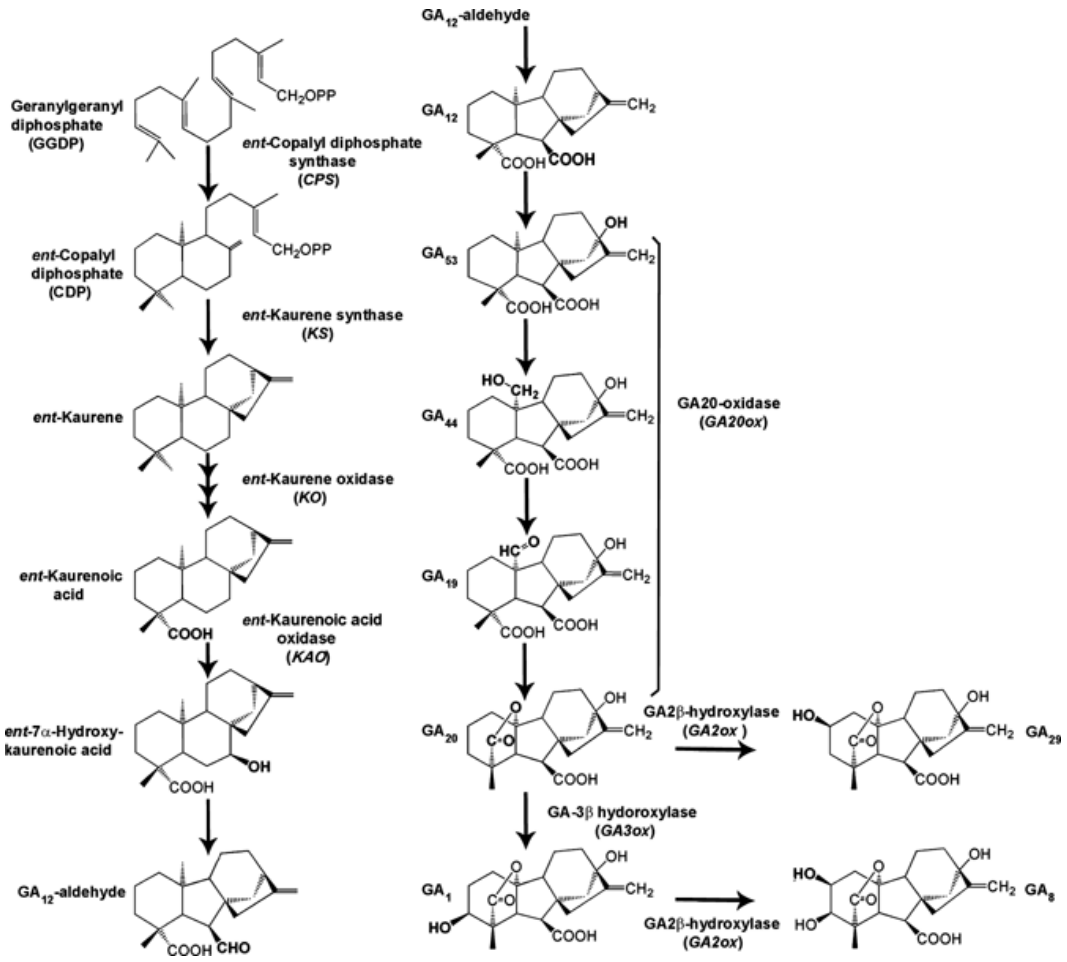

Figure 1.1. Gibberellin biosynthesis pathway from geranylgeranyl diphosphate in *Pisum sativum* L. (Source: Ayele et al., 2006).

The intermediate GGPP is synthesized in plastids from isopentenyl diphosphate, shown recently to be formed in these organelles from glyceraldehyde 3-phosphate and pyruvate rather than mevalonic acid as was previously assumed (Lichtenthaler et al., 1997). The first phase of GA biosynthesis involves a two-step cyclization by two diterpene cyclases (Terpene synthases, TPs) in plastids. The first cyclization involves the conversion of GGDP to *ent*-copalyl diphosphate (CDP) via protonation of the C-14-C-15 double bond,

and is catalyzed by *ent*-copalyl diphosphate synthase (CPS). The second cyclization step involves the conversion of CDP to the tertracyclic hydrocarbon *ent*-kaurene by *ent*-kaurene synthase (KS). As GGDP is a common precursor for other diterpenes (e.g. carotenoids, phytol chain of chlorophyll), which are present at concentrations several orders of magnitude greater than the GAs, *ent*-kaurene synthesis is likely to be a point of control for the biosynthesis of GAs (Hedden and Proebsting, 1999).

In the second phase of GA biosynthesis, *ent*-kaurene is converted to GA_{12}-aldehyde by microsomal NADPH-dependant cytochrome P450 mono-oxygenases (*ent*-kaurene oxidase and *ent*-kaurenoic acid oxidase). *ent*-Kaurene oxidase (KO) catalyses the sequential oxidation of *ent*-kaurene at the C-19 carbon producing *ent*-kaurenol, *ent*-kaurenal and *ent*-kaurenoic acid. *ent*-Kaurenoic acid is subsequently hydroxylated to *ent*-7α-hydroxykaurenoic acid by another P450 enzyme, *ent*-kaurenoic acid oxidase (KAO). The conversion of *ent*-7α-hydroxykaurenoic acid to GA_{12}-aldehyde involves contraction of the B ring from a C_6 to a C_5 structure with extrusion of the C-7 carbon. KO was shown to be localized to the outer membrane of the plastid and KAO to the endoplasmic reticulum by expression of these enzymes fused to green fluorescent protein in Arabidopsis (Helliwell et al., 2001).

In the third phase of GA biosynthesis, GA_{12}-aldehyde is converted to various C-19 GA intermediates and bioactive GAs primarily in the cytosol via either early 13-hydrolylation, which produces GA_{20} and GA_1, or non-13-hydroxylation, which produces GA_9 and GA_4, depending on species and tissue (Crozier et al., 2000). In

pea, the third phase of GA biosynthesis is mainly through the early 13-hydroxylation pathway (Sponsel, 1995). GA_{12}-aldehyde is oxidized by GA 7-oxidase to GA_{12}, which, in turn, is converted to GA_{53} by GA 13-hydroxylase. These intermediates (GA_{12} or/and GA_{53}) are metabolized further by two dioxygenases (which require 2-oxoglutarate as a co-substrate, and Fe^{2+} and ascorbate as cofactors for their activity; Hedden and Phillips, 2000). In pea, the multifunctional GA 20-oxidase (GA20ox) oxidizes the C-20 methyl group to the alcohol (GA_{44}) then an aldehyde (GA_{19}), followed by cleavage of C-20 carbon and formation of a lactone ring characteristic of the C-19 GAs (GA_{20}). Secondly, a hydroxyl group is introduced at the 3-β position on the A ring by GA 3β-hydroxylase (GA3ox) producing bioactive GA (GA_1). It has been found that some GA 3β-hydroxylase enzymes possess minor catalytic activity to synthesize GA_3 and GA_6 from GA_{20} via GA_5 (Yamaguchi, 2008).

Bioactive GA (GA_1) and its precursors (GA_{20}/GA_9) are metabolically deactivated by a third 2-oxoglutarate-dependant dioxygenase, GA 2β-hydroxylase (GA2ox) which hydroxylates at the 2-β position on the A ring. Recently, a new type of GA2ox that accepts only C-20 GAs was reported and is likely to play a role in depleting pools of GAs (such as GA_{12} and GA_{53}) that are otherwise converted to bioactive forms (Lee and Zeevaart, 2005; Schomburg et al., 2003). It was recently reported that the rice *EUI* gene (Elongated Uppermost Internode; codes for a cytochrome P450) epoxidizes the 16, 17-double bond of non 13-hydroxylated GAs, including GA_4, GA_9, and GA_{12}, thus making them inactive or depleting the pools of precursors for conversion to bioactive GAs (Zhu et al.,

2006). Recently, gibberellin methyltransferases were reported as GA deactivation enzymes in *Arabidopsis*. These enzymes catalyze methylation of the C-6 carboxyl group of GAs using S-adenosine-L-methionine as a methyl donor (Varbanova et al., 2007) but it is yet to be concluded as a common deactivation reaction.

Regulation of GA biosynthesis

Genetic evidence of GA biosynthesis regulation in pea

The majority of the GA biosynthesis and catabolism genes and enzymes have been identified and this allows a clearer view of the mechanisms by which a large variety of GAs are produced in plants. Because of the multifunctionality of several enzymes in the pathway and the ability of many GA-modifying enzymes to accept multiple GAs as substrates, fewer enzymes are required than the number of catalytic steps in the GA biosynthesis pathway (Yamaguchi, 2008). Each enzyme is encoded by a single gene or a small family of genes (Hedden and Phillips, 2000). Mutation of these genes can give rise to GA biosynthesis mutants, which can either over-produce or under-produce bioactive GA levels, resulting in phenotypic traits deviating from wild type traits. *na-1* mutants are substantially shorter than the wild type [*na-1* mutation results from a 5 base deletion in the *NA (PsKAO1)* gene, producing a premature stop codon, and the corresponding predicted protein is only 194 amino acids long as opposed to 485 in the case of *NA*; Davidson et. al., 2003]. s*ln* mutants show longer internodes in pea seedlings. In *sln* only three adenosines compared to four are present at positions 744-747 in the wild type *PsGA2ox1* cDNA sequence, yielding a null mutation resulting in a premature stop codon and the predicted protein consequently lacks essential

catalytic regions including residues required for oxoglutarate binding (Lester et. al., 1999). These mutant phenotypes are evidence that GAs are essential factors for normal plant growth and development.

To date, only one gene coding for *ent*-copalyl diphosphate synthase (CPS) has been cloned from pea: *PsCPS1* (corresponding to the *LS* locus) (Ait-Ali et al, 1997). A mutation in the *LS* gene (*ls-1*) which involves an intronic single nucleotide change at position 1914 (guanine to adenine) disrupts the normal mRNA splicing resulting in three different mutant mRNAs, all of which are predicted to encode a truncated protein with reduced enzyme activity. The plants homozygous for the *ls-1* mutation possesses a dwarf phenotype because of a reduction in internode lengths of approximately 75% compared with wild type plant (Ait-Ali et al, 1997).

The gene encoding *ent*-kaurene oxidase (KO) in pea has been cloned (*PsKO1)* and it corresponds to the *LH* locus (Davidson et al, 2004). The *lh-1* mutation, involves a single base change of guanine to adenine, which translates to a serine to asparagine substitution in the encoded protein resulting in a dramatic reduction in the enzyme activity. The *lh-2* mutation disrupts normal RNA splicing due to a single base substitution of adenine for guanine at the beginning of an intron, also resulting in reduced enzyme activity. Neither the *lh-1* and *lh-2* mutations are null mutations (Davidson and Reid, 2004). In the *lh-2* mutant, GA levels were reduced in the shoots and the young seeds. Consequently, the seeds develop slowly and/or abort (Swain et al., 1992). These observations were the first to demonstrate that GAs are required for normal seed development.

Two genes encoding *ent*-kaurenoic acid oxidase (KAO) have been isolated from pea: *PsKAO1* (corresponding to the *NA* locus) and *PsKAO2* (Davidson et. al., 2003). The *na-1* mutant (described above) is one of the shortest pea plant GA mutants characterized to date. The *na-1* mutant also has markedly reduced GA levels in roots, and root elongation and *na-1* roots respond in growth to added GA. These results indicate that GAs are required for normal root growth (Yaxley et al., 2001). *PsKAO1* is mainly expressed in the stem, apical bud, leaf, pod, and root organs whereas *PsKAO2* is expressed mainly in seeds which explains the normal seed development and normal GA biosynthesis in seeds of *na* plants.

In pea, two GA 20-oxidase genes have been cloned: *PsGA20ox1* (Martin et al., 1996) and *PsGA20ox2* (Lester et. al, 1996). There are no known mutants in pea that specifically affect this step. In fact, there is only one mutation known to primarily affect GA 20-oxidation in any species: *ga5*, in Arabidopsis (Reid et. al., 2004).

The *PsGA3ox1* gene (corresponding to *LE* locus), which encodes for GA 3β-hydroxylase (GA 3-oxidase) was cloned in two separate laboratories in the 1990s. It encodes a protein predicted to consist of 374 amino acids (Lester et. al., 1997 and Martin et. al., 1997). Sequencing the *LE* and *le-1* alleles showed that the *le-1* mutation arose from a guanine to adenine substitution at position 685 (Lester et. al., 1997), substituting threonine for alanine in the protein, and this resulted in reduced affinity for the GA substrate. The *le-1* mutant is dwarf (reaches only about 40% of the wild type height) and produces 10-20 fold less GA_1 in the stems than the wild type (Reid et al., 2004). The *le-1* is a leaky mutant (a mutant that

results from a partial rather than a complete inactivation of the wild-type function; Lester et. al., 1997). The *le-2* mutation contains a base deletion at position 376 of the *le-1* allele, and results in a severely truncated protein with undetectable enzyme activity. Therefore, the *le-2* allele encodes a non-functional protein, and it is categorized as a "null" mutation. The *le-2* mutant is even shorter and more GA_1 deficient than *le-1* (Reid et. al., 2004). A third mutant allele, *le-3* involves a cytosine to thymine substitution in the coding region, and dramatically reduces GA 3-oxidase activity (Martin et. al., 1997).

Two genes encoding GA 2-oxidases have been cloned in pea; *PsGA2ox1* (Lester et al., 1999; Martin et al., 1999; corresponding to the *SLN* locus) and *PsGA2ox2* (Lester et al., 1999). Recombinant expression of *PsGA2ox1* cDNA in *E.coli* converted GA_1, GA_4, GA_9, and GA_{20} to the corresponding 2β-hydroxylated products. The *PsGA2ox2* gene product also converted GA_1 to GA_8, but was much less effective in the catalyzing the conversion of GA_{20} to GA_{29} and did not convert GA_{29} to GA_{29}-catabolite. Seedlings of *sln* (mutation in *PsGA2ox1* described above) are elongated and "slender" and this phenotype is especially obvious in the lower internodes. The cause of the *sln* phenotype was traced to the seeds. Wild type pea seeds contain relatively high amounts of GA_{20} during development in the pod; although GA_1 is undetectable at this stage. As the seeds mature, GA_{20} is metabolized to GA_{29} and GA_{29}-catabolite. Both these steps are blocked in the *sln* mutant, and therefore GA_{20} accumulates in the seeds to very high levels (Reid et. al., 1992). When these seeds germinate, GA_{20} moves from

the cotyledons to the seedling and is converted to bioactive GA_1, which promotes internode elongation.

Feedback and feed forward regulation of GA metabolism

Gibberellin homeostasis in plants is maintained via feedback and feed forward regulation of GA metabolism (Hedden and Phillips, 2000; Olszewski et al., 2002). Transcript analysis shows that regulation of bioactive GA levels is mainly targeted the 2-oxoglutarate dependent dioxygenases (2ODDs) in the GA metabolism pathway. Increasing the bioactive GA level by treatment with GA_3 substantially reduced the transcript levels of the *PsGA20ox1* in pea pericarps (van Huizen et al., 1997) and expanding pea shoots (Martin et al., 1996). Ayele et al. (2006) observed that the transcript levels of two GA biosynthesis genes, *PsGA20ox1* and *PsGA3ox1* were decreased in response to GA_3 application. Treatment of the apical buds of pea seedlings with GA_1 significantly decreased the mRNA levels of the *PsGA3ox1* gene (Ait-Ali et al., 1999). Furthermore, Ozga et al. (1992) showed that treatment with GA_3 markedly decreased the conversion of [^{14}C]GA_{12} to putative [^{14}C]GA_{20} in pea fruits. Conversely, Ross et al. (1999) showed that in GA deficient lines (*ls-1* and *na*) the rate of conversion of applied radio-labeled GA_{20} to GA_1 is greatly increased. In Arabidopsis, numerous authors have shown that the expression of GA biosynthesis genes, *AtGA20ox1* and *AtGA3ox1* is highly elevated in a GA-deficient background, whereas these genes are down regulated after application of bioactive GAs (Chiang et al., 1995; Matsushita et al., 2007; Phillips et al., 1995; Xu et al., 1999; Yamaguchi et al.,

1998). These data suggest that substrate-induced feedback regulation occurs to maintain GA homeostasis in these species.

The level of bioactive GA also controls the GA catabolism genes. Elliott et al. (2001) showed reduced expression of both *PsGA2ox1* and *PsGA2ox2* in two different GA deficient mutants of pea, *ls-1* and *na*. The reduced expression of *PsGA2ox1* in the *na* mutant was reversed by treatment with exogenous GA_1. Ayele et al. (2006) observed that the transcript levels of *PsGA2ox1* were up-regulated in shoots and *PsGA2ox2* in roots in response to GA_3 application. Treatment of immature flower buds of the Arabidopsis *ga1-2* mutant (*GA1* codes for CPS and *ga1-2* is a GA deficient mutant) with GA_3 also upregulated the transcript abundance of *AtGA2ox1* and *AtGA2ox2* (Thomas et al., 1999).

It appears that feedback regulation does not occur in the early part of the GA biosynthesis pathway (Hedden and Phillips, 2000). The expression of *PsCPS1 (LS), PsKO1 (LH), PsKAO1 (NA)* and *PsKAO2* in pea shoots remained similar among GA deficient mutants (*ls-1, lh-1, lh-2, na-1*) and their wild types and application of the GA biosynthesis inhibitor, paclobutrazol, to both wild type and GA-deficient lines did not affect the expression of these genes (Davidson et al., 2005). Fleet et al. (2003) observed that overexpression of *AtCPS1* in Arabidopsis dramatically increased *ent*-kaurene synthesis but had no effect on the expression of the late GA biosynthesis genes (*AtGA20ox1* and *AtGA3ox1*) and the levels of GAs (GA_9, GA_4, GA_{34} and GA_{51}). Similar results were reported by Swain et al. (2005), whereby when *AtKO1* was overexpressed, there was no change in levels

of endogenous GAs, including the biologically active GA_4. These results suggest that precursors early in the GA pathway do not regulate levels of bioactive GA.

Little is known about the molecular mechanisms underlying GA homeostatic regulation. However, the central GA signaling components that appear to be required for this response including the recently cloned GA receptor, the GA DELLA proteins and F-box proteins (Yamaguchi, 2008; Sun and Gubler, 2004; Ueguchi-Tanaka et al., 2007). In the rice *gid1* and *gid2* mutants (which show severe dwarf phenotypes and GA-insensitive mutants), expression of *OsGA20ox2* is upregulated and levels of bioactive GA_1 are highly elevated (Sasaki et al., 2003; Ueguchi-Tanaka et al., 2005). These data suggest that the loss of GA responsiveness leads to upregulation of GA biosynthesis genes and bioactive GA levels to compensate for the loss of GA sensitivity (Ueguchi-Tanaka et al., 2005) Conversely, an Arabidopsis DELLA loss-of-function mutant (DELLA proteins are negative regulators in the GA signal transduction pathway) has reduced levels of *AtGA3ox1* transcripts suggesting that increased activity in GA response can down regulate GA biosynthesis (Dill and Sun, 2001). Moreover, an increase in GA signaling from *GID1*-overexpression in aspen resulted in lower levels of bioactive GAs (GA_1 and GA_4) and their immediate precursors (GA_{20} and GA_9) and higher levels of immediate catabolites of bioactive GAs (GA_8 and GA_{34}). This suggests an increase in GA signaling induces a feedback mechanism that represses the GA biosynthesis pathway (Mauriat and Moritz, 2009).

Additional mechanisms and components involved in GA homeostasis are beginning to be uncovered. In Arabidopsis, the AT-hook protein that binds to a 43

bp *cis*-acting sequence (designated by GNFEI) present in the *AtGA3ox1* promoter has been implicated in the GA negative feedback response (Matshushita et al., 2007). A mutation in GNFEI abolished both AGF1 binding and the GA-negative feedback response, suggesting that GNFEI and AGF1 are novel *cis-trans* regulatory factors involve in the GA homeostasis (Matshushita et al., 2007). However, this *cis*-element appears to be absent in the promoter of *AtGA20ox1*, suggesting that the GA signal may regulate *AtGA3ox1* and *AtGA20ox1* transcription by different mechanisms (Matshushita et al., 2007). Dai et al. (2007) suggested that YABBY1 in rice (encoded by *OsYAB1*; rice contains six members of the YABBY transcription regulators; Yamaguchi et al., 2004) may be a mediator of GA homeostasis downstream of the DELLA proteins because its expression is dependent on the DELLA proteins. Overexpression of *OsYAB1* results in a semi-dwarf phenotype and it is correlated with a decrease in GA_1, down-regulation of GA biosynthesis gene *OsGA3ox2,* and upregulation of the GA catabolic gene *OsGA2ox3*.

Auxin interaction with the GA biosynthesis pathway

Auxin was the first growth hormone to be discovered in plants (www.plant-hormones.info). The investigation carried out by Charles Darwin and his son Francis during the 1880s on phototropism using seedlings of canary grass (*Phalaris canariensis*) laid the foundation for auxin discovery (Darwin, 1880). Indole-3-acetic acid (IAA) was first isolated by Salkowski in 1885 in fermentation media (Salkowski, 1885; www.plant-hormones.info), but the isolation of IAA from plant tissues came much later from its discovery by Fritz

Went in 1926 (Went, 1926). Marumo et al. (1968) isolated another endogenous auxin, 4-chloroindoleacetic acid (4-Cl-IAA) from immature seeds of *Pisum sativum*. Additionally, IPA (3-indolepropionic acid) was detected in the roots and IBA (3-indolebutryic acid) in the roots and epicotyls of three-day old pea seedlings (Schneider et al., 1985). Schneider et al. (1985) also found PAA (phenylacetic acid), which has weak auxin-like properties, in roots, cotyledons and epicotyls of three-day old pea seedlings. Although it has long been known that the various plant hormones interact in the regulation and coordination of plant growth and development (Brian and Hemming, 1957), the exact mechanisms are poorly understood. Starting in the 1990's several reports were published that began to address the mechanisms of hormonal interactions and how these interactions can affect hormone biosynthesis and signal transduction and influence plant growth and development. Two mechanisms involved with the interaction of auxins and GAs have been reported: auxin regulation of GA metabolism (van Huizen et al., 1995; van Huizen et al., 1997; Ozga et al., 2003; Ross et al., 2000; O'Neill and Ross, 2002; Wolbang et al., 2004) and auxin-induced degradation of the negative GA-signaling element RGA, which thereby promotes GA signaling (Fu and Harberd, 2003).

The first indication of how auxin promotes GA biosynthesis came from studies in pea fruits. Seeds are required for normal pea pericarp growth. If seeds were removed from young pea pericarps, pericarp growth was inhibited and they eventually senesced (Ozga et al., 1992). When seeds were present, pericarp *PsGA20ox1* and *PsGA3ox1* mRNA levels and flux through the GA biosynthesis

pathway were maintained ([^{14}C]GA_{12} and [^{14}C]GA_{19} were converted to GA_{20}; van Huizen et al., 1995). However, when the seeds were removed, the pericarp transcript levels of *PsGA20ox1* and *PsGA3ox1* dramatically declined and production of GA_{20} and GA_1 in the pericarp was inhibited (van Huizen et al., 1997; Ngo et al., 2002; Ozga et al., 2003). 4-Cl-IAA (but not IAA) was found to mimic the seeds in the stimulation of pericarp growth (Reinecke et al., 1995) and *PsGA20ox1* and *PsGA3ox1* transcript abundance (van Huizen et al., 1997; Ngo et al., 2002; Ozga et al., 2003) in deseeded pericarps. The 4-Cl-IAA-induced increase in *PsGA20ox1* and *PsGA3ox1* transcript abundance was correlated with production of GA_{20} and GA_1 in the deseed pericarps (van Huizen et al., 1995; Ozga et al., 2009). 4-Cl-IAA was also found to reduce and maintain low *PsGA2ox1* transcript levels in deseeded pericarps, but IAA was not (Ozga et al., 2009). The ability of 4-Cl-IAA to upregulate the transcript levels of GA biosynthesis genes *PsGA20ox1* and *PsGA3ox1*, and downregulate the transcript levels of the catabolic gene *PsGA2ox1* in the pea pericarp supports the hypothesis that 4-Cl-IAA exported from the seed stimulates GA biosynthesis and growth in the pericarp (Ozga et al., 2009).

Ross et al. (2000) showed that IAA promoted GA_1 biosynthesis in pea stems. Removal of the stem apex (decapitation) reduced IAA levels in the subtending elongating internode (presumably by removing the source of auxin). ^{3}[H]GA_{20} applied to the decapitated stumps was converted mainly to the biologically inactive products ^{3}[H]GA_{29} and ^{3}[H]GA_{29}-catabolite. However, application of IAA to the cut stump enabled the elongating internode to convert

^{3}[H]GA_{20} to ^{3}[H]$GA_{1,}$ and its immediate catabolite ^{3}[H]GA_{8}. IAA induction of GA_1 levels in the elongating internodes was correlated with an increase in *PsGA3ox1* transcript levels and a decrease in *PsGA2ox1* levels (O'Neil and Ross, 2002). A similar auxin-GA interaction has been reported in stems of tobacco plants (Wolbang and Ross, 2001). In barley, auxin from the developing inflorescence plays a role in stem elongation by upregulating GA 3-oxidation and downregulating GA 2-oxidation (Wolbang et al., 2004). Frigerio et al. (2006) showed that auxins control the expression of *AtGA20ox1* and *AtGA20ox2* in Arabidopsis seedlings supporting the model that auxin promotes GA biosynthesis. In addition, it has been noted that certain *GA2ox* genes are also upregulated by auxin treatment in Arabidopsis (Frigerio et al., 2006). Similar results were reported by Ozga et al. (2009), where by application of 4-Cl-IAA to deseeded pericarps decreased the transcript abundance of *PsGA2ox1*, but also transiently increased the transcript abundance of *PsGA2ox2*. Most systems studied show that stimulation of GA biosynthesis by auxin correlates with upregulation of GA biosynthesis genes, but the particular GA biosynthesis or catabolism genes vary.

Fu and Harberd (2003) demonstrated that shoot apex-derived auxin regulates root growth by modulating the effect of GA in Arabidopsis. They observed that when polar auxin transport or auxin signaling is weakened, the GA-induced disappearance of nuclear RGA is delayed and growth is restricted, indicating auxin promotes the growth of roots by enhancing the GA-induced destabilization of RGA and probably of other DELLA proteins. Even though their results related to the growth of Arabidopsis roots, they suggested that this

mechanism is likely to be involved in controlling the growth of other plant organs. Interestingly, Brian and Hemming (1957) noted that the internodes of decapitated GA-deficient pea plants are less responsive to GA than the internodes of intact GA-deficient pea plants.

Hormonal response pathways

Ubiquitin-mediated proteolysis

Many developmental and metabolic processes (e.g. signal transduction, cell-cycle progression, transcriptional regulation and endocytosis) are known to be regulated via the selective degradation of short-lived proteins in the cell (Hershko and Ciechanover, 1998). In Arabidopsis, it has been predicted that approximately 1200 of the predicted 25,000 proteins are involved in the ubiquitin-proteasome pathway (cited from Hellmann and Estelle, 2002). Ubiquitin is a small 76 amino acid protein that can be attached to substrate proteins, and once the protein is marked with ubiquitin, it can be identified and degraded by the 26S proteasome. The conjugation process of ubiquitin to a specific protein involves three steps and needs the sequential action of three enzymes. First, the ubiquitin C-terminus is activated by the ubiquitin activating enzyme (E1). The activated ubiquitin is then trans-esterified to a member of a family of ubiquitin-conjugating enzymes (E2). Finally, the specificity providing ubiquitin protein ligase (E3) brings the E2-ubiquitin complex into proximity to the target protein and covalently attaches ubiquitin to the specific target protein. Repetition of these enzymatic events results in the generation of a polyubiquitin chain on the target protein. The 26S proteasome recognizes this chain and degrades this tagged

protein, releasing free ubiquitin in the process (Hagen et. al., 2004). The most important step in ubiquitin conjugation is the selection of specific substrates by the E3 ubiquitin protein ligase.

More than 1000 E3 enzymes have been predicted in the Arabidopsis genome, the majority of which have not been assigned a specific function (cited from Hellmann and Estelle, 2002). E3 proteins are divided into two main groups; a HECT domain group and a RING-finger domain group. SCF-type E3s belong to RING-finger group and SCFs consist of four subunits, a SKP1, a Cullin, an F-box, and a RING finger protein (RBX1/HRT1/ROC1, mostly referred as RBX1; Hellmann and Estelle, 2002). The F-box proteins bring the specificity to the SCF complex. They have a SKP1 interacting domain (the F box) and a domain that recognizes the novel substrate (Hellmann and Estelle, 2002).

Auxin signal perception and transduction

Recent molecular and biochemical studies have revealed an intracellular auxin signaling pathway and most of its components are ubiquitin-proteasome dependent (Dharmasiri and Estelle, 2004).

The current model for auxin-regulated gene expression is based on de-repression of Auxin Response Elements (AuxRE) which are in the promoter region of auxin-regulated genes (Figure 1.2; Salmon et al., 2008). Auxin Response Factors (ARFs) are a family of transcription factors that mediate auxin-regulated gene expression by binding to AuxRE (Guilfoyle and Hagen, 2001). Under low-auxin conditions, Aux/IAA (18- to 35-kD, short-lived nuclear proteins

that function as transcriptional repressors) generally represses auxin response by binding with ARF via heterodimerization (Leyser, 2002).

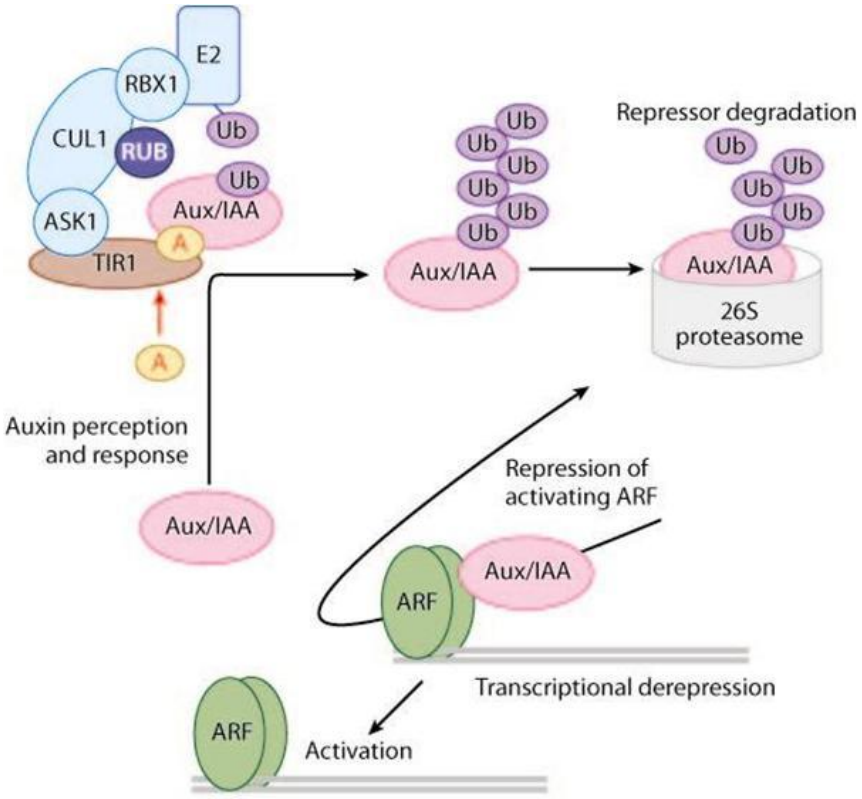

Figure 1.2. Model for auxin perception and signal transduction (source: Mockaitis and Estelle, 2008; Reprinted, with permission, from the *Annual Review of Cell & Developmental Biology*, Volume 24 © 2008 by Annual Reviews; www.annualreviews.org)

When auxin levels are elevated, Aux/IAAs are marked for degradation via ubiquitin-mediated proteolysis. Auxin induces the association of F-box protein TIR1 of E3 ligases complex $SCF^{TIR1/ABF1-3}$ [TIR1 also functions as an auxin receptor (Dharmasiri et al., 2005; Kepinski and Leyser, 2005)] with Aux/IAA proteins that catalyzes the ubiquitination (Dharmasiri et al., 2005, Kepinski and Leyser, 2005, Tan et al., 2007). Once ubiquitinated Aux/IAAs are degraded by the

26S proteasome and enabling specific ARF proteins to activate the expression of auxin-inducible genes as they are no longer dimerized with Aux/IAA proteins (Salmon et al., 2008).

GA signal perception and transduction

GA signaling operates similar to auxin signaling by de-repression of repressors (Figure1.3). DELLA proteins are transcriptional regulators that repress GA responses in the absence of GA. GA induces the degradation of DELLA-repressor proteins through the ubiquitin-proteasome pathway, mediated by the SCF complex (Gomi and Matsuoka, 2003; Fleet and Sun, 2005; Hirano et al., 2008). These proteins are referred to as DELLA proteins because of the unique "DELLA" motifs in their N-terminal domain. The DELLA proteins are members of the plant specific GRAS protein family and are located in the nucleus (Sun, 2004).

There are five Arabidopsis DELLA protein genes identified to date: *RGA* (repressor of ga1-3), *GAI* (gibberellic-acid insensitive), *RGL1* (RGA-like), *RGL2*, and *RGL3*. Several other DELLA protein genes have been identified in various crop species: maize *D8* (Dwarf 8); wheat *RHT* (reduced height); rice *SLR1* (slender rice), barley *SLN1* (slender1) and grape *VvGAI* (Olszewski et. al., 2002; Boss and Thomas, 2002; Ueguchi-Tanaka et al., 2007). More recently, Weston et al (2008) found that *PsLA* and *PsCRY* genes encode DELLA proteins in pea.

Identification of a GA receptor facilitated understanding of the molecular mechanism of GA perception and signal transduction (Fig. 1.3). Under low GA concentrations, GA action is repressed by DELLA proteins (Hirano et al., 2008).

Under high GA concentrations, the soluble GA receptor GID1 (GIBBERELLIN INSENSITIVE DWARF1) binds to GA (Ueguchi-Tanaka et al., 2005). The GID1-GA complex then interacts with DELLA proteins at the site of their DELLA and TVHYNP domains (both domains were named after the first five amino acids of conserved domains at the protein's N-terminus). This GID1-GA-DELLA protein complex is more stable than that of GID1-GA complex and does not easily dissociate (Ueguchi-Tanaka et al., 2007). The resulting trimer complex is in turn recognized by $SCF^{GID2/SLY1}$ E3 enzyme complex for polyubiquitination. ($SCF^{GID2/SLY1}$ E3 ligase complex consists of an adaptor protein Skp1 that links Cullin with F-box protein and Rbx1). The F-box protein GID2 (in Arabidopsis) and SLY1 (in rice) are the substrate receptor subunits of E3 ligase complex. The polyubiquitinated DELLA protein is degraded through the 26S proteasome pathway releasing the repressive state of GA responsive genes (Ueguchi-Tanaka et al., 2007).

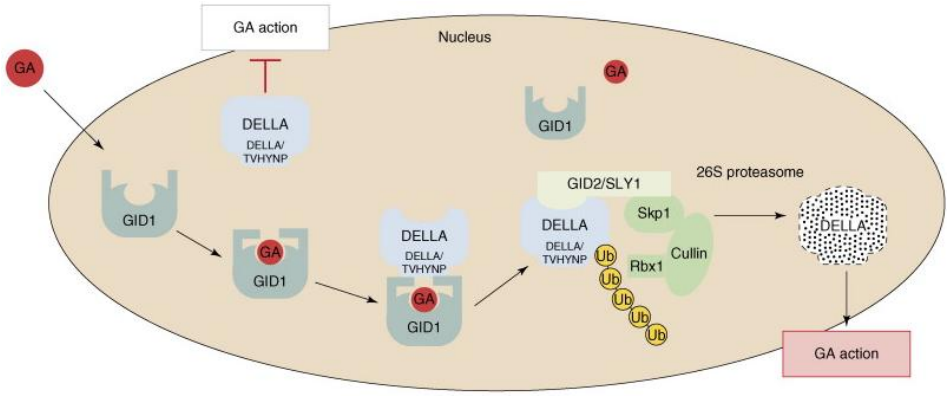

Figure 1.3. Model for GA perception and action through DELLA protein degradation (source: Hirano et al., 2008; Reprinted from Trends in Plant Science, Vol. 13, Hirano K, Ueguchi-Tanaka M, Matsuoka M, GID-1 mediated gibberellin signaling in plants, 192-199, with permission from Elsevier).

The action of GA in shoot elongation

Although GAs have been associated with many aspects of plant growth and development, their role in shoot elongation has been a central research focus. Shoot elongation is based on increased cell division and cell elongation activity in defined zones of the shoot. In deep water rice, GA-induced stem growth resulted from increased cell number and cell size (Kende et al.,1998; Cho and Cosgrove, 2004). The mechanism of GA-induced stem growth was attributed to greater extensibility of the shoot cell walls (Kende et al.,1998; Cho and Cosgrove, 2004).

Plant cell walls function as structural support, determine cell shape, and protect the cell against external biotic and abiotic stresses. To grow, plants must loosen their rigid cell walls in a precisely controlled temporal and spatial pattern and plant cells grow by expanding their cell walls through a process of controlled polymer extension (Cosgrove, 2005). The expansin proteins, discovered by McQueen-Mason et al. (1992), are prime candidates for cell wall-loosening factors that mediate the growth of plant cells (Cosgrove et al., 2000). They were shown to cause stress relaxation of isolated cell walls in a pH-dependent manner, and the prevailing model predicts that expansins act by disrupting hydrogen bonds between cellulose microfibrils and matrix polysaccharides or between the matrix polysaccharides themselves (Cosgrove, 2000). The role of expansins as mediators of plant cell growth has been tested by a number of experimental approaches. In many instances, a close correlation has been found between growth and the presence and activity of expansin proteins (McQueen-Mason et al., 1992; Cho and Kende, 1997a). There also is increasing evidence for a close correlation between

growth and the expression of expansin genes (Lee et al., 2001; Cosgrove et al., 2002).

Expansins appear to be regulated by most of the major plant hormones (Cho and Cosgrove, 2004). The role of expansins in GA action has been studied mainly in relevance to cell growth. Several families of expansins were identified in rice when genes were separated on the phylogenetic tree; expansin genes, α-expansin genes, β-expansin genes and expansin-like genes (Lee et al., 2001). Four expansin genes have been identified from rice (Cho and Kende, 1997a). The transcript levels of one (*OsEXP4*) of these expansin genes were induced within 30 minutes after 50 μM GA_3 treatment. Further investigation showed that five α-expansins, four β-expansins and one expansin-like genes were up-regulated by GA in the deepwater rice stem. These results support the hypothesis that part of the GA-induced elongation in deepwater rice is mediated by increased expression and activity of expansins (Cho and Kende, 1997a; Lee et. al., 2001).

The effect of GA on cell division was studied in the intercalary meristem region of rice internodes where cell divisions generate new internodal cells (Metraux and Kende, 1984). Progression of the cells through the cell cycle was monitored by measuring the [^{3}H]thymidine incorporation into the cells in the intercalary meristem by flow cytometry and also by determining the expression of genes whose products regulate the entry of cells into the S phase of the cell cycle and mitosis (Lorbiecke and Sauter, 1998). In all eukaryotes, the $p34^{cdc2\text{-}CDC28}$ protein kinase plays a central role in the onset of mitosis (Nurse, 1990) and it was found that GA enhanced the gene expression and the activity of this protein

suggesting that GA is involved in the activation of the cell cycle (Sauter et al., 1995). In addition, the transcript levels of two cyclin genes (cyclin is a fundamental regulator of the plant cell cycle) *cycOs1* and *cysOs2* were elevated in GA-treated internodes of rice during the G2 phase, indicating the corresponding cyclins of those two genes may control the cell's entry into the mitosis phase (Sauter et al., 1995). Taken together, these data suggest that GA is involved in promoting the two factors responsible for tissue elongation, increase in cell number and cell size.

The role of GA in leaf elongation appears to be multifaceted. Application of GA_3 on leaves of *Aegiops* species showed that it increased leaf elongation rate by increasing both cell number and cell size whereas application of a GA biosynthesis inhibitor, paclobutrazol, had the opposite effects (Bultynck and Lambers, 2004). Studies conducted on leaf sheath elongation of dwarf rice cultivar 'Tanginbozu' revealed that application of GA_3 enhanced the growth of leaf sheath; however, measurement of the mitotic index and cell size revealed that cell elongation was enhanced rather than cell division by GA_3 (Matsukura et al., 1998). They also reported that greater cell elongation was the result of increased wall extensibility. In garden pea (*Pisum sativum*), the *na-1* mutant (*PsKAO1* gene null mutation with markedly reduced bioactive GA levels) exhibits a dramatic reduction in stipule size (Reid and Ross, 1993) indicating the importance of bioactive GA in pea leaf development. In sweet pea (*Lanthyrus odoratus* L.), leaflets of *l* mutants (corresponding to *le* mutant of *P. sativum*), are consistently smaller and more ovate than those of wild type plants (Ross et al., 1990).

However, *le* mutants in garden pea show reduced leaflet size only at lower nodes and no difference in leaf shape (Reid and Ross, 1993).

Auxin transport

Auxin is involved in a number of plant growth and development processes including embryogenesis, organogenesis, vascular tissue differentiation, root meristem maintenance, hypocotyl and root elongation, apical hook formation, stem elongation, apical dominance, fruit development, and growth response to environmental stimuli (Davies, 2004; Vieten et al., 2007). Pharmacological and genetic studies combined with direct and indirect visualization of auxin distribution has implied that directional intercellular transport of auxin and its resulting local accumulation play key roles in a number of these auxin-regulated responses (Vieten et al., 2007).

Auxin is distributed throughout the plant by two main pathways. One pathway is the fast, non-directional transport system through the phloem, and the second is the slower, more controlled, cell-to-cell and directional carrier-dependant transport system (polar auxin transport; PAT; see review, Morris et al., 2004). The existence of auxin phloem transport was established through radio-labeled auxin experiments in maize seedlings and this transport occurs relatively fast (5-20 cm/h) in both basipetal and acropetal directions; the direction and speed of auxin translocation in this pathway is subjected to the factors that influence phloem translocation (Friml and Palme, 2002; Morris et al., 2004; Morris and Thomas, 1978; Nowacki and Bandurski, 1980). Polar auxin transport occurs in a cell-to-cell manner and it is unidirectional. The main PAT system runs from the

stem apex basipetally with a velocity of 5-20 mm/h towards the base of the plant (Friml and Palme, 2002; Lomax et al., 1995; Goldsmith, 1977). PAT requires energy and is sensitive to protein synthesis inhibitors (Friml and Palme, 2002). In roots, polar auxin transport is mainly acropetal towards the root tip, where part of the auxin is transmitted backwards and transported basipetally through the root epidermis to the elongation zone (Rashotte et al., 2000).

In the mid 1970s, the chemiosmotic hypothesis was formulated to explain the mechanism of PAT (Rubery and Sheldrake, 1974; Raven, 1975). According to this hypothesis, the IAA molecule is present in both ionized and protonated forms [about 15% of IAA exists in its protonated form (IAAH)] in the relatively acidic environment of the cell wall (about pH 5.5). Hydrophobic, protonated IAAH enters the cell passively by diffusion through the plasma membrane. In the more basic cytoplasm (pH 7), the IAAH dissociates and the resulting IAA^- anion cannot passively move out of the cell due to its poor membrane permeability. In addition to simple diffusion, the auxin influx carriers also transport auxin anions (IAA^-) into the cell (Vieten et al., 2007). Furthermore, the presence of auxin efflux carriers asymmetrically localized within cell was postulated to transport IAA- ions out of the cell in a unidirectional manner (Friml and Palme, 2002). It has also been reported that the polarity of auxin flow can be modulated by changes in the subcellular localization of auxin efflux carriers within auxin transporting cells (Wisniewska et al., 2006). Experiments conducted using labeled auxin showed that auxin transported in the phloem was later found in the PAT system indicating the two transport systems might be linked (Cambridge and Morris, 1996). The

known PAT inhibitor 2, 3, 5-triiodobenzoic acid (TIBA) induced the net uptake of labeled IAA in wheat coleoptiles segments indicating TIBA inhibits auxin efflux rather than influx. This observation together with chemical properties of IAA suggested that auxin efflux is the limiting step in PAT (Morris et al, 2004).

PIN auxin efflux carriers

Okada et al. (1991) described existence of the knitting needle-like *pin-formed1 (pin1)* mutant in Arabidopsis and this mutant resembled plants treated with inhibitors of auxin efflux. They also found that the basipetal auxin transport was also strongly reduced in this mutant. Galweiler et al. (1998) cloned the *AtPIN1* gene and found that it encodes a transmembrane protein with some similarity to a group of bacterial transporters. Eight *PIN* genes have been identified in Arabidopsis, but all have not been functionally characterized (Vieten et al., 2007). The functionally characterized AtPIN1 appears to mediate organogenesis and vascular tissue differentiation (Galweiler et al., 1998; Reinhardt et al., 2003). AtPIN2 appears to be involved in root gravitropic growth (Muller et al., 1998), AtPIN3 in shoot differential growth and root tropic growth responses (Friml et al., 2002b), AtPIN4 in root meristem activity (Friml et al., 2002a), and AtPIN7 in early embryo development (Friml et al., 2003; Vieten et al., 2007). Members of the PIN protein family were found to be homologous and functionally redundant as indicated by the increasingly severe phenotypes with increasing *pin* mutant gene members within a single genome (Vieten et al., 2005, Vieten et al., 2007).

Almost all the PIN proteins analyzed so far show polar subcellular localization, even though some of them can be found without marked polarity in specific cell types (Vieten et al., 2007). This fits well with the chemiosmotic hypothesis. There are several reports showing the correlation between the polarity of PIN proteins and the direction of auxin transport or with the local accumulation of auxin in adjacent cells (Vieten et al., 2007). Wisniewska et al (2006) demonstrated that the polarity of PIN protein localization is determined not only by cell type-specific signals, but also by sequence-specific signals within PIN proteins.

Auxin efflux carriers in pea

To date, two genes coding PIN auxin efflux carriers have been cloned in pea, *PsPIN1* (Chawla and DeMason, 2004) and *PsPIN2* (Hoshino et al., 2005). *PsPIN1* is most similar to that of *AtPIN1* in sequence and in expression pattern (ubiquitously expressed in all organs and plant parts). *PsPIN1* transcript is also more abundant in growing or developing plant parts (Chawla and DeMason, 2004). The predicted PsPIN1 amino acid sequence has high homology to its orthologs, PsPIN1 is 96.8% similar to *Medicago* MtPIN4, 88.4% to *Populus* PtPIN1, and 83.3% to *Arabidopsis* AtPIN1 (Chawla and DeMason, 2004). Sequence analysis of the promoter region of *PsPIN1* revealed the presence of three auxin responsive elements and two possible GA-responsive elements (Chawla and DeMason, 2004).

The predicted PsPIN1 amino acid sequence has high homology to its Arabidopsis orthologs; PsPIN2 is similar to AtPIN4 (74%), AtPIN3 (74%) and

AtPIN7 (72%). Phylogenetic analysis shows that PsPIN2 belongs to a different class than PsPIN1, suggesting different roles for PsPIN1 and PsPIN2 in auxin transport (Hoshino et al., 2005) in pea. Northern blot analysis showed that *PsPIN2* is expressed in the shoot apical hook, internode (both in the elongation zone and the basal zone of the 1st internode) and root (mature root regions and root tips) of 6-d-old etiolated pea seedlings (Hoshino et al., 2005). *PsPIN2* expression was relatively low in roots compared to shoots suggesting a greater role for *PsPIN2* in regulating auxin transport in the shoot tissues (Hoshino et al., 2005).

IAA and 4-Cl-IAA induced *PsPIN1* expression within 1 h of auxin treatment to 7-day-old dark grown shoot tips, with *PsPIN1* transcript abundance peaking within 2 hours of hormone application (Chawla and DeMason, 2004). *PsPIN1* transcript induction maximum for IAA was 50 µM while that of 4-Cl-IAA was 25 µM, suggesting that 4-Cl-IAA is more effective than IAA in stimulating *PsPIN1* mRNA levels in this tissue (Chawla and DeMason, 2004). IAA stimulation of *PsPIN* mRNA levels was also reported by Hoshino et al (2005). When pea epicotyl segments were pre-incubated with distilled water for 2 h to reduce endogenous auxin concentrations within the tissue, gene expression of *PsPIN1* and *PsPIN2* were substantially reduced. When the pretreated segments were incubated with a relatively low concentration of auxin (10^{-7} M), expression of *PsPIN1* and *PsPIN2* substantially increased. A 4 h treatment with 50 µM GA_3 also stimulated *PsPIN1* mRNA abundance in pea internode segments (Hoshino et al 2005). No additive or synergistic response with respect to *PsPIN1* gene

expression was observed with simultaneous application of GA_3 and IAA (Chawla and DeMason, 2004).

Thesis objectives

The overall objective of the research described in this thesis was to test the hypothesis that GA 3β-hydroxylation is a rate limiting step in GA biosynthesis in pea. To test this hypothesis, transgenic pea lines overexpressing *PsGA3ox1* were phenotypically, molecularly and biochemically characterized with respect to stem growth and during seed germination and early seedling growth. In order to understand the phenotypic alterations in the *PsGA3ox1*-overexpression lines, possible regulation mechanisms of GA biosynthesis were investigated along with expression profiles of the putative auxin efflux carriers *PsPIN1* and *PsPIN2*.

Literature cited:

Ait-Ali T, Frances S, Weller JL, Reid JB, Kendrick RE, et al. (1999) Regulation of gibberellin 20-oxidase and gibberellin 3β-hydroxylase transcript accumulation during de-etiolation of pea seedlings. Plant Physiol **121**: 783-791

Ait-Ali T, Swain SM, Reid JB, Sun T, Kamiya Y (1997) The *LS* locus of pea encodes the gibberellin biosynthesis enzyme *ent*-kaurene synthase A. Plant J **11**:443-454

Ayele BT, Ozga JA, Reinecke DM (2006) Regulation of GA biosynthesis genes during germination and young seedling growth of pea (*Pisum sativum* L.). J Plant Growth Regul **25**:219-232

Backer DA (2000) Long-distance vascular transport of endogenous hormones in plants and their role in source: sink regulation. Israel J Plant Sci **48**:199-203

Boss PK, Thomas MR (2002) Association of dwarfism and floral induction with a grape 'green revolution' mutation. Nature **416**:847-50

Brian PW, Hemming HG (1957) A relation between the effects of gibberellic acid and indolylacetic acid on plant cell expansion. Nature **179**: 417

Bultynck L, Lambers H (2004) Effect of applied gibberellic acid and paclobutrazol on leaf expansion and biomass allocation in two *Aegilops* species with contrasting leaf elongation rates. Physiol Plant **122**: 143-151

Cambridge AP, Morris DA (1996) Transfer of exogenous auxin for the phloem to the polar auxin transport pathway in pea (*Pisum sativum* L.) Planta **199**: 583-588

Chawla R, DeMason DA (2004) Molecular expression of *PsPIN1*, a putative auxin efflux carrier gene form pea (*Pisum sativum* L.) Plant Growth Reg **44**: 1-14

Chen R, Hilson P, Sedbrook J, Rosen E, Caspar T, et al. (1998) The *Arabidopsis thaliana AGRAVITROPIC 1* gene encodes a component of the polar-auxin-transport efflux carrier. Proc Natl Acad Sci USA **95**: 15112-15117

Chiang HH, Hwang I, Goodman HM (1995). Isolation of the *Arabidopsis GA4* locus. Plant Cell **7**:195-201

Cho HT, Cosgrove DJ (2004) Expansins as agents in hormone action. *In* PJ Davis, ed, Plant hormones: Biosynthesis, signal transduction, action. Ed 3. Kluwer Academic Publishers, Dordrecht, The Netherlands, pp 262-281

Cho HT, Kende H (1997) Expansins in deepwater rice internodes. Plant Physiol **113**: 1137-1143

Cho HT, Kende H (1997a) Expression of expansin genes is correlated with growth in deepwater rice. Plant Cell **9**:1661-1671

Cosgrove DJ (2000) Loosening of plant cell wall by expansins. Nature **407**: 321-326

Cosgrove DJ (2005) Growth of the plant cell wall. Nature rev mol cell bio **6**: 850-861

Cosgrove DJ, Li LC, Cho HT, Hoffmann-Bennings S, Moor RC, et al (2002) The growing world of expansins. Plant Cell Physiol **43**:1436-1444

Crozier A, Kamiya Y, Bishop G, Yakota T (2000) Biosynthesis of hormone and elicitor molecule. *In* B Buchanan, W Gruissem, R Jones, eds, Biochemistry and molecular biology of plants. American Society of Plant Biologists, Rockville, USA, pp 851-865

Dai M, Zhao Y, Ma Q, Hu Y, Hedden P et al. (2007) The rice *YABBI* gene is involved in the feedback regulation of gibberellin metabolism Plant Physiol **144**:121-131

Darwin, CR (1880) The power of movement in plants. Murray, London

Davidson SE, Reid JB (2004) The Pea gene *LH* encodes *ent*-kaurene oxidase. Plant Physiol **134:** 1123-1134

Davidson SE, Elliott RC, Helliwell CA, Poole AT, Reid JB (2003) The pea gene NA encodes ent-kaurenoic acid oxidase. Plant Physiol **130**: 335-344

Davidson SE, Swain SM, Reid JB (2005) Regulation of the early GA biosynthesis pathway in pea. Planta **222**: 1010-1019

Davies PJ (2004) The plant hormones: their nature, occurrence, and functions. *In* PJ Davis, ed, Plant hormones: Biosynthesis, signal transduction, action. Ed 3. Kluwer Academic Publishers, Dordrecht, The Netherlands, pp 1-15

Dharmasiri N, Dharmasiri S, Estelle M (2005) The F-box protein TIR1 is an auxin receptor. Nature **435**: 441-445

Dharmasiri N, Estelle M (2004). Auxin signaling and regulated protein degradation. Trends Plant Sci **9**: 302-308

Dill A, Sun T-P (2001) Synergistic derepression of gibberellin signaling by removing RGA and GAI function in *Arabidopsis thaliana* Genetics **159**: 777-785

Elliott RC, Ross JJ, Smith JJ, Lester DR, Reid JB (2001) Feed-forward regulation of gibberellin deactivation in pea. J Plant Growth Regul **20**: 87-94

Fleet CM, Sun T-p (2005) A DELLAcate balance: the role of gibberellin in plant morphogenesis. Curr Opin Plant Biol **8**: 77-85

Fleet CM, Yamaguchi S, Hanada A, Kawaide H, David CJ, et al (2003) Overexpression of *AtCPS* and *AtKS* in *Arabidopsis* confers increased *ent*-kaurene production but no increase in bioactive gibberellins. Plant Physiol **132**: 830-839

Frigerio M, Alabadi D, Perez-Gomaez J, Garcia-Carcel L, Phillips AL, et al. (2006) Transcriptional regulation of gibberellin metabolism genes by auxin signaling in *Arabidopsis*. Plant Physiol **142**: 553-563

Friml J, Benkova E, Blilou I, Wisniewska J, Hamann Y, et al. (2002a) AtPIN4 mediates sink-driven auxin gradients and root patterning in *Arabidopsis*. Cell **108**: 661-673

Friml J, Palme K (2002) Polar auxin transport- old questions and new concepts? Plant Mol Biol **49**: 273-284

Friml J, Vieten A, Sauer M, Weijers D, Schwarz H, et al. (2003) Efflux-dependent auxin gradients establish the apical-basal axis of Arabidopsis. Nature **426**: 147-153

Friml J, Wisniewska J, Benkova EMendgen K, Palme K (2002b) Lateral relocation of auxin efflux regulator PIN3 mediates tropism in *Arabidopsis*. Nature **415**:806-809

Fu X, Harberd NP (2003) Auxin promotes Arabidopsis root growth by modulating gibberellin response. Nature 421: 740-743

Galweiler L, Guan C, Muller A, Wisman E, Mendgen K et al (1998) Regulation of polar auxin transport by AtPIN1 in Arabidopsis vascular tissue. Science **282**: 2226-2230

Goldsmith MHM (1977) The polar transport of auxin. Annu Rev Plant Physiol **28**: 439-478

Gomi K, Matsuoka M (2003) Gibberellin signaling pathway. Curr Opin Plant Biol **6**: 489-493

Guilfoyle TJ, Hagen G (2001) Auxin response factors. J Plant Growth Regul **10**:281-291

Hagen G, Guilfoyle TJ, Gray WM (2004) Auxin signal transduction. *In*: PJ Davis, ed, Plant hormones: Biosynthesis, signal transduction, action. Ed 3. Kluwer Academic Publishers, Dordrecht, The Netherlands, pp 282-303

Hedden P, Phillips AL (2000) Gibberellin metabolism: new insights revealed by the genes. Trends Plant Sci **5**: 523-530

Hedden P, Proebsting W (1999) Genetic analysis of gibberellin biosynthesis. Plant Physiol **119**: 365-370

Helliwell CA, Chandler PM, Poole A, Dennis ES, Peacock WJ (2001) The CYP88A cytocrome P450, ent-kaurenoic acid oxidase, catalyzes three steps of the gibberellin biosynthesis pathway. Proc Natl Acad Sci USA **98**:2065-2070

Hellmann H, Estelle M (2002) Plant development: regulation by protein degradation. Science **297**: 793-797

Hershko A, Ciechanover A (1998) The ubiquitin system. Annu Rev Biochem **67**:425-479

Hirano K, Ueguchi-Tanaka M, Matsuoka M (2008). GID-1 mediated gibberellin signalling in plants. Trends Plant Sci **13**: 192-199

Hori S (1898) Some observations on "Bakanae" disease of the rice plant. Mem Agric Res Sta (Tokyo) **12**: 110-119

Hoshino T, Hitotsubashi R, Miyamoto K, Tanimoto E, Ueda J (2005) Isolation of *PsPIN2* and *PsAUX1* from etiolated pea epicotyls and their expression of three-dimensional clinostat. Adva Space Res **36**: 1284-1291

Kende H, van der Knaap E, Cho HT (1998) Deepwater rice: A model plant to study stem elongation. Plant Physiol **118**: 1105-1110

Kepinski S, Leyser O (2005) The Arabidopsis F-box protein TIR1 is an auxin receptor. Nature **435**: 446-451

Lee DJ, Zeevaart JA (2005) Molecular cloning of GA 2-oxidase3 from spinach and its ectopic expression in *Nicotiana sylvestris*. Plant Physiol **138**: 243-254

Lee Y, Choi D, Kende H (2001) Expansins: ever-expanding numbers and functions. Curr Opin Plant Biol **4**:527-532

Lester DR, Ross JJ, Ait-Ali T, Martin DN, Reid JB (1996) A gibberellin 20-oxidase cDNA (Accession no. U58830) from pea seed. Plant Physiol **111**: 1353

Lester DR, Ross JJ, Davies, Reid JB (1997) Mendel's stem length gene (*Le*) encodes a gibberellin 3β-hydroxylase. Plant Cell **9**:1453-1443

Lester DR, Ross JJ, Smith JJ, Elliot RC, Reid JB (1999) Gibberellin 2-oxidation and the *SLN* gene of *Pisum sativum*. Plant J **19**:1435-1443

Leyser O (2002) Molecular genetics of auxin signaling. Annu. Rev. Plant Biol. **53**: 377-398

Lichtenthaler H, Rohmer M, Schwender J (1997) Two independent biochemical pathways for isopentenyl diphospate and isoprenoid biosynthesis in higher plants. Physiol Plant **101**: 643-652

Lomax TL, Muday GK, Rubery PH (1995) Auxin transport. In PJ Davis ed, Plant hormones: Physiology, biochemistry and molecular biology, Ed 2. Kluwer Academic Publishers, Dordrecht, Boston, London, pp 509-530

Lorbiecke R, Sauter M (1998) Induction of cell growth and cell division in the intercalary meristem of submerged deep water rice (*Oryza sativa* L.). Planta **204**: 140-145

Macmillan J Seaton JC Suter PJ (1960) Isolation of gibberellin A_1 and gibberellin A_5 from *Phaseolus multiflorus*. Tetrahedron **11**: 60-66

Macmillan J Seaton JC Suter PJ (1962) Isolation and structures of gibberellin A_6 and gibberellin $A_{8.}$ Tetrahedron **18**: 349-355.

Macmillan J, Seaton JC Suter PJ (1959) A new plant-growth promoting acid-gibberellin A_5 from the seed of *Phaseolus multiflorus* Proc Chem Soc **325**:1

Macmillan J, Suter PJ (1958) The occurence of gibberellin A_1 in higher plants: Isolation from the seed of runner bean (*Phaseolus multiflorus*). Naturwiss **45**: 46

MacMillan J, Takahashi N (1968). "Proposed procedure for the allocation of trivial names to the gibberellins". *Nature* **217**:170-171

Martin DN, Proebsting WM, Hedden P (1997) Mendel's dwarfing gene: cDNAs from the *le* alleles and function of the expressed protein. Proc Natl Acad Sci USA **94**:8907-8911

Martin DN, Proebsting WM, Hedden P (1999) The *SLENDER* gene of pea encodes a gibberellin 2-oxidase. Plant Physiol **121**:775-781

Martin DN, Proebsting WM, Parks TD, Dopugherty WG, Lange T, et al. (1996) Feedback regulation of gibberellin biosynthesis and gene expression in *Pisum sativum* L. Planta **200**: 159-166

Marumo S, Abe H, Hattori H, Munakata K (1968) Isolation of a novel auxin, methyl 4-chloroindole acetate from immature seeds from *Pisum sativum.* Agric Biol Chem **32**: 117-118

Matsukura C, Itoh S, Nemoto K, Tanimoto E, Yamaguchi J (1998) Promotion of leaf sheath growth by gibberellic acid in a dwarf mutant of rice. Planta **205**: 145-152

Matsushita A, Furumoto T, Ishida S, Takahashi Y (2007) AGF1, an AT-hook protein is necessary for the negative feedback of *AtGA3ox1*encoding GA 3-oxidase. Plant Physiol **143**: 1152-1162

Mauriat M, Moritz T (2009) Analysis if GA20ox- and GID1-over-expressing aspen suggest that gibberellins play two distinct roles in wood formation. Plant J **58**: 989-1003

McQueen-Mason SJ, Durachko DM, Cosgrove DJ (1992) Two endogenous proteins that induce cell wall extension in plants. Plant Cell **4**: 1425-1433

Metraux J-P, Kende H (1984) The cellular basis of the elongation response in submerged deep-water rice. Planta **160**: 66-72

Mockaitis K, Estelle M (2008) Auxin Receptors and Plant Development: A New Signaling Paradigm. Ann Rev Cell Dev Biol 24: 55-80

Morris DA, Friml J, Zazimalova E (2004) The functioning of hormones in plant growth and development. *In* PJ Davis, ed, Plant hormones: Biosynthesis, signal transduction, action. Ed 3. Kluwer Academic Publishers, Dordrecht, The Netherlands, pp 437-470

Morris DA, Thomas AG (1978) A microautoradiographic study of auxin transport in the stem of intact pea seedlings (*Pisum sativum* L.) J Exp Bot **29**:147-157

Muller A, Guan C, Galweiler L, Tanzler P, Huijser P et al. (1998) AtPIN2 defines a locus of Arabidopsis for root gravitropism control. EMBO J **17**: 6903-6911

Mutasa-Gottegens E, Hedden P (2009) Gibberellin as a factor in floral regulatory networks. J Experi Bot **60**: 1979-1989

Ngo P, Ozga JA, Reinecke DM (2002) Specificity of auxin regulation of GA 20-oxidase gene expression in pea pericarp. Plant Mol Biol **49**:439-448

Nowacki J, Bandurski RS (1980) Myo-inositol esters of indole-3-acetic acid as seed auxin precursors of Zea mays L. Plant Physiol **65**:422-427

Nurse P (1990) Universal control mechanism regulating onset of M-phase. Nature **344**:503-508

O'Neill DP, Ross JJ (2002) Auxin regulation of gibberellin pathway in pea. Plant Physiol **130**: 1974-1982

Okada K, Udea J, Komaki MK, Bell CJ, Shimura Y (1991) Requirement of the auxin polar transport system in the early stages of *Arabidopsis* floral bus formation. Plant Cell **3**:677-684

Olszewski N, Sun T, Gubler F (2002) Gibberellin signaling: Biosynthesis, catabolism, and response pathways. Plant Cell **14**: S61- S80

Ozga JA, Brenner ML, Reinecke DM (1992) Seed effects on gibberellin metabolism in pea pericarp. Plant Physiol **100**:88-94

Ozga JA, Reinecke DM, Ayele BT, Ngo P, Nadeaue C, Wickramarathna AD (2009) Developmental and hormonal regulation of gibberellin biosynthesis and catabolism in pea fruit. Plant Physiol **150**: 448-462

Ozga JA, Yu J, Reinecke DM (2003) Pollination-, development-, and auxin-specific regulation of gibberellin 3β-hydroxylase gene expression in pea fruit and seeds. Plant Physiol **131**: 1137-1146

Phillips AL, Ward DA, Uknes S, Appleford NE, Lange T, et al. (1995) Isolation and expression of three gibberellin 20-oxidase cDNA clones from *Arabidopsis*. Plant Physiol **108**: 1049-1057

Phinney BO, West CA, Ritzel MB, Neely PM (1957) Evidence for gibberellin-like substances from flowering plants. Proc Nat Acad Sci USA **43:** 398-404

Phinney BO (1983) The history of gibberellins. *In* A Crozier, ed, The biochemistry and physiology of gibberellins. Vol 1. Praeger, New York, USA pp 19-52

Radley M (1956) Occurrence of substances similar to gibberellic acid in higher plants. Nature **178:** 1070-1071

Rashotte AM, Brady S, Reed R, Ante S, Muday GK (2000) Basipetal auxin transport is required for gravitropism in roots of *Arabidopsis*. Plant Physiol **122**: 481-490

Raven JA (1975) Transport of indole acetic acid in plant cells in relation to pH and electrical potential gradients, and its significance for polar IAA transport. New Phytol **74**: 163-172

Reid JB, Ross JJ (1993) A mutant-based approach, using *Pisum sativum*, to understanding plant growth. Int J Plant Sci **154**:22-34

Reid JB, Ross JJ, Swain SM (1992) Internode length in *Pisum*. A new slender mutant with elevated levels of C19 gibberellins. Planta **188**: 462-467

Reid JB, Symons GM, Ross JJ (2004) Regulation of gibberellin and brassinosteroid biosynthesis by genetic, environmental and hormonal factors. *In* PJ Davis, ed, Plant hormones: Biosynthesis, signal transduction, action. Ed 3. Kluwer Academic Publishers, Dordrecht, The Netherlands, pp 179-203

Reinecke DM, Ozga JA, Magnus V (1995) Effect of halogensubstitution of indole-3-acetic acid on biological activity in pea fruit. Phytochemistry **40:** 1361–1366

Reinhardt D, Pesce E, Stieger P, Mandel T, Baltensperger K, et al. (2003) Regulation of phyllotaxis by polar auxin transport. Nature **426**: 255-260

Ross JJ, Davis NW, Reid JB, Murfet IC (1990) Internode length in *Lanthyrus odoratus*: effects of mutants l and lb on gibberellin metabolism and levels. Physiol Plant **79**:453-458

Ross JJ, MacKenzie-Hose AK, Davis PJ, Lester DR, Twitchin B, et al (1999) Firther evidence for feedback regulation of gibberellin biosynthesis in pea. Physiol Plant **105**: 532-538

Ross JJ, O'Neill DP (2001) New interactions between classical plant hormones. Trends Plant Sci **6**:2-4

Ross JJ, O'Neill DP, Smith JJ, Kerckhoffs LH, Elliott RC (2000) Evidence that auxin promotes gibberellin A_1 biosynthesis in pea. Plant J **21**: 547-552

Rubery PH, Sheldrake AR (1974) Carrier-mediated auxin transport. Planta **188**: 101-121

Salkowski E (1885) Uber das verhalten der skatolcarbonsaure im organismus. Zeitschr Physiol Chem **9**:23-33

Salmon J, Ramos J, Callis J (2008) Degradation of the auxin response factor ARF-1. Plant J **54**:118-128

Sasaki A, Itoh H, Gomi K, Ueguchi-Tanaka M, Ishiyama K, et al. (2003). Accumulation of phosphorylated repressor for gibberellin in an F-box mutant. Science **299**: 1896-1898

Sauter M, Mekhedov SL, Kende H (1995) Gibberellins promotes histone H1kinase activity and the expression of cdc2 and cyclin genes during the induction of rapid growth in deep water rice internodes. Plant J **7**:623-632

Schneider EA, Kazakoff CW, Wightman F (1985) Gas chromatography-mass spectrometry evidence for several endogenous auxins in pea seedling organs. Plants **165**: 232-241

Schomburg FM, Bizzell CM, Lee DJ, Zeevaart JA, Amasino RM (2003) Overexpression of a novel class of gibberellin 2-oxidase decreases gibberellin levels and creates dwarf plants. Plant Cell **15**: 151-63

Schwechheimer C (2008) Understanding gibberellic acid signaling – are we there yet? Curr Opi Plant Biol **11**: 9-15

Sponsel VM (1995) The biosynthesis and metabolism of gibberellins in higher plants. *In* PJ Davies, ed, Plant hormones: Physiology, biochemistry and molecular biology. Kluwer Academic, Dordrecht, The Netherlands, pp 66-97

Sun T-P, Gubler F (2004) Molecular mechanisms of gibberellin signaling in plants. Annu Rev Plant Biol **55**: 197-223

Sun T-P (2004) Gibberellin signal transduction in stem elongation and leaf growth. *In* PJ Davis, ed, Plant hormones: Biosynthesis, signal transduction, action. Ed 3. Kluwer Academic Publishers, Dordrecht, The Netherlands, pp 304-320

Swain SM, Reid JB (1992) Internode length in *Pisum*. A new allele at the *Lh* locus. Physiol Plantarum **86**: 124-130

Swain SM, Sing Dp, Helliwell CA, Poole AT (2005) Plants with increased expression of ent-kaurene oxidase are resistant to chemical inhibitors of this gibberellin biosynthesis enzyme. Plant Cell Physiol **46**: 284-291

Swarup R, Parry G, Graham N, Allen T, Bennett M (2002) Auxin cross talk: integration of signaling pathways to control plant development. Plant Mol Biol **49**:411-426

Tan X, Calderon-Villalobos LI, Sharon M, Zheng C, Robinson CV, et al. (2007) Mechanism of auxin perception by the TIR1 ubiquitin ligase. Nature **446**: 640–645

Thomas SG, Phillips AL, Hedden P (1999) Molecular cloning and functional expression of gibberellin 2-oxidases, multifunctional enzymes involved in gibberellin deactivation. Proc Natl Acad Sci USA **96**:4698-4703

Trewavas AJ (1981) How do plant growth substance work? Plant, Cell and Environment **4**: 203-228

Ueguchi-Tanaka M, Ashikari M, Nakajima M, Itho H, Katoh E, et al. (2005) *Gibberellin Insensitive DWARF1* encodes a soluble receptor for gibberellin. Nature **437**: 693-698

Ueguchi-Tanaka M, Nakajima M, Motoyuki A, Matsuoka M (2007) Gibberellin receptor and its role in gibberellin signalling in plants. Annu Rev Plant Biol **58**: 183-198

Umehara M, Hanada A, Yoshida S, Akiyama K, Arite T et al (2008) Inhibition of shoot branching by new terpinoid plant hormones. Nature **455**: 195-200

van Huizen R, Ozga JA, Reinecke DM (1997) Seed and hormonal regulation of gibberellin 20-oxidase expression in pea pericarp. Plant Physiol **115**: 123-128

van Huizen R, Ozga JA, Reinecke DM, Twitchin B, Mander LN (1995) Seed and 4-chloroindole-3-acetic acid regulation of gibberellin metabolism in pea pericarp. Plant Physiol **119**: 1213-1217

Varbanova M, Yamaguchi S, Yang Y, McKelvey K, Hanada A, et al. (2007) Methylation of gibberellins by Arabidopsis GAMT1 GAMT2. Plant Cell **19**: 32-45

Vieten A, Sauer M, Brewer P, Friml J (2007) Molecular and cellular aspects of auxin-transport-mediated development. Trend Plant Sci **12**:160-168

Vieten A, Vanneste S, Wisniewska J, Benkova E, Benjamins R, et al. (2005) Functional redundancy of PIN proteins is accompanied by auxin-dependant cross-regulation of PIN expression. Development **132**: 4521-4531

Went FW (1926) On growth-accelerating substances in the coleoptiles of Avena sativa. Proc Kon Ned Akad Wet **30**:10-19.

Weston DE, Elliott RC, Lester DR, Rameau C, Reid JB, et al. (2008) The pea DELLA proteins *LA* and *CRY* are important regulators of gibberellin synthesis and root growth. Plant Physiol **147**: 199-205

Wightman F, Lighty DL (1982) Identification of phenylacetic acetic acid as a natural auxin in the shoots of higher plants. Physiol Planta **55**: 17-24

Wisniewska J, Xu J, Seifertova D, Brewer PB, Ruzicka K et al. (2006) Polar PIN localization directs auxin flow in plants. Science **312**: 883

Wolbang CM, Chandler PM, Smith JJ, Ross JJ (2004) Auxin from the developing inflorescence is required for the biosynthesis of active gibberellins in barley stems. Plant Physiol **134**:769-776

Wolbang CM, Ross JJ (2001) Auxin promotes gibberellin biosynthesis in decapitated tobacco plants. Planta **214**: 153-157

Woodward AW, Barterl B (2005) Auxin: Regulation, action and interaction. Ann Bot **95**: 707-735

http://www.plant-hormones.info/gibberellins.htm

Xu YL, Li L, Gage DA, Zeevaart JA (1999) Feedback regulation of GA5 expression and metabolic engineering of gibberellin levels in *Arabidopsis*. Plant Cell **11**:927-936

Yabuta T (1935) Biochemistry of the "bakanae" fungus of rice. Agr Hort **10:**17-22

Yamaguchi S (2008) Gibberellin metabolism and its regulation. Annu Rev Plant Biol **59**: 225-251

Yamaguchi S, Smith MW, Brown RG, Kamiya Y, Sun T-p (1998) Phytochrome regulation and differential expression of gibberellin 3β-hydroxylase genes in germinating Arabidopsis seeds. Plant Cell **10**:2115-2126

Yamaguchi T, Nagasawa N, Kawasaki S, Matsuoka M, Nagato Y, et al (2004) the *YABBY* gene *DROOPING LEAF* regulates carpel specification and midrib development in *Oryza sativa*. Plant Cell **16**:500-509

Yaxley JR, Ross JJ, Sherriff LJ, Reid JB (2001) Gibberellin biosynthesis mutations and root development in pea. Plant Physiol **125**: 627-633

Zhu Y, Nomura T, Xu Y, Zhang Y, Peng Y, et al. (2006) Elongated uppermost internode encodes a cytochrome P450 monooxygenase that epoxidizes gibberellins in a novel deactivation reaction in rice. Plant Cell **18**: 442-456

Chapter 2

Characterization of pea plants transformed to overexpress *PsGA3ox1*

Introduction

The general biosynthesis pathway has been elucidated and genes identified for many of the enzymes involved in the synthesis of GAs in plants (for a review, see Hedden and Phillips, 2000a; Olszewski et al, 2002; Yamaguchi, 2008). Changing the expression of these genes within plant tissues provides new opportunities to study the regulation of GA biosynthesis and catabolism as well as the functions of GAs in plant growth and development. Furthermore, it should be possible to introduce agriculturally-useful traits into crops through the modification of bioactive GA levels, in some cases reproducing the effects obtained by the application of chemical growth regulators (Hedden and Phillips, 2000b). In addition, overexpression of GA metabolism genes in plants could provide useful information on the rate-limiting steps of GA biosynthesis.

Modulation of the expression of GA biosynthesis genes through transgenic approaches has lead to a greater understanding of the regulation of this pathway. Fleet et al. (2003) observed that overexpression of *AtCPS1* (codes for *ent*-copalyl diphosphate synthase which converts GGDP to CDP, the first committed step in GA biosynthesis) in Arabidopsis dramatically increased *ent*-kaurene synthesis, but had no effect on either the expression of late GA biosynthesis genes (*AtGA20ox1* and *AtGA3ox1*) or the levels of GA_9, GA_{34}, GA_{51} and bioactive GA_4. Similar results were observed when *AtKO1* (codes for *ent*-kaurene oxidase, which is responsible for the three step oxidation of *ent*-kaurene to *ent*-kauronic acid) was

overexpressed (Swain et al. 2005). *AtKO1*-overexpressor lines exhibited increased expression of *KO* mRNA, but there was no change in levels of endogenous bioactive GAs (GA_4 and GA_1). These results suggest that regulation of bioactive GA levels occurs after these steps, later in the GA biosynthesis pathway. Feedback regulation of transcript abundance by bioactive GA also appears to be specific to the later part of the GA biosynthesis pathway (Hedden and Phillips, 2000a). The expression of the early GA biosynthesis genes, *PsCPS1 (LS), PsKO1 (LH), PsKAO1 (NA)* and *PsKAO2*, in pea shoots remained similar between GA deficient mutants (*ls-1, lh-1, lh-2*, *na-1*) and the wild-type controls (Davidson et al., 2005). Consistently, the application of the GA biosynthesis inhibitor, paclobutrazol, to both wild-type and GA-deficient lines did not affect the expression of these genes (Davidson et al., 2005). Similarly, the application of GA_3 or the GA biosynthesis inhibitor, prohexadione (inhibits both 2-oxidation and 3-oxidation of GA_{20} and 2-oxidation of GA_1), modified the transcript levels of several late GA biosynthesis genes in the shoots and roots of young seedlings but the transcript levels of *PsCPS1* were unaffected (Ayele et al., 2006).

Overexpression of Arabidopsis GA 20-oxidase genes (*AtGA20ox1*, *AtGA20ox2* and *AtGA20ox3*; Coles et al., 1999 and *AtGA20ox1*; Huang et al., 1998; produce the immediate precursor to bioactive GA) in Arabidopsis resulted in longer hypocotyls, early flowering, increased stem elongation and reduced seed dormancy associated with an increase in GA_4, the main bioactive GA in this species (Huang et al., 1998; Coles et al., 1999). Arabidopsis plants expressing antisense *AtGA20ox1* had shorter hypocotyls and reduced stem elongation,

resulting in a semi-dwarf phenotype. The amount of GA_4 in the semi-dwarf plants was reduced to approximately one third of that of control plants (Coles et. al., 1999). Overexpression of *StGA20ox1* cDNA in potato resulted in taller plants that required a longer induction photoperiod to tuberize. Potato plants expressing anti-sense copies of *StGA20ox1* had shorter stems, decreased internode length, and tuberized earlier than control plants in a shorter induction photoperiod (Carrera et al., 2000). Biemelt et al. (2004) reported that stem growth, biomass production and rate of photosynthesis of transgenic tobacco were enhanced when *AtGA20ox1* was overexpressed and reduced when *AtGA2ox1* (encodes for the catabolic GA 2-oxidase) was overexpressed. Overexpression of citrus *GA20ox* (*CcGA20ox1*) in tobacco resulted in a shift to the non 13-hydroxylation pathway from the early-13-hydroxylation pathway, which tobacco normally follows, and GA_4 became the predominant bioactive GA (Vidal et al., 2001). In rice, overexpression of *OsGA20ox1* resulted in internode overgrowth that was approximately twice that of the wild-type (Oikawa et. al., 2004).

Overexpression of *AtGA20ox1* in hybrid aspen resulted in faster growth in stem height and diameter, larger leaves, more numerous and longer xylem fibers, and increased biomass (Eriksson et al., 2000). However, the *AtGA3ox1* overexpressor lines of aspen did not exhibit any major changes in morphology, even though they had increased GA 3β-hydroxylation activity (Israelsson et. al., 2004). The nearly unaltered growth pattern was associated with relatively small changes in GA_1 and GA_4 levels. The small increase in bioactive GA levels did not appear to be due to feedback or feed forward regulation of GA dioxygenase

transcripts, according to semi-quantitative reverse transcription polymerase chain reaction (RT-PCR) analysis of *PttGA20ox1, PttGA3ox1,* and two putative *PttGA2ox* genes. Therefore, it was concluded that GA 20-oxidation was the limiting step, rather than 3β-hydroxylation, in the formation of GA_1 and GA_4 in elongating shoots of hybrid aspen, and ectopic *GA3ox* expression alone could not increase the flux toward bioactive GAs.

Variation in the phenotypes has been reported when *GA3ox* has been overexpressed in Arabidopsis. Phillips (2004) reported that overexpression of Arabidopsis *GA3ox* did not produce any discernable effect on plant development in Arabidopsis. However, Radi et al. (2006) reported that overexpression of pumpkin *CmGA3ox1* in Arabidopsis resulted in seedlings with elevated hypocotyl and leaf growth and increased number of trichomes with increased levels of GA_4 compared to wild-type plants. Overexpression of pea *GA3ox* (*PsGA3ox1*) in tobacco also resulted in longer hypocotyls, taller plants and larger leaves, and was associated with a small but significant increase of bioactive GA_1 (Gallego-Giraldo et al., 2008). These researchers also observed a large increase in transcript abundance of the GA catabolism genes *NtGA2ox3* and *NtGA2ox5* (between 10- and 60-fold) in the *PsGA3ox1* overexpression lines of tobacco.

Pea (*Pisum sativum* L.) has been a valuable genetic model plant and was used by Gregor Mendel in his classical genetic studies over 100 years ago (Mendel, 1866; Sutcliffe, 1977). Pea is a self-pollinating diploid plant with a relatively short life cycle. It has been particularly useful in studying hormone biology because of the availability of mutants affected in GA biosynthesis and the

fact that its large-sized fruits and seeds and plentiful vegetative tissues have made the extraction and quantification of GAs more practical (Ayele, 2006; Marx, 1977). Moreover, it can be transformed using *Agrobacterium*-mediated transformation procedures (Schroeder et al., 1993; Krejci et al., 2007).

A number of GA biosynthesis gene mutations that result in a reduction in bioactive GA have been reported in pea (Reid et al., 2004). One such example is the *le-1* mutant allele of the GA 3β-hydroxylase gene (*PsGA3ox1; LE*), which leads to a dwarf phenotype. It has been shown that the *le-1* mutation dramatically reduces the conversion of GA_{20} to GA_1 in pea stems (Ingram et al., 1984) and *le-1* stems contain much less GA_1 than wild type stems (Potts et al., 1982; Ross et al., 1992). The application of GA_1 to the *le-1* mutant promoted stem elongation, resulting in plants that resemble the wild type. Also Ross et al. (2003) observed that pea lines containing the *le-1* mutation bear narrower (suture to suture) and more tapered pods than pea lines with the *LE* allele.

Only one GA biosynthesis gene mutation (*sln*) has been observed to increase bioactive GA_1 levels. The pea *sln* mutant is impaired in GA 2β-hydroxylation activity. (GA 2β-hydroxylase converts GA_1 to biologically inactive GA_8 and removes GA_{20}, the immediate precursor to GA_1 from the pathway by conversion to GA_{29}). As a result of this mutation, GA_{20} accumulates in the cotyledons of developing seeds and upon germination, GA_{20} moves into the seedling where it is converted to GA_1, promoting stem elongation growth. Increased internode elongation is mainly observed in the first six internodes of *sln* compared to the wild-type, consistent with the life-span of the cotyledons.

GA biosynthesis mutants with increased GA 3β-hydroxylase activity have not been reported in pea. In this study, transgenic pea lines that were transformed to overexpress *PsGA3ox1* were characterized to determine if GA 3β-hydroxylation is a rate limiting step in the GA biosynthetic pathway during vegetative growth of this species.

Materials and Methods

Plant material

Transgenic pea lines (*Pisum sativum* L. cv. Carneval) that were generated to overexpress *PsGA3ox1* (*LE*; a fully functional wild-type GA 3β-hydroxylase gene) by *Agrobacterium*-mediated transformation of *PsGA3ox1* fused to a CaMV-35S constitutive promoter (Figure 2.1) were used in this study (Reinecke and Ozga, unpublished). 'Carneval' is a semi-dwarf (*le-1*; single base-pair mutation in *PsGA3ox1*) and semi-leafless (*af*; *afila*, leaflets are replaced by tendrils of normal anatomy) field pea cultivar. It has white flowers and yellow cotyledons at maturity. In brief, the generation of the homozygous transgenic lines used in this study by the Ozga-Reinecke lab was as follows: The plants that were putatively transformed (grew on kanamycin containing culture medium) in culture were grafted to root stocks and grown out to produce T_1 generation seeds. T_1 plants were tested for the presence of the *NPTII* marker gene by PCR, and T_2 seeds from the NPTII-positive lines were selected for homozygosity using a kanamycin assay (Reinecke and Ozga, unpublished).

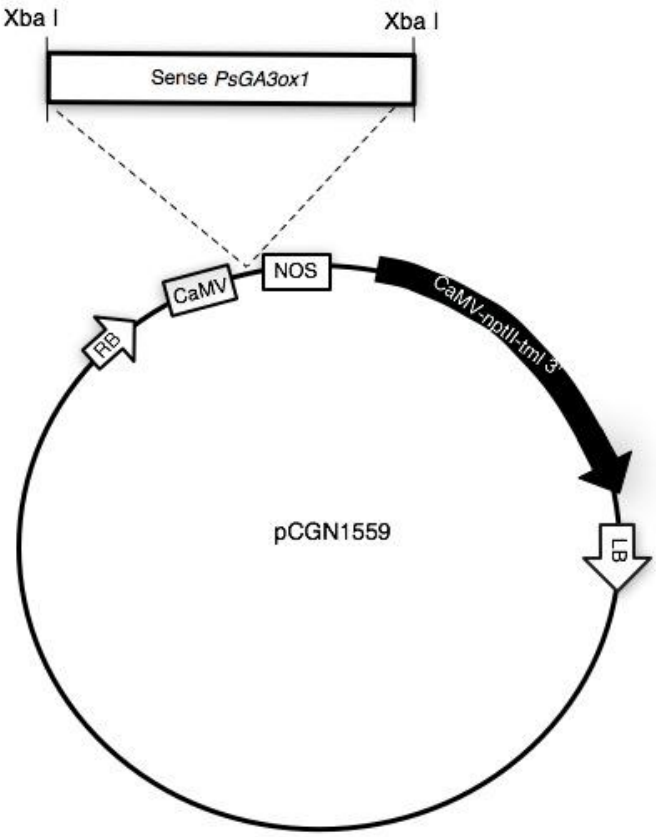

Figure 2.1: Schematic diagram of the *PsGA3ox1 (LE)* sense gene construct used for *Agrobacterium*-mediated transformation of *Pisum sativum* L. cv. Carneval. LB, left T-DNA border; RB, right T-DNA border; CaMV, CaMV 35S promoter; NOS, NOS terminator; nptII, neomycin phosphotransferase gene II; tml 3´, tumor morphology large gene.

Morphological, biochemical and molecular characterizations were performed on three independent homozygous transgenic lines (TG1, TG2 and TG3) that segregated at the T_2 generation consistent with carrying one copy of the transgenic *PsGA3ox1 (LE)* gene per haploid genome (assessed by screening the T_2 generation for the kanamycin selection gene, *nptII*) along with two transformation control lines (C1 and C3, where the transgene has segregated out)

and a wild-type line (C2; non-tissue-cultured). All transgenic and transgenic control null lines were from generations T_4 to T_6.

Growth conditions

Mature air-dried seeds were planted at a depth of approximately 2.5 cm into Sunshine Mix #4 (Mixture of peat moss, coarse grade perlite, gypsum, dolomitic lime and a wetting agent; Sungro Horticulture, Seba Beach, AB) potting medium in 1.5 L plastic pots (one seed per pot). Pots were arranged in a completely randomized design in a 2.5 × 1.4 m Conviron growth chamber and grown at 19°C/17°C (day/night) with a 16/8-h photoperiod under cool-white fluorescent lights (F54/I5/835/HO high fluorescent bulbs, Phillips, Holland; 366 μE m^2 s^{-2}). For the morphological characterization studies, the plants were watered every three days and fertilized at 22, 42 and 62 days after planting with a fertilizer mix of N:P:K (15:30:15). Lateral shoots were removed as they emerged to facilitate the maximum extension of the main stem. For the gene expression studies and GA analyses, seedlings were watered once every three days, but were not fertilized. For GA analyses, pots were arranged in a completely randomized design in a 7.5 × 3 m space in a growth chamber set at 19°C/17°C (day/night) with a 16/8-h photoperiod under cool-white fluorescent lights (F54/I5/835/HO high fluorescent bulbs, Phillips, Holland; 350 μE m^2 s^{-2}).

Morphological assessment

The total number of internodes at plant maturity (the first internode was defined as the one between the cotyledon attachment and the first stem node), the length of each internode at maturity from position 1 to 20, the number of nodes to

first flower, and the number of fruits aborted before the first fruit set were recorded. The area of the larger stipule of each pair at specific nodes was measured at maturity using a leaf area meter (LI-3100 Area Meter, LI-COR, Inc. Lincoln, Nebraska, USA). The petiole length of tendrils at selected nodes was measured at maturity from the point of attachment to the main stem to the first tendril branching point. The data presented are from one experiment consisting of eight to ten plants per line (biological replications). This experiment has been repeated twice over time with TG1 and C1 and two to four times at selected internodes and nodes with all lines. The morphological data were analyzed using the General Linear Model of SAS 9.1 statistical software (SAS Institute Inc., Cary, NC, USA) following a completely randomized design, and mean separation was by LSD at $P \leq 0.05$.

Tissue harvest for gene expression and GA analyses

Three different types of vegetative tissues (internode, tendril and stipule) were harvested for gene expression and GA analyses. Internodes from position 8 (between nodes 7 and 8) were harvested when at 5-7 mm in length (approximately 15%-20% of final length). Tendrils were harvested at 4 different maturity stages: 10-15% of final length (total tendril; stage 1), 35-40% of final length (stage 2), 75-80% of final length (stage3) and at maturity (stage 4). Stipules were also harvested at 4 different maturity stages: 15-20% of final size (stage 1), 35-40% of final size (stage 2), 75-80% of final size (stage 3) and at maturity (stage 4). All tendril and stipule tissues for stages 2, 3 and 4 were collected from node eight. In order to obtain enough tissue for RNA isolation from the smallest development

stage (stage 1), tendril and stipule tissues from nodes 7 and 8 were pooled. The gene expression data presented are results from one experiment consisting of three biological replicates per tissue and stage, where each replicate contained tissues from two individual plants. In addition, two to three independent gene expression experiments using internodes, tendrils, and stipules of selected stages were also run for comparison.

For GA analysis, internodes from position 8 (between nodes 7 and 8) were harvested when at 15-20 mm in length (approximately 45%-55% of final length); tendrils and stipules at node eight were also harvested when at 35-40% and 75-85% of final size. The data are from one experiment, where two biological replicates per tissue were collected (each replicate contained tissues from nearly two hundred plants). Tissues were immediately frozen in liquid nitrogen upon harvesting and were stored at -80^{o}C until RNA extraction or freeze-drying for endogenous GA analysis.

Light microscopy

Tissues for histological studies were harvested from pea seedlings of two transgenic lines (TG1 and TG2) and the control line C1 (transgenic null control line 1). Internodes from two different maturity classes were selected for sectioning, internodes from position 2 (between nodes 1 and 2) and 4 (between nodes 3 and 4) were harvested at maturity and internodes from position 8 (between nodes 7 and 8) were harvested at 50% of their full length. Internode sections (5 mm sections from the uppermost part of the internode) from each nodal position were harvested into a fixing solution containing 2.5% (v/v)

glutaraldehyde in 0.1M phosphate buffer at pH 7.5 and vacuum-aspirated overnight at room temperature, then placed at atmospheric pressure for 6 h to achieve sufficient penetration of the fixing reagent. Thereafter, the specimens were dehydrated in a graded ethanol series starting with 30% (v/v) ethanol in 0.1M phosphate buffer followed by increasing ethanol concentrations in 15% (v/v) increments to 100% (v/v). Samples were incubated for 20 min between each ethanol wash and the final wash at 100% (v/v) ethanol was performed twice. After dehydration, specimens were sequentially infiltrated with 2.5, 5, 10, 15, 25, 50 and 75% (v/v) n-butanol in ethanol and the infiltration was completed with two washes in 100% (v/v) n-butanol (2 h intervals). The tissues were then embedded in Paraplast Plus paraffin (Oxford Labware, St. Louis, MO) as described by O'Brien and McCully (1981), with the following minor modifications: The n-butanol incubation time was decreased to 1 d, the vials containing tissues were directly placed at 40^{o}C for 1 d followed by 59^{o}C for 1 day. Internode tissues were cut into cross-sections 7 µm thick with a rotary microtome (Spencer Lens Co., Buffalo, NY,USA) and stained with 1% (w/v) safranin O and 0.25% (w/v) fast green FCF according to the following procedure. Paraffin was removed from the tissues using two changes of toluene and tissues were hydrated to 70% (v/v) ethanol by passing through an ethanol gradient series starting with absolute ethanol. Rehydrated tissues were stained with 1% (w/v) safranin O for 1 hour. Slides were then rinsed with absolute ethanol and, if excessively stained, 90% (v/v) ethanol was used for further destaining. Afterwards, slides were dipped in 0.25% (w/v) fast green FCF for 30 seconds then washed with absolute ethanol

followed by 90% (v/v) ethanol. Sections were dehydrated in absolute ethanol for two changes and dipped in toluene for two more changes to remove any residual water. Coverslips were mounted on the sections with DPX mounting medium immediately after the toluene wash. Slides were kept in toluene until moments before mounting to avoid tissue drying. Coverslip-mounted slides were incubated overnight at 37^{o}C before being transferred to storage boxes.

The sections were viewed through a compound microscope (Primo Star, Carl Zeiss SM, Inc. Peabody, MA, USA) at 10×, 4× and 2.5× magnification and the images were captured with a digital camera (Photometrics Col Snap cf, Roper Scientific Photometrics, Tucson, AZ, USA). The cross-sectional area was estimated using the image capturing and analyzing software, MetaMorph, version 7 (Molecular Devices, Sunnyvale, CA, USA). The cross-sectional areas of the internode vasculature stele, cortex, and the xylem and phloem enriched areas of the vascular stele were determined at internode 2 (fully matured internode) using MetaMorph. The number of vascular bundles per internode cross-section was also determined at internode 8 at 50% final length. Sections from four to five biological replicates per internode position per line were assessed (each biological replicate consisted of one plant sampled at internode 2, 4 and 8 as described). Two technical replicates per section were averaged for each cross-sectional area value.

DNA extraction

Approximately 1 g of young stipule tissue from transgenic and transgenic control lines (T_2 generation; see appendix table A.1.1 for details on lines assessed)

was finely ground in liquid nitrogen and the DNA was isolated using the Cetyltrimethylammonium bromide (CTAB) method (Aldrich and Cullis, 1993). After initial extraction with the CTAB and centrifugation, the supernatant was partitioned with phenol/chloroform/isoamyl alcohol (25:24:1; v/v/v), followed by chloroform/isoamyl alcohol (24:1; v/v). The DNA was precipitated from the aqueous phase by adding 3M sodium acetate (pH 5.2):100% ethanol (1:25; v/v). The pelleted DNA was washed twice with 75% aqueous ethanol and resuspended in autoclaved double distilled water. Sample DNA concentration was determined in duplicate by A_{260} measurement using a NanoDrop ND-100 spectrophotometer (Nano Drop Technologies, Wilmington, DE, USA).

Confirmation of stable gene transformation into plant genome

Stable transformation was confirmed by monitoring for the presence of both the reporter gene *neomycin phosphotransferase II* (*NPTII*) and the transgenic *PsGA3ox1* gene in plant DNA samples using PCR. The *NPTII* gene was monitored by PCR amplification using the forward primer: 5'-GAA GCC GAT AGA AGG CGA TG-3', and the reverse primer: 5'-GAT GGA TTG CAC GCA GGT TC-3', which generate an amplicon of 776 bp (*NPTII-776*). The transgenic *PsGA3ox1* gene was amplified using the forward primer: 5'-CGA CAT AAG CGG GTT ACA GG-3', which anneals to the 3' end of the *PsGA3ox1* coding sequence, and the reverse primer: 5'-TCT AGA ACT AGT GGA TCC CC-3', which anneals to the small vector sequence upstream from the NOS terminator sequence, generating an amplicon of 447 bp (*TPsGA3ox1*-447; see appendix figure A.1.1). Thermocycler conditions used for *nptII* amplification were 94^{o}C

for 3 min for DNA polymerase activation, and 30 cycles of denaturation at 94^{o}C for 1 min followed by annealing at 55^{o}C for 1 min and extension at 72^{o}C for 1 min. Samples were then held at 72^{o}C for 10 min for extension completion. Similar thermocycler conditions were used for transgenic *PsGA3ox1* gene amplification except the annealing temperature of 51^{o}C was used.

RNA extraction

Plant tissues were finely ground in liquid nitrogen (see appendix tables A.1.2 and A.1.3 for details on tissues) and total RNA was isolated using a modified TRIzol (Invitrogen) protocol (Ayele et al., 2006). After initial extraction with the TRIzol reagent and centrifugation, a phase separation using chloroform (0.2 mL mL^{-1} TRIzol) was performed and organic phase discarded. RNA was precipitated from the aqueous phase by first using an isopropanol solution (0.25 mL mL^{-1} TRIzol) followed by a high salt solution (1M sodium citrate and 0.8M sodium chloride) to remove polysaccharides and proteoglycans. The RNA samples were further precipitated with 4M lithium chloride and finally with a mixture of 3M sodium acetate (pH 5.2): 100% ethanol (1:20, v/v). The precipitate was resuspended in DEPC-treated water. After extraction, the total RNA samples were treated with DNase (DNA-free kit, Ambion, Austin TX, USA) to remove any residual DNA. RNA integrity was verified by determination of 260 to 280 nm ratio by spectrophotometry and gel electrophoresis (viewing by two tight bands of 28S and 18S rRNA after ethedium bromide staining) of representative samples. Sample RNA concentration was determined in duplicate by A_{260} measurement using a NanoDrop ND-100 spectrophotometer (NanoDrop

Technologies, Wilmington, DE, USA). The samples were stored at -80^{o}C until quantitation by qRT-PCR.

Confirmation of transgene PsGA3ox1 mRNA

First strand cDNA synthesis from total RNA was performed using the SuperScript First-Strand Synthesis System for RT-PCR (Invitrogen). Total RNA (2 µg) was mixed with 1 µL of 10 mM dNTP and 1 µL of 0.5 µg/µL Oligo $(dT)_{12-18}$ and the mixture was brought up to 10 µL using DEPC-treated water. The sample was incubated at 65^{o}C for 5 min followed by incubation on ice for 4 min. A reaction mixture containing 2 µL of 10× reverse transcription buffer, 4 µL of 25 mM $MgCl_2$, 2 µL of 0.1 M DTT and 1 µL of RNaseOUT Recombinant RNase inhibitor was added to the sample and it was incubated for 2 min at 42^{o}C, followed by the addition of 1 µL (50 units) of SuperScript II reverse transcriptase and further incubation for 50 min at 42^{o}C. The reaction was terminated by placing samples at 70^{o}C for 15 min followed by immediate chilling on ice. The sample was finally treated with 1 µL of RNase H before proceeding to the amplification step.

The presence of transgenic *PsGA3ox1* mRNA transcript was confirmed using PCR and the resulting amplicon was sequenced to confirm specificity of the PCR product. Transgenic *PsGA3ox1* transcript was amplified using the forward primer: 5'-TCA ACG TGG GCG ACC TCT TTC ATA-3', which anneals to the coding sequence of *PsGA3ox1 (LE)*, and the reverse primer: 5'-TAA TCA TCG CAA GAC CGG CAA CAG-3', which anneals to the NOS terminator region of the transformation cassette generating an amplicon of 445 bp (*TPsGA3ox1*-445;

see appendix for details; Figure A.1.2). Thermocycler conditions used were 95^{o}C for 10 min for activation of HotStar Taq (Qiagen) and 35 cycles of denaturation at 94^{o}C for 1 min followed by annealing at 55^{o}C for 1 min and extension at 72^{o}C for 1 min. Finally, samples were held at 72^{o}C for 10 min for extension completion. The PCR product was separated on a 0.8% (w/v) agarose gel, purified from the gel using a Qiagen gel elution kit and directly sequenced using the Applied Biosystems 3.1 Dye terminator method at the Molecular Biology Facility, University of Alberta.

qRT-PCR gene expression analysis

Primers and probes

Primers and probe for the transgene *PsGA3ox1* quantifying amplicon (T*PsGA3ox1-130*) were designed using Primer Express software (version 3, Applied Biosystems, Foster City, CA, USA) to produce a transgene-specific quantifying amplicon based on the composite sequence of the *PsGA3ox1* vector construct (see appendix for details; Figure A.1.3): forward primer: 5'-AAC ATT TCA ACA AAG CAC TCT CAT CT-3'; reverse primer: 5'-GGG CTG CAG GAA TTC GAT ATC-3'; Probe: 5'-AGT GTC CAA GTG GGC TA-3'. The amplicon spans the 3' coding region of *PsGA3ox1 (LE)* through to a small remnant vector sequence situated prior to the NOS terminator sequence, thus providing specificity for the transgenic *PsGA3ox1* transcript. The qRT-PCR product produced by the T*PsGA3ox1-130* primers was separated on a 0.8% (w/v) agarose gel, purified from the gel using a Qiagen gel elution kit and directly

sequenced using the Applied Biosystems 3.1 Dye terminator method at the Molecular Biology Facility, University of Alberta.

The T*PsGA3ox1-130* primers produced a single product with the desired length (Figure A.1.4) and sequencing of the fragment further confirmed the specificity of the primers for transgenic *PsGA3ox1* mRNA (for details, see appendix; Figure. A.1.5). Primers and probes for the target gene quantifying amplicon *PsGA3ox1-87* [used for total *PsGA3ox1* (endogenous+ transgene) transcript quantitation] and for the reference gene amplicon, *18S-62* (used for pea 18S rRNA transcript quantitation) were designed as described by Ozga et al. (2003). Primers and probes for the target gene quantifying amplicon *GA2ox1-73* (used for *PsGA2ox1* quantification), *GA2ox2-83* (used for *PsGA2ox2* quantification), *PsGA20ox1-104* (used for *PsGA20ox1* quantification), and *GA20ox2-88* (used for *PsGA20ox2* quantification) were designed as described by Ayele et al. (2006). Primers and probes for the *PsGA3ox2* quantitation (*PsGA3ox2-104*) were designed as described by Ozga et al. (2009).

All probes were Taqman-based (Applied Biosystems). The probes for the GA genes were labeled at the 5' end with the fluorescent reporter dye, FAM, and at the 3' end with a minor-grove binding non-fluorescent quencher (MGB, Applied Biosystems). The *18S-62* reference gene probe was labeled at the 5' end with the VIC fluorescent reporter dye and at the 3' end with the TAMRA quencher (Applied Biosystems). The PCR efficiency for the qRT-PCR primers used to quantify the GA genes was calculated (see appendix; table A.1.4) using a dilution series of a single RNA sample over several log concentrations (from 500

ng/reaction to 0.05 ng/reaction). qRT-PCR was performed for those RNA samples as previously described and resulting average Ct values were plotted against log input RNA, and a linear regression was calculated. Provided the r^2 value was satisfactory, the slope of this equation was then used to calculate reaction efficiency (%) using the following formula;

$$\text{Efficiency} = (10^{[-1/\text{slope}]}-1)*100$$

qRT-PCR assay

Quantitative real-time RT-PCR assays were performed on a model 7700 sequence detector (Applied Biosystems) using a TaqMan One-Step RT-PCR Master Mix reagent kit (Applied Biosystems). For each 25 µL TaqMan reaction, 5 µL (200 ng) of total RNA for target genes or 10 pg for 18S rRNA was mixed with 12.5 µL of 2× Master Mix (containing AmpliTaq Gold DNA Polymerase), 0.6 µL of 40× Multiscribe (reverse transcriptase and RNase inhibitor mix), 1.5 µL of forward primer (5 µM; final concentration 300 nM), 1.5 µL of reverse primer (5 µM; final concentration 300 nM), 0.5 µL of probe (5 µM; final concentration 100 nM), and 3.4 µL of DEPC-treated water. Samples were subjected to thermal cycling conditions of reverse transcription at 48^{o}C for 30 min, DNA polymerase activation at 95^{o}C for 10 min, and 40 cycles of denaturation at 95^{o}C for 15 sec followed by anneal/ extension at 60^{o}C for 1 min. PCR amplification of each sample was carried out in duplicate in 96-well optical reaction plates covered with optical caps (Applied Biosystems) and the average of the two sub-samples (technical replicates) was used to calculate the sample transcript abundance. One common total RNA sample from each tissue was chosen as the plate

normalization sample and was run on each plate and used to correct for plate-to-plate amplification differences. The Ct value of the very first run of the common sample was arbitrarily used as the standard run for normalization.

*Normalized Ct value of sample = (Ct value of the common sample in the standard run / Ct value of the common sample in the sample run) * Ct value of sample*

The relative transcript abundance of the target genes in the individual plant sample was determined by $2^{-\Delta Ct}$ (Livak and Schmittgen, 2001) where ΔCt was the difference between the Ct of the target sample and the average Ct of the reference sample. Transcript levels of *PsGA20ox1*, *PsGA20ox2*, transgenic *PsGA3ox1*, total (transgenic + endogenous) *PsGA3ox1*, *PsGA2ox1*, and *PsGA2ox2* were standardized across genes, tissues and developmental stages using the lowest sample average Ct value (37.96; line: TG1, tissue: tendril stage 2, gene: *PsGA20ox2*). At least two, more often three biological replicate plant samples were assayed.

The pea 18S small subunit nuclear ribosomal RNA gene was used as a loading control to estimate variation in input total RNA concentration across all samples. The coefficient of variation (CV) of the 18S rRNA amplicon Ct value across all samples was 2.7% and, therefore, the target amplicon mRNA values were not normalized to the 18S signal (Livak and Schmittgen, 2001, Ozga et al., 2009).

Analysis of endogenous GA levels

Endogenous GA levels in the elongating internodes (approximately 50% of the final size), developing tendrils (approximately 40% and 80% of the final size) and developing stipules (approximately 40% and 80% of the final size) were

analyzed by Dr. Leonid Kurepin at the University of Calgary using a procedure adopted from Kurepin et al. (2007) and described below.

Stored tissues (at -80^{o}C) were freeze-dried in a FreeZone^{12} freeze-dryer (Labconco Corp., Kansas City, MO, USA) prior to analysis and 25 to 40 mg dry weight (DW) of each tissue sample was ground with liquid N_2, washed with sea sand (Fisher Scientific, New Jersey, USA), and extracted in 80% MeOH (H_2O:MeOH = 20:80, v/v). Following this, 20 ng of [$^2H_2$]GA_1, 33.33 ng of [$^2H_2$]GA_8, 40 ng of [$^2H_2$]GA_{20} and 20 ng of [$^2H_2$]GA_{29} (deuterated GAs were obtained from Prof. L.N. Mander, Research School of Chemistry, Australian National University, Canberra, Australia) were added to the aqueous MeOH extraction solvent as internal standards. The 80% MeOH extract was filtered through Whatman #2 filter paper (55 mm, Whatman International Ltd, Maidstone, England) and then purified with a C_{18} preparative column (C_{18}-PC) made of a syringe barrel (inside diameter 2 cm) filled with 3 g of C_{18} preparative reversed-phase material (Waters Ltd.; Koshioka et al., 1983). The 80% MeOH eluate from this column was dried *in vacuo* at 35°C. The dry sample was dissolved in 1 ml of 10% (v/v) MeOH with 1% (v/v) acetic acid and injected into the HPLC using the method described by Koshioka et al. (1983). The HPLC (Waters Ltd.) apparatus consisted of two pumps (model M-45), an automated gradient controller (model 680), and a Rheodyne injector (model 7125). The solvents were, pump A: 10% MeOH in 1% acetic acid [H_2O: MeOH: acetic acid=89:10:1, (v/v)], pump B: 100% MeOH. A reversed phase C_{18} Radial-PAK (μ-Bondapak) column (8 mm × 10 cm) was used with a manually implemented 10–73% gradient program at a

flow rate of 2 ml min^{-1} [i.e. 0–10 min (pump A, 100%; pump B, 0%), 10–50 min (pump A, 30%; pump B, 70%), 50–80 min (pump A, 0%; pump B, 100%), 80–90 min (pump A, 100%; pump B, 0%)]. The HPLC fractions (4 mL) were dried *in vacuo* at 35ºC. Fractions from the C_{18} HPLC were divided into two groupings with 100% MeOH and dried *in vacuo*. Each group was run separately on Nucleosil $N(CH_3)_2$ HPLC (nucleosil, 5 μm, 5/16" OD × 4.6 mm ID) which was isocratically eluted with 0.1% (v/v) HOAc in MeOH at 1.2 ml min^{-1} (Jacobsen et al. 2002). Three minute fractions from $N(CH_3)_2$ HPLC were dried *in vacuo*. Subsequently, fractions containing GAs were transferred with 100% (v/v) MeOH to 2 mL glass vials and dried *in vacuo*. The GA-containing 2 ml vials were methylated by ethereal CH_2N_2 for 20 min and the methylated samples were trimethylsilylated by N,O,-bis(trimethylsilyl)trifluoroacetamide (BSTFA) with 1% trimethylchlorosilane (TMCS) (Hedden, 1987; Gaskin and MacMillian, 1991).

The identification and quantification of plant hormones was carried out using a gas chromatograph connected to a mass spectrometer (GC-MS) using the -selected ion monitoring (SIM) mode. The derivatized samples were injected into a capillary column installed in an Agilent 6890 GC with a capillary direct interface to the Agilent 5973 mass selective detector (MSD). The dimensions of the capillary column were 0.25 μm film thickness, 0.25 mm internal diameter, 30 m DB-1701 (Model No.: J&W122-0732, J&W Scientific, Inc.). The GC temperature program was: 1 min at 60°C, followed by an increase to 240°C at 25°C min^{-1}, then an increase at 5°C min^{-1} to 280°C where it remained constant for 15 min before

returning to 60°C. The interface temperature was maintained at 280°C. The dwell time was 100 ms and data was processed using HP G1034C MS ChemStation Software. For identification of the endogenous GAs, comparison of GC-retention times (Rts) of the GAs as well as a comparison of the relative intensities of the molecular ion (M^+) pairs with standards was completed. The relative intensities of at least two other characteristic mass to charge (m/z) ion pairs for each endogenous GA and its deutero standard was also completed. Quantification was accomplished by reference to the stable isotope-labelled internal standard using equations for isotope dilution analysis, adapted by DW Pearce (see Jacobsen et al., 2002) from Gaskin and MacMillan (1991).

Results

Confirmation of stable gene transformation into plant genome and transgene expression

Stable integration of *PsGA3ox1* (driven by the constitutive CaMV-35S promoter) into the pea genome was confirmed by PCR analysis using genomic DNA from the T_2 generation of a number of independently transformed pea lines. Transgenic lines produced the expected amplicon size for *TPsGA3ox1*-447 (Figures A.1.1 and A.1.6). Based on preliminary morphological characterization, three independently transformed lines and two transgenic control lines (for which the transgene had segregated out) were selected for further characterization.

To determine whether the *PsGA3ox1* transgene was expressed in these selected lines, PCR was performed on cDNA (made from total RNA extracts) from various tissues of the transgenic and transgenic control lines. The transgenic

lines TG1, TG2, and TG3 produced a single band at the desired size of 445 bp (Figure 2.2) with the transgenic specific primers *TPsGA3ox1*-445 (Figure. A.1.2), confirming that transgenic *PsGA3ox1* was expressed in these lines. The 445 bp amplicon was not detected in the control lines C1 (Figure 2.2) and C3, and wild-type (data not shown). The 445 bp amplicon was subsequently sequenced and it was found to be specific to the transgenic *PsGA3ox1* sequence targeted (Figure A.1.7).

Effect of PsGA3ox1-overexpression on plant phenotype

The TG1 line produced significantly ($P<0.05$) longer internodes compared to C1 (transgenic null line) from internode 1 to 15 (Figure 2.3A), with the greatest increase in internode length occurring at internodes 2, 3, and 4 in the transgenic line compared to the control (average internode length was 22% greater in TG1 than the control). The TG2 line also produced significantly longer internodes than C1 at most internode positions from 1 to 15 (with the exception of internodes 4, 5 and 6; Figure 2.3A), and exhibited an average increase in internode length of 13% compared to the control (C1). The control transgenic null line (C1) and the wild-type line (C2) exhibited similar internode lengths from internode 1 to 20 (Figure 2.3C). The TG3 line produced significantly longer internodes than its corresponding transgenic null line (C3) at a number of nodal positions (1, 2, 4, 5, 7, 8, 9, 10, 11, and 14; Figure 2.3B), and the average internode length was 8% greater in TG3 than the control.

Tendril petiole length and stipule area were measured at selected nodal positions. The transgenic line TG1 produced significantly longer tendril petioles

than the control (C1) at nodes 8, 16 and 25 (Figure 2.4A). The TG2 line produced significantly longer tendrils than C1 at nodes 8 and 10 (Figure 2.4A). The TG3 line had significantly longer petioles than its transgenic null control (C3) at nodes 6, 8, 10, 16, and 18 (Figure 2.4B).

The transgenic lines TG1 and TG3 also produced significantly larger stipules than the controls at nodes 6 and 8 (Figure 2.5A and B) while TG2 produced larger stipules than the control at node 8 (Figure. 2.5A). Stipule area in the transgenic lines (TG1, TG2 and TG3) was not significantly different from that in the controls at nodal positions 16, 18, and 20 (data not shown).

The transgenic lines TG1 and TG3 produced significantly ($P<0.05$) more internodes per plant compared to their respective controls (C1 and C3, respectively; Table 2.1). Transition from the vegetative to the reproductive phase also occurred later in TG1 and TG3 lines compared to their controls (Table 2.1). The transgenic line TG1 exhibited significantly more fruit abortion prior to first fruit set compared to the control (Table 2.1).

Effect of PsGA3ox1-overexpression on internode anatomy

The effects of *PsGA3ox1*-overexpression on internode anatomy were investigated in two transgenic lines (TG1 and TG2) and a control (C1) line. Transverse cross-sections of internode 8 at 50% maturity revealed that the transgenic lines had significantly more vascular bundles compared to the transgenic control line at this developmental stage and nodal position (Table 2.3 and Figure. 2.6). No difference in the cross-sectional area of internode 8 at maturity was observed between the transgenic line TG1 and the control (Table

2.3). However, at internode 2, both TG1 and TG2 lines had reduced internode cross-sectional area compared to the control line at maturity (24% and 9% reduction, respectively; Table 2.2 and Figure 2.7A). The cross-sectional areas of the cortex and the vascular stele in internode 2 at maturity were approximately equal in the transgenic and control lines (Table 2.2). However, the phloem-enriched area of the vascular stele in internode 2 was significantly reduced in the transgenic lines compared to the control (Table 2.2; Figure 2.7B). Additionally, although the cross sectional areas of the xylem-enriched region of the vascular stele varied in the transgenic and control lines, both TG1 and TG2 contained larger xylem vessel elements (in cross-section) than the control (Table 2.2; Figure 2.7B). Minimal differences were observed between transgenic and control lines when cross-sections of internode 4 (at maturity) were examined (Figure 2.8).

Expression analysis of GA biosynthesis and catabolism genes

Expression of transgenic and total (transgenic + endogenous) *PsGA3ox1* was determined in internodes, tendrils and stipules in the transgenic lines, TG1, TG2, and TG3 and controls. In addition, the expression patterns of the late GA biosynthesis and catabolism genes (*PsGA20ox1, PsGA20ox2, PsGA3ox1, PsGA3ox2, PsGA2ox1, and PsGA2ox2*) were monitored to determine if *PsGA3ox1*-overexpression altered their expression patterns during vegetative development.

Internodes

The greatest abundance of transgenic *PsGA3ox1* mRNA was observed in the internodes of the TG1 line (more than 5-fold greater than TG2), followed by the TG2 line, then the TG3 line (Figure 2.9C). No transgenic *PsGA3ox1*

transcripts were detected in the control lines (data not shown). Total *PsGA3ox1* (transgenic + endogenous) transcript levels in the internode were higher in the transgenic lines TG1 (more than 4-fold higher) and TG2 (1.2-fold higher) than in the control (C1; Figure 2.9D). Total *PsGA3ox1* transcript abundance was also greater in the transgenic TG3 line compared to its transgenic null line (C3; Figure 2.9D). The endogenous *PsGA3ox1* gene contains the *le-1* mutation and the GA 3-oxidase coded by *le-1* is substantially less efficient (Lester et al., 1997; Martin et al., 1997) than that coded by the transgene (wild-type *PsGA3ox1*). *PsGA3ox2* transcripts were not detected in transgenic or control lines in the 8th internode (data not shown). In a separate experiment, *PsGA3ox2* transcripts were detected in internodes 1 to 4 when monitored at 15-20% full length, but were not detected in internodes 5 to 7 in either transgenics (TG1, TG2 and TG3) and controls (C1 and C3; Chapter 3; Figures 3.6D, E, F).

Transcript levels of the GA biosynthesis gene, *PsGA20ox1* (codes for the enzyme that converts GA_{53} to GA_{20}) were moderately increased by the presence of the *PsGA3ox1* transgene (Figure 2.9A). There was no consistent effect of *PsGA3ox1*-overepression on *PsGA20ox2* transcript levels (Figure. 2.9B). Transcript abundance of the GA catabolic gene mainly responsible for conversion of GA_{20} to GA_{29}, *PsGA2ox1,* was elevated in the elongating internodes of all three transgenic lines (TG1, TG2, and TG3) compared to the controls (Figure 2.9E). Transcript levels of the GA catabolic gene *PsGA2ox2,* which is mainly involved in the conversion of bioactive GA_1 to inactive GA_8, were markedly higher in

transgenic lines TG2 and TG3, but not in the TG1 when compared to their controls (Figure 2.9F).

Tendrils

PsGA3ox1-overexpression increased tendril petiole length in all three transgenic lines (Figure. 2.4); therefore, the temporal expression patterns of the transgenic and total *PsGA3ox1* genes and other GA metabolism genes were monitored in the tendrils during growth and development in these lines. In the controls, endogenous *PsGA3ox1* transcript abundance was highest in tendrils at 10 to 15% of final length (stage 1), and decreased with increasing maturity (Figures 2.10 H, I, and J). Similarly, tendril *PsGA3ox1* transgene transcript abundance was higher during the early- to mid-elongation stage, and declined as the tendrils reached maturity, with the highest level of transgenic *PsGA3ox1* mRNA observed in the transgenic TG1 line throughout tendril development, followed by the TG2 line, then the TG3 line (Figure 2.10G). No transgenic *PsGA3ox1* transcript was detected in the control lines (data not shown). Tendrils from the TG1 line had higher total *PsGA3ox1* transcript abundance throughout development compared to the control (Figure 2.10 H). Tendrils from the TG2 line contained approximately double the total *PsGA3ox1* transcript abundance at stage 1 than the control, with minimal differences in the later developmental stages (Figure 2.10I). Minimal differences in total *PsGA3ox1* transcript levels were observed between TG3 and its control (Figure 2.10J). No *PsGA3ox2* transcripts were detected in stage 1 tendrils of either the transgenic or control lines (data not shown).

Transcript levels of the GA biosynthesis gene, *PsGA20ox1* (codes for the enzyme that converts GA_{53} to GA_{20}) declined from stage 2 (35-40% final length) to stage 4 (mature length) in the controls (Figures 2.10 A, B and C). The presence of the *PsGA3ox1* transgene elevated *PsGA20ox1* transcript levels at stage 3 (75-80% full length) in all transgenic lines compared to the controls (Figures 2.10 A, B, and C). Endogenous (control) *PsGA20ox2* levels remained very low in tendrils from 10 to 40% full length (stages 1 and 2), then increased as the tendrils matured (stages 3 and 4; Figures 2.10 D, E, and F). In transgenic lines TG1 and TG2, this trend was amplified (Figures 2.10 D and E).

Transcript abundance of the GA catabolic gene, *PsGA2ox1,* increased with maturity in the tendrils of the controls (Figures 2.10 K, L, and M). In the transgenic lines TG2 and TG3, *PsGA2ox1* mRNA levels were elevated above the controls at stages 2 to 4, peaking at stage 3 (Figures 2.10L and M). Similar to the expression pattern of the catabolic gene *PsGA2ox2* in the TG1 internodes, *PsGA2ox1* mRNA levels in TG1 did not increase in the tendrils during development compared to the control (Figure 2.10K). Transcript abundance of the GA catabolic gene, *PsGA2ox2*, also increased with maturity in the tendrils of the controls (Figure 2.10N, O, and P). All three transgenic lines (TG1, TG2, and TG3) exhibited higher *PsGA2ox2* transcript abundance at some point during tendril growth compared to the controls.

Stipules

Since the transgenic lines also produced larger stipules at earlier nodal positions (nodes 6 and 8; Figure 2.5), the temporal expression patterns of

transgenic and total *PsGA3ox1* and other GA metabolism genes were monitored during stipule development in the transgenic and control lines. Endogenous *PsGA3ox1* transcript levels in the control lines were low when the stipules were at 15 to 20% full length (stage 1) and they increased and remained elevated from 35 to 80% stipule expansion (stage 2 and 3), followed by a decrease to low levels at maturity (stage 4; Figures 2.10H, I, and J). The abundance of transgenic *PsGA3ox1* transcript in the stipules was highest in the TG1 line throughout development, followed by TG2, and then TG3 (Figure 2.11G). No transgenic *PsGA3ox1* transcript was detected in the stipules of the control lines (data not shown). The total stipule *PsGA3ox1* transcript abundance was higher in all three transgenic lines when stipules were at 35 to 80% full expansion (stages 2 and 3), with the TG1 transgenic line having elevated total *PsGA3ox1* levels throughout development (stages 1 to 4; Figure 2.11H). No *PsGA3ox2* transcripts were detected in stage 1 stipules of either transgenic or control lines (data not shown).

Transcript levels of the GA biosynthesis gene, *PsGA20ox1* (codes for the enzyme that converts GA_{53} to GA_{20}) were high during early stipule expansion and decreased as the stipules matured in both transgenic and control lines (Figures 2.11A, B, and C). The control line had higher *PsGA20ox1* transcript levels than the TG1 at the earlier expansion stages (1 and 2; Figure 2.11A). *PsGA20ox1* transcript levels in transgenic lines TG2 and TG3 were minimally affected by the presence of the *PsGA3ox1* transgene (Figures 2.11B and C). Stipule *PsGA20ox2* transcript levels were higher at 15-20% expansion (stage 1), then decreased to minimal levels by 35-40% expansion (stage 2) and remained at these low levels

until maturity (stage 4) in the control lines. Stipule *PsGA20ox2* transcript abundance was not affected by the presence of the *PsGA3ox1* transgene during development (Figures 2.11D, E, and F).

The presence of the *PsGA3ox1* transgene slightly elevated expression of the GA catabolic gene, *PsGA2ox1*, in the TG2 and TG3 lines compared to the controls at mid to late development, but minimal to no increase was observed in the TG1 line (Figures 2.11K, L, and M). Transcript levels of the catabolic gene, *PsGA2ox2*, increased dramatically during the last phase of development in both the transgenic and controls lines (Figures 2.11N, O, and P). *PsGA2ox2* transcript abundance in stipules during development was minimally affected by the presence of the *PsGA3ox1* transgene.

Endogenous GAs

In order to examine the effect of *PsGA3ox1*-overexpression on tissue steady-state GA levels, endogenous GA_{20} (precursor to bioactive GA_1), GA_{29} (the 2β-hydroxylated catabolite of GA_{20}), bioactive GA_1, and GA_8 (the 2β-hydroxylated inactive catabolite of GA_1) were determined in the internodes (at 50% full length, position 8), tendrils (at 40% and 80% full length from 8th node) and stipules (at 40% and 80% full size from the 8th node) of transgenic TG1 and TG2 lines and a transgenic null control line (C1).

Elongating internodes of the transgenic TG1 line contained higher steady-state GA_1 and GA_8 levels compared to the control line indicating increased flux through to bioactive GA_1 in this *PsGA3ox1*-overexpresser line (Figures 2.12B and C). No changes in internode steady-state GA_1 or GA_8 levels were observed

between TG2 and the control line (Figures 2.12B and C). Steady-state GA_{20} levels were not affected by *PsGA3ox1*-overexpression in the internodes of these transgenic lines (Figure 2.12A). However, higher GA_{29} levels were observed in elongating internodes of transgenics TG1 and TG2 compared to the control (Figure 2.12D).

Elongating tendrils in transgenic lines TG1 and TG2 (at 40% full length) had elevated GA_1 levels compared to the control suggesting that the tendrils from these *PsGA3ox1*-overexpressor lines had increased flux to bioactive GA_1 (Figure 2.13 B). Similar to that in elongating internodes, elongating tendril GA_{20} levels were minimally affected by the presence of the *PsGA3ox1* transgene (Figure 2.13 A). TG1 tendrils had slightly lower levels of GA_{29} than that observed in either TG2 or the control lines at 40% full length; however, as the tendrils matured, both transgenic lines had higher levels of GA_{29} than the control line (Figure 2.13D). As the tendrils matured from 40 to 80% full length, the levels of GA_{20}, GA_1, GA_8 and GA_{29} decreased (Figures 2.13A, B, C and D)

Expanding stipules in the transgenic TG1 line contained lower GA_{20}, similar GA_1, and higher GA_8 levels (at 40% full size) than the control, suggesting increased flux through to bioactive GA_1 in the transgenic stipules of this line (Figures 2.14A, B, and C). Only higher steady-state GA_8 levels were observed in the expanding stipules of TG2 compared to the control (Figures 2.14A, B, C and D). However, the expanding stipules of both transgenic lines TG1 and TG2 contained less of the GA_{20} catabolite, GA_{29}, than the control (Figure 2.14D). Similar to that of developing tendrils, GA_{20}, GA_1, GA_8 and GA_{29} levels markedly

decreased as stipules matured from 40 to 80% full size (Figures 2.14A, B, C and D).

Pericarp length at maturity (in fruit containing the same number of seeds per pericarp) was greater in the *PsGA3ox1*-overexpressor line TG1 than the control line (Table 2.4).

Discussion

GA 3β-hydroxylation is the critical step for bioactive GA production in plants, as this step converts biologically inactive GAs to the biologically active form. Overexpression of genes in the GA biosynthesis pathway has been a useful research tool to investigate the effects of a specific GA on the flux through the GA biosynthesis pathway, on GA homeostasis, and on plant morphology (Phillips, 2004). Overexpression of *GA3ox* genes has led to different phenotypes in different species (Phillips, 2004; Radi et. al, 2006; Israelsson et. al., 2004; Gallego-Giraldo et al., 2008) suggesting that GA 3-oxidation is regulated in a species-dependent manner. To investigate the role of GA 3-oxidation in modulating GA biosynthesis, determine if GA 3-oxidation is a rate limiting step in the GA biosynthetic pathway, and determine the effects of overexpression on phenotype in pea, I characterized pea lines generated to overexpress *PsGA3ox1*.

Internodes

A range in expression of the transgenic *PsGA3ox1* gene was observed in the elongating internodes of the three independently transformed *PsGA3ox1*-overexpression lines characterized. The TG1 line produced the highest levels of transgenic *PsGA3ox1* transcript in the elongating internode 8, followed by the

TG2 line and then the TG3 line (Figure 2.9C). Total *PsGA3ox1* (transgenic + endogenous) transcript levels were more than 5-fold higher in TG1 than the control (C1; Figure 2.9D). Transgenic expression of a wild-type *PsGA3ox1* gene in 'Carneval', which contains the *le-1* form of *PsGA3ox1* that codes for a GA 3-oxidase that is substantially less efficient than the wild-type enzyme, has resulted in an increase in steady-state levels of bioactive GA_1 and its immediate catabolic product GA_8 (Figure 2.12B and C) in the TG1. These data suggest that overexpression of *PsGA3ox1* in pea can increase the flux through the GA biosynthesis pathway to bioactive GA_1 in elongating internodes. Consistent with this elevated flux through the GA pathway in the stem, we observed longer internodes (about 22% longer in the TG1 than the control (C1; Figure 2.3A), increased apical meristem half-life (TG1 line had approximately 10 more nodes per plant; Table 2.1), and delayed apical meristem transition from the vegetative phase to the reproductive phase (the node to first flower was node 30 in TG1 compared to node 25 in the control; Table 2.1).

Transgenic lines TG2 and TG3 also contained transgenic *PsGA3ox1* transcript in elongating internodes, but the levels were much less that that observed in TG1 (Figure 2.9C). Likely due to lower transgenic *PsGA3ox1* levels in the internodes of TG2, an increase in steady-state GA_1 and GA_8 levels was not detected in this line (Figures 2.12B and C). However, significantly longer internodes were observed in TG2 compared to the control (Figure 2.3A), indicating that an increased flux through the GA pathway may have also occurred in the internodes of this line (and in the TG3 line). These phenotypic changes in

the pea *PsGA3ox1*-overexpressing transgenic lines are, in general, consistent with phenotypes observed in other species that contain higher than normal GA levels via transgenic expression of GA biosynthesis genes or phenotypes observed after the exogenous application of bioactive GAs in pea. Overexpression of heterologous *GA3ox* genes in Arabidopsis (*CmGA3ox1*; Radi et al., 2006) and in tobacco (*PsGA3ox1*; Gallego-Giraldo et al., 2008) resulted in longer internodes and shoots. However, overexpression of *AtGA3ox1* in hybrid aspen did not result in dramatic changes in internode length or the number of internodes formed (Israelsson et. al., 2004). Consistent with our results in the transgenic TG1 line, Spiker et al. (1976) observed an increase in the number of nodes per plant when pea plants (at the three expanded leaves stage) were treated with gibberellic acid (50 nmol/plant) once or on a weekly basis (similar results were obtained in an exogenous GA experiments using 'Carneval'; Chapter 3, Table 3.1). The increase in shoot apical meristem longevity caused by increased levels of bioactive GA appears to be due to increased mitotic activity in the shoot apex. Likewise, exogenous GA_3 increased the mitotic activity in the shoot apex of *Silene* and *Perilla* (for review, Pharis and King, 1985; Besnard-Wibaut et al., 1983).

Furthermore, it has been observed that high concentrations of bioactive GAs can stimulate vegetative growth (Dennis, 1973) and lengthen the morphological age to flowering in some species (*Fushsia*, *Hieracium* and *Fragaria*; for review, Pharis and King, 1985). These GA-induced phenotypic changes are similar to those observed in the transgenic TG1 line.

The mature internodes at position 2 were smaller (9-24% less) in cross-sectional area in the *PsGA3ox1*-overexpressor lines TG1 and TG2 than in the control line (Table 2.2 and Figure 2.7). This observation is consistent with that of Fagoaga et al (2007), who observed a decrease in stem diameter when the GA biosynthesis gene coding for GA 20-oxidase (*CcGA20ox1*) was overexpressed in citrus. However, later in morphological development (internode 8), the internode cross-sectional area of transgenic line TG1 was similar to that of the control (Table 2.3). These data suggest that the lower internodes of TG1 have higher bioactive GA levels and/or they are more sensitive to bioactive GA levels than the later internodes of pea. Interestingly, the ratio of cortex to vascular stele tissue was similar in the transgenic and control internodes at position 2 (Table 2.2), indicating that the bioactive GA-induced decrease in stem cross-sectional area likely reflects reductions in both cortical and vascular stele regions. Within the vascular stele of internode 2, the phloem-enriched region was reduced in the transgenics, and although the cross-sectional area of the xylem-enriched region varied in the transgenics, larger xylem vessel elements were present in the *PsGA3ox1*-overexpressor lines compared to the control (Table 2.2). Biemelt et al. (2004) observed an increase in the number of xylem vessel elements when *AtGA20ox1* was overexpressed and a decrease when *AtGA2ox1* was overexpressed in tobacco. Consistently, tissue-specific localization of GAs and expression of GA-biosynthetic and signaling genes in wood forming tissues of aspen indicated that the last stages of GA biosynthesis occur in expanding xylem,

suggesting that GA plays a role in the expansion and/or elongation of xylem elements (Israelsson et al., 2005).

Pate (1975) noted that the architecture of the shoot vascular system of pea followed the model depicted by Devadas and Beck (1972) for *Trifolium*, where 12 vascular strands can occur in an internode (after vascular re-patterning is complete following early seedling growth; internode 4 and after) depending on its nodal position: 4 main shoot traces, 4 axillary shoot traces, 2 tendril petiole traces, and two stipule traces. Variation in the number of traces per internode will depend on the presence of the axillary shoot traces. More vascular bundle traces were observed in the internodes of transgenic TG1 and TG2 at 50% maturity, likely indicating that their axillary shoot vascular strands were stimulated to develop in advance of those in the control.

The higher transcript abundance of the GA catabolic gene, *PsGA2ox1* (Figure 2.9D), concomitant with higher GA_{29} levels (Figure 2.12D) in elongating internodes of the transgenic lines compared to the controls is indicative of feedback regulation of GA biosynthesis due to increased levels of bioactive GA. Similarly, upregulation of GA catabolism genes (*NtGA2ox3* and *NtGA2ox5*) was observed in 7 d-old seedlings when *PsGA3ox1* was overexpressed in tobacco (Gallego-Giraldo et al., 2008). GA_{20} levels did not change in the transgenic lines (TG1 and TG2) compared to the controls. Both Gallego-Giraldo et al. (2008; in the apical portions of tobacco) and Israelsson et al. (2004; in internodes of hybrid aspen) reported that GA_{20} (in tobacco) and GA_{20} and GA_9 (in hybrid aspen) markedly decreased in *GA3ox*-overexpression lines, suggesting that transgenic

GA3ox expression quickly depleted the immediate bioactive GA substrate pool. The discrepancy between our results and those from tobacco and hybrid aspen might be explained by the elevated transcript levels of *PsGA20ox1* observed in the pea transgenic lines that could result in increased production of the GA_{20} and circumvent the depletion of this substrate pool for conversion to bioactive GA_1. Upregulation of *NtGA20ox1* was not observed in the *PsGA3ox1*-overexpression transgenic tobacco lines (Gallego-Giraldo et al., 2008). It is possible that overexpression of an endogenous *GA3ox* gene (as is the case in the pea transgenics) affects regulation of the GA biosynthesis pathway differently than overexpression of an ortholog from a different species (as was the case in the tobacco transgenics from the Gallego-Giraldo et al. 2008 study).

Tendrils

'Carneval' is semi-leafless (*af*; *afila*, leaflets are replaced by tendrils of normal anatomy) and, therefore, provides a simple tendril organ for developmental studies. The tendril transcript profile of the GA biosynthetic genes *PsGA20ox1* and *PsGA3ox1* decreased with organ maturity in all lines (Figures 2.10A, B, C, H, I and J). The higher *PsGA3ox1* transcript levels of TG1 and TG2 at the earlier developmental stages, concomitant with increased bioactive GA_1 in the rapidly elongating tendrils (40% of final size; stage 2; Figure 2.13B) suggest that *PsGA3ox1*-overexpression increased the flux through the GA biosynthesis pathway to bioactive GA_1. Consistently, tendril petiole length in the transgenic lines TG1 and TG2 was about 12-13% greater than that in the control (Figure 2.4). Similar to the internodes, a consistent increase in *PsGA20ox1* and

PsGA20ox2 was observed in stage 3 (80% full size) tendrils of the transgenic lines, following the increase in flux to bioactive GA_1 observed in stage 2 (40% full size) tendrils (Figure 2.10). Consistently, the levels of GA_{20} did not decline in the tendrils of the transgenic lines at either 40% or 80% expansion (Figure 2.13A).

The increase in the transcript abundance of the GA catabolic genes *PsGA2ox1* and *PsGA2ox2* concomitant with the decrease in transcript abundance of the GA biosynthesis genes *PsGA20ox1* and *PsGA3ox1* during tendril development (Controls; Figures 2.10 A, C, H, J, K, M, N, and P) is indicative of decreased flux through the GA pathway to bioactive GA_1, and decreased GA_{20} and GA_1 half-life in tendrils as they complete their development. Concomitantly, a decrease in the steady-state levels of GA_{20} and GA_1 occurred as the tendrils matured from 40 to 80% full size (in transgenic and control; Figures. 2.13A, B, C, and D). Ross et al. (2003) reported that mature pea shoot tissues (combined leaves and internode tissues) contained lower levels of GA_{20} and GA_1 compared to young apical bud tissues. Using data from [^{14}C]GA_{20} metabolism studies, they suggested that the low GA_{20} and GA_1 levels observed in mature shoot tissues was due to rapid 2-oxidation of these GAs. Our GA expression data along with endogenous GA levels in tendril tissues during development suggest that the lower levels of GA_{20} and GA_1 in mature tendrils (compared to immature tendrils) are likely the result of both a decrease in GA biosynthesis capacity as well as an increase in GA 2-oxidation.

The transgenic lines TG2 and TG3 had higher tendril *PsGA2ox1* levels from stage 2 to 4, and higher *PsGA2ox2* mRNA levels were detected in the tendrils of all three transgenic lines at some point during development compared to the controls (Figures 2.10K, L, M, N, O and P). Higher GA_{29} levels were observed in tendrils at 80% expansion in the transgenic lines compared to the controls (Figure 2.13D). Similar to the internodes, the tendril GA expression pattern and endogenous GA content data are indicative of feedback regulation due to elevated bioactive GA levels in the transgenics. *PsGA2ox1* transcript abundance was lower (more than 10-fold lower in tendrils than in internodes in the control line at similar growth stages) in the tendrils than that in the internodes (controls) suggesting that *PsGA2ox1* plays a larger role in maintaining GA homeostasis in the internodes than the tendrils.

Stipules

Developmental regulation of *PsGA3ox1* expression in the stipules differed from that in the tendrils. Total *PsGA3ox1* transcript levels were low at 15 to 20% full size (stage 1), peaked at 35 to 80% full size (stage 2 and 3), and then decreased as stipules reached full maturity (controls; Figures 2.11H, I and J). Markedly higher levels of bioactive GA_1 and its immediate catabolite, GA_8, were observed in rapidly expanding stipules (40% full size) compared to elongating internodes or tendrils at a similar growth stage (controls; Figures 2.12, 2.13 and 2.14). Bioactive GA_1 decreased more than 5-fold as the stipules matured from 40 to 80% full size (control; Figure 2.14 B).

Higher transgene-specific *PsGA3ox1* transcript levels were observed in TG1 compared to the other transgenic lines, and although minimal changes in bioactive GA_1 levels were observed in the stipules of both TG1 and TG2 compared to the control, increased levels of GA_8 (the immediate catabolite of GA_1) in the TG1 transgenic line suggest an increased flux through the GA biosynthesis pathway in the stipules of this line at 40% full size compared to the control (Figure 2.14C). Both TG1 and TG2 exhibited larger stipules (approximately 15%) at nodal position 8; therefore, it is likely that an increased flux through the GA biosynthesis pathway also occurred in the stipules at this node in TG2, but due to a smaller increase in bioactive GA in this transgenic line, increased flux was not reflected in the steady-state levels of GA_1 or GA_8. Additionally, stipules were only larger at the lower internodes in both TG1 and TG2 compared to the controls (Figure 2.5A), suggesting that the dynamics of GA biosynthesis in the stipules vary with nodal position on the plant. Increased leaf area was also observed when *PsGA3ox1* and *CmGA3ox1* were heterologously overexpressed in tobacco (Gallego-Giraldo et al., 2008) and Arabidopsis (Radi et al., 2006), respectively.

The expression of *PsGA20ox1* and *PsGA20ox2* was high early in stipule development, and then decreased with maturity (controls; Figures 2.11A, B and C). Overexpression of *PsGA3ox1* minimally affected the expression of these *PsGA20ox* genes in the stipules (Figures 2.11 A, B, C, D, E, and F), and TG1 stipules had lower levels of GA_{20} at 40% stipule expansion compared to the control. In this tissue, it appears that upregulation of *PsGA20ox* genes does not

occur in the *PsGA3ox1*-overexpressing lines, and a concomitant decrease in GA_{20} levels was observed (Figure 2.14A).

A substantial increase in transcript abundance of the catabolic gene, *PsGA2ox2*, occurred in the stipules from stage 3 (75-80% full size) to 4 (full size), suggesting that the enzyme encoded by *PsGA2ox2* is the major catabolic enzyme responsible for deactivating bioactive GA_1, as part of the developmental program to limit growth for stipule maturation. Overexpression of *PsGA3ox1* had minimal effects on *PsGA2ox* genes in the stipules (Figures 2.11K, L, M, N, O and P) in contrast to that observed in the internode and tendril tissues (Figures 2.9E and F, for internodes and Figures. 2.10K, L, M, N, O, and P for tendrils). The difference in catabolic *PsGA2ox* gene expression between these organs in response to *PsGA3ox1*-overexpression is likely due to the different developmental paradigm in the stipules compared to that in the internodes and tendrils.

Reproductive morphology

Previous work has documented that higher concentrations of GA_3 can inhibit embryogenesis in excised embryos of *Phaseolus coccineus* (Yeung and Sussex, 1979; Pharis and King, 1985) and, therefore, it is possible that higher than optimum levels of bioactive GA in the fertilized ovules of TG1 might have acted to inhibit embryogenesis. Since the presence of viable seeds is required for pericarp (fruit) growth in pea (Ozga et al., 1992), embryo abortion due to super-optimal levels of bioactive GA in the ovule tissues could have led to more fruit abortion in the TG1 line compared to the control line (Table 2.1). Longer pericarps were observed in the *PsGA3ox1*-overexpressor line TG1 than in the

control line when pericarps containing a similar number of seeds were compared (Table 2.4). Rodrigo et al., (1997) reported a linear relationship between GA concentration and pericarp growth from 0.1 to 2 ng g^{-1} fresh weight. Consistently, *PsGA3ox1*-overpression increased pericarp length in the highest *PsGA3ox1*-expressor line TG1.

In summary, *le* pea lines generated to overexpress *PsGA3ox1* exhibited modified plant stature and internode anatomy. The presence of transgenic *PsGA3ox1* transcript was associated with increased steady state GA_1 and GA_8 levels indicative of increased flux through the GA biosynthesis pathway in the transgenic lines. The highest *PsGA3ox1*-overexpressor line had characteristics of bioactive GA overproduction including longer internodes and tendrils, larger stipules in lower nodes, more nodes per plant, smaller stem diameter in the lower internodes, delayed flowering, more fruit abortion before fruit set and increased fruit size. Increased levels of GA catabolic genes *PsGA2ox1* (in internodes) and *PsGA2ox2* (in tendrils) in elongating internodes and tendrils of the transgenic lines compared to the controls is indicative of feedback regulation of GA biosynthesis due to the increased levels of bioactive GA. The overall expression profile of the GA biosynthesis and catabolism genes studied during stipule development was different from that in the tendrils and internodes suggesting that the vegetative development of stipules has unique GA requirements.

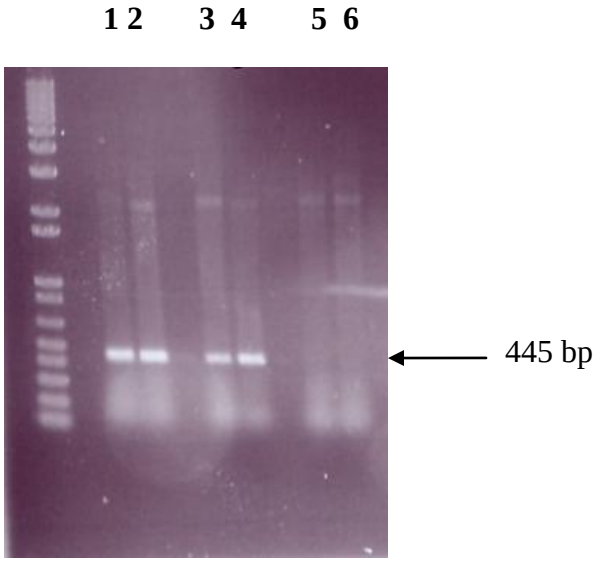

Figure 2.2. Confirmation of the presence of transgenic *PsGA3ox1* transcript in transformed pea lines by RT-PCR. Total RNA isolated from TG1 internodes (1), TG2 tendrils (2), TG2 pods (3), TG3 internodes (4), C1 internodes (5), and C1 pods (6) was reverse-transcribed to cDNA and the presence of transgenic *PsGA3ox1* transcripts was determined using PCR with transgene specific primers designed to obtain the amplicon *TPsGA3ox1*-445. Transgenic lines produced an amplicon of expected size (445 bp), whereas no bands were detected in the control line.

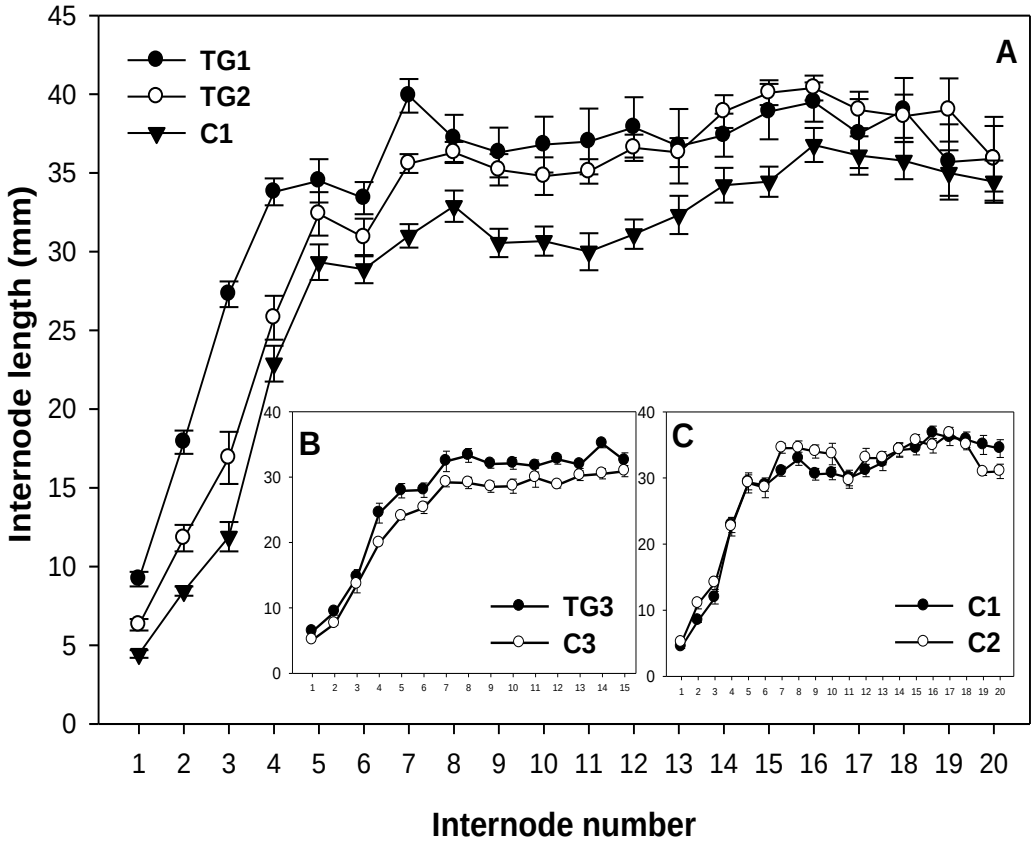

Figure 2.3. Internode lengths at maturity of transgenic and control lines from internode 1 to 20 (A, TG1, TG2, and C1) or internode 1 to 15 (B, TG3 and C3) or internode 1 to 20 (C, C1 and C2). Data are means ± SE, n= 8 to 10.

TG1= Transgenic line 1; TG2= Transgenic line 2; C1= Control transgenic null line 1; C2= Wild-type line; TG3= Transgenic line 3; C3= Control transgenic null line 3 grown with TG3.

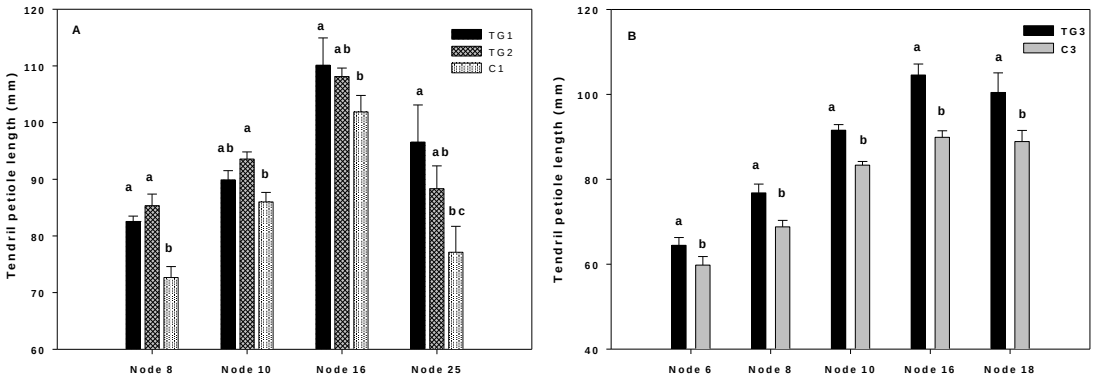

Figure 2.4. Tendril petiole lengths at maturity of transgenic and control lines at different nodal positions. Petiole length was measured from the point of attachment to the stem to the first tendril branchlet. Data are means ± SE, n= 8 to 10. Letters indicate significant differences among tendril lengths within nodal position by LSD at $P<0.05$. [A, TG1 (transgenic line 1), TG2 (transgenic line 2) and C1 (control transgenic null line 1); B, TG3 (transgenic line 3) and C3 (control transgenic null line 3 grown with TG3)].

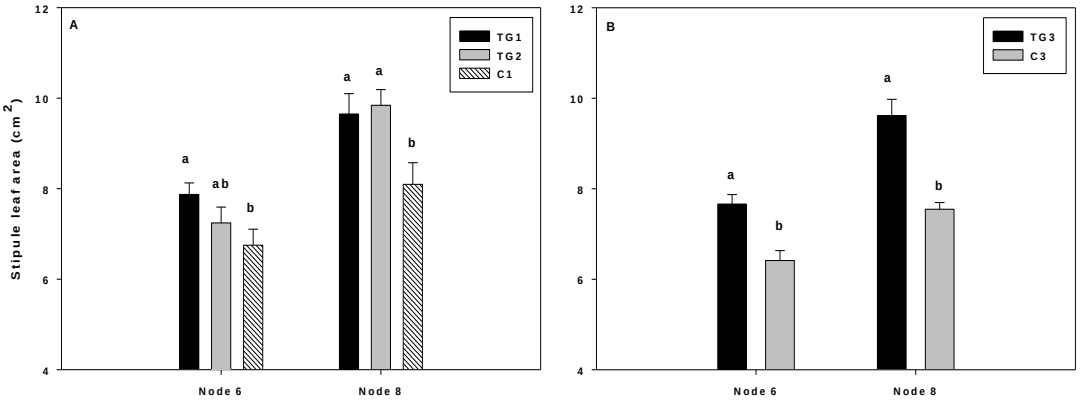

Figure 2.5. Stipule area at maturity of transgenic and control lines at different nodal positions. Data are means ± SE, n= 8 to 10. Letters indicate significant differences among stipule area within nodal position by LSD at P<0.05. [A, TG1 (transgenic line 1), TG2 (transgenic line 2) and C1 (control transgenic null line 1); B, TG3 (transgenic line 3) and C3 (control transgenic null line 3 grown with TG3)].

Table 2.1. Number of internodes per plant, nodes to first flower, and number of fruits aborted before first fruit set in transgenic and control lines.

Line	Total number of internodes	Nodes to first flower	Number of fruits aborted before first fruit set
TG1	46.4±1.3[x]a[y]	30.1±0.06a	5.9±1.00a
TG2	38.2±1.0b	25.5±0.03b	3.2±0.06b
C1	36.6±0.6bc	25.7±0.03b	1.3±0.05bc
TG3	38.5±0.3a	25.6±0.04a	1.1±0.09a
C3	35.2±0.5b	24.3±0.04b	0.5±0.40a

[x] Data are means ± SE, n= 8 to 10.

[y] Means followed by different letters (a, b, c) indicate significant difference among TG1, TG2 and C1, or TG3 and C3 lines by LSD, $P<0.05$.

Table 2.2. Cross-sectional areas of the internode, cortex, vascular stele, xylem-enriched region, phloem-enriched region, and xylem vessels of transgenic (TG1, TG2) and control (C1) lines of internode 2 at maturity. The ratios of cortex to vascular area and xylem- to phloem-enriched regions are also presented.

Line	Cross-sectional area ($\times 10^3$µm)	Cortex area ($\times 10^3$µm)	Vascular stele area ($\times 10^3$µm)	Ratio of cortex to vascular stele	Xylem-enriched area ($\times 10^3$µm)	Phloem-enriched area ($\times 10^3$µm)	Ratio of xylem to phloem enriched area	Xylem vessel area (µm)[b]
TG1	422.2 ± 57.6[a]	230.6±39.1	191.8±6.1	1.19±0.18	118.2±7.4	67.5±2.4	1.8 ± 0.13	517.0±16.5
TG2	511.24 ± 15.4	260.4±5.2	250.8±11.3	1.04±0.04	175.7±10.0	69.7±4.6	2.5 ± 0.12	595.9±18.1
C1	562.26 ± 21.2	301.3±19.7	260.9±7.6	1.16±0.08	150.5±4.2	101.9±5.7	1.48 ± 0.09	431.3±26.8

[a] Data are means ± SE of four to five biological replicates. Each replicate value is the average of values obtained from two subsample cross-sections.

[b] Average of the 20 largest xylem vessel elements per cross-section.

Table 2.3. Number of vascular bundles and stem cross-sectional area at 50% full length and at maturity in transverse sections of internode 8 of transgenic (TG1 and TG2) and control (C1) lines.

Line	Number of vascular bundles[a]	Cross-sectional area at 50% full length ($\times 10^3$ µm)	Cross-sectional area at full length ($\times 10^3$ µm)
TG1	11.2 ± 0.49	385.3±6.5	1006.4±61.1
TG2	10.25 ± 0.22	258.7±19.4	n.d.[b]
C1	8 ± 0.0	248.6±6.9	935.2±39.1

[a] Data are means ± SE of four to five biological replicates. Each replicate value is the average of values obtained from two subsample cross-sections.

[b] n.d= not determined

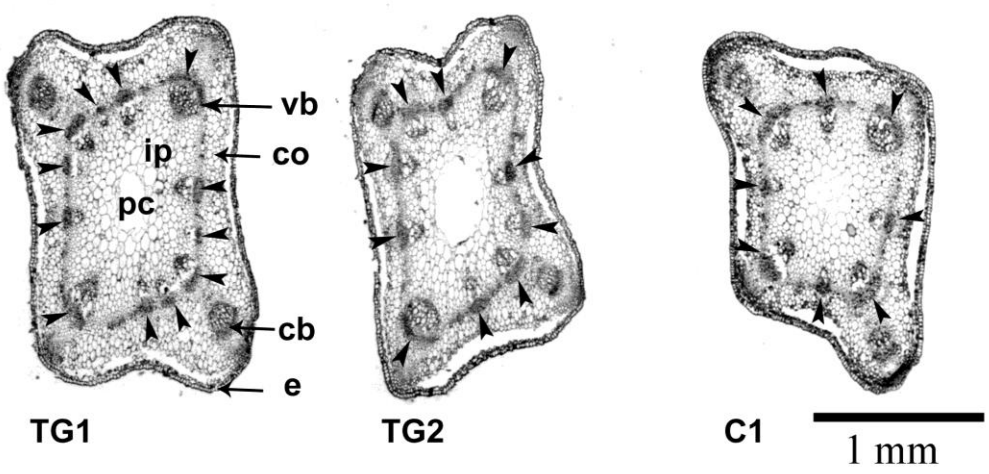

Figure 2.6. Representative light micrographs of transverse cross-sections from internode 8 at 50% maturity in transgenic lines TG1 and TG2, and in the control line C1. Each arrow indicates an individual developing vascular bundle. Magnification is 2.5×. e, epidermis; cb, cortical fibre bundle; co, cortex; ip, intact pith; pc, pith cavity; vb, vascular bundle.

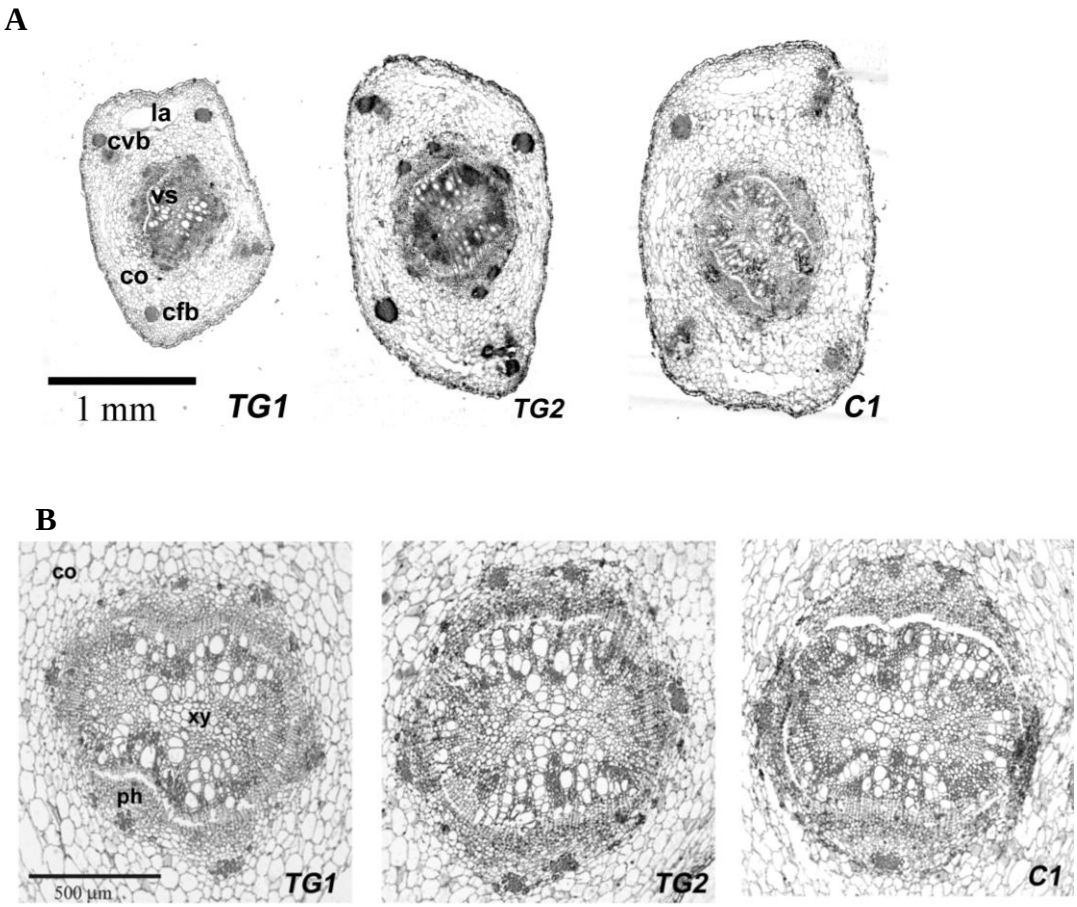

Figure 2.7. (A) Representative light micrographs of transverse cross-sections from internode two at maturity in transgenic lines TG1 and TG2, and in the control line C1. Magnification is 2.5×. cvb, cortical vascular bundle; cfb, cortical fiber bundle co, cortex; vs, vascular style; la, lacunae.

(B) Representative light micrographs of the vascular region of internode two at maturity in the transgenic lines TG1 and TG2, and the control line C1. Magnification is 10×. co, cortex; ph, phloem; xy, xylem.

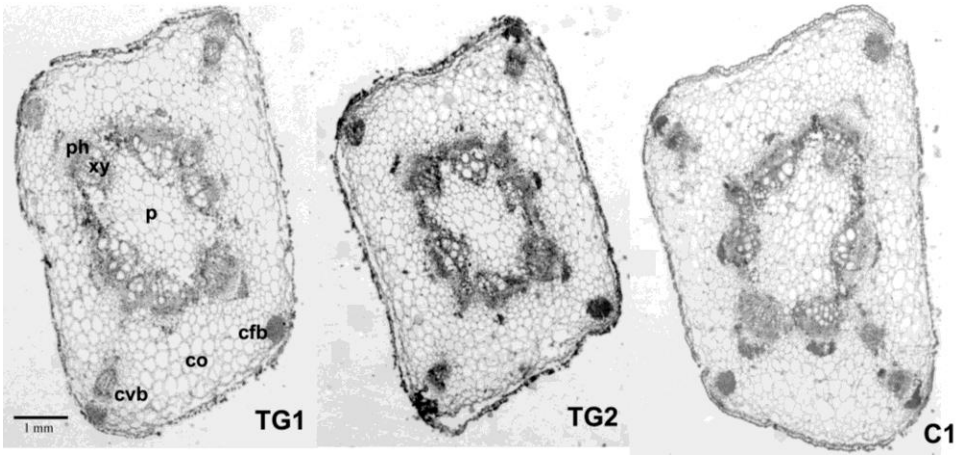

Figure 2.8. Representative light micrographs of transverse cross-sections from internode four at maturity in transgenic lines TG1 and TG2, and in the control line C1. Magnification is 2.5×. cvb, cortical vascular bundle; cfb, cortical fiber bundle; co, cortex; xy, xylem; ph, phloem; p, pith.

Figure 2.9. Relative transcript abundance of A, *PsGA20ox1;* B, *PsGA20ox2*; C, transgenic *PsGA3ox1;* D, total *PsGA3ox1* (transgenic + endogenous); E, *PsGA2ox1*, and F, *PsGA2ox2* in elongating internodes of the transgenic lines TG1, TG2 and TG3, and their controls (C1 for TG1 and TG2; C3 for TG3). Transcript levels were compared across genes and lines using the tendril stage 2 *PsGA20ox2* (Ct = 37.96) sample of the TG1 line as a reference for normalization. Data are means ± SE of two to three biological replicates. Internodes were harvested at 15-20% of their final length from internode position 8.

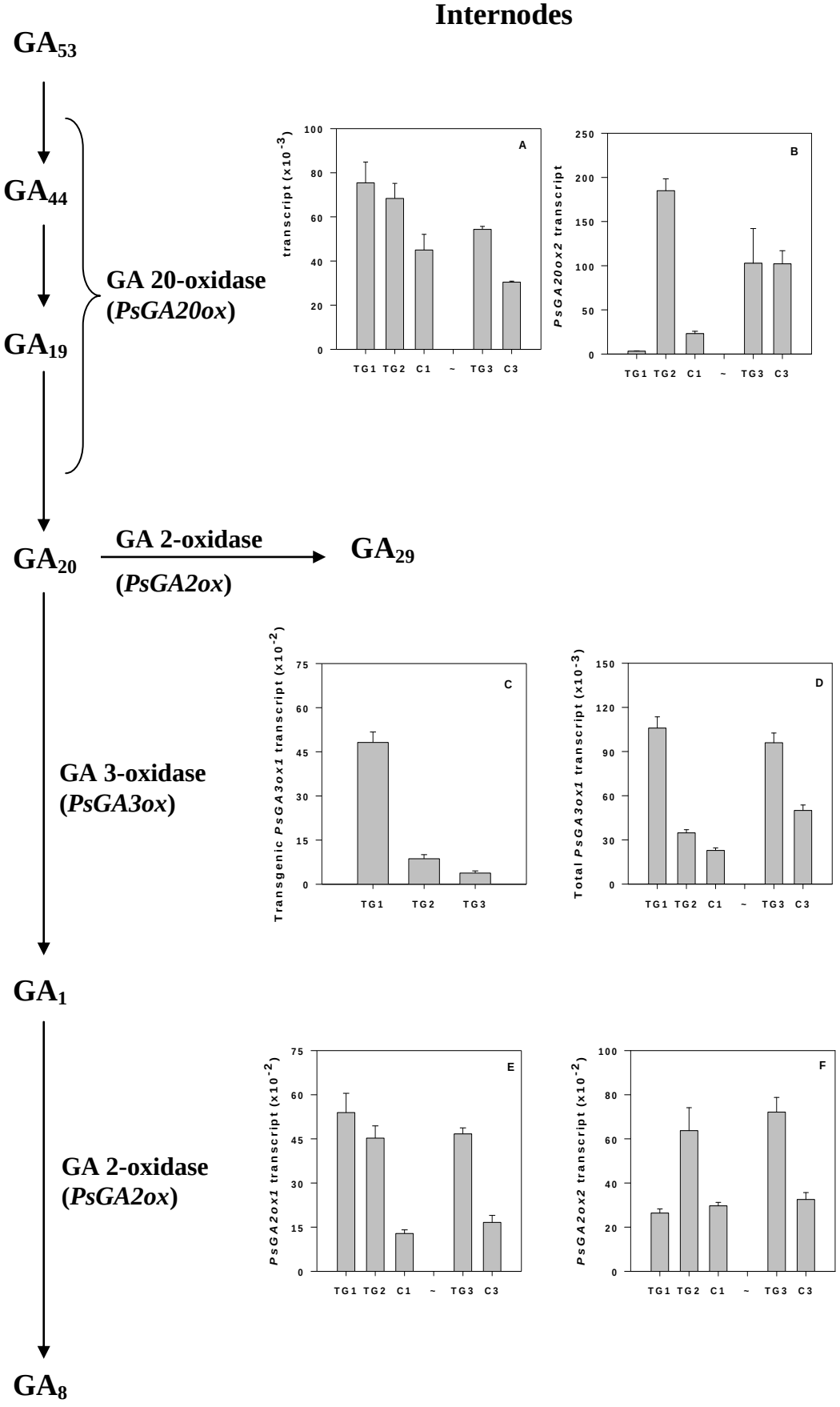
Internodes
GA53
GA44
GA19
GA20
GA29
GA1
GA8
GA 20-oxidase
(PsGA20ox)
GA 2-oxidase
(PsGA2ox)
GA 3-oxidase
(PsGA3ox)
GA 2-oxidase
(PsGA2ox)
A
B
C
D
E
F
TG1 TG2 C1 ~ TG3 C3
TG1 TG2 TG3
Transgenic PsGA3ox1 transcript (x10-2)
Total PsGA3ox1 transcript (x10-3)
PsGA2ox1 transcript (x10-2)
PsGA2ox2 transcript (x10-2)

Figure 2.10. Relative transcript abundance of A, B and C, *PsGA20ox1*; D, E and F, *PsGA20ox2*; G, transgenic *PsGA3ox1*; H, I and J, total *PsGA3ox1* (transgenic + endogenous); K, L and M, *PsGA2ox1*; and N, O and P, *PsGA2ox2* in the tendrils of transgenic lines TG1, TG2 and TG3, and their controls (C1 for TG1 and TG2; C3 for TG3) over development. Transcript levels were compared across genes and lines using the tendril stage 2 *PsGA20ox2* (Ct = 37.96) sample of the TG1 line as a reference for normalization. Data are means ± SE of two to three biological replicates. Tendrils were harvested over development at 10-15% of final length (stage 1), 35-40% of final length (stage 2), 75-80% of final length (stage3) and at maturity (stage 4) for total RNA extraction.

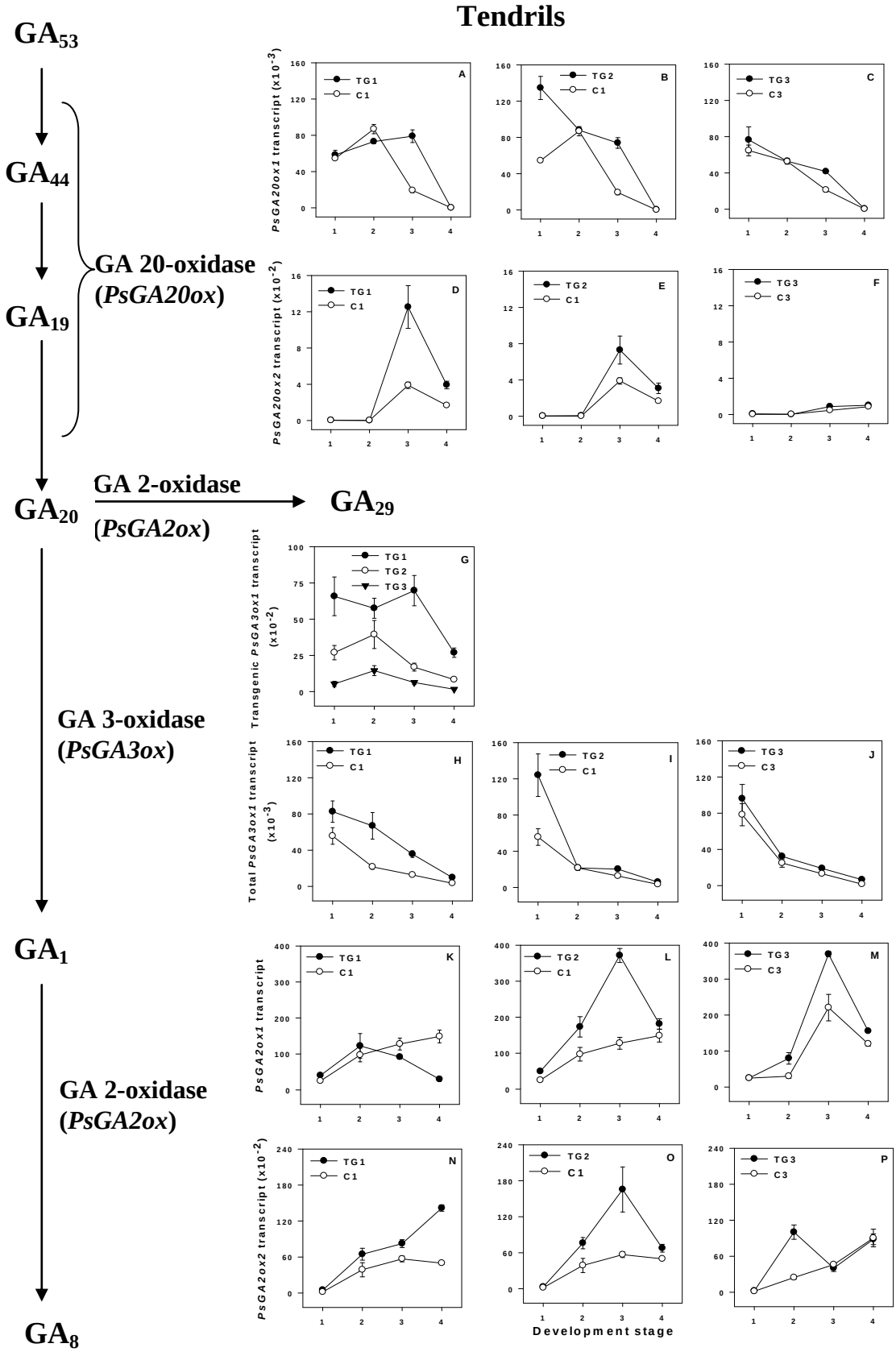
Tendrils
GA53
GA44
GA 20-oxidase
(PsGA20ox)
GA19
GA 2-oxidase
(PsGA2ox)
GA20
GA29
GA 3-oxidase
(PsGA3ox)
GA1
GA 2-oxidase
(PsGA2ox)
GA8
PsGA20ox1 transcript (x10-3)
PsGA20ox2 transcript (x10-2)
Transgenic PsGA3ox1 transcript (x10-2)
Total PsGA3ox1 transcript (x10-3)
PsGA2ox1 transcript
PsGA2ox2 transcript (x10-2)
TG1
TG2
TG3
C1
C3
A
B
C
D
E
F
G
H
I
J
K
L
M
N
O
P
Development stage

Figure 2.11. Relative transcript abundance of A, B and C, *PsGA20ox1*; D, E and F, *PsGA20ox2*; G, transgenic *PsGA3ox1*; H, I and J, total *PsGA3ox1* (transgenic + endogenous); K, L and M, *PsGA2ox1*; and N, O and P, *PsGA2ox2* in the stipules of transgenic lines TG1, TG2 and TG3, and their controls (C1 for TG1 and TG2; C3 for TG3) over development. Transcript levels were compared across genes and lines using the tendril stage 2 *PsGA20ox2* (Ct = 37.96) sample of the TG1 line as a reference for normalization. Data are means ± SE of two to three biological replicates. Stipules were harvested over development at 15-20% of final size (stage 1), 35-40% of final size (stage 2), 75-80% of final size (stage3) and at maturity (stage 4) for total RNA extraction.

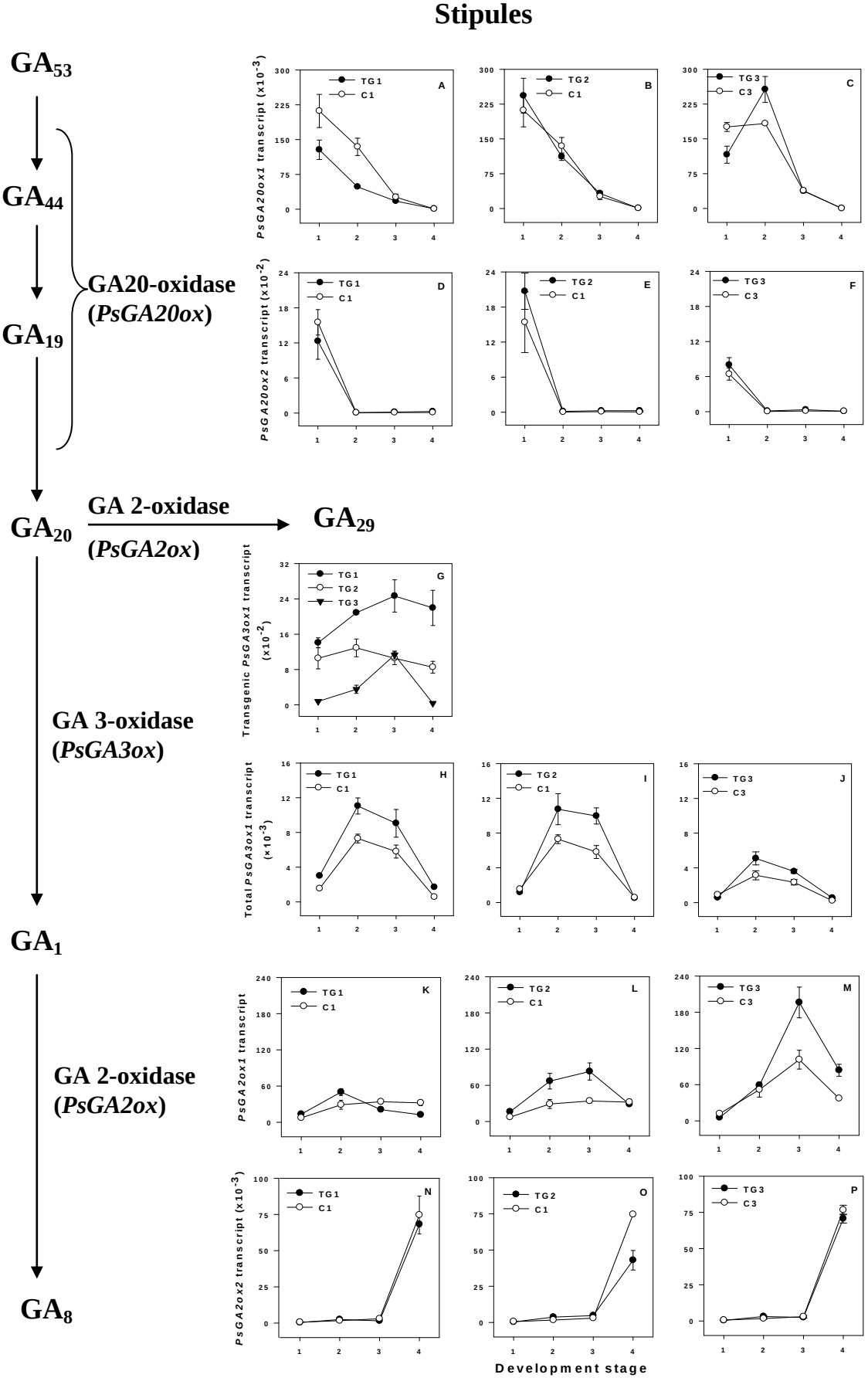
Stipules
GA53
GA44
GA20-oxidase
(PsGA20ox)
GA19
GA20
GA 2-oxidase
(PsGA2ox)
GA29
GA 3-oxidase
(PsGA3ox)
GA1
GA 2-oxidase
(PsGA2ox)
GA8
PsGA20ox1 transcript (x10-3)
PsGA20ox2 transcript (x10-2)
Transgenic PsGA3ox1 transcript (x10-2)
Total PsGA3ox1 transcript (x10-3)
PsGA2ox1 transcript
PsGA2ox2 transcript (x10-3)
TG1
TG2
TG3
C1
C3
A
B
C
D
E
F
G
H
I
J
K
L
M
N
O
P
Development stage

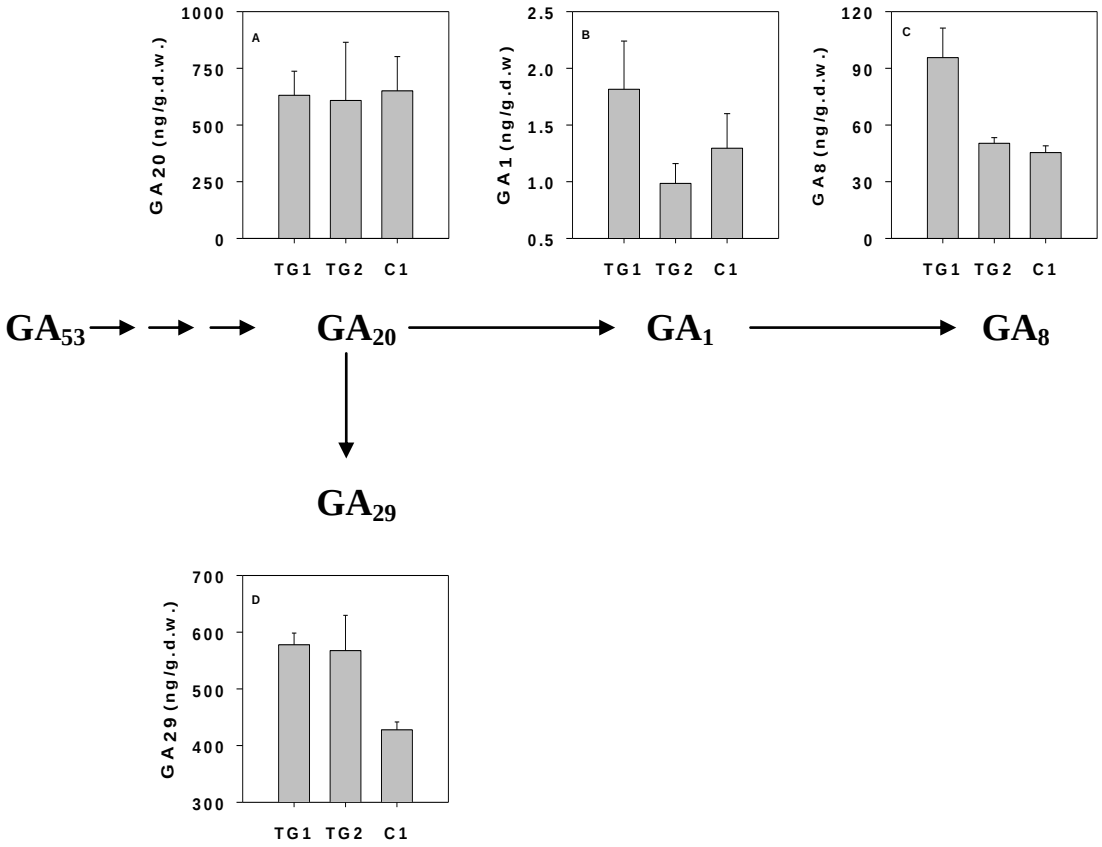

Figure: 2. 12. Endogenous A, GA_{20}; B, GA_1; C, GA_8; and D, GA_{29} content in elongating internodes (internode 8 at 50% full length) of transgenic lines TG1 and TG2, and the control line C1. Data are means ± SE, n=2.

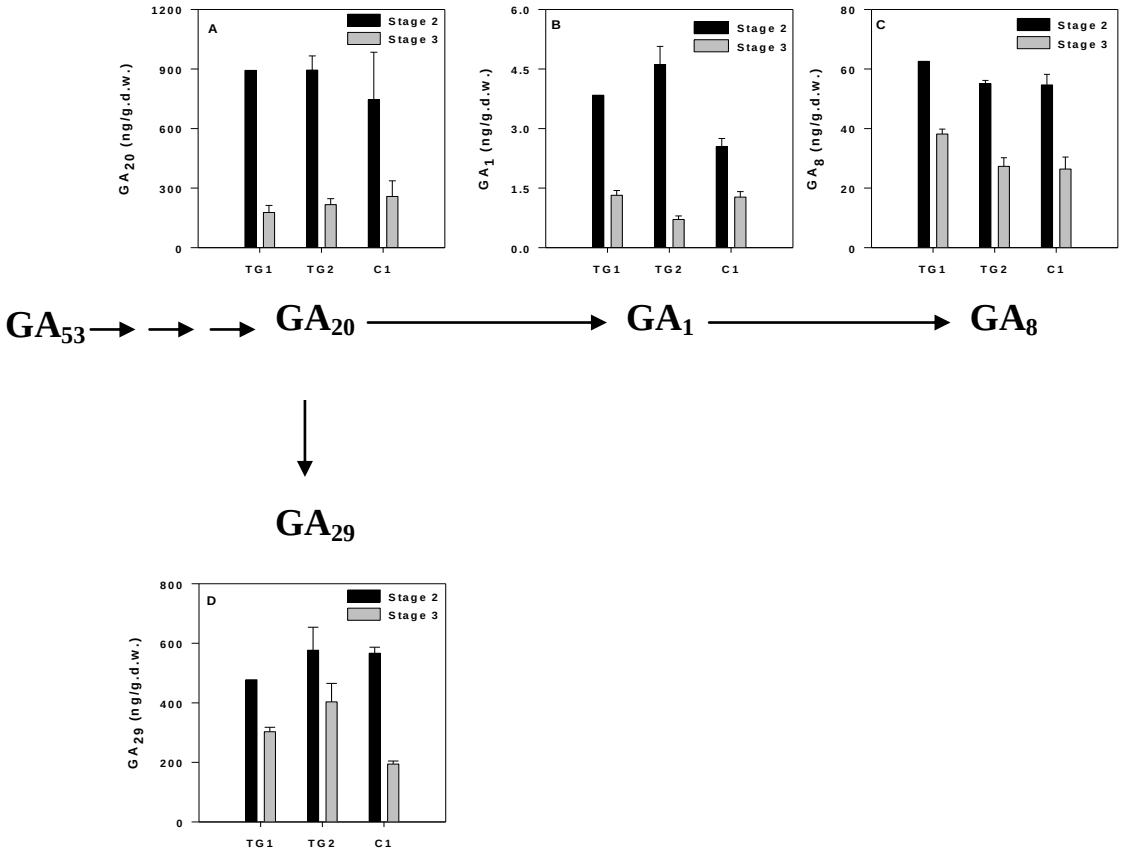

Figure 2.13. Endogenous A, GA_{20}; B, GA_1; C, GA_8; and D, GA_{29} content in elongating tendrils at 40% (stage 2) and 80% full length (stage 3) at nodal position 8 of the transgenic lines TG1 and TG2, and the control line C1. Data are means ± SE, n= 2, with one exception, 40% full length tendrils of TG1, n=1.

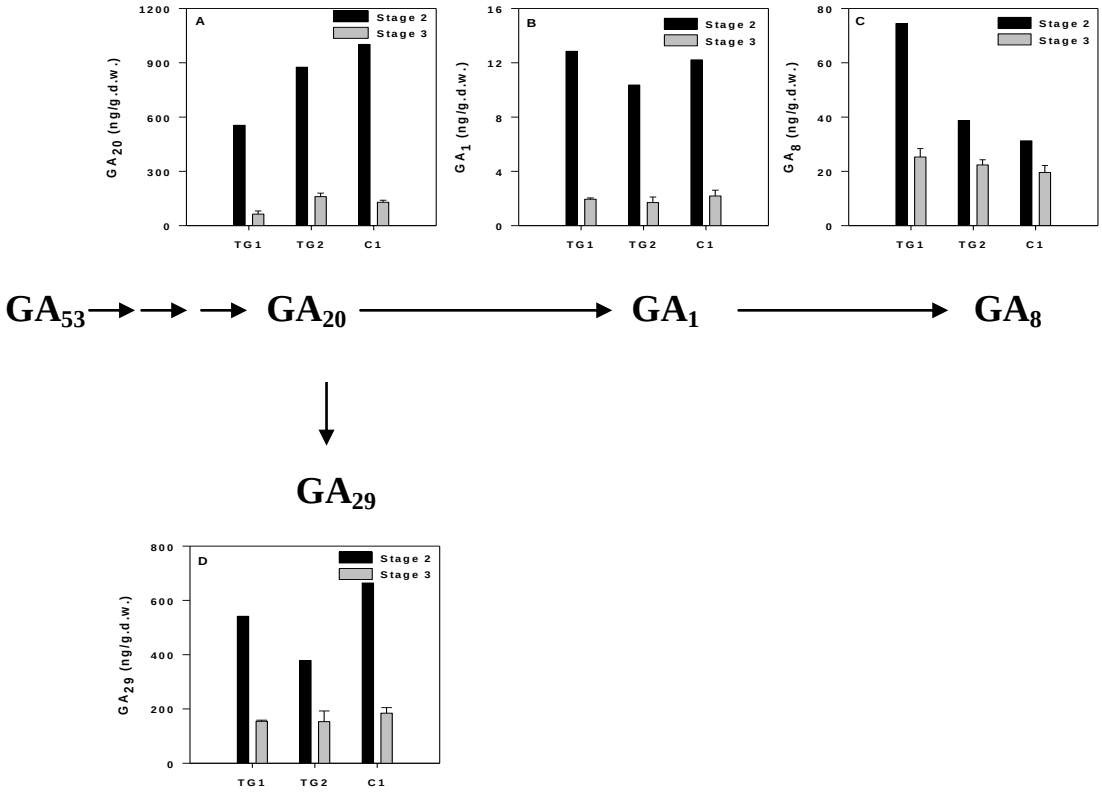

Figure 2.14. Endogenous A, GA_{20}; B, GA_1; C, GA_8; and D, GA_{29} content in stipules at 40% full size (stage 2) and 80% full size (stage 3) at nodal position 8 of transgenic lines TG1 and TG2, and the control line C1. Data are means ± SE, n= 1 for 40% full size samples, n= 2 for 80% full size samples.

Table 2.4. Length of pericarps at maturity of transgenic (TG1 and TG2) and control (C1) lines.

Line	Pericarp length at maturity (mm)			
	3 seeds[a]	4 seeds	5 seeds	6 seeds
TG1	61.5±3.2[b]z[c]	62.0±1.4z	68.4±1.4z	75.7±1.8z
TG2	49.6±2.5y	54.5±1.9y	62.1±3.8y	68.5±1.5y
C1	47.8±2.1y	57.5±2.3y	60.6±2.3y	65.6±1.3y

[a] number of seeds per fruit

[b] Data are means ± SE, n=7 to 16 (from 7 to 10 individual plants).

[c] Means followed by different letters (y, z) indicate significant difference among lines by LSD, $P<0.05$.

Literature cited:

Aldrich J, Cullis CA (1993) RAPD analysis in flax: Optimization of yield and reproducibility using Klen *Taq* 1 DNA polymerase, Chelex 100, and gel purification of genomic DNA. Plant Mol Biol Repo **11**:128-141

Ayele BT (2006) Gibberellin biosynthesis during germination and young seedling growth of pea. PhD thesis. University of Alberta, Canada.

Ayele BT, Ozga JA, Reinecke DM (2006) Regulation of GA biosynthesis genes during germination and young seedling growth of pea (*Pisum sativum* L.). J Plant Growth Regul **25**: 219-232

Besnard-Wibaut C, Noin M, Zeevat JAD (1983) Mitotic activities and levels of nuclear DNA in the apical meristem of *Silene armeria* (Strain S1.2) following application of gibberellin A_3. Plant Cell Physiol **24**: 1269-1279

Biemelt S, Tschiersch H, Sonnewald U (2004) Impact of altered gibberellin metabolism on biomass accumulation, lignin biosynthesis and photosynthesis of transgenic tobacco plants. Plant Physiol **135**:254-265

Carrera E, Bou J, Gracia-Martinez JL, Prat S (2000) Changes in GA 20-oxidase gene expression strongly affects stem length, tuber induction and tuber yield of potato plants. Plant J **22**:247-256

Coles JP, Phillips AL, Croker SJ, Garcia-Lepe R, Lewis MJ, et al (1999) Modification of gibberellin production and plant development in potato by sense and antisense expression of gibberellin 20-oxidase genes. Plant J **17**:547-556

Davidson SE, Swain SM, Reid JB (2005) Regulation of the early GA biosynthesis pathway in pea. Planta **222**: 1010-1019

Dennis FG (1973) Physiological control of fruit set and development with growth regulators. Acta Hort **34**: 251-259

Devadas C, Beck CB (1972) Comparative morphology of the primary vascular systems in some species of Rosaceae and Leguminosae. Amer J Bot **59**: 557-567

Eriksson M, Israelsson M, Olsson O, Moritz T (2000) Increased gibberellin biosynthesis in transgenic trees promotes growth, biomass production and xylem fiber length. Nature Biotech **18**: 784-788

Fagoaga C, Tadeo FR, Iglesias DJ, Huerta L, Lliso I, et al. (2007) Engineering of gibberellin levels in citrus by sense and antisense overexpression of a GA 20-oxidase gene modifies plant architecture. J Experi Bot **58**: 1407-1420

Fleet CM, Yamaguchi S, Hanada A, Kawaide H, David CJ, et al (2003) Overexpression of *AtCPS* and *AtKS* in *Arabidopsis* confers increased *ent*-kaurene production but no increase in bioactive gibberellins. Plant Physiol **132**: 830-839

Gallego-Giraldo L, Ubeda-Tomas S, Gisbert C, Garcia-Martinez JL, Moritz T, et al. (2008) Gibberellin homeostasis in tobacco is regulated by gibberellin metabolism genes with different gibberellin sensitivity. Plant Cell Physiol **49**: 679-690

Gaskin P, MacMillan J (1991) GC-MS of the gibberellins and related compounds: Methodology and a library of spectra. University of Bristol (Cantock's Enterprises), Bristol, UK

Hedden P (1987) Gibberellins. *In* Rivier L, Crozier A, eds, Principles and practice of plant hormone analysis, Vol. 1. Academic Press, London, pp 9–110

Hedden P, Phillips AL (2000a) Gibberellin metabolism: new insights revealed by the genes. Trends Plant Sci **5**: 523-530

Hedden P, Phillips AL (2000b) Manipulation of hormone biosynthetic genes in transgenic plants. Curr Opin Biotech **11**: 130-137

Huang S, Raman AS, Ream JE, Fujiwara H, Cerny RE, et al. (1998) Overexpression of 20-oxidase confers a gibberellin-over production phenotype in *Arabidopsis*. Plant Physiol **118**:773-781

Ingram TJ, Reid JB, Murfet IC, Gaskin P, Willis CL, et al. (1984) Internode length in *Pisum*: the Le gene controls the 3β-hydroxylation of gibberellin A_{20} to gibberellin A_1. Planta **106**: 455-463

Israelson M, Sundberg B, Moritz T (2005) Tissue-specific localization of gibberellins and expression of gibberellin-biosynthetic and signaling genes in wood forming tissues in aspen. Plant J **44**: 494-504

Israelsson M, Mellerowic E, Chono M, Gullberg J, Moritz T (2004) Cloning and overproduction of gibberellin 3-oxidase in hybrid aspen trees. Effects on gibberellin homeostasis and development. Plant Physiol **135**:221-230

Jacobsen JV, Pearce DW, Poole AT, Pharis RP, Mander LN (2002) Abscisic acid, phaseic acid, and gibberellin contents associated with dormancy and germination in barley. Physiol Plant **115**: 428–441

Koshioka M, Takeno K, Beall FD, Pharis RP (1983) Purification and separation of gibberellins from their precursors and glucosyl conjugates. Plant Physiol **73**: 398–406

Krejci P, Matuskova P, Hanacek P, Reinohl V, Prochazka S (2007) The transformation of pea (*Pisum sativum* L.): applicable methods of *Agrobacterium tumefaciens*-mediated gene transfer. Acta Physiol Plant **29**: 157-163

Kurepin LV, Emery RJN, Pharis RP, Reid DM (2007) Uncoupling light quality from light irradiance effects in Helianthus annuus shoots: putative roles for plant hormones in leaf and internode growth. J Exp Bot **58**: 2145-2157

Livak KJ, Schmittgan TD (2001) Analysis of relative gene expression data using real-time quantitative PCR and the $2^{-\Delta\Delta Ct}$ method. Methods **25**: 402-408

Lester DR, Ross JJ, Davies, Reid JB (1997) Mendel's stem length gene (*Le*) encodes a gibberellin 3β-hydroxylase. Plant Cell **9**:1453-1443

Lester DR, Ross JJ, Smith JJ, Elliot RC, Reid JB (1999) Gibberellin 2-oxidation and the *SLN* gene of *Pisum sativum*. Plant J **19**:1435-1443

MacKenzie-Hose AK, Ross JJ, Davis NW, Swain SM (1998) Expression of gibberellin mutations in fruits of *Pisum sativum*. Planta **204**: 397-403

Marx GA (1977) Classification, Genetics and Breeding. *In* Sutcliffe JF, Pate JS, eds, The Physiology of the Garden Pea. Academic Press, London, pp21-44

Mendel G (1866) Versuche u¨ber Pflanzen-Hybriden. Verh Naturforsch Ver.Bru¨nn. 4:3-47

O'Brian TB, McCully ME (1981) The study of plant structure: principles and selected methods. Termarcarphi, Melbourne, Australia

Oikawa T, Koshioka M, Kojima K, Yoshida H, Kawata M (2004) A role of *OsGA20ox1*, encoding an isoform of gibberellin 20-oxidase, for regulation of plant stature in rice. Plant Mol Biol **55**:687-700

Olszewski N, Sun T-P, Gubler F (2002) Gibberellin signaling: Biosynthesis, catabolism, and response pathways. Plant Cell **14**: S61- S80

Ozga JA, Reinecke DM, Ayele BT, Ngo P, Nadeau C, Wickramarathna AD (2009) Developmental and hormonal regulation of gibberellin biosynthesis and catabolism in pea fruit. Plant Physiol **150**: 448-462

Ozga JA, Yu J, Reinecke DM (2003) Pollination-, development-, and auxin-specific regulation of gibberellin 3β-hydroxylase gene expression in pea fruit and seeds. Plant Physiol **131**: 1137-1146

Ozga JA, Brenner ML, Reinecke DM (1992) Seed effects on gibberellin metabolism in pea pericarp. Plant Physiol **100**: 88-94

Pate JS (1975) Pea. *In* LT Evans, ed, Crop physiology: some case histories. Syndics of the Cambridfe University Press, Great Britain, pp 191-224

Pharis RP, King RW (1985) Gibberellins and reproductive development in seed plants. Ann Rev Plant Physiol **36**: 517-568

Phillips AL (2004) Genetic and transgenic approaches to improve crop performace. *In* PJ Davis, ed, Plant hormones: biosynthesis, signal transduction, action. Ed 3. Kluwer Acedemic Publishers, Dordrecht, The Netherlands, pp 582-609

Potts WC, Reid JB, Murfet IC (1982) Internode length in *Pisum.* I. The effect of the *Le/le* gene difference on endogenous gibberellin-like substances. Physiol. Plant **55**: 323-328

Radi A, Lange T, Tomoya N, Koshioka M, Pimienta LMP (2006) Ectopic expression of pumpkin gibberellin oxidases alters gibberellin biosynthesis and development of transgenic *Arabidopsis* plants. Plant Physiol **140**:528-536

Reid JB, Ross JJ, Swain SM (1992) Internode length in *Pisum*. A new slender mutant with elevated levels of C19 gibberellins. Planta **188**: 462-467

Reid JB, Symons GM, Ross JJ (2004) Regulation of gibberellin and brassinosteroid biosynthesis by genetic, environmental and hormonal factors. *In* PJ Davis, ed, Plant hormones: biosynthesis, signal transduction, action. Ed 3. Kluwer Academic Publishers, Dordrecht, The Netherlands, pp 179-203

Rodrigo MJ, Garcia-Martinez JL, Santes CM, Gaskin P, Hedden P (1997) The role of gibberellins A_1 and A_3 in fruit growth of *Pisum sativum* L. and the identification of gibberellins A_4 and A_7 in young seeds. Planta **201**: 446-455

Ross JJ, Davidson SE, Wolbang CM, Bayly-Stark E, Smith JJ, et al. (2003) Developmental regulation of the gibberellin pathway in pea shoots. Funct Plant Biol **30**: 83-89

Ross JJ, Reid JB, Dungey HS (1992) Ontogenetic variation levels of gibberellin A_1 in *Pisum*. Planta **186**: 166-171

Ross JJ, Reid JB, Gaskin P, MacMillan J (1989) Internode length in *Pisum*. Estimation of GA_1 levels in genotypes *Le*, *le* and le^d. Physiol Plant **76**: 173-176

Santes CM, Hedden P, Sponsel VM, Reid JB, Garcia-Martinez JL (1993) Expression of the *le* mutation in young ovaries of *Pisum sativum* and its effect on fruit development. Plant Physiol **101**: 759-764

Schroeder HE, Schotz AH, Wardley-Richardson T, Spencer D, Higgins TJV (1993) Transformation and regeneration of two cultivars of pea (*Pisum sativum* L.). Plant Physiol **101**: 751-757

Spiker S, Mashkas A, Yunis M (1976) The effect of single and repeated gibberlic acid treatment on internode number and length in dwarf peas. Physiol Plant **36**: 1-3

Sutcliffe JF (1977) History of the use of the pea in plant physiological research. *In* Sutcliffe JF, Pate JS, eds, The physiology of the garden pea. Acedemic Press, London, pp1-19

Swain SM, Sing D P, Helliwell CA, Poole AT (2005) Plants with increased expression of ent-kaurene oxidase are resistant to chemical inhibitors of this gibberellin biosynthesis enzyme. Plant Cell Physiol **46**: 284-291

Vidal AM, Gisbert C, Talon M, Primo-Millo E, Lopez-Diaz I, et al. (2001) The ectopic over-expression of a citrus gibberellin 20-oxidase enhances the non 13-hydroxylation pathway of gibberellin biosynthesis and induces an extremely elongated phenotype in tobacco. Physiol Plant **112**:251-260

Yamaguchi S (2008) Gibberellin metabolism and its regulation. Annu Rev Plant Biol **59**: 225-251

Yeung EC, Sussex IM (1979) Embryogeny of *Phaseolus coccineus*: the suspensor and the growth of the embryo-proper in vitro. Z Pflanzenphysiol **91**: 423-433

Chapter 3

Dynamics of GAs and auxins in the elongation pea stem

Introduction

Overexpression of *PsGA3ox1* in pea led to increased flux through the GA biosynthesis pathway in elongating pea internodes (Chapter 2) and resulted in longer internodes (approximately 22% increase in the highest transgenic expression line). However, Ross et al. (1992) found that the internode length of a tall pea (*Le*) line was up to 300% longer than that in its isogenic dwarf (*le-1*) line (*le-1* contains a mutation in *PsGA3ox1* making the GA 3-oxidase it encodes much less efficient). The difference in internode lengths between the isogenic lines of *LE* and *le* reported by Ross et al. (1992) and the *PsGA3ox1*-overexpressor lines could be due to the expression dynamics of the endogenous promoter versus the 35S CaMV promoter, and/or that a bioactive GA homeostatic mechanism is triggered in the transgenics decreasing the levels of bioactive GA and resulting in a more modest increase in internode length. Bioactive GA homeostasis in plants is maintained via feedback and feed forward regulation of GA metabolism (Hedden and Phillips, 2000). It appears that feedback regulation does not occur in the early part of the GA biosynthesis pathway, but is mainly targeted to the 2-oxoglutarate dependent dioxygenases (2ODDs) in the GA metabolism pathway (Hedden and Phillips, 2000). In transgenic tobacco, up-regulation of GA catabolism genes (*NtGA2ox3* and *NtGA2ox5*) was observed in 7 d-old seedlings when *PsGA3ox1* was overexpressed (Gallego-Giraldo et al., 2008), however there was no effect on

the expression of the *AtGA20ox1* and *AtGA3ox1* or the levels of GA_9, GA_4, GA_{34} and GA_{51} when *AtCPS1* was overexpressed in Arabidopsis (Fleet et al., 2003).

It is also known that plant hormones interact to regulate and coordinate plant growth and development (Brian and Hemming, 1957), but the exact mechanisms generally are poorly understood. Mechanisms of hormone interaction began to be more intensely studied in the 1990's and one focus was on the mechanisms of interaction between GAs and auxins. Two specific mechanisms of interaction between these classes of plant hormones have been reported: auxin regulation of GA metabolism (van Huizen et al., 1995; van Huizen et al., 1997; Ozga et al., 2003; Ross et al., 2000; O'Neill and Ross, 2002; Wolbang et al., 2004) and auxin-induced degradation of the negative GA-signaling element RGA, thereby promoting GA signaling (Fu and Harberd, 2003). Therefore, understanding the interaction of auxins and GAs during stem growth and development will enhance our knowledge of hormonal regulation of these processes.

Additionally, plant hormones can elicit their effects near their sites of synthesis, or they can be transported and cause their effects at a distance from the point of synthesis (Davies, 2004). In order to more fully understand the role of GAs and the interaction between auxins and GAs in stem elongation, it is necessary to understand the synthesis capacity of these hormones in the internodes per se, as well as other possible sources of these hormones that could be transported to the internode. The transport of GAs has been studied using excised plant tissues and grafted or intact plants, and results from these studies

suggest that GAs, in general, are transported in a non-directional manner via the phloem (Jacobs and Jacobs, 2001). Studies conducted by Jacobs et al. (1988) in runner bean provided evidence that GA_1 is more effectively transported than GA_5, indicating that specific GAs may be preferred transport forms. They also suggested that different GAs may have different transport properties. Based on grafting and radiolabelled GA application studies in pea, Proebsting et al. (1992) concluded that it is likely that GA_{20} is the major GA transported, and that GA_1 is also transported but somewhat less efficiently than GA_{20}. However initial radiolabel uptake into the source tissue was not taken into consideration in this study.

Auxin is transported throughout the plants by two main pathways. One pathway is the fast, non-directional transport system through the phloem, and the second is the slower, more controlled, cell-to-cell and directional carrier-dependant transport system (polar auxin transport; PAT; for review, Morris et al., 2004). In the mid 1970s, the chemiosmotic hypothesis was formulated to explain the mechanism of PAT (Rubery and Sheldrake, 1974; Raven, 1975) and this model explains the cell-to cell movement of auxin by the action of simple diffusion and specific auxin carriers. In brief, the IAA molecule is present in both ionized and protonated forms [about 15% of IAA exists in its protonated form (IAAH)] in the relatively acidic environment of the cell wall (pH around 5.5). Hydrophobic, protonated IAAH enters the cell passively by diffusion through the plasma membrane. In the more basic cytoplasm (pH 7), the IAAH dissociates and the resulting IAA^- anion cannot passively move out of the cell due to its poor

membrane permeability. In addition to simple diffusion, auxin influx carriers are proposed to transport auxin anions (IAA^-) into the cell (Vieten et al., 2007) and the presence of auxin efflux carriers asymmetrically localized within cell postulated to transport IAA- ions out of the cell in a unidirectional manner (Friml and Palme, 2002). This model was further reinforced by the identification and characterization of auxin influx and efflux carrier proteins (Rubery and Sheldrake, 1974; Raven, 1975; Galweiler et al., 1998; Muller et al., 1998; Friml et al., 2003; for review, Vieten et al., 2007). To date, two genes coding auxin efflux carriers have been cloned in pea, *PsPIN1* (Chawla and DeMason, 2004) and *PsPIN2* (Hoshino et al., 2005). *PsPIN1* is similar to that of *AtPIN1* in that it is ubiquitously expressed in all organs and plant parts; *PsPIN1* transcript is also more abundant in growing or developing plant parts (Chawla and DeMason, 2004). Northern blot analysis showed that *PsPIN2* is expressed in the shoot apical hook, internode (both in the elongation zone and the basal zone of the 1st internode) and root (mature root regions and root tips) of 6-d-old etiolated pea seedlings and the expression of *PsPIN2* was relatively low in roots compared to shoots suggesting a role of *PsPIN2* in regulating auxin transport in shoot tissues (Hoshino et al., 2005).

In order to more fully understand the regulation of bioactive GA levels in the *PsGA3ox1*-overexpressor lines, the response of stems to exogenous bioactive GA_3 was monitored in the highest transgenic expression line (TG1), expression profiles of the transgenic *PsGA3ox1* and other late GA biosynthesis and catabolism genes were determined in internodes of the transgenic and control

lines at nodal positions 2 to 9 of the elongating stem, and GA levels were determined in the internodes at specific internodal positions. For further understanding of GA and auxin transport in the stem and possible sources of these hormones for the elongating internode, transport of GA_1 in the stem was monitored at specific nodal positions in the transgenic and control lines, gene expression profiles of the auxin efflux carriers *PsPIN1* and *PsPIN2* were determined in the transgenic and control lines at nodal positions 2 to 9 of the elongating stem, and GA and IAA levels were monitored in various stem organs at specific nodal positions.

Materials and Methods

Plant Materials and hormone application

Mature air-dried seeds of the *PsGA3ox1*-overexpressor lineTG1, transgenic null C1 and wild-type lines (*Pisum sativum* L. cv. Carneval) were planted at a depth of approximately 2.5 cm into Sunshine Mix #4 potting medium (mixture of peat moss, coarse grade perlite, gypsum, dolomitic lime and a wetting agent; Sungro Horticulture, Seba Beach, AB) in 1.5 L plastic pots at one seed per pot. The pots were arranged in three blocks, where plant lines were randomized within the block [8 to 12 plants (biological replicates) per line per block]. The left block received the GA_3 treatment, the right block received the Apogee treatment and the center block received the control treatment. Plants were completely wetted with 100 μM GA_3 (Abbot Laborataries, North Chicago, IL, USA) in 0.1% Tween 80, 3.61 mM prohexadione-calcium (Apogee; BASF, Triangle Park NC,

USA) in 0.1% aqueous Tween 80 or with 0.1% Tween 80 (control) using compressed air sprayers (Model # 2512 RONA Inc. Boucherville, QC) when seedlings were at the three fully expanded leaves stage and a second application was made two weeks after the first application. Polyethylene baffles were set up to prevent cross-contamination while treatments were being applied and they were kept erected for 6 h after treatment application. The experiment was carried out in a 2.5 × 1.4 m Conviron growth chamber and plants were grown at 19^{o}C/17^{o}C (day/night) with a 16/8 h photoperiod under cool-white fluorescent lights (F54/I5/835/HO high florescent bulbs, Phillips, Holland; 366 µE m^2 s^{-2}). The total number of internodes at plant maturity (the first internode was defined as the one between the cotyledon attachment and the first stem node) and the length of each internode at maturity from position 1 to 15 were recorded.

Tissue harvest for gene expression and GA analysis

For gene expression analysis three independently-transformed, homozygous transgenic lines (T_4 to T_6 generation; TG1, TG2 and TG3) along with two transgenic null control lines (C1 and C3) were used, and endogenous GA levels were analyzed in the TG1, TG2 and C1 lines.

For the gene expression studies, mature air-dried seeds were planted as described above, and the pots were arranged in a completely randomized designed in a in a 2.5 × 1.4 m Conviron growth chamber and grown at 19^{o}C/17^{o}C (day/night) with a 16/8-h photoperiod under cool-white fluorescent lights (F54/I5/835/HO high florescent bulbs, Phillips, Holland; 366 µE m^2 s^{-2}). Plants were watered once every three days, and were not fertilized. Internodes from

position 2 to 9 (Figure 3.1) were harvested when at 5-7 mm in length (approximately 15-20% of final length). The data presented are from one experiment consisting of three biological replicates per tissue where each replicate contained tissues from two plants. This experiment has been repeated twice over time at selected internodes in lines TG1, TG2, and C1.

For endogenous GA and IAA analyses, mature air-dried seeds were planted as described above, and pots were arranged in a completely randomized design in a 7.5 × 3 m growth chamber space grown at $19^{o}C/17^{o}C$ (day/night) with a 16/8-h photoperiod under cool-white fluorescent lights (F54/I5/835/HO high florescent bulbs, Phillips, Holland; 350 $\mu E\ m^2\ s^{-2}$). Internodes from position 7 and 8 (Figure 3.1) were harvested when at 15-20 mm in length (approximately 45-55% of final length) and internodes from position 6 and 7 (Figure 3.1) were harvested when at 26-30 mm in length (approximately 75-85% of final length). Stipules at node eight when at 35-40% and 75-85% of final size were also harvested. The data presented are from one experiment, where two biological replicates per tissue were collected (each replicate contained tissues from nearly two hundred plants). Tissues were immediately frozen upon harvesting in liquid nitrogen and stored at $-80^{O}C$ until RNA extraction or freeze-drying (as described in Chapter 2) for hormone extraction.

Defoliation and tissue collection

To examine the effect of defoliation and tendril removal on GA biosynthesis and catabolism gene expression profiles in expanding internodes, stipules and tendrils located above and below the expanding internode of interest

were removed 24 h prior to internode harvesting (Figure 3.2). Internode tissues were harvested when 5-7 mm in size at the seventh, eighth and ninth positions (Figure 3.1) for expression studies. The data presented are from one experiment consisting of three biological replicates per internode position per treatment. Each replicate contained tissues from 2 plants. Each replicate was harvested over time (1 to 6 days).

qRT-PCR gene expression analysis

RNA isolation

Internode tissues were finely ground in liquid nitrogen (50 to 80mg FW) and total RNA was isolated using a modified TRIzol (Invitrogen) method as described previously (Chapter 2). After initial extraction, the total RNA samples were treated with DNase (DNA-free kit, Ambion, Austin TX, USA) to remove any residual DNA. RNA integrity was verified by gel electrophoresis in representative samples of each extraction run and the 260 to 280 nm ratio was determined by spectrophotometry in all samples. Sample RNA concentration was determined in duplicate by A_{260} measurement using a NanoDrop ND-100 spectrophotometer (NanoDrop Technologies, Wilmington, DE). The total RNA samples were stored at -80^{o}C until quantitation by qRT-PCR.

Primers and probes

Primers and probe for the transgene *PsGA3ox1* quantifying amplicon (T*PsGA3ox1-130*) were designed using Primer Express software (version 3, Applied Biosystems, Foster City, CA, USA) as described previously (Chapter 2). Primers and probes for the target gene quantifying amplicon *PsGA3ox1-87* [used

for total *PsGA3ox1* (endogenous+ transgene) transcript quantitation] and for the reference gene amplicon *18S-62* (used for pea 18S rRNA transcript quantitation) were designed as described by Ozga et al. (2003). Primers and probes for the target gene quantifying amplicon *GA2ox1-73* (used for *PsGA2ox1* quantification), *GA2ox2-83* (used for *PsGA2ox2* quantification), *PsGA20ox1-104* (used for *PsGA20ox1* quantification), *GA20ox2-88* (used for *PsGA20ox2* quantification) were designed as described by Ayele et al. (2006). Primers and probes for the *PsGA3ox2* quantitation (*PsGA3ox2-104*) were designed as described by Ozga et al (2009).

For *PsPIN1* and *PsPIN2* quantitation, the following primers and probes were designed using Primer Express software (version 3, Applied Biosystems, Foster City, CA, USA). For *PsPIN1*, a 64-bp amplicon (*PsPIN1-64*; spans nucleotides 868 to 931 of AY222857; Chawla and DeMason, 2004) was used for quantitation: FP, 5'-CCG AGG CCG TCT AAT TAC GA-3'; RP, 5'-GAG CCG GAT AAT GTT TCA ACT TCT-3'; Probe, 5'-AAG ATG CTT CGA ATG C-3' (appendix Figure A. 2.1). For *PsPIN2*, a 100-bp amplicon (*PsPIN2-100*; spans nucleotide 951 to 1050 of AB 112364; Hoshino et al., 2005) was used for quantitation: FP, 5'-CCA CGC CGA GTT TTA CTC CAT-3'; RP, 5'-AGG AGT GGG TCC TCT AGA AGA CTG A-3'; Probe, 5'-TTT GGT ACT ACT GAT CTC TAT TC-3' (appendix Figure A.2.4). The *PsPIN-64* and *PsPIN2-100* primers each produced single a product of desired length as determined by gel electrophoresis and sequencing of the PCR products confirmed the specificity of

the primers (Figures A. 2. 2 and A. 2. 3 for *PsPIN1-64* and Figures A. 2. 5 and A. 2. 6 for *PsPIN2-100*).

All probes were Taqman-based (Applied Biosystems). The *GA* and *PIN* genes were labeled at the 5' end with the fluorescent reporter dye FAM and at the 3' end with a minor-grove binding non-fluorescent quencher (MGB, Applied Biosystems). The *18S-62* reference gene probe was labeled at the 5' end with VIC fluorescent reporter dye and the 3' end with the TAMRA quencher (Applied Biosystems).

qRT-PCR assay

The qRT-PCR assays were performed on an Applied Biosystems StepOnePlus sequence detector (defoliation and tendril removal experiment) or an Applied Biosystems model 7700 sequence detector (all other samples) using the TaqMan One-Step RT-PCR Master Mix reagent Kit (Applied Biosystems) as described previously (Chapter 2). The relative transcript abundance of the target genes in the individual plant sample was determined by $2^{-\Delta Ct}$ (Livak and Schmittgen, 2001) where ΔC_t was the difference between the C_t of the target sample and the average C_t of the reference sample. Transcript levels of *PsGA20ox1*, *PsGA20ox2*, transgenic *PsGA3ox1*, total (transgenic + endogenous) *PsGA3ox1*, *PsGA3ox2*, *PsGA2ox1*, *PsGA2ox2*, *PsPIN1* and *PsPIN2* were standardized across genes, development and treatments using the sample average Ct value (37.96; line: TG1, tissue: tendril stage 2, gene: *PsGA20ox2*; chapter 2). At least two, but more often three, biological replicate plant samples were assayed.

The pea 18S small subunit nuclear ribosomal RNA gene was used as a loading control to estimate variations in input total RNA concentration across all samples. 10 pg of DNase-treated total RNA was used for 18S rRNA quantitation using the reaction conditions described above. The coefficient of variation (CV) of the 18S rRNA amplicon Ct value among the samples was 2.7% and, therefore, the target amplicon mRNA values were not normalized to the 18S signal (Livak and Schmittgen, 2001, Ozga et al., 2009).

Analysis of endogenous GA and IAA levels

Endogenous GA and IAA levels in the elongating internodes 7 and 8 (approximately 45-55% of the final length), internodes 6 and 7 (approximately 75-85% of the final length) and the stipules at node 8 (two growth stages; approximately 35-45% of the final size and 75-85% of the final size) were analyzed by Dr. Lenoid Kurepin at the University of Calgary as described by Kurepin et al. (2007).

GA transport in elongating stems

In order to study the pattern of GA_1 transport in elongating pea stems, [^{14}C]GA_1 transport studies were initiated. Preliminary studies revealed that very little radioactivity was transported after 12 hours to tissues apical to the application site when [^{14}C]GA_1 was applied directly to the internode at position 8 when 15-20% full length (approximately 0.03% of total radioactivity applied was transported). However, when [^{14}C]GA_1 was applied to the stipules at node 7, accumulation of ^{14}C in tissues apical to the application site was detectable after both 24 h (approximately 2.1% of total radioactivity applied transported) and 48

h (approximately 4% of total radioactivity applied transported) after application. Therefore, distribution of ^{14}C was determined in the stipules, tendrils, internodes (mainly apical to the application site) and the shoot apex of pea stems after supplying [^{14}C]GA_1 to expanding stipules. Pea plants from the TG1 and C1 lines were grown in individual pots as described above. [^{14}C]GA_1 (34 μC/μM) in 50% aqueous methanol (154,000 dpm total) per plant was applied to the stipules at nodes 6 or 7 (5 μL per stipule leaf; 10 uL total per stipule pair at the target node) when the internode immediately above the stipules to be treated with [^{14}C]GA_1 was 5-7 mm (15-20% of final size). Forty hours after [^{14}C]GA_1 application (when the next elongating internode developed to a size of 5-7 mm; 8th and 9th internodes respectively), internode tissues from three positions (I-1, I-2 and I-3), stipule tissues from two positions (S-1 and S-2), tendril tissues from two positions (T-1 and T-2) and the shoot apex (A) were harvested (see Figures 3.14 and 3.15) and stored at -80C until extraction. The tissues were macerated using a mini pestle and a small amount of 100% methanol. The methanol was removed under vacuum using a SpeedVac concentrator, and 7 mL of EcoLite (+) liquid scintillation fluid (MP Biomedicals, Irview, CA, USA) was added to each sample. Samples were gently shaken overnight prior to determining radioactivity content using a LS 6500 Multi-Purpose Scintillation Counter (Backman Coulter, Inc., Fullerton, CA, USA. Quenching of radioactivity was determined by adding 10,500 dpm of [1-^{14}C] lenoleic acid (100 μL in 50% aqueous methanol; 55 mCi/mmol; GE healthcare, Baie d'Urfe, QC) to each sample vial after initially determining ^{14}C radioactive content, then gently shaking samples overnight prior

to recounting. The ^{14}C dpm values for each sample were determined using the following equation:

$$\text{Counting efficiency} = \frac{(\text{sample CPM} + [^{14}C]\text{lenoleic acid CPM}) - (\text{sample CPM})}{\text{DPM of } [^{14}C]\text{lenoleic acid standard}}$$

$$\text{Sample DPM} = \frac{(\text{sample CPM} - \text{background CPM})}{\text{Counting efficiency}}$$

Data from the exogenous GA_3 and Apogee treatment study were analyzed using the General Linear Model of SAS 9.1 statistical software (SAS Institute Inc., Cary, NC, USA) following a completely randomized design, and mean separation was by single tail *t*-test at $P \leq 0.05$.

The data presented are one experiment consisting of two to three biological replicates per tissue. The experiment was repeated twice over time for the control lines.

Results

Bioactive GA response is not saturated in the PsGA3ox1-overexpression lines

To investigate whether the internode elongation response to bioactive GA was saturated in the highest transgenic *PsGA3ox1*-overexpression line (TG1), bioactive GA_3 was applied to elongating TG1 and control seedlings and internode length and number were monitored at plant maturity. Application of GA_3 increased the internode length in both the transgenic TG1 and control lines (Figures 3.3A and B), and increased the total number of internodes per plant to a much greater extent in the control than the *PsGA3ox1*-overexpressor line TG1 (Table 3.1). Application of prohexadione-calcium (Apogee; a GA biosynthesis

inhibitor) decreased internode length in both TG1 and C1 lines (Figures 3.3A and B), with a greater decrease in internode length exhibited in the TG1 line compared to the control line (Figure 3.2C). The total number of internodes per plant was decreased by Apogee treatment only in the *PsGA3ox1*-overexpressor line (Table 3.1).

Expression of GA biosynthesis and catabolism genes in sequential internodes

To obtain a more complete developmental picture of bioactive GA and internode growth in elongating pea stems, the expression patterns of the late GA biosynthesis and catabolism genes were monitored in sequentially growing internodes (from internode number two through nine; Figure 3.1) at a similar growth stage (15-20% final size) of the *PsGA3ox1*-overpressor and control lines.

The highest level of transgenic *PsGA3ox1* mRNA was observed in the internodes of TG1 at all nodal positions analyzed, followed by the TG2, then the TG3 (Figure 3.5). Interestingly, transgenic *PsGA3ox1* mRNA of TG1 internodes oscillated from higher to lower levels in the adjacent internodal positions. A similar, but much less pronounced oscillation pattern was exhibited by TG2, but not in the lowest transgenic *PsGA3ox1*-expressor line, TG3 (Figure 3.5). No transgenic *PsGA3ox1* transcripts were detected in transgenic control null lines (data not shown). Total *PsGA3ox1* transcript levels were higher in the internodes at most nodal positions in the TG1 compared to the control, with 4.5- and 3-fold higher levels observed in TG1 internodes at positions eight and nine compared to the control (Figure 3.6A). Total *PsGA3ox1* transcript levels in the internodes of TG2 and TG3 lines were greater than the controls only at the early and later nodal

positions (Figures 3.6B and C). The transcript abundance of *PsGA3ox2* in the elongating internodes was several orders of magnitude lower than that of *PsGA3ox1* when detected (Figures 3.6D, E and F; quantifying *PsGA3ox1* amplicon has a lower efficiency than *PsGA3ox2*; Table A.1.4). In the transgenic lines, *PsGA3ox2* transcript levels were higher than those in the controls in the internodes at position two. However, *PsGA3ox2* transcript abundance markedly decreased in the internode at position three and no transcript was detected in the fourth to seven internodes in either transgenic or control lines (Figures 3.6D, E and F).

In the early nodal positions (internodes 2 to 4), a marked oscillation in *PsGA20ox1* levels occurred in the highest *PsGA3ox1*-overexpressor line TG1, but not in the lower expressor lines TG2 and TG3 (Figures 3.7A, B and C). Elongating internodes from positions five to nine were minimally affected by the presence of the *PsGA3ox1* transgene. Interestingly, the elongating internodes of TG1 exhibited higher *PsGA20ox1* transcript levels in most of the internode positions monitored, but this was not observed in the TG2 and TG3 lines. With the exception of a small peak in elongating internodes at position 3, *PsGA20ox2* transcript abundance was low at all the internode positions assayed, and this expression pattern was minimally affect by the presence of the transgene (Figures 3.7D, E and F).

PsGA2ox1 mRNA levels oscillated from high to low in adjacent internodes of elongating pea stems of the transgenic lines (Figures 3.8A, B and C). Transcript levels were markedly reduced at internodes three, five, seven and

nine, where as transcript levels were increased 130 to 960 times in internodes two, four, six and eight in TG1 and TG2 lines (Figures 3.8A and B). The control lines also exhibited a less pronounced oscillation pattern of *PsGA2ox1* mRNA abundance at earlier and later internode positions. A small peak in *PsGA2ox2* transcript levels occurred in the elongating internodes at position four, and higher levels were observed at position 9 (Figures 3.8 D, E and F). The transgenic lines exhibited higher levels of *PsGA2ox2* mRNA at internode positions two and nine compared to the control lines.

Expression of PIN auxin efflux carrier genes in sequential elongating internodes

Auxin efflux carriers (PIN proteins) are known to play important roles in vascular patterning and their presence and location can influence cellular IAA levels. The expression patterns of the *PsPIN1* and *PsPIN2* (putatively code for PIN proteins in pea) were monitored in sequential elongating internodes [from elongating internodes (15-20% final size) at position two through nine] to determine if their expression patterns are correlated with vascular development, GA flux, and/or other aspects of internode stem growth and development.

PsPIN1 transcript levels were elevated in the elongating internodes at positions 2, 4, 5, 6, and 8 of the transgenic line TG1 compared to the controls (Figure 3.9A). Slightly higher *PsPIN1* transcript levels were also observed in the elongating internodes at most positions assayed in TG2 (Figure 3.9B). A transient decrease in *PsPIN1* transcript levels in the elongating internodes at position 3 followed by a marked increase in *PsPIN1* transcripts in the internodes at position

4 occurred in the transgenic and control lines, with the greatest change in transcript abundance observed in the transgenic TG1 line (Figures 3.9A, B and C). Similarly, another transient decrease in *PsPIN1* transcript levels in the elongating internodes at position 7 followed by an increase in *PsPIN1* transcripts in the internodes at position 8 occurred in the transgenic and control lines, with TG1 exhibiting the greatest change in transcript abundance. Elevated levels of *PsPIN2* transcript were also observed at most nodal positions in TG1 and TG2 compared to the control, and a similar transient decrease in *PsPIN2* transcripts at internode position 3 followed by a marked increase at position 4 also occurred in all lines (Figures 3.9D, E and F).

Defoliation and tendril removal changes expression pattern of PsGA2ox1 and PsPIN1 in elongating internodes

In order to determine the effect of defoliation and tendril removal on the expression pattern of the late GA biosynthesis and catabolism genes and the putative auxin efflux carrier genes *PsPIN1* and *PsPIN2*, removal of tendrils and stipules above and below the elongating internode at positions 7, 8, and 9 was performed when the internode was approximately 2-3 mm in length. Defoliation and removal of tendrils above and below internode 8 when it was at 2-3 mm in size reduced internode length by approximately 20% (when measured in control plants after full length was reached; internode length (mm, n=3) in intact plants 33.0 ± 1.1; in defoliated and tendril removed plants, 25.7 ± 1.4). Defoliation and tendril removal had relatively minor effects on the transcript abundance of transgenic or total *PsGA3ox1* in the internodes at positions 7, 8, and 9 in the

transgenic or control lines (Figures 3.10A, B, C and D). However, the oscillation of *PsGA2ox1* and *PsPIN1* transcript abundance between elongating internodes at positions 7, 8, and 9 was eliminated by removal of these stem organs (Figures 3.11A, B, C and D).

Endogenous GA and IAA levels in sequential elongating internodes

In order to determine if the expression patterns of the GA biosynthesis and catabolism genes are translated into changes in steady-state GA levels, endogenous GA_{20} (precursor to bioactive GA_1), GA_{29} (the 2β-hydroxylated catabolite of GA_{20}), bioactive GA_1, and GA_8 (the 2β-hydroxylated inactive catabolite of GA_1) were determined in the sequential elongating internodes at position 7 and 8 when internodes were approximately at 50% full length, and in the internodes at positions 6 and 7 when internodes were approximately at 80% full length. IAA was also determined in these internodes in order to correlate levels of this hormone with internode growth and flux through the GA pathway.

The elongating internode at position 7 (50% full length) contained higher levels of GA_1 and was longer than the internode at position 8 (50% full length) in the higher *PsGA3ox1*-overexpessor line TG1 (Table 3.2; Figure 3.12). No difference in GA_1 level or internode length was observed between internode 7 and 8 in TG2 or the control lines (Table 3.2; Figure 3.12). Comparison between internodes at positions 6 and 7 at 80% full length in the TG1 line revealed that internode 7 contained significantly higher levels of GA_1 and had longer internodes than that in internode 6 (Table 3.3; Figure 3.13). IAA levels were

generally higher in elongating internodes at 50% full size than those at 80% full size in both the transgenics and the controls (Tables 3.2 and 3.3)

GA_1 transport in pea shoots

In order to more fully understand the role of GAs in stem elongation, it is necessary to understand the synthetic capacity for these hormones in the internodes per se, as well as other possible sources of these hormones that could be transported to the internode. In order to study the pattern of GA_1 transport in elongating pea stems, the distribution of ^{14}C was determined in various parts of the stem after supplying [^{14}C]GA_1 to a pair of expanding stipules. When [^{14}C]GA_1 was applied to the stipules at the 6th node (40-50% of the full size), higher levels of [^{14}C] were detected in the transgenic TG1 line compared to the control line in most tissues assayed (internode -2, I-2; internode -3, I-3; tendril -2, T-2; and apex, A; Figure 3.14). When [^{14}C]GA_1 was applied to the stipules at the 7th node (40-50% of the full size), higher levels [^{14}C] were detected in most tissues assayed (internode -2, I-2; internode -3, I-3; stipule -2, S-2; tendril -1, T-1 and apex, A) in the control line than that in the transgenic TG1 line (Figure 3.15).

Discussion

Ross et al. (1992) reported that the internode length of a tall pea (*Le*) line was up to 300% longer than that in its isogenic dwarf (*le*) line. However, overexpression of *PsGA3ox1 (LE)* in pea, cv. Carneval (which has the *le-1* mutation) only increased internode length approximately 22% in the highest transgenic expression line (Chapter 2). The difference in internode lengths

between the isogenic lines of *LE* and *le* reported by Ross et al. (1992) and the *PsGA3ox1*-overexpressor lines could be due to the expression dynamics of the endogenous promoter versus the 35S CaMV promoter, and/or that a bioactive GA homeostatic mechanism is triggered in the transgenic lines decreasing the levels of bioactive GA and resulting in a more modest increase in internode length. GA_3 application studies revealed that the response of elongating internodes to bioactive GA in the highest *PsGA3ox1*-overexpressor line was not saturated (Fig 3.2A and B). Similar observations were reported when *AtGA20ox1* was overexpressed in Arabidopsis, where hypocotyl length was increased when treated with GA_3 in both transgenic and wild-type lines (Huang et al., 1998). Application of the GA biosynthesis inhibitor prohexadione-calcium (Apogee) decreased internode length in the *PsGA3ox1*-overexpressor line TG1 to a greater extent than the control line (Figure 3.4). Since Apogee reduces growth mainly by inhibiting conversion of GA_{20} to bioactive GA_1 (by competing for 2-oxoglutarate, a required cofactor for GA 3β-hydroxylases; Rademacher, 2000), the greater reduction in growth observed in the Apogee-treated *PsGA3ox1*-overexpressor line compared to the Apogee-treated control line is confirmatory that the increased internode length in TG1 was the result of higher GA_1 levels.

GA homeostasis in elongating pea shoots

Expression analysis of late GA biosynthesis and catabolism genes and determination of endogenous GA levels in transgenic and control internodes (at position 8) demonstrated that the transcript levels of the GA catabolic gene *PsGA2ox1* (Chapter 2; Figure 2.9D) and GA_{29} levels (the product of enzyme

coded for by *PsGA2ox1*; Chapter 2; Figure 2.12D) were higher in the internodes (at position 8) of the *PsGA3ox1*-overexpressor lines than in the control line. These data suggested that feedback regulation of GA biosynthesis in elongating internodes was triggered by the overexpression of *PsGA3ox1*. In order to broaden our understanding of the effects of *PsGA3ox1*-overexpression on coordination of tissue growth and development in the stem, expression of the late GA biosynthesis and catabolism genes and GA as well as IAA levels were monitored in sequentially growing internodes.

GA expression analysis of elongating internodes (at 15 to 20% full length) at positions 2 to 9 (Figure 3.1) revealed a much greater and more consistent oscillation of the transcript levels of the GA catabolite gene *PsGA2ox1* between adjacent internodes in the *PsGA3ox1*-overexpressor lines than the control lines (Figures 3.7A, B and C). Furthermore, in the highest *PsGA3ox1*-overexpressor line TG1, endogenous GA_1 levels and internode length were greater in internode 7 (which had lower *PsGA2ox1* transcript levels), whereas GA_1 levels and internode length were lower in internode 8 (which contained higher *PsGA2ox1* mRNA levels) when internodes were assessed at approximately 50% final length (Table 3.2 and Figures 3.8A, B and C; Figure 3.12). A similar pattern of bioactive GA_1 levels, internode length, and *PsGA2ox1* transcript levels was observed in the internodes at position 6 and 7 of TG1 when they were assessed at approximately 80% final length (Table 3.3 and Figures 3.8A, B and C; Fig 3.13). These data suggest that, when a specific threshold level of bioactive GA_1 in the internode is exceeded, a feedback mechanism is triggered in the adjacent elongating internode

resulting in the upregulation of the GA catabolic gene *PsGA2ox1*, that in turn, will reduce the levels of bioactive GA_1 in this developing internode as part of a mechanism to regulate bioactive GA levels to maintain internode elongation within a specific range.

GA expression analysis of elongating internodes (at 15 to 20% full length) at positions 2 to 9 also revealed that levels of transgenic *PsGA3ox1* mRNA oscillated from higher to lower levels in the adjacent nodal positions, with the most pronounced oscillation detected in the internodes of the highest transgenic *PsGA3ox1*-expressor line TG1, followed by a modest oscillation pattern in TG2, and no discernable pattern detected in the lowest transgenic *PsGA3ox1*-expressor line TG3 (Figure 3.5). The transgenic *PsGA3ox1* mRNA oscillation pattern is similar to that observed for *PsGA2ox1* in TG1. It is possible that in the internodes at nodal positions that have high *PsGA2ox1* expression and lower bioactive GA_1, the half-life of transgenic *PsGA3ox1* is greater (degradation of message is slower) leading to higher levels of this mRNA than in internodes at nodal position that have lower *PsGA2ox1* and higher bioactive GA_1 levels. These data suggest that regulation of bioactive GA levels likely occurs at both the transcriptional and post-transcriptional levels.

In order to determine other possible sources of GAs that could be transported to the internode, the pattern of [^{14}C] accumulation was assessed after application of [^{14}C]GA_1 to the stipules at nodes 6 and 7 (Figures 3.14 and 3.15). When stipules at node 6 were treated with [^{14}C]GA_1, more [^{14}C] was detected in internode 7 of the TG1 line (contains higher GA_1 levels and lower *PsGA2ox1*

transcript levels), as well as in the tendril (T-2) and apex (A) tissues of TG1 than in the control line (Fig. 3.14). In contrast, when stipules at node 7 were treated with [^{14}C]GA_1, less [^{14}C] was detected in internode 8 of the TG1 line (contains lower GA_1 levels and higher *PsGA2ox1* transcript levels) as well as in internode (I-3), stipule (S-2), and apex (A) tissues of TG1 than in the control line (Fig. 3.15). These data suggest that the stipules could be another source of bioactive GA_1 for the elongating internodes, if required. Consistently, data from Probsting et al. (1992) support that both GA_{20} and GA_1 can be transported within the pea stem. Furthermore, removal of stipules and tendrils above and below the elongating internodes 7, 8 and 9 eliminated the oscillation pattern of *PsGA2ox1* transcripts in the adjacent internodes of the *PsGA3ox1*-overexpressor lines TG1 and TG2, as well as in the control line (Figures 3.11A and B) indicating that the stipules or both stipules and tendrils affect GA homeostasis in the elongating pea internodes. Consistently, it was noted that a marked reduction in pea internode GA_1 levels when the upper mature leaves including leaflets, petioles and tendrils were removed from 21-day old wild-type plants (Jager et al., 2007).

Putative auxin efflux carrier gene expression and vascular development

In general, both *PsPIN1* and *PsPIN2* transcript levels were observed to be higher in most internodes of the transgenic lines compared to the controls (Figures 3.8A, B, C, D, E, and F). Chawla and DeMason (2004) also observed an increase in *PsPIN1* mRNA levels in pea internode segments when the uppermost internodes of the 7 d-old pea seedlings were treated with 50µM GA_3. Expression

of *PttPIN1* was also induced in *Populus* stem tissues by about 50% with bioactive GA_4 treatment (Bjorklund et al., 2007).

The capacity of auxin to stimulate vascular differentiation is well established (Aloni, 2004). Exogenous auxin can trigger the formation of new vascular strands in mature organs (Jacobs, 1952) and IAA-overproducing transgenic petunia plants produced approximately twice the number of vascular tissues compared to wild-type plants (Klee et al., 1987). The Arabidopsis *pin-formed* mutant *pin1* exhibited reduced auxin transport activity relative to that in the wild-type plants (Okada et al., 1991). Genetic disruption of *AtPIN1* led to enhanced xylem formation just below the young auxin synthesizing leaves in Arabidopsis (Galweiler et al., 1998) and Mattsson et al., (1999) observed enhanced vascularization in leaves of the *pin1* mutant in Arabidopsis. Based on these observations, Berleth and Mattsson, (2000) suggested that the increased vascularization observed in these studies was due to the auxin accumulation in these mutants.

A transient decrease in *PsPIN1* and *PsPIN2* transcript levels in the elongating internodes at position 3 followed by a marked increase of these transcripts in the internodes at position 4 occurred in the transgenic and control lines (Figures 3.9A, B, C, D, E and F). According to Hayward (1938), the first three internodes in pea (*Pisum sativum* L.) exhibit a vascular structure that is transitioning from vascular connections to the cotyledons to that which is present in the stem proper (vascular connection to stipules, tendrils, and axillary vegetative and floral branches). At the second internode, the vascular structure

within the stele is composed of two polar bundles which supply the leaves, two bands of exarch xylem, and six groups of phloem (two are subtending the polar bundles and the other four are arranged in pairs lateral to the xylem; Figure 2.7B; Chapter 2). By the fourth internode, the transition of the vascular structure to that found in the mature stem is complete. There are two polar vascular bundles which supply the leaves and at right angles to them, two more vascular bundles which supply the stipules, and no exarch xylem is present. The number of vascular bundles can be increased in the ring because of the downward divergence of the vascular traces from the vegetative axes such as axillary shoots (Figure 2.8; Chapter 2). The drop in transcript levels of the putative auxin efflux genes *PsPIN1* and *PsPIN2* observed at internode 3 likely reflect the requirement of auxin accumulation at specific sites within this internode for the vascular re-patterning events occurring in this internode which are completed by internode 4 (Figures 3.9 A, B, C, D, E, and F). Additionally, the *PsGA3ox1*-overexpressor line TG1 exhibited a second decrease in *PsPIN1* transcript levels at internode 7 which was not mimicked to this extent in the other transgenic or control lines (Figures 3.9A, B and C). Transverse cross-sections of internode 8 at 50% maturity revealed that the TG1 line had significantly higher number of vascular bundles compared to both TG2 and the control line at this developmental stage and nodal position (Table 2.3 and Figure 2.6). The marked decrease in transcript abundance of *PsPIN1* and *PsPIN2* in internode 7 of TG1 is correlated with the significant increase in stem vascular bundles appearing in internode 8 of this line (Table 2.3 and Figure 2.6). Therefore, these data suggest that bioactive GA can advance the

formation of the vascular connections from the internode to the axillary bud at higher nodal positions in the plant.

In summary, GA_3 application studies revealed that the response of elongating internodes to bioactive GA in the *PsGA3ox1*-overexpressor lines was not saturated. Expression analysis of transgenic *PsGA3ox1* and other late GA genes of elongating internodes (at 15 to 20% full length) at positions 2 to 9 revealed a consistent and a much greater oscillation of the transcript levels of the GA catabolic gene *PsGA2ox1* between adjacent internodes in the *PsGA3ox1*-overexpressor lines. In the highest *PsGA3ox1*-overexpressor line, steady state endogenous GA_1 levels and internode length were inversely correlated with the *PsGA2ox1* mRNA levels. These data suggest that when a specific threshold level of bioactive GA_1 in the internode is exceeded, a feedback mechanism is triggered in the adjacent elongating internode resulting in the upregulation of the GA catabolic gene *PsGA2ox1*, that in turn, will reduce the levels of bioactive GA_1 in this developing internode as part of a mechanism to regulate bioactive GA levels and growth. The distribution patterns of ^{14}C-label after application of [^{14}C]GA_1 to expanding stipules suggested that expanding stipules could be another source of bioactive GA_1 for the elongating internodes. And lastly, the expression patterns of the putative auxin efflux carrier genes, *PsPIN1* and *PsPIN2* reflected vascular re-patterning events occurring in internodes of the growing stem.

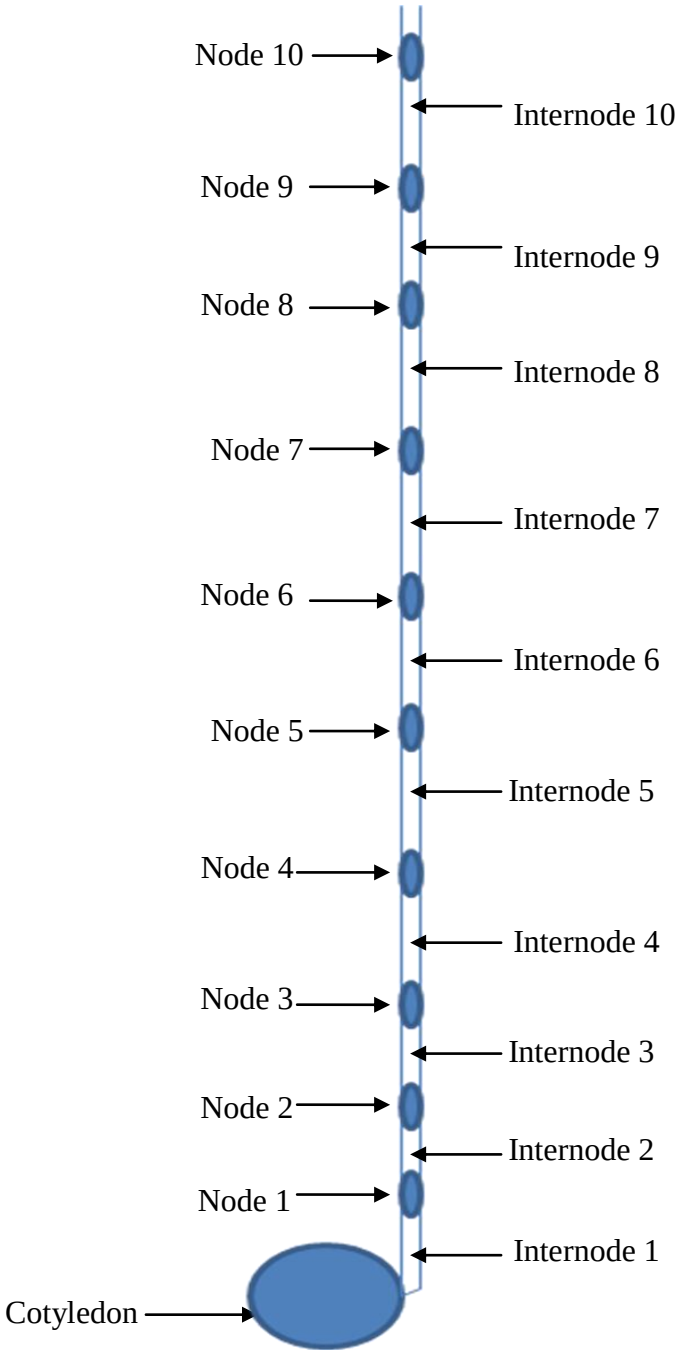

Figure 3.1. Schematic representation of the node and internode numbering system used in this study.

Figure 3.2. Defoliation and tendril removal experiment. A representative plant prior to harvesting of internode. Arrows indicate the nodes in which stipules and tendrils were removed 24 h prior to harvesting. The internodes between defoliated nodes were harvested when 5-7 mm in size for total RNA extraction.

Table 3.1. Number of internodes per plant in transgenic and control lines in response to 100 μM GA_3 in 0.1% aqueous Tween 80, 3.61 mM prohexadione-calcium (Apogee) in 0.1% aqueous Tween 80 or control (0.1% aqueous Tween 80) solutions.

Lines	Treatments		
	Control	GA_3 treated	Apogee treated
TG1	39.0±0.4[a]y[b]	42.3±0.6y	35.6±0.9y
C1	31.1±0.7z	40.5±1.3y	34.5±0.7y

[a] Data are means ± SE, n=8 to 12.

[b] Means followed by different letters (y, z) indicate significant difference between TG1 and C1 within treatments by ANOVA and mean separation using single tail *t*-test ($P<0.05$). Variation between treatments cannot be directly compared due to a significant treatment × line interaction.

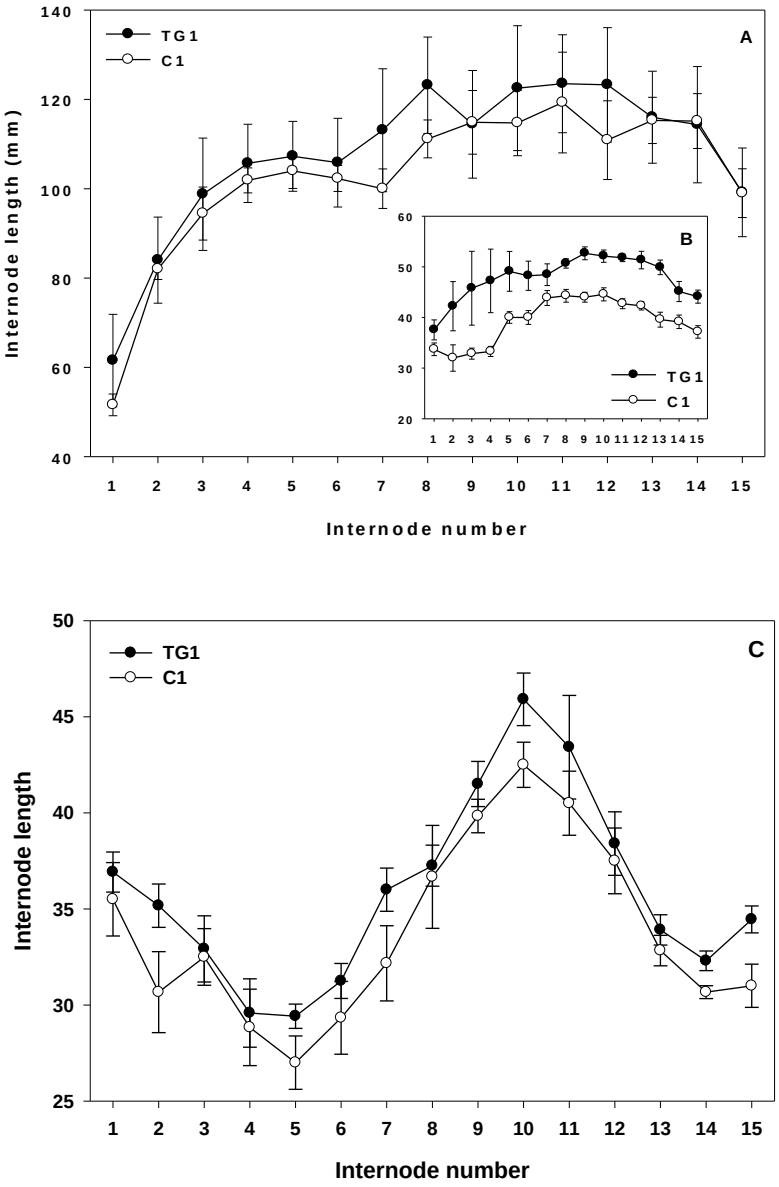

Figure 3.3. Internode lengths at maturity of the transgenic line TG1 and the control line C1 from internode 1 to 15 treated with A, 100 μM GA_3 in 0.1% aqueous Tween 80; C, 3.61 mM prohexadione-calcium (Apogee) in 0.1% aqueous Tween 80; B, 0.1% aqueous Tween 80 solutions (control treatment) . Data are means ± SE, n= 7 to 12.

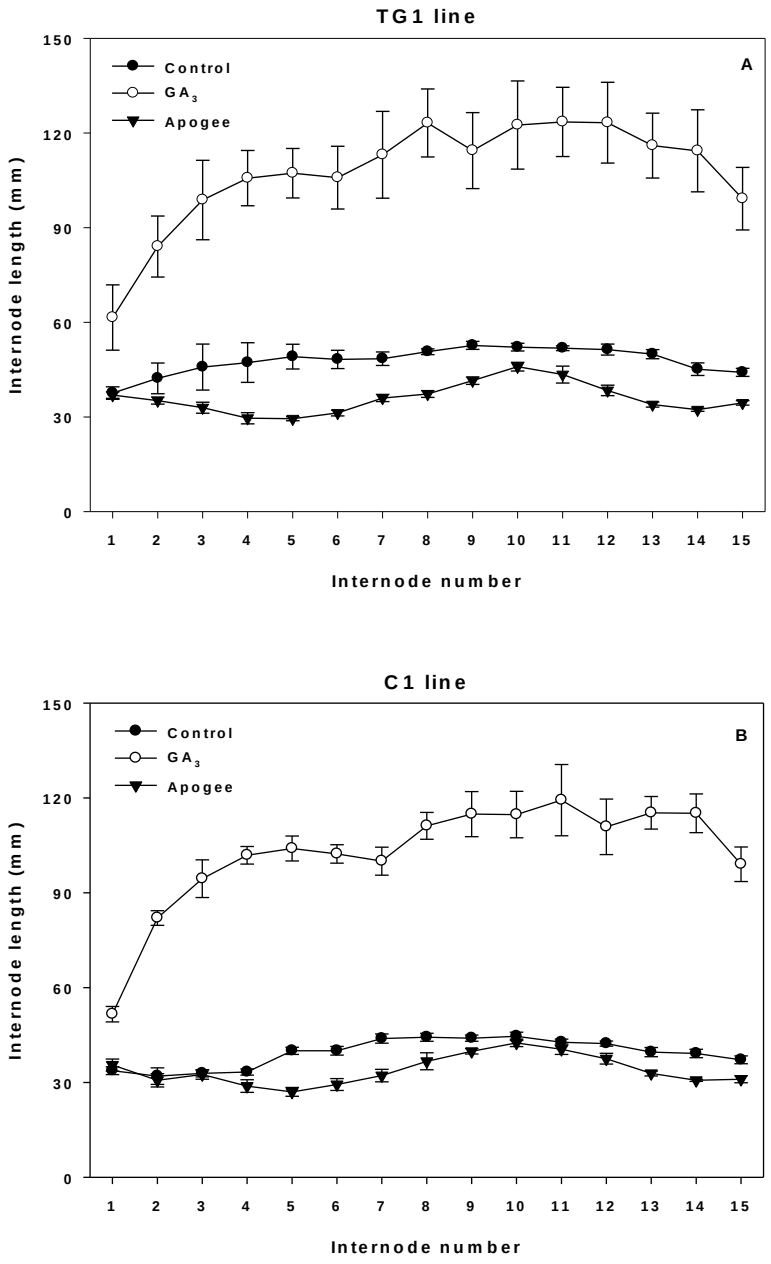

Figure 3.4. Internode lengths at maturity of A, the transgenic line TG1; and B, the control line C1 from internode 1 to 15 treated with 100 µM GA_3 in 0.1% aqueous Tween 80, 3.61 mM prohexadione-calcium (Apogee) in 0.1% aqueous Tween 80 or 0.1% aqueous Tween 80 (control treatment) solutions. Data are means ± SE, n= 7 to 12.

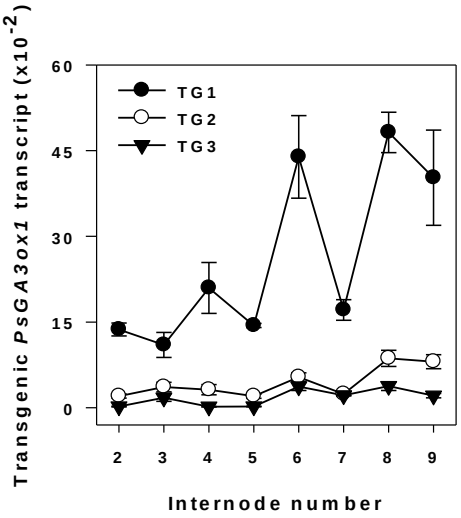

Figure 3.5. Relative abundance of transgenic *PsGA3ox1* transcripts in internodes two through nine of transgenic lines TG1, TG2, and TG3. Transcript levels were compared across lines using the tendril stage 2 *PsGA20ox2* (Ct=37.96) samples of TG1 as a reference for normalization (Chapter2). Data are means ± SE of two to three biological replicates. Internodes were harvested at 15-20% of their final length for total RNA extraction.

Figure 3.6. Relative transcript abundance of A, B and C, total *PsGA3ox1* (transgenic + endogenous); and D, E and F, *PsGA3ox2* in internodes two through nine of transgenic lines TG1, TG2, and TG3 and controls (C1 and C3). Transcript levels were compared across genes and lines using the tendril stage 2 *PsGA20ox2* (Ct=37.96) samples of TG1 as a reference for normalization (Chapter 2). Data are means ± SE of two to three biological replicates. Internodes were harvested at 15-20% of their final length for total RNA extraction.

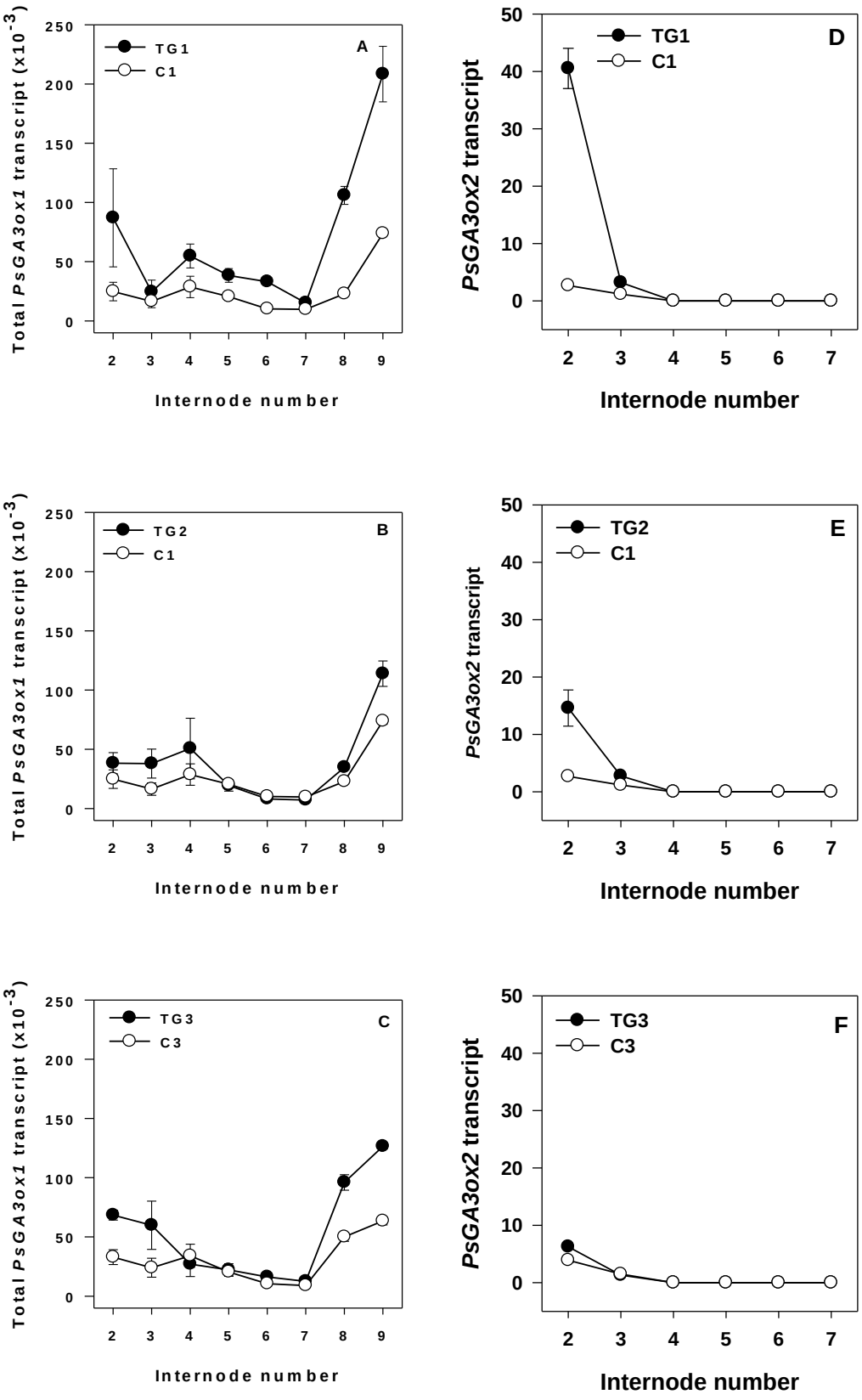
A
TG1
C1
Total PsGA3ox1 transcript (x10-3)
Internode number
B
TG2
C1
Total PsGA3ox1 transcript (x10-3)
Internode number
C
TG3
C3
Total PsGA3ox1 transcript (x10-3)
Internode number
D
TG1
C1
PsGA3ox2 transcript
Internode number
E
TG2
C1
PsGA3ox2 transcript
Internode number
F
TG3
C3
PsGA3ox2 transcript
Internode number

Figure 3.7. Relative transcript abundance of A, B and C, *PsGA20ox1*; and D, E and F, *PsGA20ox2* in internodes two through nine of transgenic lines TG1, TG2, and TG3 and their controls (C1 and C3). Transcript levels were compared across genes and lines using the tendril stage 2 *PsGA20ox2* (Ct=37.96) samples of TG1 as a reference for normalization (Chapter 2). Data are means ± SE of two to three biological replicates. Internodes were harvested at 15-20% of their final length for total RNA extraction.

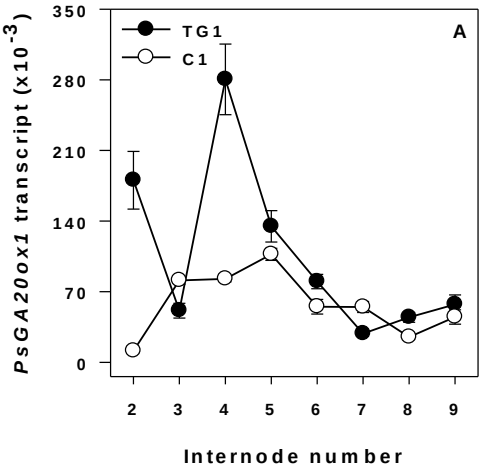
TG1
C1
A
PsGA20ox1 transcript (x10-3)
350
280
210
140
70
0
2 3 4 5 6 7 8 9
Internode number

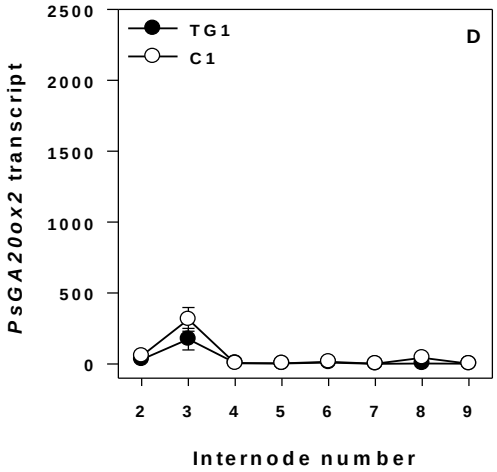
TG1
C1
D
PsGA20ox2 transcript
2500
2000
1500
1000
500
0
2 3 4 5 6 7 8 9
Internode number

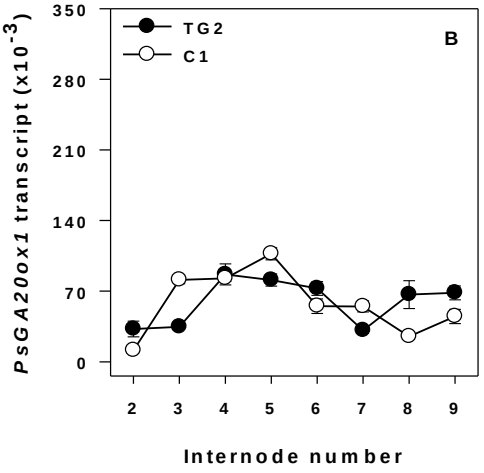
TG2
C1
B
PsGA20ox1 transcript (x10-3)
350
280
210
140
70
0
2 3 4 5 6 7 8 9
Internode number

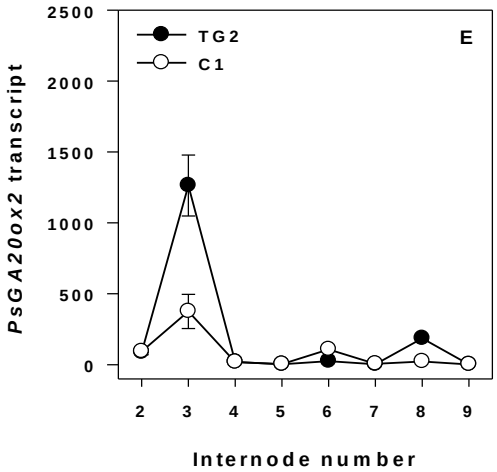
TG2
C1
E
PsGA20ox2 transcript
2500
2000
1500
1000
500
0
2 3 4 5 6 7 8 9
Internode number

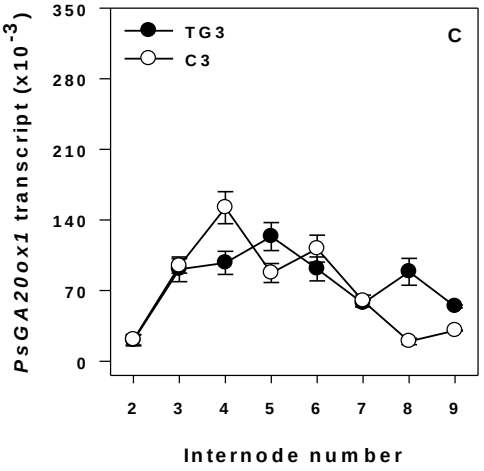
TG3
C3
C
PsGA20ox1 transcript (x10-3)
350
280
210
140
70
0
2 3 4 5 6 7 8 9
Internode number

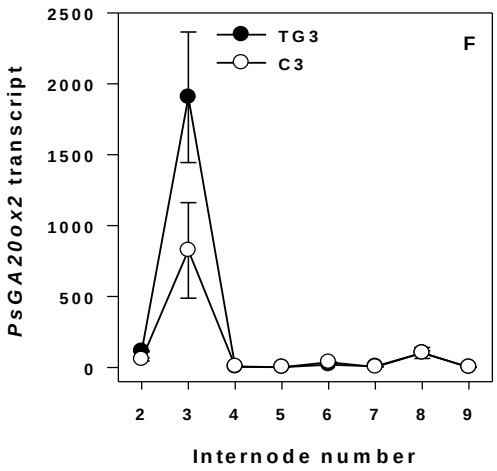
TG3
C3
F
PsGA20ox2 transcript
2500
2000
1500
1000
500
0
2 3 4 5 6 7 8 9
Internode number

Figure 3.8. Relative transcript abundance of A, B and C, *PsGA2ox1*; and D, E and F, *PsGA2ox2* in internodes two through nine of transgenic lines TG1, TG2, and TG3 and their controls (C1 and C3). Transcript levels were compared across genes and lines using the tendril stage 2 *PsGA20ox2* (Ct=37.96) samples of TG1 as a reference for normalization (Chapter 2). Data are means ± SE of two to three biological replicates. Internodes were harvested at 15-20% of their final length for total RNA extraction.

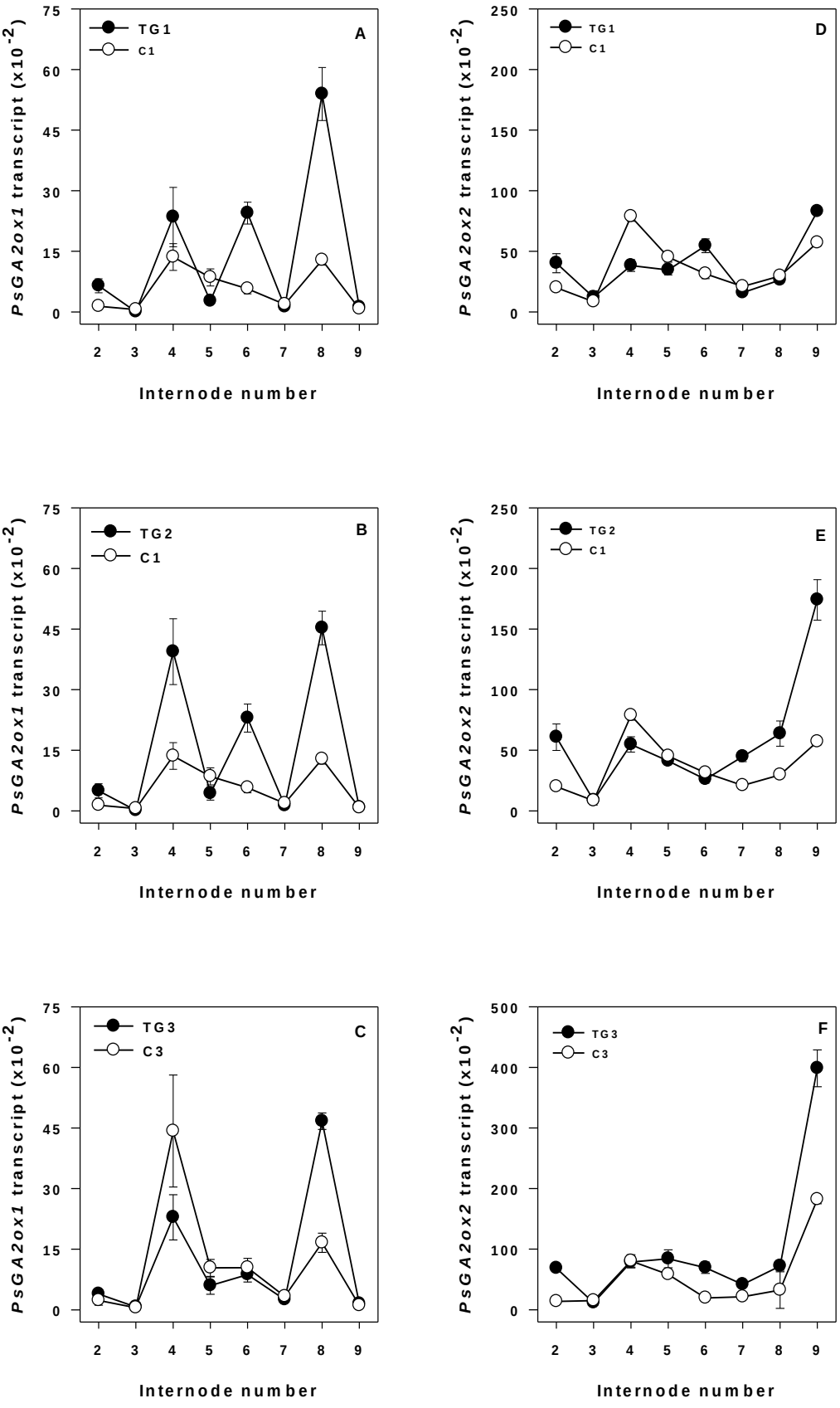
A
TG1
C1
PsGA2ox1 transcript (x10-2)
Internode number
B
TG2
C1
PsGA2ox1 transcript (x10-2)
Internode number
C
TG3
C3
PsGA2ox1 transcript (x10-2)
Internode number
D
TG1
C1
PsGA2ox2 transcript (x10-2)
Internode number
E
TG2
C1
PsGA2ox2 transcript (x10-2)
Internode number
F
TG3
C3
PsGA2ox2 transcript (x10-2)
Internode number

Figure 3.9. Relative transcript abundance of A, B and C, *PsPIN1*; and D, E and F, *PsPIN2* in internodes two through nine of transgenic lines TG1, TG2, and TG3 and their controls (C1 and C3). Transcript levels were compared across genes and lines using the tendril stage 2 *PsGA20ox2* (Ct=37.96) samples of TG1 as a reference for normalization (Chapter 2). Data are means ± SE of two to three biological replicates. Internodes were harvested at 15-20% of their final length for total RNA extraction.

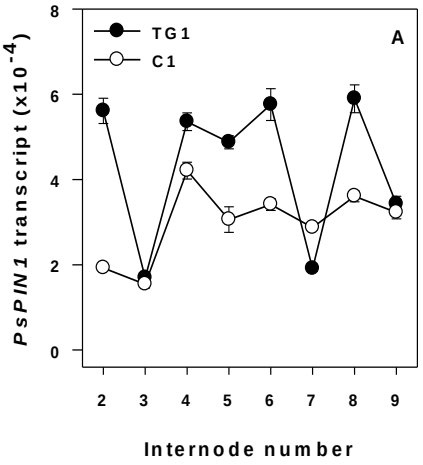
TG1
C1
A
PsPIN1 transcript (x10-4)
Internode number

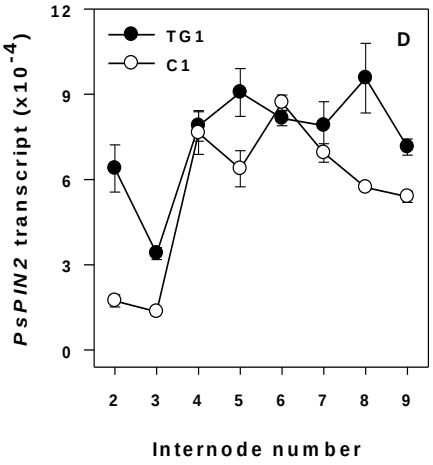
TG1
C1
D
PsPIN2 transcript (x10-4)
Internode number

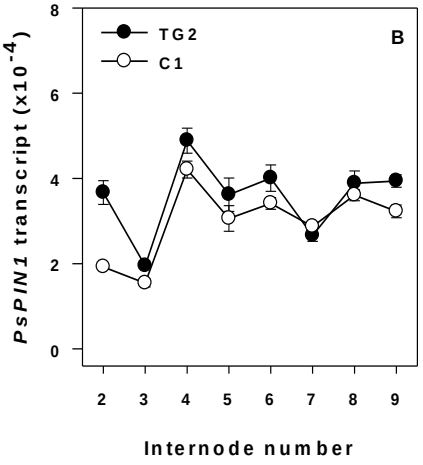
TG2
C1
B
PsPIN1 transcript (x10-4)
Internode number

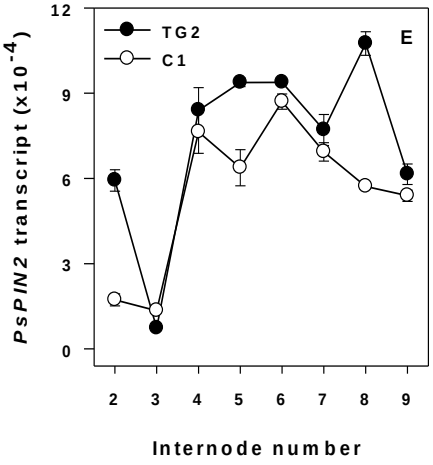
TG2
C1
E
PsPIN2 transcript (x10-4)
Internode number

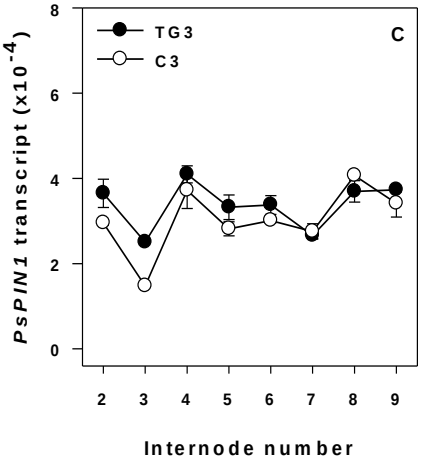
TG3
C3
C
PsPIN1 transcript (x10-4)
Internode number

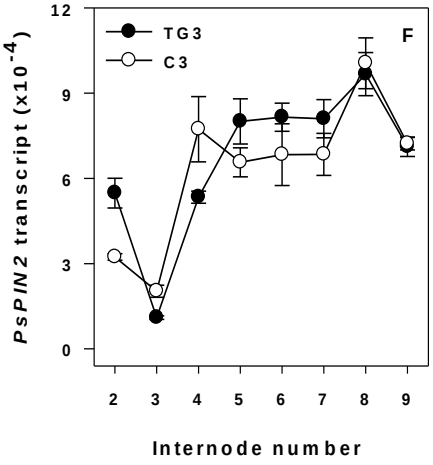
TG3
C3
F
PsPIN2 transcript (x10-4)
Internode number

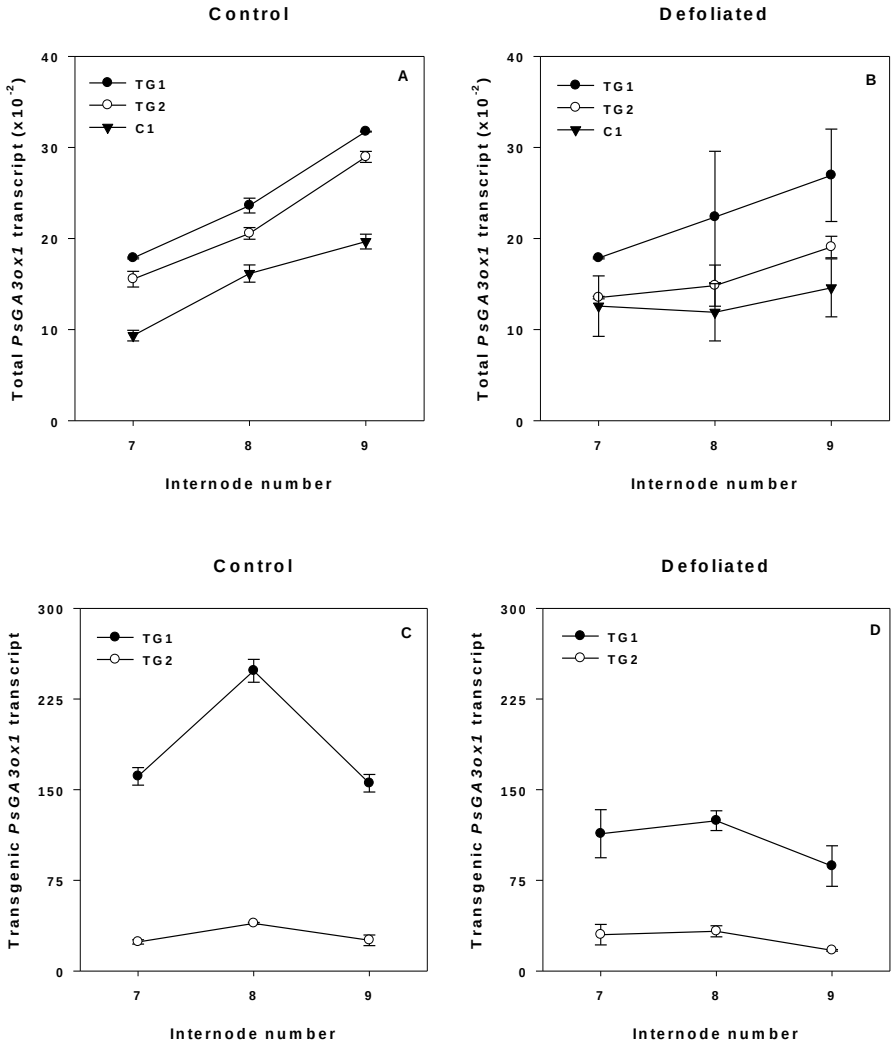

Figure 3.10. Relative transcript abundance of A and B, total *PsGA3ox1*; and C and D, transgenic *PsGA3ox1* in the internodes at positions 7, 8, and 9 of intact (control) and defoliated and tendril removed plants of transgenic lines TG1, TG2, and the control line, C1. Transcript levels were compared across genes and lines using the tendril stage 2 *PsGA20ox2* (Ct=37.96) samples of TG1 as a reference for normalization (Chapter 2). Data are means ± SE of two to three biological replicates. Internodes were harvested at when they were 5-7 mm in size for total RNA extraction.

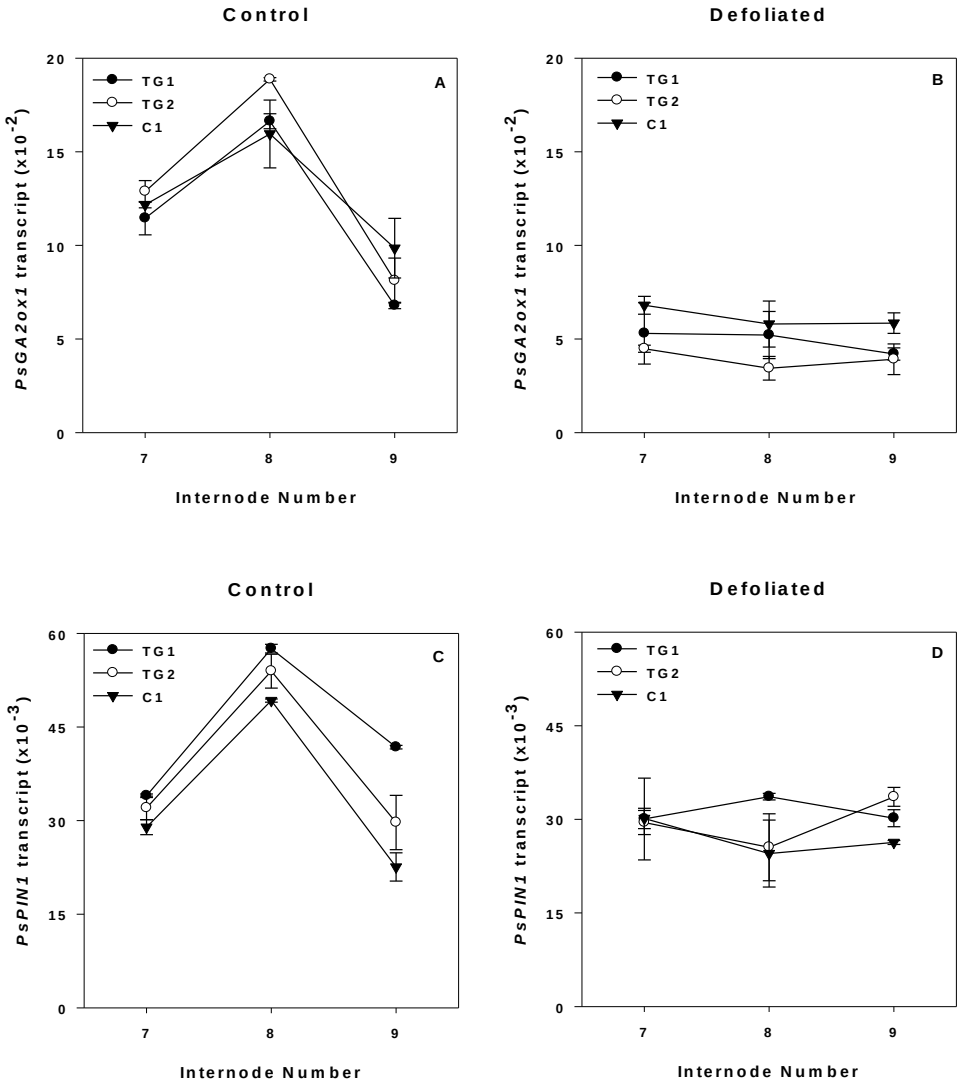

Figure 3.11. Relative transcript abundance of A and B, *PsGA2ox1*; and C and D, *PsPIN1* in the internodes at positions 7, 8, and 9 of intact (control) and defoliated and tendril removed plants of transgenic lines TG1, TG2, and the control line, C1. Transcript levels were compared across genes and lines using the tendril stage 2 *PsGA20ox2* (Ct=37.96) samples of TG1 as a reference for normalization (Chapter 2). Data are means ± SE of two to three biological replicates. Internodes were harvested at when they were 5-7 mm in size for total RNA extraction.

Table 3.2. Endogenous GAs and IAA content in internodes 7 and 8 (50% final size) of transgenic lines TG1 and TG2, and the control line C1.

		ng gdw^{-1}				
Line	Internode	GA_1	GA_8	GA_{20}	GA_{29}	IAA
TG1	8	1.82±0.43[a]	95.7±15.6	630.7±106.4	577.9±20.6	784.4±67.9
TG2	8	0.99±0.18	50.3±3.0	608.1±256.4	567.4±62.3	873.4±65.7
C1	8	1.30±0.31	45.4±3.6	650.3±151.0	427.7±13.9	682.3±59.1
TG1	7	4.24±0.94	48.0±1.4	424.8±157.9	833.9±156.2	715.3[b]
TG2	7	1.39±0.46	47.9±1.1	1059±154.8	487.3±23.9	804.2
C1	7	1.22±0.56	85.7±0.6	447.0±38.7	1125.5±193.1	782

[a] Data are means ± SE, n=2.

[b] 1 sample.

Table 3.3. Endogenous GAs and IAA content in internodes 6 and 7 (80% final size) of transgenic lines TG1 and TG2, and the control line C1.

		ng gdw^{-1}				
Line	Internode	GA_1	GA_8	GA_{20}	GA_{29}	IAA
TG1	7	2.07±0.46[a]	22.88±5.78	150.5±81.6	290.8±72.9	699.2±83.8
TG2	7	Lost	20.81±4.14	170.0±34.6	296.3±19.7	533.6±59.0
C1	7	0.35±0.04	18.61±1.9	178.3±30.3	314.8±9.0	623[b]
TG1	6	0.34±0.1	14.8±3.9	142.7±0.3	208.7±24.5	546.9±18.2
TG2	6	0.65±0.0	17.1±4.5	225.5±5.1	169.1±20.6	613.7[b]
C1	6	0.48±0.2	18.4±1.0	246.4±34.1	157.1±3.6	646.6±98.0

[a] Data are means ± SE, n= 2.

[b] 1 sample.

Table 3.4. Endogenous GAs and IAA content in stipules at nodal position 8 at 40% full size and 80% final size of transgenic lines TG1 and TG2, and the control line C1.

		ng gdw^{-1}				
Line	Stipule size	GA_1	GA_8	GA_{20}	GA_{29}	IAA
TG1	40%	12.85[a]	74.47	554.44	541.24	192.71
TG2	40%	10.36	38.74	875.86	378.44	83.93
C1	40%	12.22	31.26	1001.6	664.17	82.83
TG1	80%	1.94±0.09 [b]	25.28±3.08	63.80±17.29	154.67±4.12	591.72±5.7
TG2	80%	1.70±0.41	22.38±1.89	160.46±19.13	153.32±39.4	559.08[c]
C1	80%	2.18±0.42	19.60±2.54	129.19±11.34	184.29±20.4	476.58±3.6

[a] Data are means ± SE, n= 1 for 40% full size samples.

[b] Data are means ± SE, n= 2 for 80% full size samples.

[c] 1 sample.

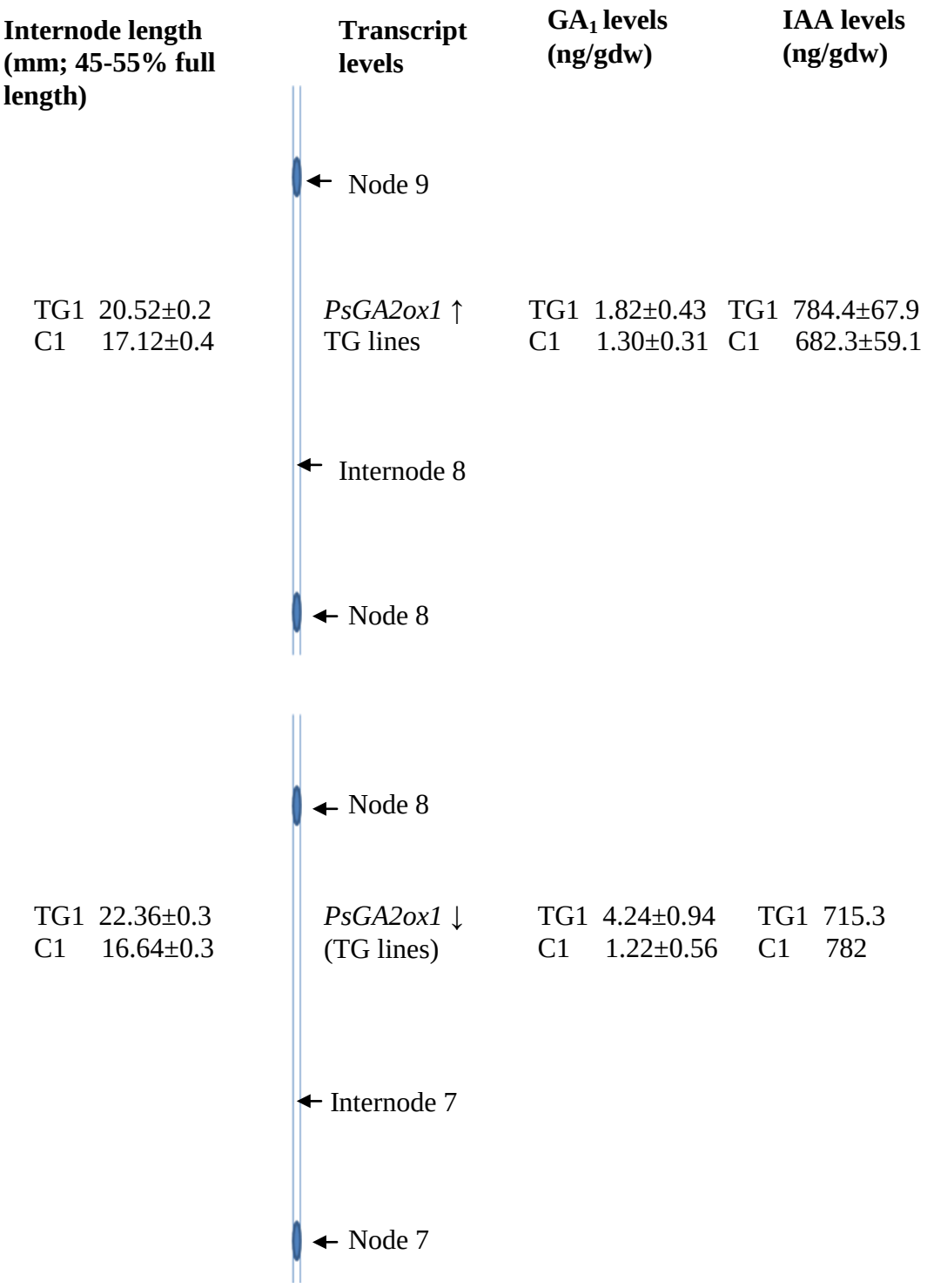

Figure 3.12. Internode length, GA_1 and IAA contents of internodes 7 and 8 (45-55% full length) and *PsGA2ox1* oscillation pattern.

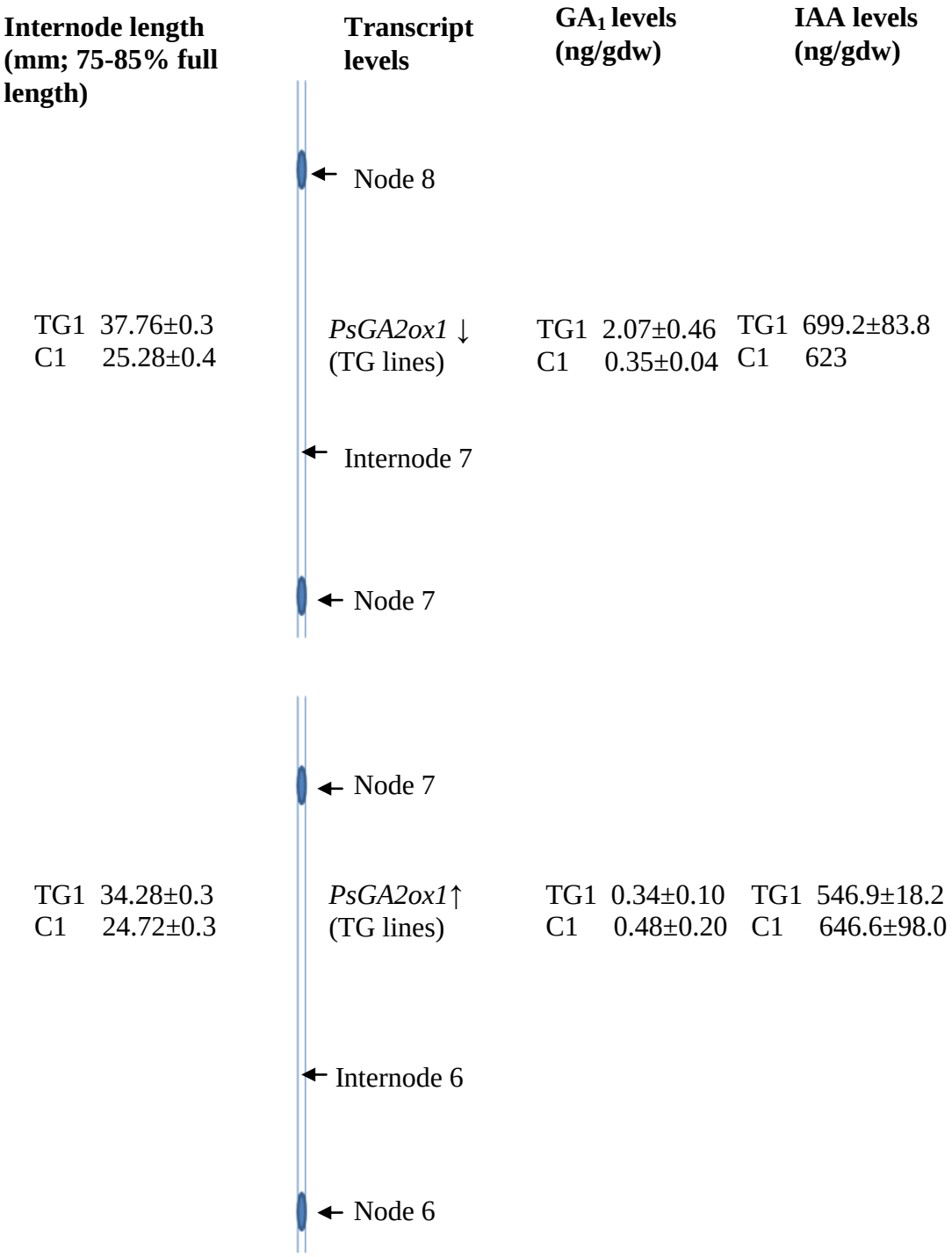

Figure 3.13. Internode length, GA_1 and IAA contents of internodes 6 and 7 (75-85% full length) and *PsGA2ox1* oscillation pattern.

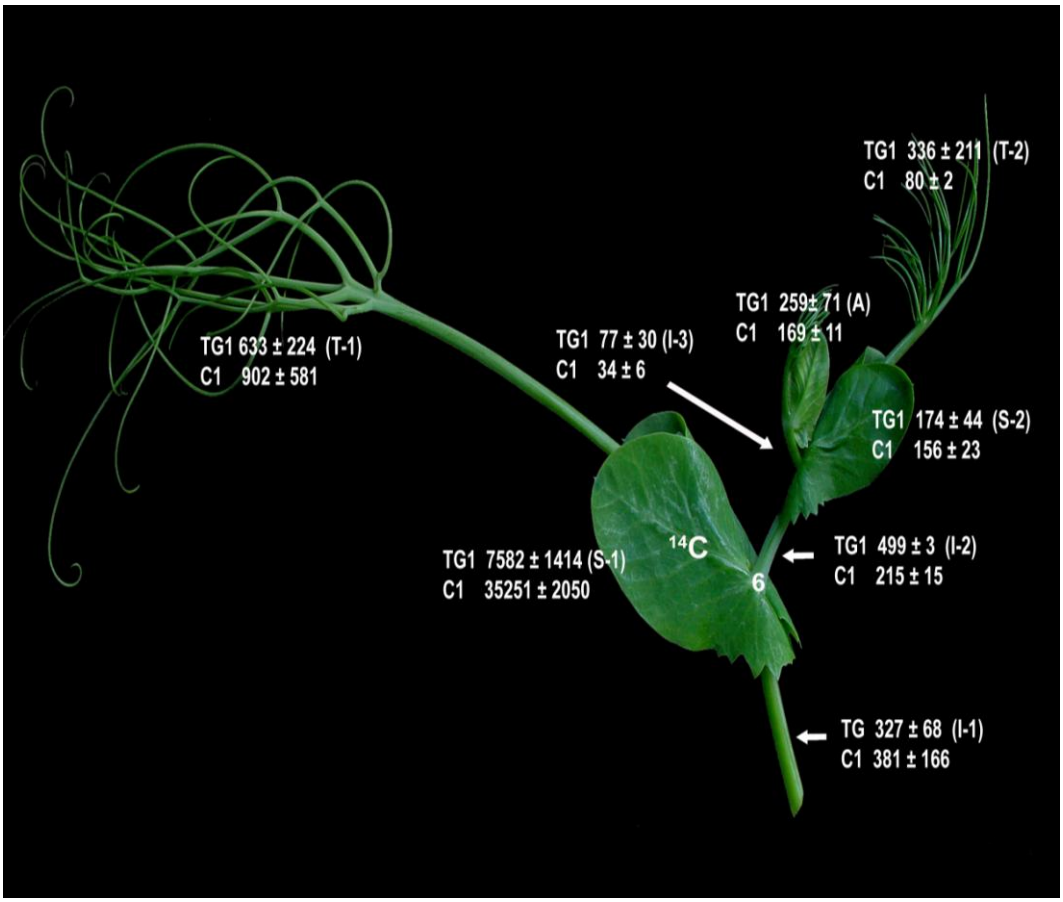

Figure 3.14. Transport of ^{14}C to different organs in the developing pea shoot when [^{14}C]GA_1 was applied to the stipules at node 6. The tissues were harvested 40 h after [^{14}C]GA_1 application and extractable radioactivity (dpm) is denoted in individual tissues assayed. Data are means ± SE, n= 2 to 3.

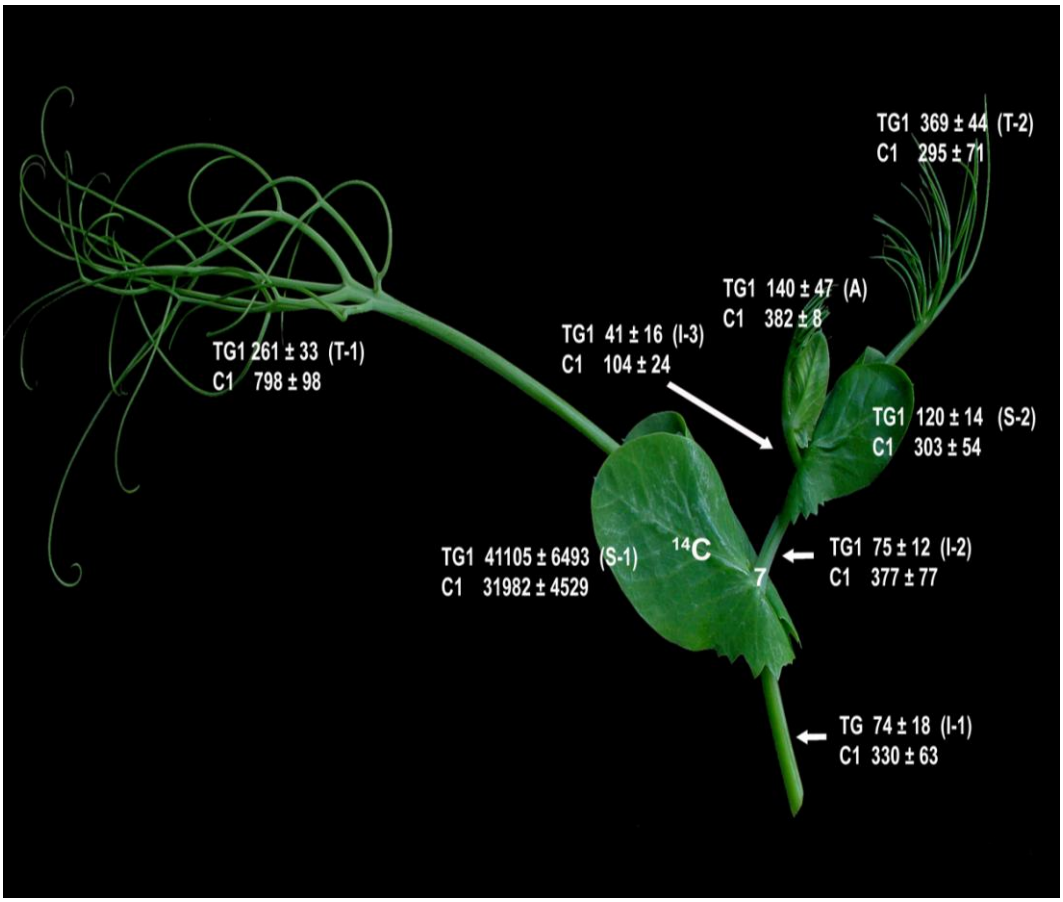

Figure 3.15. Transport of ^{14}C to different organs in the developing pea shoot when [^{14}C]GA_1 was applied to the stipules at node 7. The tissues were harvested 40 h after [^{14}C]GA_1 application and extractable radioactivity (dpm) is denoted in individual tissues assayed. Data are means ± SE, n= 2 to 3.

Literature cited:

Aloni, R (2004) The Induction of Vascular Tissues by Auxin: *In* PJ Davis, ed, Plant hormones: Biosynthesis, signal transduction, action. Ed 3. Kluwer Academic Publishers, Dordrecht, The Netherlands, pp 471-492

Ayele BT, Ozga JA, Kurepin LV, Reinecke DM (2006) Developmental and embryo axis regulation of gibberellin biosynthesis during germination and young seedling growth of pea. Plant Physiol **142**: 1267-1281

Berleth T, Mattsson J (2000) Vascular development: tracing signals along veins. Curr Opin Plant Biol **3**: 406-411

Bjorklund S, Antti H, Uddestrand I, Mortiz T, Sundberg B (2007) Cross-talk between gibberellin and auxin in development of *Populus* wood: gibberellin stimulates polar auxin transport and has a common transcriptome with auxin. Plant J **52**: 499-511

Brian PW, Hemming HG (1957) A relation between the effects of gibberellic acid and indolylacetic acid on plant cell expansion. Nature **179**: 417

Chawla R, DeMason DA (2004) Molecular expression of *PsPIN1*, a putative auxin efflux carrier gene form pea (*Pisum sativum* L.) Plant Growth Reg **44**: 1-14

Davies PJ (2004) The plant hormones: their nature, occurrence, and functions. *In* PJ Davis, ed, Plant hormones: Biosynthesis, signal transduction, action. Ed 3. Kluwer Academic Publishers, Dordrecht, The Netherlands, pp 1-15

Fleet CM, Yamaguchi S, Hanada A, Kawaide H, David CJ, et al (2003) Overexpression of *AtCPS* and *AtKS* in *Arabidopsis* confers increased *ent*-kaurene production but no increase in bioactive gibberellins. Plant Physiol **132**: 830-839

Frigerio M, Alabadi D, Perez-Gomaez J, Garcia-Carcel L, Phillips AL, et al. (2006) Transcriptional regulation of gibberellin metabolism genes by auxin signalling in *Arabidopsis*. Plant Physiol **142**: 553-563

Friml J, Palme K (2002) Polar auxin transport- old questions and new concepts? Plant Mol Biol **49**: 273-284

Friml J, Vieten A, Sauer M, Weijers D, Schwarz H, et al. (2003) Efflux-dependent auxin gradients establish the apical-basal axis of Arabidopsis. Nature **426**: 147-153

Fu X, Harberd NP (2003) Auxin promotes Arabidopsis root growth by modulating gibberellin response. Nature **421**: 740-743

Gallego-Giraldo L, Ubeda-Tomas S, Gisbert C, Garcia-Martinez JL, Moritz T, et al. (2008) Gibberellin homeostasis in tobacco is regulated by gibberellin metabolism genes with different gibberellin sensitivity. Plant Cell Physiol **49**: 679-690

Galweiler L, Changhui G, Muller A, Wiseman E, Mendgen K et al (1998) Regulation of polar auxin Transport by AtPIN1 in *Arabidopsis* Vascular Tissue. Science 282: 2226-2230

Hayward HE (1938) Leguminosae, pisum (pea): *In* HE Heyward, ed, The structure of economic plants. The Macmillan Company, New York

Hedden P, Phillips AL (2000) Gibberellin metabolism: new insights revealed by the genes. Trends Plant Sci **5**: 523-530

Hertel R, Evans ML, Leopold AC, Sell HM (1969) The specificity of the auxin transport system. Planta **85**: 238-249

Hoshino T, Hitotsubashi R, Miyamoto K, Tanimoto E, Ueda J (2005) Isolation of *PsPIN2* and *PsAUX1* from etiolated pea epicotyls and their expression of three-dimensional clinostat. Adva Space Res **36**: 1284-1291

Huang S, Raman AS, Ream JE, Fujiwara H, Cerny RE, et al. (1998) Overexpression of 20-oxidase confers a gibberellin-over production phenotype in *Arabidopsis*. Plant Physiol **118**:773-781

Jacobs WP (1952) The role of auxin in differentiation of xylem around a wound. Am J Bot **39**: 301-309

Jacobs WP, Frederick D, Pharis B, Pharis RP (1988) The transport and metabolism of gibberellins A_1 and A_5 in excised segments of internodes of *Phaseolus coccinesus*. Physiol Planta **72**: 529-534

Jacobs WP, Jacobs M (2001) Gibberellin movement: review and new evidence. (2001) Phytomorphology **51**: 201-215

Jager CE, Symons GM, Glancy NE, Reid JB, Ross JB (2007) Evidence that the mature leaves contribute auxin to the immature tissues of pea (*Pisum sativum* L.). Planta **226**: 361-368

Klee HJ, Horsch RB, Hinchee MA, Hein MB, Hoffmann N (1987) The effects of overproduction of two Agrobacterium tumerfaciens T-DNA auxin biosynthesis gene products in transgenic petunia plants. Gens Dev **1**: 86-89

Kurepin LV, Emery RJN, Pharis RP, Reid DM (2007) Uncoupling light quality from light irradiance effects in *Helianthus annuus* shoots: putative roles for plant hormones in leaf and internode growth. J Exp Bot **58**: 2145-2157

Livak KJ, Schmittgen TD (2001) Analysis of relative gene expression data using real-time quantitative PCR and the $2^{-\Delta\Delta Ct}$ method. Methods **25**: 402-408

Mattsson J, Sung R, Berleth T (1999) Response of plant vascular systems to auxin transport inhibition. Development **126**: 2979-2991

Morris DA, Friml J, Zazimalova E (2004) The functioning of hormones in plant growth and development. *In* PJ Davis, ed, Plant hormones: Biosynthesis, signal transduction, action. Ed 3. Kluwer Academic Publishers, Dordrecht, The Netherlands, pp 437-470

Muller A, Guan C, Galweiler L, Tanzler P, Huijser P et al. (1998) AtPIN2 defines a locus of Arabidopsis for root gravitropism control. EMBO J **17**: 6903-6911

O'Neill DP, Ross JJ (2002) Auxin regulation of gibberellin pathway in pea. Plant Physiol **130**: 1974-1982

Okada K, Ueda J, Komaki M, Bell J, Shimura Y (1991) Requirement of auxin polar transport system in early stages of *Arabidopsis* floral bud formation. Plant Cell **3**: 677-684

Ozga JA, Reinecke DM, Ayele BT, Ngo P, Nadeau C, Wickramarathna AD (2009) Developmental and hormonal regulation of gibberellin biosynthesis and catabolism in pea fruit. Plant Physiol **150**: 448-462

Ozga JA, Yu J, Reinecke DM (2003) Pollination-, Development-, and auxin-specific regulation of gibberellin 3β-hydroxylase gene expression in pea fruit and seeds. Plant Physiol **131**: 1137-1146

Phillips ID, Hartung W (1974) Basipetal and acropetal transport of [3,4-^{3}H] gibberellin A_1 in shoot and long segments of *Phaseolus coccineus* second internode. Planta **116**: 109-121

Probebsting WM, Hedden P, Lewis MJ, Croker SJ, Proebsting LN (1992) Gibberellin concentration and transport in genetic lines of pea. Plant Physiol **100**:1354-1360

Rademacher W (2001) Growth retardants: effects on gibberellin biosynthesis and other metabolic pathways. Annu Rev Plant Physiol Plant Mol Biol **50**: 501-531

Raven JA (1975) Transport of indole acetic acid in plant cells in relation to pH and electrical potential gradients, and its significance for polar IAA transport. New Phytol **74**: 163-172

Ross JJ, O'Neill DP, Smith JJ, Kerckhoffs LH, Elliott RC (2000) Evidence that auxin promotes gibberellin A1 biosynthesis in pea. Plant J **21**: 547-552

Ross JJ, Reid JB, Dungey HS (1992) Ontogenetic variation in levels of gibberellin A_1 in *Pisum*: Implications for the control of stem elongation. Planta **186**: 166-171

Rubery PH, Sheldrake AR (1974) Carrier-mediated auxin transport. Planta **188**: 101-121

van Huizen R, Ozga JA, Reinecke DM (1997) Seed and hormonal regulation of gibberellin 20-oxidase expression in pea pericarp. Plant Physiol **115**: 123-128

van Huizen R, Ozga JA, Reinecke DM, Twitchin B, Mander LN (1995) Seed and 4-chloroindole-3-acetic acid regulation of gibberellin metabolism in pea pericarp. Plant Physiol **119**: 1213-1217

Vieten A, Sauer M, Brewer P, Friml J (2007) Molecular and cellular aspects of auxin-transport-mediated development. Trend Plant Sci **12**:160-168

Wolbang CM, Chandler PM, Smith JJ, Ross JJ (2004) Auxin from the developing inflorescence is required for the biosynthesis of active gibberellins in barley stems. Plant Physiol **134**:769-776

Chapter 4

The effects of *PsGA3ox1*-overexpression in pea during seed germination and early seedling growth

Introduction

By definition, seed germination is the series of events that take place from the initial uptake of water by the dry seed (imbibition) up to the elongation of the embryonic axis. Visible germination is denoted by the protrusion of the radicle from the seed coat (Bewley and Black, 1994). Upon imbibition, the quiescent dry seed quickly resumes metabolic activities. The resumption of respiratory activity and the commencement of protein synthesis are two major changes that occur immediately after imbibition (Bewley, 1997).

As opposed to species like Arabidopsis and tomato, pea seeds are non-endospermic at maturity and cotyledons are the sole storage organs (Lovell, 1977; Petruzzelli et al., 1995). The seed-covering layers (testa), in many plant species, impose a physical constraint on radicle protrusion, which has to be overcome by the growth potential of the embryo (Kucera et al, 2005). However, in pea, the embryo-enclosing testa does not hinder the radicle protrusion (Petruzzelli et al., 1995). Based on the morphology of the cotyledons, germination can either be epigeal or hypogeal. In epigeal germination, the hypocotyl extends pushing the cotyledons out of the medium. Later, cotyledons expand and become photosynthetic (e.g. Arabidopsis, tomato, tobacco and pumpkin). In hypogeal germination, cotyledons of germinating seeds remain under the surface of the

medium and the extending epicotyl emerges from the medium giving rise to the shoot portion of the seedling (e.g. pea and broad bean; Bewlay and Black, 1994).

The vital role of gibberellins during seed germination in a wide range of plant species is well documented [Arabidopsis (Koornneef and van der Veen, 1980; Nambara et al., 1991); tomato (Groot and Karssen, 1987); tobacco (Leubner-Metzger et al., 1996); *Datura ferox* (Sanchez and de Miguel, 1997); (for review, see Bewley and Black, 1994; Sponsel and Hedden, 2004). The proposed roles of gibberellin during germination includes: the weakening of the testa (Debeaujon and Koornneef, 2000) or endosperm (Karssen et al., 1989) that act as mechanical barriers to radicle protrusion. GA may also facilitate embryo growth, possibly by enhancing the embryo growth potential (Karssen et al., 1989). For example, without exogenous gibberellin, GA-deficient mutant embryos of tomato (*gal-1*) were not able to penetrate the micropylar endosperm and did not readily germinate without applications of GA_3 or GA_{4+7} (Groot and Karssen, 1987).

There have been several studies on the effects of GAs on germination and early seedling growth of small-seeded dicots, but relatively little research has been conducted on their effects on large-seeded, non-endospermic and hypogeously-germinating seedlings such as pea. In pea, several studies conducted using different GA biosynthesis inhibitors (which block different steps in the GA biosynthesis pathway) have supported the hypothesis that *de novo* GA biosynthesis was not essential for seed germination, but that it was essential for normal seedling growth after germination (i.e. four days after imbibition). GA biosynthesis inhibitors used in these studies on pea included N,N,N-trimethyl-1-

methyl-(2′,6′,6′ -trimethylcyclohex-2′ en-1-yl)-prop-2-enylammonium iodide, which blocks *CPS* activity (Sponsel, 1983), Paclobutrazol which inhibits the oxidation of *ent*-kaurene to *ent*-kaurenoic acid (Graebe, 1986), and prohexadione which primarily inhibits the 3β-hydroxylation of GA_{20} (Ross et al., 1993).

Data from a number of studies suggest that GAs (mainly GA_{20}) sequestered in the cotyledons at the end of pea seed maturation are used during the early stages of seedling growth to maintain the normal growth of the embryo axis (Sponsel, 1983; Ross et al., 1993; Ayele et al., 2006). Experiments using GA biosynthesis inhibitors and the *sln* mutant (null mutant that results from a premature stop codon in *PsGA2ox1*; encodes GA 2-oxidase, which is responsible for metabolizing GA_{20} to GA_{29} and GA_{29}-catabolite and, therefore, GA_{20} accumulates in the seeds to very high levels during seed development) in pea suggested that cotyledonary GA_{20} is transported to the actively-growing young shoots, and that it is converted to biologically active GA_1 by 3β-hydroxylation, which is then used for shoot elongation (Ross et al., 1993). Detailed studies on spatial and temporal regulation of GA biosynthesis during germination and young seedling growth also suggested that pea cotyledons serve as a pool of GA_{20}, which can be converted to bioactive GA_1 in the cotyledon itself or transported to the embryo axis (Ayele et al., 2006). Furthermore, data suggest that following imbibition of the mature seed, the embryo axis is initially provided with precursors of bioactive GA (mainly GA_{20}) by the cotyledons; however, as the embryo axis initiates growth [by 1 day after imbibition (DAI)], it gains an increased capacity to produce bioactive GA_1 (supported by the large increase in

PsGA20ox1 and *PsGA3ox1* GA biosynthesis genes, concomitant with a substantial decrease in *PsGA2ox2* transcript levels from 0.5 to 1 DAI; Ayele et al., 2006).

Further genetic evidence for the role of GAs in early seedling growth came from the pea mutant *na*. The *na* mutation results from a 5-base deletion in the *NA* gene (*PsKAO1;* encodes *ent*-Kauronic acid oxidase and is expressed mainly in vegetative tissues), producing a premature stop codon, and the resulting enzyme has very low activity (Davidson et al., 2003). The presence of a *PsKAO2* homolog, which is mainly expressed in seeds (Potts and Reid, 1983; Davidson et al., 2003) allows seeds of *na* mutant plants to germinate readily, but the seedlings produced have extremely short internodes (Potts and Reid, 1983) and a markedly reduced tap root system (Yaxley et al., 2001). It has also been found that both expanding shoot tissues (Probsting et al., 1992) and roots (Yaxley et al., 2001) of *na* mutants have extremely low levels of bio-active $GA_{1.}$

Additionally, transcript levels of the GA catabolic gene *PsGA2ox2,* which converts biologically active GA_1 to inactive GA_8, were elevated in the mature quiescent embryo and it was suggested that this is a probable mechanism to keep bioactive GA levels at a minimum to prevent embryo-axis expansion during the later stages of seed maturation (Ayele et al., 2006). Embryo *PsGA2ox2* transcript abundance dramatically decreased upon imbibition of the mature pea seed in preparation for a phase of development where bioactive GA is required for embryo axis expansion (Ayele et al., 2006).

We observed a greater flux through the GA biosynthesis pathway to bioactive GA_1 in the stem tissues of the TG1 line compared to the transgenic null line, C1 (Chapter 2) and also the activation of a homeostatic mechanism to limit the level of bioactive GA during internode elongation. Previous data suggests that coordination of the late GA biosynthesis and catabolism genes is highly regulated both spatially and temporally during pea seed germination and early seedling growth within each organ to maintain both precursors and bioactive GA at optimum levels for successful growth dynamics (Ayele et al., 2006). Our main objective in this study was to determine how overexpression of *PsGA3ox1* affects the late GA biosynthesis and catabolism genes during seed germination and early seedling growth.

Materials and Methods

Plant Materials and Growth Conditions

Based on phenotypic and the transgene expression results (Chapter 2), the highest transgenic expressor line (TG1; T5 generation) and the transgenic null control line (C1; T6 generation) were chosen to characterize the effects of *PsGA3ox1*-overexpression on developmental parameters during germination and early seedling growth.

For germination studies, mature air-dried seeds of transgenic and control lines were surface sterilized in 1.2% (v/v) sodium hypochlorite solution for 30 min after an initial wash with 70% (v/v) ethanol, and rinsed five times with sterile deionized water. Seeds were either left with intact seed coats or the seed coats were nicked by removing a small piece of seed coat using a scalpel and then

placed on filter paper (Whatman #4) moistened with 10 mL of sterilized ddH_2O in 9 cm Petri plates (10 seeds per plate). Seeds were scored germinated when the radicle extended *ca.*3 mm or greater. This experiment was replicated twice over time. The data presented were from one experiment with three biological replications (10 seeds per replication).

For phenotypic assessment of seedling growth, mature air-dried seeds of the transgenic and control lines were planted at a depth of approximately 2.5 cm into moist vermiculite (Grace Canada, Inc. Ajax, ON) in 3 L plastic pots (10 seeds per pot). The pots were placed in a growth chamber (Conviron) set at 19^{o}C/17^{o}C (day/night) with a 16/8-h photoperiod under cool-white fluorescent lights (F54/I5/835/HO high fluorescent bulbs, Phillips, Holland; 366 µE m^2 s^{-2}) until harvest. To maintain moisture in the vermiculite, trays with approximately 3 cm of water were placed under each pot throughout the experiment. For growth measurements, 10 seedlings from each line were harvested at 3, 5, 7, 9 and 11 DAI (10 biological replicates). Shoot and root length, fresh and dry weight, root and shoot diameter, and cotyledon fresh and dry weight were recorded at the time of harvest. Dry weights were obtained after drying tissue at 60^{o}C until a constant weight was reached (approximately three days).

For gene expression studies, mature air-dry seeds of the transgenic and control lines were planted at a depth of approximately 2.5 cm into moist sterilized sand in 3 L plastic pots (10 seeds per pot) and the pots were placed in a growth chamber as described above. Seeds or seedlings of each line were harvested at 1, 2, and 3 DAI. Seedlings were separated into cotyledons and embryo axes (1 DAI)

or into cotyledons, roots and shoots (2 and 3 DAI). The data presented consist of two biological replicates, where each replicate consisted of tissues from five seedlings (1 and 2 DAI) or from three seedlings (3 DAI). Tissues were harvested into liquid nitrogen, and stored at -80^{o}C until total RNA extraction.

Gene Expression Analysis

RNA isolation

Tissues were ground finely in liquid nitrogen (30 to 200 mg fresh weight (FW) for embryo axes, shoots and roots; 150 to 200 mg FW for cotyledons) and total RNA was isolated using a modified TRIzol (Invitrogen, Carlsbad, CA, USA) protocol as described in Chapter 2. Cotyledonary total RNA samples were further purified using RNeasy columns (Qiagen, Valencia, CA, USA). After extraction, the total RNA samples were treated with DNase (DNA-free kit, Ambion, Austin TX, USA) to remove any residual DNA. RNA integrity was verified by gel electrophoresis in representative samples of each extraction run and the 260 to 280 nm ratio was determined by spectrophotometry in all samples. Sample RNA concentration was determined in duplicate by A_{260} measurement using a NanoDrop ND-100 spectrophotometer (NanoDrop Technologies, Wilmington, DE, USA). The samples were stored at -80^{o}C until quantitation by qRT-PCR.

To compare the expression patterns of *PsGA3ox1* and *PsGA3ox2* during seed germination and early seedling growth in the cultivars Alaska and Carneval, the RNA samples extracted by Ayele et al. (2006) were used.

Primers and Probes

Primers and probes for the transgene quantifying amplicon, *TPsGA3ox1-130* were designed using Primer Express software (Version 3, Applied Biosystems, Foster City, CA, USA) as described previously (Chapter 2). Primers and probes for the target gene quantifying amplicon *PsGA3ox1-87* [used for total *PsGA3ox1* (endogenous+ transgene) transcript quantitation] and for the reference gene amplicon *18S-62* (used for pea 18S rRNA transcript quantitation) were designed as described by Ozga et al. (2003). Primers and probes for the target gene quantifying amplicon *PsGA2ox1-73* (used for *PsGA2ox1* quantification), *PsGA2ox2-83* (used for *PsGA2ox2* quantification), *PsGA20ox1-104* (used for *PsGA20ox1* quantification), and *PsGA20ox2-88* (used for *PsGA20ox2* quantification) were designed as described by Ayele et al. (2006). Primers and probes for *PsGA3ox2* quantitation (*PsGA3ox2-104*) were designed as described by Ozga et al. (2009).

All probes used were Taqman-based. Probes for the GA genes were labeled at the 5' end with the fluorescent reporter dye FAM and at the 3' end with a minor-groove binding non-fluorescent quencher (MGB, Applied Biosystems). The *18S-62* reference gene probe was labeled at the 5' end with the VIC fluorescent reporter dye and at the 3' end with the TAMRA quencher (Applied Biosystems).

qRT-PCR Assay

qRT-PCR assays were performed on a StepOnePlus sequence detector (Applied Biosystems) using a TaqMan One-Step RT-PCR Master Mix reagent kit

(Applied Biosystems) as described previously (Chapter 2). PCR amplification of each sample was carried out in duplicate in fast 96-well reaction plates covered with optical adhesive covers (Applied Biosystems), and the average of the two sub-samples (two technical replicates) was used to calculate the sample transcript abundance. One total RNA sample (common sample) was run on each plate and used to correct for plate-to-plate amplification differences. The Ct value of the common sample on the first plate was used arbitrarily as the standard for normalization as follows:

*Normalized Ct value of sample = (Ct value of the common sample in the standard run / Ct value of the common sample in the sample run) * Ct value of sample*

The relative transcript abundance of the target genes in the plant samples was determined using the $2^{-\Delta Ct}$ method (Livak and Schmittgen, 2001; Ozga et al., 2009) where ΔC_t was the difference between the C_t of the target sample and the average C_t of the reference sample. Transcript levels of *PsGA20ox1*, *PsGA20ox2*, transgenic *PsGA3ox1*, total *PsGA3ox1* (transgenic + endogenous), *PsGA3ox2*, *PsGA2ox1*, and *PsGA2ox2* were standardized across genes, lines, and tissues using the lowest sample average Ct value (the reference sample; control 2 DAI cotyledons; *PsGA20ox1* Ct = 37.76). The relative transcript abundance of *PsGA3ox1* and *PsGA3ox2* in 'Alaska' and 'Carneval' was determined using the average Ct of mature embryo *PsGA3ox2* samples of 'Alaska' as the reference; Ct= 38.35. At least two biological replicate plant samples were assayed for each data value.

The pea 18S small subunit nuclear ribosomal RNA gene was used as a loading control to estimate variation in input total RNA concentration across all

samples within a data set. The coefficient of variation (CV) of the 18S rRNA amplicon Ct value among the samples was 2.17% and 2.98% among the 'Alaska' and 'Carneval' samples and therefore, the target amplicon mRNA values were not normalized to the 18S signal (Livak and Schmittgen, 2001, Ozga et al., 2009).

Root diameter data were analyzed using the General Linear Model of SAS 9.1 statistical software (SAS Institute Inc., Cary, NC, USA) following a completely randomized design, and mean separation was by LSD at $p \leq 0.05$.

Results

Seed germination and early seedling growth

Rapid imbibition arrests embryo axis growth in transgenic seeds

Germination and early seedling growth in pea seeds transformed to overexpress *PsGA3ox1* were characterized. Mature air-dried seeds of the transgenic line were significantly larger (fresh mass: 323.3±2.8 mg) than those of the control line (240.5±1.9 mg). The relative water content was similar in both transgenic and control seeds in the mature-dried state, and remained so in the cotyledons 3 days after imbibition and through 11 DAI (Table 4.1 and Figure 4.1C)

When intact transgenic and control seeds were germinated in Petri Plates, there was no difference in the percent germination at 7 DAI, mean days to germination, or Sum 7 (cumulative percent germination over 7 days), and both the transgenic and control lines exhibited normal seedling development (Table 4.2) However, when the seed coats were nicked (a small piece of seed coat was

removed prior to imbibition) to reduce the time to germination, the increased rate of water uptake that is a consequence of seed-coat nicking, arrested embryo axis growth preventing germination of the transgenic seeds (Table 4.2). Control seeds were not affected in this manner and seed coat-nicking stimulated the rate of germination (reduced the mean days to germination; increased SUM 7) and normal seedling development occurred (Table 4.2)

When seed coat-nicked transgenic seeds were germinated in a medium that would allow slower water up-take by the embryo (moist vermiculite medium), germination occurred and normal seedling development was observed (Table 4.3; Figure 4.2). However, seedlings from the seed coat-nicked transgenic seeds were observed to have less root and shoot biomass at 11 DAI than the control line (data not shown).

When intact seeds were planted in moist vermiculite, both transgenic and control lines exhibited normal seedling growth. Both root and shoot elongation was rapid from 5 to 11 DAI (Figures 4.1 and 4.3). Interestingly, roots of the *PsGA3ox1*-overexpressor line elongated more slowly than those of the control line from 3 to 11 DAI (Figures 4.1G and 4.3); however, transgenic tap roots were thicker than control tap roots 7-9 DAI (Table 4.4 and Figure 4.3). There were minimal differences in shoot length between the transgenic and the control lines from 3 to 7 DAI; however, from 9 DAI the transgenic line exhibited longer shoots than the control (Figures 4.1H and 4.3). Root and shoot fresh weights and dry weights were similar between the transgenic and control lines from 3 to 11 DAI (Figures 4.1 A, B, D, and E).

GA biosynthesis and catabolism gene expression

Expression of transgenic *PsGA3ox1* during germination and early seedling growth in pea seeds transformed to overexpress *PsGA3ox1* was characterized. In addition, the expression patterns of the late GA biosynthesis genes (*PsGA20ox1*, *PsGA20ox2*, *PsGA3ox1*, *PsGA3ox2*, *PsGA2ox1*, and *PsGA2ox2*) were also monitored to determine if *PsGA3ox1*-overexpression altered their expression patterns during this developmental period.

Expression profiles of *PsGA3ox1* and *PsGA3ox2* were also compared between the pea cultivars 'Carneval' (contains *le-1*) and 'Alaska' (contains *LE*) during germination and early seedling growth.

Cotyledons

In the cotyledons of the *PsGA3ox1*-overexpressor line, transgenic *PsGA3ox1* transcripts were present 24 h after imbibition (1 DAI), increased from 24 to 48 h after imbibition (2 DAI), and remained elevated through 3 DAI (Figure 4.4D). The presence of transgenic *PsGA3ox1* mRNA resulted in markedly higher total cotyledonary *PsGA3ox1* transcript abundance (transgenic + endogenous) in the transgenic line than in the control line by 2 DAI, and the elevated *PsGA3ox1* transcript levels were maintained through 3 DAI (Figures 4.4E, 4.5A and B)

The trend of increasing *PsGA3ox2* transcript abundance with increasing time of imbibition was similar in the cotyledons of both the transgenic and control lines; however, the transcript abundance of *PsGA3ox2* in the transgenic line was 5-fold lower than in the control line at 3 DAI (Figure 4.4F). The cotyledons of both 'Alaska' and 'Carneval' also exhibited a similar trend of increasing

PsGA3ox2 levels from 1 to 4 DAI (Figures 4.6C and F), even though 'Alaska' cotyledons contained markedly higher levels of *PsGA3ox1* than that in 'Carneval'. In general, *PsGA3ox2* transcript abundance was greatest in the cotyledons compared to the root and shoot tissues in both transgenic and control lines by 3 DAI (Figures 4.5C and D).

Transcript levels of the GA biosynthesis genes, *PsGA20ox1* and *PsGA20ox2* (code for the enzymes that convert GA_{53} to GA_{20}) were substantially higher at 2 DAI in the cotyledons of the transgenic line compared to the control, then decreased by 3 DAI to levels similar to those in the control (Figures 4.4A and B). Expression of the two catabolic GA 2-oxidase genes, *PsGA2ox1* and *PsGA2ox2* was similar in the transgenic and control cotyledons. *PsGA2ox1* transcript abundance increased at 2 DAI, then decreased by 3 DAI (Figure 4.4H), while *PsGA2ox2* transcript levels decreased sharply from 1 to 2 DAI (Figure 4.4G) and remained low at 3 DAI. The overall GA gene expression profile suggests a greater flux through the GA biosynthesis pathway to bioactive GA_1 in the cotyledons of the *PsGA3ox1*-overexpressing line compared to the control.

Shoots

The radical protrudes through the seed coat (by 1-2 DAI) and embryo axis growth is substantially initiated by 3 DAI (Figure 4.7C). Transgenic *PsGA3ox1* transcript levels were expressed during the first 3 DAI in the shoot tissues (Figure 4.7D); transgenic *PsGA3ox1* levels increased by 2 DAI and remained elevated through 3 DAI in the shoot similar to the observation in transgenic cotyledons (Figure 4.4D). *PsGA3ox1* transcript levels (transgenic + endogenous) were

similar in the transgenic and control lines at 2 DAI (Figure 4.7E). However, by 3 DAI the transgenic shoots had significantly higher *PsGA3ox1* transcript levels than the control shoots (Figure 4.7E). Minimal changes in *PsGA3ox2* transcript levels were observed in the shoots of the transgenic and control lines over the 3 days of imbibition (Figure 4.7F). 'Carneval' (*le-1*) shoots contained higher *PsGA3ox1* levels than that of 'Alaska' by 4 DAI (Figures 4.6B and E). *PsGA3ox2* transcript levels low in the shoots of both cultivars (Figures 4.6B and E).

The transcript levels of *PsGA20ox1* were substantially higher in the transgenic shoots than those in the control shoots by 2 DAI, and they remained higher in the transgenic shoots through 3 DAI (Figure 4.7A). *PsGA20ox2* transcript levels were also higher in the transgenic shoots compared to the control shoots at 2 and 3 DAI (Figure 4.7B). Transcript abundance of the catabolic GA 2-oxidase gene, *PsGA2ox1*, was significantly higher in the transgenic shoots at 2 and 3 DAI compared to the control, whereas *PsGA2ox2* transcript levels were low in the shoots of both the transgenic and control lines during this time period (Figures 4.7G and H).

The overall GA biosynthesis gene expression profile (greater transcript abundance of *GA20ox* and *GA3ox* genes) suggests a greater flux through the GA biosynthesis pathway to bioactive GA_1 in the shoots of the *PsGA3ox1*-overexpressing line compared to the control. The increase in *PsGA2ox1* transcript abundance at 3 DAI suggests that higher levels of bioactive GA_1 in the transgenic shoots resulted in feedback regulation of the pathway by increasing the transcript abundance of the catabolic gene *PsGA2ox1*. Consistently, the shoot length of the

transgenic line was observed to be significantly greater than the control by 9 DAI, when the internodes were rapidly expanding (Figure 4.1).

Roots

The rate of radicle (root) growth increased from 2 to 3 DAI in both the control and transgenic lines; however, the control line exhibited greater root growth by 3 DAI (Figure 4.8C). Transgenic *PsGA3ox1* transcripts were present in the roots of the *PsGA3ox1*-overexpressor line during the first 3 DAI, and levels were elevated from 1 to 2 DAI and slightly decreased by 3 DAI (Figure 4.8D). Total *PsGA3ox1* transcript levels (transgenic + endogenous) were higher in the control roots than in the transgenic roots by 2 DAI; however, from 2 to 3 DAI, transcript levels decreased in the control line and increased in the transgenic line (Figure 4.8E). The roots of 'Alaska' (*LE*) also exhibited increasing *PsGA3ox1* levels with increasing DAI (Figure 4.6D). Minimal changes in *PsGA3ox2* levels were observed in the roots of the transgenic and control lines over the 3 DAI (Figure 4.8F). The roots of 'Carneval' had higher levels of *PsGA3ox2* than 'Alaska' roots from 1 to 2 DAI, however, transcript levels increased substantially in 'Alaska' compared to 'Carneval' from 2 to 6 DAI (Figures 4.6A and D).

The transcript levels of *PsGA20ox1*were substantially higher in the transgenic roots than those in the control roots by 2 DAI, and remained higher than that of the control roots through 3 DAI (Figure 4.8A). Transcript levels of *PsGA20ox2* were minimally changed in the transgenic line compared to the control line (Figure 4.8B). The transcript levels of the catabolic GA 2-oxidase gene, *PsGA2ox1*, was substantially increased in the transgenic roots by 3 DAI

compared to the control roots (Figure 4.8H), while *PsGA2ox2* levels remained low from 2 to 3 DAI in the roots of both the transgenic and control lines (Figure 4.8G). In general, roots and shoots of the *PsGA3ox1*-overexpressor line and the control line exhibited similar GA gene expression profiles (except for *PsGA3ox2*) over the 3 day experimental period (Figures 4.7 and 4.8).

Discussion

Rapid imbibition damage in transgenic seeds

Imbibition damage occurs when rapid water uptake by the embryo during initial imbibition leads to rapid solute leakage and cell death within the embryo (Powell and Matthews, 1978). Powell and Matthews (1978) observed imbibition damage in pea embryos when they were imbibed in water without their seed coats (not observed in intact seeds). Rapid imbibition in seed coat-removed embryos significantly increased solute leakage from the embryo suggesting that the high levels of solute leakage were a consequence of dead or damage tissues (Powell and Matthews, 1978). Staining of the embryos with 2, 3, 5, triphenyl-tetrazolium chloride revealed the presence of dead cells in the abaxial surface of the cotyledons. Embryo damage was also revealed by differences in respiration where the seed coat-intact embryos exhibited a much higher respiration rate than that of seed coat-removed embryos (Powell and Matthews, 1978). When embryos were imbibed without their seed coats in a 30% (w/v) polyethylene glycol solution (allowing for a slower rate of water uptake by the embryo), imbibition damage was reduced, if not completely prevented (Powell and Matthews, 1978). In our experiments, it was observed that when seed coat-nicked seeds of the transgenic

and control lines were geminated in Petri Plates, total inhibition of embryo axis expansion occurred in the transgenic seeds; however, the control seeds germinated normally and produced normal seedlings (Table 4.2). This inhibition of embryo axis expansion observed in the seed coat-nicked transgenic seeds when germinated in the presence of freely available water (Petri plate system), is likely a result of rapid imbibition damage. Similar to that observed by Powell and Matthews (1978), when the transgenic seeds were germinated in vermiculite, a medium allowing slower water up-take by the embryo, imbibition damage (as measured by the ability of the embryo axis to expand and form normal seedlings) was substantially reduced (Table 4.3).

Severe imbibition damage observed in the transgenic seeds when the seed coats were nicked is most likely due to changes in the embryo as the result of overexpression of *PsGA3ox1* during seed development. Previous work suggests that bioactive GA is required for the early stages of pea seed development in which, cell division and expansion predominate, but may not be a required for the later stages of storage deposition and maturation of the embryo (Reid et al., 2004). It is possible that higher levels of bioactive GA in the developing transgenic seeds prolonged the pre-storage phase of development at the expense of the later maturation stages making the mature embryo more susceptible to imbibition damage. The larger seed size of the mature air-dried transgenic seeds compared to the control seeds may reflect a GA-induced expansion of the pre-storage phase of seed development

Effect of PsGA3ox1-overexpression on cotyledons

Pea seeds exhibit hypogeal germination and the cotyledons remain underground during seedling development; thus, the cotyledons are not involved in photosynthetic activity. Cotyledon fresh and dry weights were consistently greater in the transgenic seeds and seedlings than the control seeds from 1 to 11 DAI (1 to 3 DAI, Figure 4.4C; 3 to 11 DAI; Figures 4.1C and F). The percent relative water content was similar in both the transgenic and control seeds when in their mature air-dry state and in the imbibed cotyledons from 3 through 11 DAI (Table 4.1). Thus, the larger cotyledonary fresh weight of the transgenic seeds reflects the larger embryos at maturity compared to those of the controls. The overall cotyledonary GA gene expression profile suggests a greater flux through the GA biosynthesis pathway to bioactive GA_1 in the transgenic cotyledons during germination and early seedling growth. Transcript levels of the GA biosynthesis genes *PsGA20ox1* and *PsGA20ox2* (code for the enzymes that convert GA_{53} to GA_{20}) (*PsGA20ox1*about 7-fold and *PsGA20ox2* about 2-fold higher at 2 DAI; Figures 4.4A and B), and total *PsGA3ox1* (more than 4-fold; Figure 4.4E at 2-3 DAI) were higher in the transgenic line than in the control line. Additionally, expressions of the GA catabolic genes (*PsGA2ox1* and *PsGA2ox2*) were minimally changed by *PsGA3ox1*-overexpresssion (Figures 4.4G and H).

Bioactive GAs play a critical role in hydrolyzing and mobilizing of reserves in endosperm during cereal seed germination (Woodger et al., 2004), but the role of bioactive GAs on cotyledonary reserve mobilization in dicots is unclear (Ayele et al., 2006; Bewley and Black, 1994). It has been reported that

pea cotyledonary endogenous GA_1 levels increased during the first DAI and then decreased to undetectable levels from 1 to 2 DAI (Ayele et al., 2006). If the modified cotyledonary GA gene expression profile in the transgenic line (Figure 4.4) resulted in greater bioactive GA_1 levels in this tissue, it would be of great interest to compare cotyledon morphology at the tissue and cellular level as well as nutrient mobilization patterns in the transgenic and control lines.

Ayele et al. (2006) also investigated the importance of the embryo axis on GA biosynthesis in the cotyledons. They observed that removal of the embryo axis within 2 h after imbibition substantially reduced the transcript abundance of cotyledonary GA biosynthesis genes *PsGA20ox1, PsGA20ox2,* and *PsGA3ox1* and resulted in more than a 7-fold reduction in the conversion of [^{14}C]GA_{20} to [^{14}C]GA_8 in the 2 DAI cotyledons. These data suggested that GA biosynthesis in the cotyledons is controlled by a signal(s) from the embryo axis. It would be interesting to test if this relationship was altered in the *PsGA3ox*1-overexpressing line.

Effects of PsGA3ox1-overexpression on young seedling shoots

Overexpression of *PsGA3ox1* appears to have stimulated feed forward regulation of *PsGA20ox1* and *PsGA20ox2* in the 2 to 3 DAI shoots (Figures 4.7A and B). Concomitant with increased *PsGA20ox* transcript abundance was an increase in the abundance of the catabolic gene *PsGA2ox1* in the transgenic line suggesting that increased levels of bioactive GA_1 also stimulated feedback regulation of bioactive GA levels in the developing shoot. Gallego-Giraldo et al. (2008) observed similar upregulation of GA catabolic genes in 7-day-old tobacco

seedlings when *PsGA3ox1* was overexpressed. Even with bioactive GA-induced feedback regulation of GA biosynthesis occurring in the shoots, longer shoots were observed in the transgenic line compared to the control line by 9 DAI when internodes were rapidly expanding (Figure 4.1H).

Effects of PsGA3ox1-overexpression on young seedling roots

The effects of overexpression of *PsGA3ox1* on the GA gene expression profile was similar in the shoot and root tissues for the *PsGA20ox and GA2ox* genes monitored (Figures 4.8A, B, G, H). The total *PsGA3ox1* transcript abundance profile was also similar in the roots and shoots; however, higher levels of total *PsGA3ox1* were present in the roots of the transgenic lines than in the control lines at 3 DAI (5.2-fold higher; Figure 4.8E; Figures 4.5A and B) than in the similar comparison in the shoots (transgenic shoots had 2.9-fold higher transcripts than the control; Figure 4.7E; Figures 4.5A and B). Roots also had higher levels of *PsGA3ox2* transcript at 2 DAI than the shoots in both transgenic and control lines (Figures 4.5 C and D). The *PsGA3ox2* transcript profile was minimally modified in the roots by *PsGA3ox1*-overexpression. Interestingly, the control line had longer primary roots and exhibited earlier lateral root initiation (control line was about 2 d earlier) than the transgenic line (Figures 4.1G and 4.3). The transgenic line also had thicker primary roots compared to the control line at 7 to 9 DAI (Table 4.4; Figure 4.3). Root and shoot organs respond differently to exogenous GAs levels. Pea roots in general are more sensitive to applied GAs than shoots (lower GA concentration is required for optimal growth response) and it is suggested that a much lower concentration of GA is required for normal root

growth than for normal shoot growth (Tanimoto, 1990). Roots from pea seedlings of GA_3- or prohexadione-treated seeds (prohexadione is a GA biosynthesis inhibitor) did not exhibit a difference in length by 6 DAI or lateral root initiation, but shoots of GA_3-treated seeds were significantly longer by 6 DAI, and shoots of prohexadione-treated seeds were shorter by 4 DAI (Ayele, 2006). It is possible that overexpression of *PsGA3ox1* in pea resulted in higher bioactive GA levels in the roots leading to a less than optimal GA: auxin ratio for root growth and development. Ectopic expression of *CmGA3ox1* in Arabidopsis resulted in more lateral roots that were thicker compared to the wild type plants (Raid et al., 2006) suggesting that the response of roots to increased levels of bioactive GA may be species-specific.

Tissue specific expression of PsGA3ox2

Weston et al. (2008) measured *PsGA3ox2* transcript abundance in the roots and shoots of 6-d-old pea seedlings and suggested that *PsGA3ox2* is expressed primarily in the root. Transcript profiling of *PsGA3ox2* in the roots, shoots, and cotyledons of 'Alaska' and 'Carneval' during germination and early seedling growth revealed that, in general, *PsGA3ox2* transcript levels were higher in the roots than in the shoots (Figures 4.6A, B, D, and E) consistent with the observations of Weston et al. (2008). In addition, *PsGA3ox2* mRNA is substantially expressed and temporally regulated in the cotyledons (*PsGA3ox2* mRNA levels markedly increased by 4 DAI in both 'Alaska' and 'Carneval cotyledons; Figures 4.6C and F). Moreover, Ozga et al. (2009) observed that

PsGA3ox2 is minimally expressed in pea pericarps, but markedly expressed in the developing seeds of pea.

Overexpression of *PsGA3ox1* minimally altered the expression pattern of *PsGA3ox2* in cotyledons, roots, and shoots suggesting that *PsGA3ox1* and *PsGA3ox2* are independently regulated. Consistent with this hypothesis, Weston et al. (2009) observed that *PsGA3ox1* mRNA levels increased while those of *PsGA3ox2* were reduced when pea roots were treated with an auxin action inhibitor, *p*-chlorophenoxyisobutric acid (PCIB). It was suggested that reduced GA_1 content of PCIB-treated roots might have led to increased *PsGA3ox1* mRNA levels due to feedback regulation, but *PsGA3ox2* levels were reduced due to the overall effect of PCIB.

In summary, *PsGA3ox1*-overexpression resulted in larger embryos (seeds) at maturity and these seeds were more susceptible to rapid imbibition damage. The GA biosynthesis and catabolism gene expression profiles suggest that an increased flux through the GA biosynthesis pathway to bioactive GA_1 occurred in the transgenic cotyledons, roots and shoots during early seedling growth. Shoots and roots of the pea seedlings exhibited different phenotypic responses to *PsGA3ox1*-overexpression. Seedling shoots exhibited a typical response to increased bioactive GA levels (longer shoots), although, increased transcript abundance of the catabolic gene *PsGA2ox1* by 3 DAI suggests that substrate-induced feedback regulation may have been induced by higher levels of bioactive GA in this tissue. Although seedling roots from the *PsGA3ox1*-overexpressor line exhibited a similar GA gene transcription profile as that in the shoots, transgenic

roots were shorter and lateral root initiation was delayed compared to control roots. This may be the result of higher bioactive GA levels in the roots leading to a less than optimal GA: auxin ratio for root growth and development.

Table 4.1. RWC of mature air-dry seeds and cotyledons at 3 to 11 DAI in transgenic and control lines

	% RWC	
	Transgenic	Control
Mature air-dry seeds	7.5±2.3[a]	6.0±1.9
3 DAI	55.0±2.2	54.6±1.9
5 DAI	57.4±2.4	60.0±5.1
7 DAI	59.4±1.5	61.7±2.1
9 DAI	58.8±2.2	60.5±2.8
11 DAI	62.0±1.4	59.1±0.8

[a] Data are means ± SE, n= 9 to 10

Table 4.2. Germination of transgenic and control lines in Petri Plates over seven days. Seeds were scored germinated when the radical protruded through the seed coat *ca.* 3 mm.

	Seed coat-intact seeds		Seed coat-nicked seeds[a]	
	Transgenic	Control	Transgenic	Control
Mean days to germination	3.2±0.0[b]	3.0±0.0	4.5±0.3	2.8±0.0
SUM 7[c]	489.6±5.8	496.7±3.3	56.7±8.8	583.3±8.8
Seeds germinated at 7 DAI (%)	96.7±3.3	96.7±3.3	16.7±5.8	100
Abnormal seedlings at 7 DAI (%)	0	0	100	0

[a] A small piece of seed coat was removed immediately before placing them in the moist Petri Plates.

[b] The results of 10 seeds per Petri Plate were averaged for one replication. Data are means ± SE; three replications per treatment.

[c] Cumulative % germination over 7 days.

Table 4.3. Germination of seed coat-nicked transgenic and control seeds in vermiculite medium over seven days. Seeds were scored germinated when the radical protruded through the seeds coat *ca.* 3 mm.

	Transgenic	Control
Mean days to germinate	1.4±0.3[a]	1.3±0.2
Seeds germinated at 7 DAI (%)	80	100
Abnormal seedlings at 7 DAI (%)	0	0

[a] Data are means ± SE, n=10.

Figure 4.1. Seedling growth of the transgenic (TG) and control (C) lines. A, root fresh weight; D, root dry weight; G, root length; B, shoot fresh weight; E, shoot dry weight; and H, shoot length from 3 to 11 DAI . C, cotyledon fresh weight; and F, dry weight from 3 to 11 DAI. Data are means ± SE, n=10.

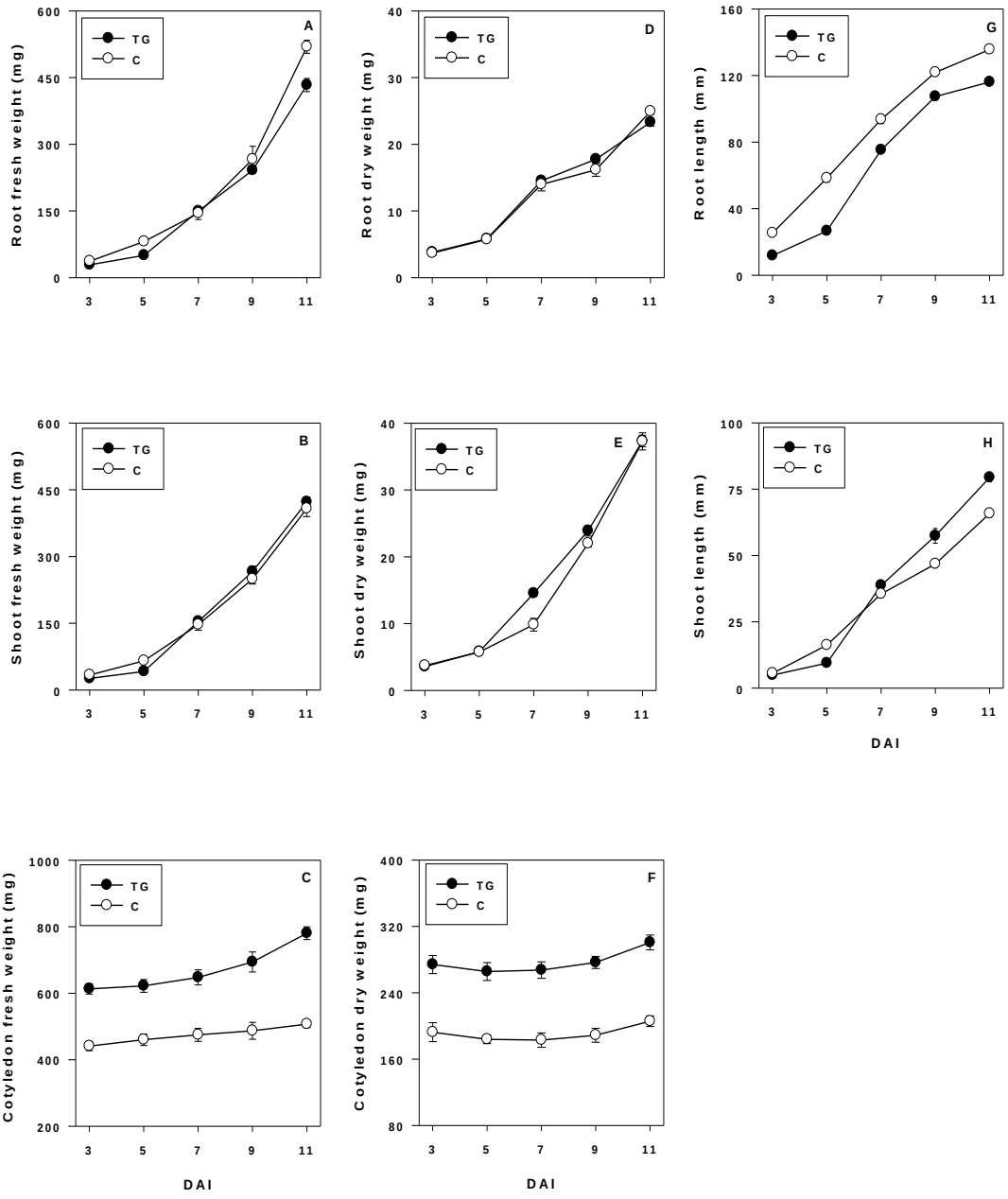
A
TG
C
Root fresh weight (mg)
600
450
300
150
0
3
5
7
9
11
D
Root dry weight (mg)
40
30
20
10
0
G
Root length (mm)
160
120
80
40
B
Shoot fresh weight (mg)
E
Shoot dry weight (mg)
H
Shoot length (mm)
100
75
50
25
DAI
C
Cotyledon fresh weight (mg)
1000
800
600
400
200
F
Cotyledon dry weight (mg)
320
240
160
80

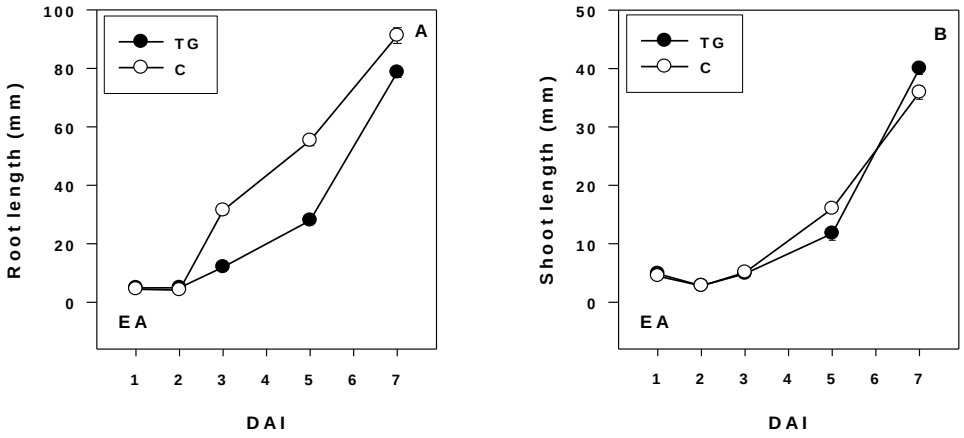

Figure 4.2. Growth of transgenic and control seedlings in vermiculite medium from 1 to 7 DAI days when seed coats were nicked prior to imbibition; A, root length; B, shoot length. Data are means ± SE, n = 8 to 10.

Table 4.4. Root diameter of the transgenic and control lines at 9 and 11 DAI.

	Root diameter ($x10^{-2}$mm)[x]	
	Transgenic	Control
9 DAI	18.2±0.4[y]a[z]	14.9±0.8b
11 DAI	18.5±0.7a	14.8±0.8b

[x] Root diameter was measured 20 mm below the point of attachment to the cotyledon.

[y] Data are means ±SE, n=10.

[z] Means followed by different letters (a, b) indicate significant difference among lines within DAI by LSD, ($P<0.05$).

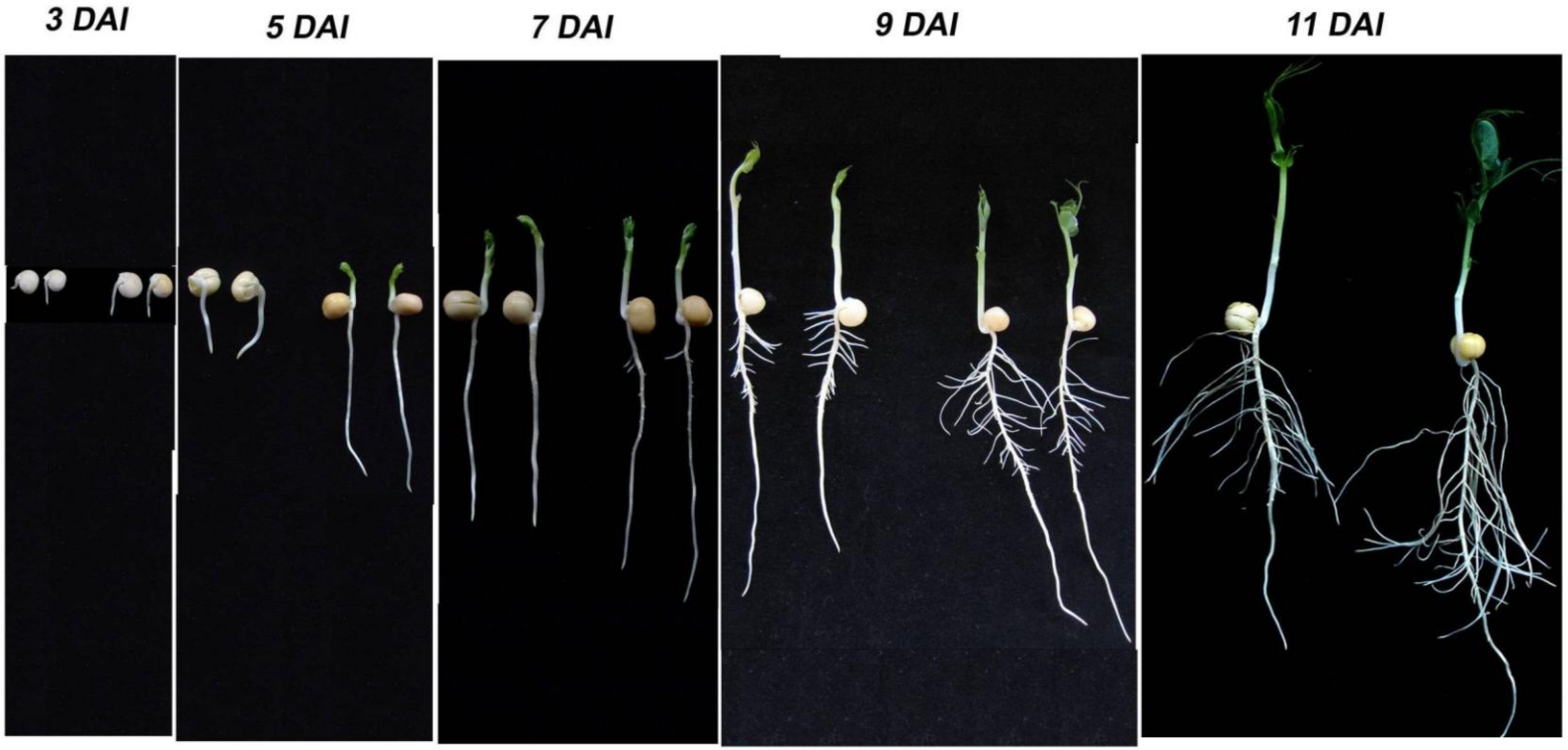

Figure 4.3. Seedling growth of the *PsGA3ox1*-overexpressor line (left in each seedling pair) and the control line (right in each seedling pair) from 3 to 11 DAI.

Figure 4.4. Relative transcript levels of A, *PsGA20ox1*; B, *PsGA20ox2*; D, transgenic *PsGA3ox1*; E, total *PsGA3ox1* (transgenic + endogenous); F, *PsGA3ox2*; H, *PsGA2ox1*; and G, *PsGA2ox2* in cotyledonary tissue from 1 to 3 DAI; and C, cotyledon fresh weight of transgenic (TG) and transgenic null (C) lines during germination and early seedling growth from 0 (mature seed) to 3 DAI. Data are means ± SE of two biological replicates for transcription profiling and means ± SE, n=10 to 13 for cotyledon fresh weight.

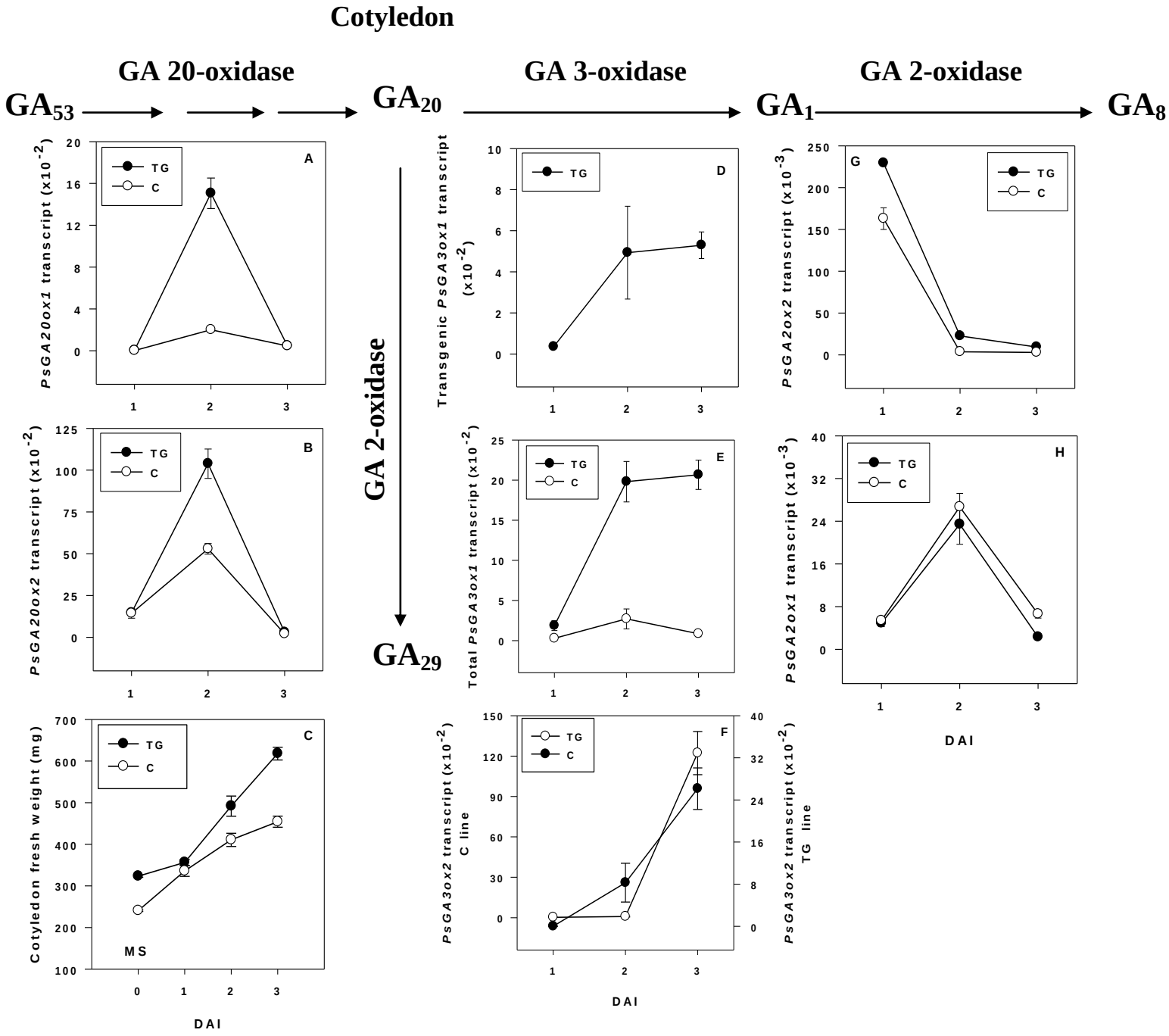
Cotyledon
GA 20-oxidase
GA 3-oxidase
GA 2-oxidase
GA53
GA20
GA1
GA8
GA 2-oxidase
GA29
A
B
C
D
E
F
G
H
TG
C
MS
DAI
PsGA20ox1 transcript (x10-2)
PsGA20ox2 transcript (x10-2)
Cotyledon fresh weight (mg)
Transgenic PsGA3ox1 transcript (x10-2)
Total PsGA3ox1 transcript (x10-2)
PsGA3ox2 transcript (x10-2) C line
PsGA3ox2 transcript (x10-2) TG line
PsGA2ox2 transcript (x10-3)
PsGA2ox1 transcript (x10-3)

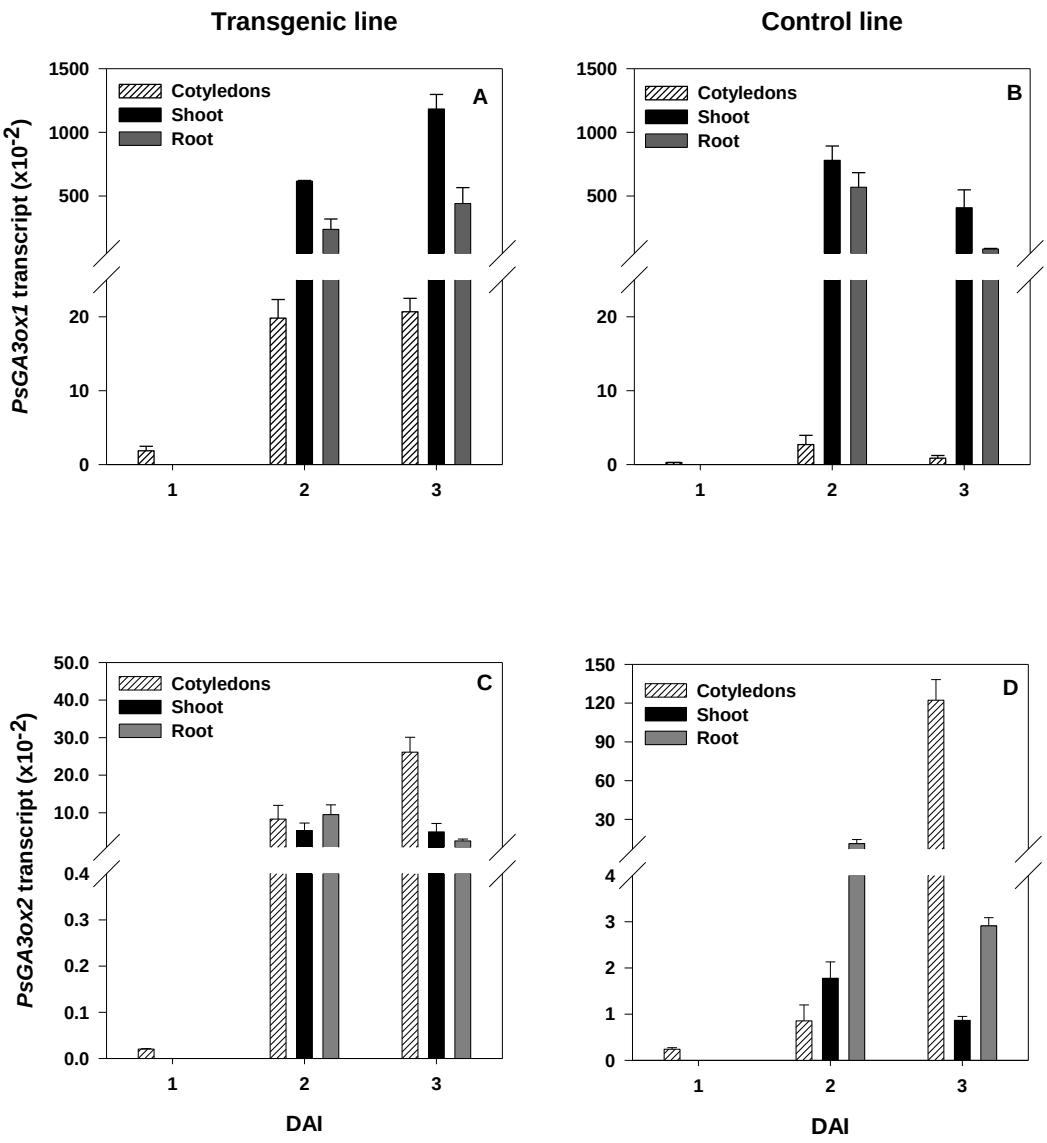

Figure 4.5. Relative transcript abundance of A and B, total (endogenous + transgenic) *PsGA3ox1*; and C and D, *PsGA3ox2* in cotyledons (1-3 DAI), shoots (2-3 DAI) and roots (2-3 DAI) during germination and early seedling growth of transgenic and control lines. Data are means ± SE, n= 2.

Figure 4.6. Relative transcript levels of *PsGA3ox1* (left Y-axis) and *PsGA3ox2* (right Y-axis) during seed germination and early seedling growth of A, B and C, 'Carneval'; and D, E, and F, 'Alaska'. Relative transcript levels were determined in C and F, mature embryos and cotyledons (0.5-6 DAI); A, B, D and E, embryo axes (0.5 and 1 DAI); A and D, roots (2-6 DAI); and B and E, shoots (2-6 DAI). Data are means ± SE, n= 2 to 3.

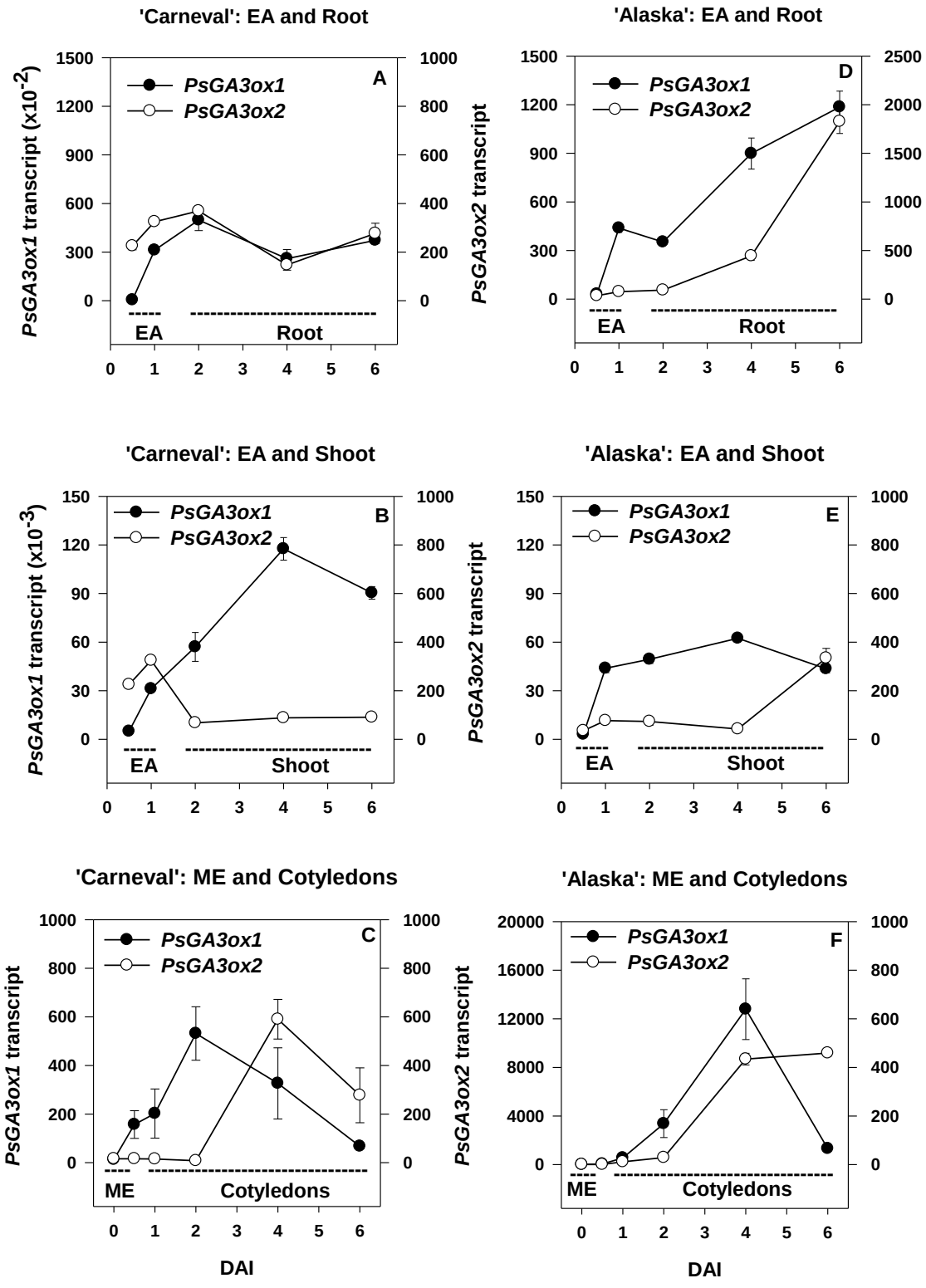
'Carneval': EA and Root
'Alaska': EA and Root
'Carneval': EA and Shoot
'Alaska': EA and Shoot
'Carneval': ME and Cotyledons
'Alaska': ME and Cotyledons
PsGA3ox1
PsGA3ox2
PsGA3ox1 transcript (x10-2)
PsGA3ox2 transcript
PsGA3ox1 transcript (x10-3)
PsGA3ox1 transcript
EA
Root
Shoot
ME
Cotyledons
DAI
A
B
C
D
E
F

Figure 4.7. Relative transcript levels of A, *PsGA20ox1*; B, *PsGA20ox2*; D, transgenic *PsGA3ox1*; E, total *PsGA3ox1* (transgenic + endogenous); F, *PsGA3ox2*; H, *PsGA2ox1*; and G, *PsGA2ox2* in embryo axis (EA) and shoot tissues and; C, fresh weights of EA and shoot of transgenic (TG) and transgenic null (C) lines during germination and early seedling growth (from 1 to 3 DAI). Data are means ± SE of two biological replicates for transcription profiling and means ± SE, n=10 to 13 for EA and shoot fresh weight.

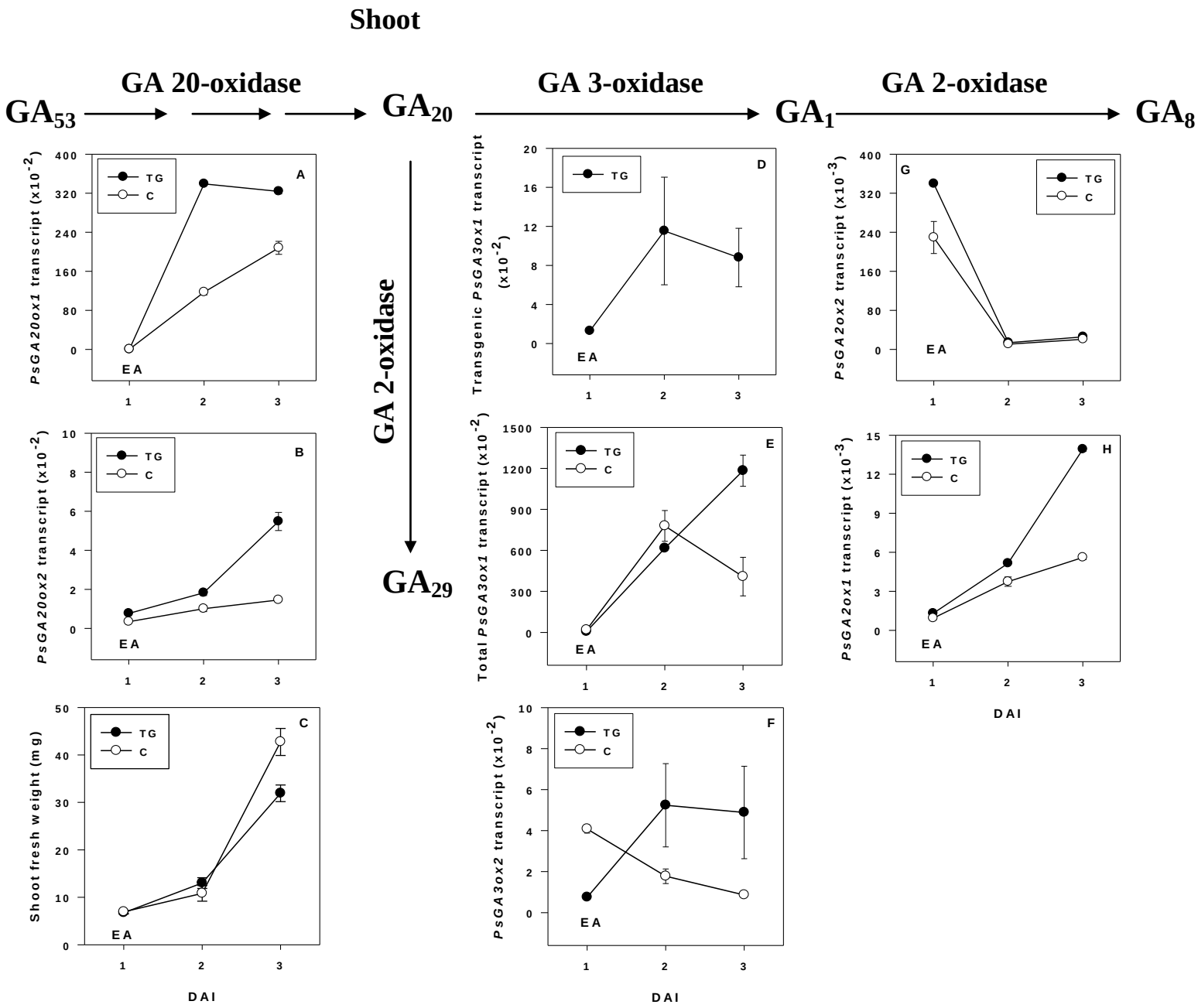
Shoot
GA 20-oxidase
GA 3-oxidase
GA 2-oxidase
GA53
GA20
GA1
GA8
GA 2-oxidase
GA29
PsGA20ox1 transcript (x10-2)
Transgenic PsGA3ox1 transcript (x10-2)
PsGA2ox2 transcript (x10-3)
PsGA20ox2 transcript (x10-2)
Total PsGA3ox1 transcript (x10-2)
PsGA2ox1 transcript (x10-3)
Shoot fresh weight (mg)
PsGA3ox2 transcript (x10-2)
TG
C
EA
A
B
C
D
E
F
G
H
DAI

Figure 4.8. Relative transcript levels of A, *PsGA20ox1*; B, *PsGA20ox2*; D, transgenic *PsGA3ox1*; E, total *PsGA3ox1* (transgenic + endogenous); F, *PsGA3ox2*; H, *PsGA2ox1*; and G, *PsGA2ox2* in embryo axis (EA) and root tissues; and C, fresh weights of EA and root of transgenic (TG) and transgenic null (C) lines during germination and early seedling growth (from 1 to 3 DAI). Data are means ± SE of two biological replicates for transcription profiling and means ± SE, n=10 to 13 for EA and root fresh weight.

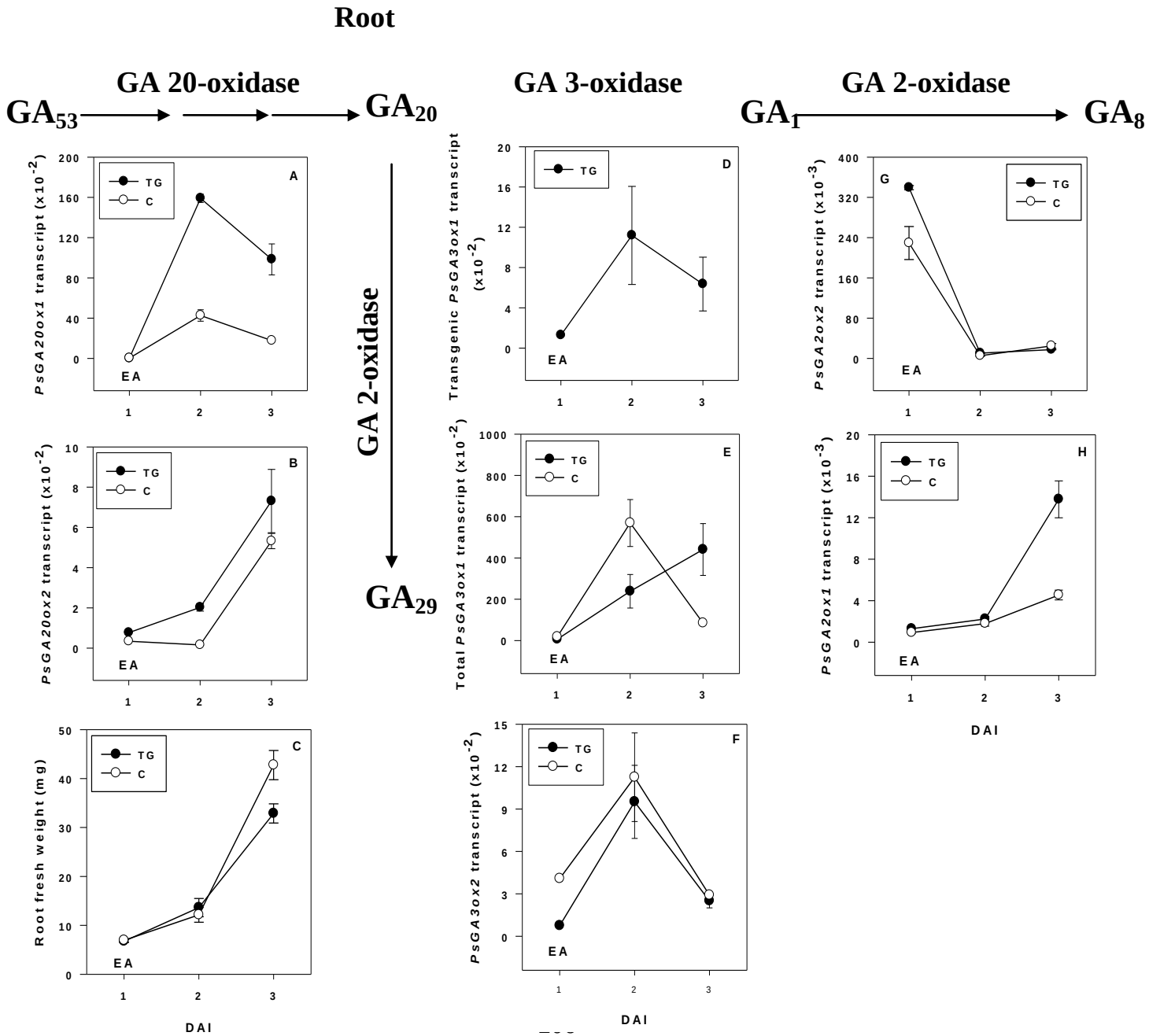
Root
GA 20-oxidase
GA 3-oxidase
GA 2-oxidase
GA53
GA20
GA1
GA8
GA 2-oxidase
GA29
A
B
C
D
E
F
G
H
TG
C
EA
DAI
PsGA20ox1 transcript (x10-2)
PsGA20ox2 transcript (x10-2)
Root fresh weight (mg)
Transgenic PsGA3ox1 transcript (x10-2)
Total PsGA3ox1 transcript (x10-2)
PsGA3ox2 transcript (x10-2)
PsGA2ox2 transcript (x10-3)
PsGA2ox1 transcript (x10-3)

Literature cited:

Ayele BT (2006) Gibberellin biosynthesis during germination and young seedling growth of pea. PhD thesis. University of Alberta, Edmonton, Alberta, Canada

Ayele BT, Ozga JA, Kurepin LV, Reinecke DM (2006) Developmental and embryo axis regulation of gibberellin biosynthesis during germination and young seedling growth of pea. Plant Physiol **142**: 1267-1281

Bewley JD (1997) Seed germination and dormancy. Plant Cell **9**: 1055-1066

Bewley JD, Black M (1994) Seeds: Physiology of development and germination, Ed 2nd. Plenum Press, New York

Debeaujon I, Koornneef M (2000) Gibberellin requirement for Arabidopsis seed germination is determined both by testa characteristics and embryonic abscisic acid. Plant Physiol **122**: 415-424

Davidson SE, Elliott RC, Helliwell CA, Poole AT, Reid JB (2003) The pea gene *NA* encodes ent-kaurenoic acid oxidase. Plant Physiol **131**: 335-344

Elliott RC, Ross JJ, Smith JJ, Lester DR, Reid JB (2001) Feed-forward regulation of gibberellin deactivation in Pea. J Plant Growth Regul **20**: 87-94

Gallego-Giraldo L, Ubeda-Tomas S, Gisbert C, Garcia-Martinez JL, Moritz T, et al. (2008) Gibberellin homeostasis in tobacco is regulated by gibberellin metabolism genes with different gibberellin sensitivity. Plant Cell Physiol **49**: 679-690

Graebe JE (1986) Gibberellin biosynthesis from gibberellin $A_{12\text{-aldehyde}}$. *In* M Bopp, ed, Plant Growth Substances 1985. Springer-Verlag, New York, pp 74-82

Groot SPC, Karssen CM (1987) Gibberellins regulate seed germination in tomato by endosperm weakening: a study with gibberellin mutants. Planta **171**: 525-531

Karssen CM, Zagorski S, Kepczynski J, Groot SPC (1989) A key role for endogenous gibberellins in the control of seed germination. Ann of Bot **63**:71-80

Koonnneef M, van der Veen JH (1980) Induction and analysis of gibberellin-sensitive mutants in *Arabidopsis thaliana* (L.) Heynh. Theor Appl Genet **58**:257-263

Kucera B, Cohn MA, Leubner-Metzger G (2005) Plant hormone interactions during seed dormancy and germination. Seed Sci Res **15**:281-307

Leubner-Metzger G, Frundt C, Meins Jr F (1996) Effects of gibberellins, darkness and osmotic on endosperm rupture and class 1 β-1-3 glucanse inductionin tobacco seed germination. Planta **199**: 282-288

Livak KJ, Schmittgan TD (2001) Analysis of relative gene expression data using real-time quantitative PCR and the $2^{-\Delta\Delta Ct}$ method. Methods **25**: 402-408

Lovell PH (1977) Correlative Influence in Seedling Growth. *In* JF Sutcliff and JS Pate, The Physiology of the Garden Pea. Academic Press Inc., New York pp 265-290

Mitchum MG, Yamaguchi S, Hanada A, Kuwahara A, Yoshioka Y, et al. (2006) Distinct and overlapping roles of two gibberellin 3-oxidases in Arabidopsis development. Plant J **45**: 804-818

Nambara E, Akazawa T, McCourt P (1991) Effects of gibberellin biosynthetic inhibitor uniconazol on mutants of Arabidopsis. Plant Physiol **97**: 736-738

Ogawa M, Hanada A, Yamauchi Y, Kuwahara A, Kamiya Y, et al. (2003) Gibberellin biosynthesis and response during Arabidopsis seed germination. Plant Cell **15**: 1591-1604

Ozga JA, Reinecke DM, Ayele BT, Ngo P, Nadeaue C, Wickramarathna AD (2009) Developmental and hormonal regulation of gibberellin biosynthesis and catabolism in pea fruit. Plant Physiol **150**: 448-462

Petruzzelli L, Harren F, Perrone C, Reuss J (1995) On the role of ethylene in seed germination and early growth of *Pisum sativum*. J Plant Physiol **145**:83-86

Potts WC, Reid JB (1983) Internode length in *Pisum.* III. The effect and interaction of the *Na/na* and *Le/le* gene differences on endogenous gibberellin-like substances. Physiol Plant **57**: 448-454

Powell A, Matthews S (1978) The damaging effect of water on dry pea embryos during imbibition. J Exp Bot **29**: 1215-1229

Probsting WM, Hedden P, Lewis MJ, Croker SJ, Probsting LN (1992) Gibberellin concentration and transport in genetic lines of pea: effects of grafting. Plant Physiol **100:** 1354-1360

Radi A, Lange T, Tomoya N, Koshioka M, Pimienta LMP (2006) Ectopic expression of pumpkin gibberellin oxidases alters gibberellin biosynthesis and development of transgenic *Arabidopsis* plants. Plant Physiol **140**:528-536

Reid JB, Symons GM, Ross JJ (2004) Regulation of gibberellin and brassinosteroid biosynthesis by genetic, environmental and hormonal factors. *In* PJ Davis, ed, Plant hormones: Biosynthesis, signal transduction, action. Ed 3. Kluwer Academic Publishers, Dordrecht, The Netherlands, pp 179-203

Ross JJ, Reid JB, Swain SM (1993) Control of stem elongation by gibberellin A_1: evidence from genetic studies including the slender mutant *sln*. Aust J Plant Physiol **20**: 585-599

Sachez RA, de Miguel L (1997) Phytochrome promotion of mannan-degrading enzyme activities in the micropylar endosperm of *Datura ferox* seeds requires the presence of the embryo and gibberellin synthesis. Seed Sci Res **7**:27-33

Sponsel VM (1983) The localization, metabolism and biological activity of gibberellins in maturing and germinating seeds of *Pisum sativum* cv. Progress No.9. Planta **159**: 454-469

Sponsel VM, Hedden P (2004) Gibberllin biosynthesis and inactivation. *In* PJ Davis, ed, Plant hormones: Biosynthesis, signal transduction, action. Ed 3. Kluwer Academic Publishers, Dordrecht, The Netherlands, pp 63-94

Tanimoto E (1990) Gibberellin requirement for the normal growth of roots. *In* N Takahashi, B Phinney, J MacMillan, eds, Gibberellins. Springer-Verlag, New York, pp 229-240

Weston DE, Elliott RC, Lester DR, Rameau C, Reid JB, et al. (2008) The pea DELLA proteins *LA* and *CRY* are important regulators of gibberellin synthesis and root growth. Plant Physiol **147**: 199-205

Weston DE, Reid JB, Ross JJ (2009) Auxinregulation of gibberellin biosynthesis in the roots of pea (*Pisum sativum*). Funct Plant Biol **36**: 362-369

Woodger F, Jacobsen JV, Gubler F (2004) Gibberellin action in germinating cereal grains. *In* PJ Davis, ed, Plant hormones: Biosynthesis, signal transduction, action. Ed 3. Kluwer Academic Publishers, Dordrecht, The Netherlands, pp 221-240

Yaxley JR, Ross JJ, Sherriff LJ, Reid JB (2001) Gibberellin biosynthesis mutations and root development in pea. Plant Physiol **125**: 627-633

Chapter 5

General Discussion and Conclusions

Modulation of expression of GA genes within plant tissues provides new opportunities to study the regulation of GA biosynthesis and catabolism as well as the functions of GAs in plant growth and development. Maintaining optimum bioactive GA levels and right temporal and spatial patterns as well as controlling the responsiveness of a particular tissue to bioactive GA are vital processes for the plant to successfully complete its growth and development. Several studies have so far indicated that regulation of bioactive GA levels is mainly targeted at the 2-oxoglutarate dependent dioxygenases in the GA metabolism pathway (Fleet et al., 2003; Swain et al., 2005; Davidson et al., 2005; Ayele et al., 2006; Huang et al., 1998; Coles et al., 1999; Carrera et al., 2000; Vidal et al., 2001; Eriksson et al., 2000; Radi et. al., 2006; Gallego-Giraldo et al., 2008). Overexpression of sense and anti-sense copies of genes encoding the GA dioxygenases has been a useful research technique in GA studies. Overexpression of *GA20ox* genes in several species resulted in consistent outcomes whereas the effects of *GA3ox* overexpression appear to be species specific. Therefore, this study focused on characterizing *PsGA3ox1*-overexpressing transgenic pea plants and investigating the effects of overexpression on vegetative development, germination and early seedling growth. The mechanisms of GA homeostasis during the key growth and developmental events were also investigated.

In the first part of the study, the transgenic pea (cv. Carneval) lines generated to overexpress *PsGA3ox1* were characterized to understand how pea

responded to this overexpression (instead of orthologs of *GA3ox*). Morphological characterization revealed that the transgenic lines had modified plant stature and internode anatomy, delayed flowering, more fruit abortions before fruit set and longer fruits. Expression studies revealed that the transgenic *PsGA3ox1* expression was different in independently transformed lines and also among different organs. The increased steady state GA_1 and GA_8 levels were indicative of increased flux through the GA biosynthesis pathway in transgenic lines in the tissues tested. Increased levels of GA catabolic genes *PsGA2ox1* (in internodes) and *PsGA2ox2* (in tendrils) in elongating internodes and tendrils of the transgenic lines compared to the controls was indicative of feedback regulation of GA biosynthesis. This feedback regulation was due to the increased levels of bioactive GA to maintain GA homeostasis in fast growing organs.

Overall expression dynamics of GA genes during stipule development were different from tendril expression dynamics suggesting that the vegetative development of different organs is regulated differently by GA to match with their unique developmental patterns. Stipules and tendrils exhibited marked differences in bioactive GA_1 levels at similar growth stages suggesting different vegetative organs have diverse sensitivities for bioactive GA.

Phenotypic characterization studies revealed interesting changes in reproductive morphology of the transgenic lines. These changes are likely due to the increased flux through the GA biosynthesis pathway during pea pod development. Detailed growth dynamic studies along with expression studies on GA biosynthesis and catabolism genes would provide valuable information to

further understand the developmental regulation of the GA biosynthesis and catabolism pathways during pea fruit development and effects of GA on fruit development. Radiolabeled-GA_{20} metabolic profiling and/or analysis of endogenous GA levels of transgenic and control lines along with gene expression studies would further reinforce our understanding of the aspects described. Although the transgene exhibited stable inheritance and the observed phenotypes were consistent from one generation to the next, the plants used for phenotypic characterization and tissues used for expression studies of transgenic and control lines were from different generations (T_4 and T_6) due to limitations in seed availability for some lines. Using plants from the same generation for the phenotypic characterization and gene expression studies would have been ideal and future studies will likely be performed to address this experimental issue.

GA_3 application studies revealed that the response of elongating internodes to bioactive GA in the *PsGA3ox1*-overexpressor lines was not saturated. Expression analysis of transgenic *PsGA3ox1* and other late GA genes of elongating internodes (at 15 to 20% full length) at positions 2 to 9 revealed a consistent and a much greater oscillation of the transcript levels of the GA catabolic gene *PsGA2ox1* between adjacent internodes in the *PsGA3ox1*-overexpressor lines. Steady state endogenous GA_1 levels were higher in the internode with lower *PsGA2ox1* and GA_1 levels were lower in the internode with higher *PsGA2ox1* when internodes were assessed at 50% final length in TG1. A similar pattern of GA_1 levels and *PsGA2ox1* levels was observed when TG1 internodes were analyzed for GA content at 80% final length. Consistently, the

internodes of TG1 that contained higher GA_1 levels were longer than those that contained lower GA_1. These data suggest that when a specific threshold level of bioactive GA_1 in the internode is exceeded, a feedback mechanism is triggered in the adjacent elongating internode resulting in the up-regulation of the GA catabolic gene *PsGA2ox1*. This feedback mechanism will maintain internode elongation within a specific range by reducing the levels of bioactive GA_1 in this developing internode.

Data gathered from studies into [^{14}C]GA_1 application to the stipules suggested that stipules could be another source of bioactive GA_1 for the elongating internodes, if required. The movement of bioactive GA_1 from the internodes which have higher GA_1 levels to the next elongating internode was inconclusive. The uptake of [^{14}C]GA_1 by the internodes was extremely low when [^{14}C]GA_1 was applied to the surface of the internode. Therefore, using a better application technique, possibly direct injection (needs to find out through preliminary experiments) of the right amount of [^{14}C]GA_1 without inducing the pharmacological effect would provide better evidence of the triggering of the homeostasis mechanism in the adjacent elongating internode of the TG1 line. A large scale experiment to collect enough tissue to analyze different radiolabelled GAs by HPLC after the internode has been treated with [^{14}C]GA_1, would provide conclusive evidence for transport of GA_1 in elongating internodes. A similar large scale experiment involving the treatment of stipules with [^{14}C]GA_1 to gather further evidence that stipules can be a source of bioactive GA_1 for the elongating internodes should also be performed.

The auxin efflux carrier genes, *PsPIN1* and *PsPIN2* exhibited a transient decrease in expression at internode position 3 followed by a marked increase at internode position 4 in all lines analyzed. This likely reflects the requirement of auxin accumulation within this internode for vascular re-patterning events. Comparative auxin inhibitor application studies with auxin application studies aimed at higher elongating internodes would further reinforce our hypothesis that was based on observations of transcript levels and internode anatomy.

In the third part of the study, I expanded our inferences on how GA biosynthesis is regulated and GA homeostasis is maintained during seed germination and early seedling development. Overexpression of *PsGA3ox1* resulted in larger embryos (seeds) at maturity that were more vulnerable to rapid imbibition damage. Overall GA gene expression analysis suggests an increased flux through the GA biosynthesis pathway to bioactive GA_1 in the transgenic cotyledons; however, the endogenous levels of bioactive GA_1 and/or radiolabeled-GA_{20} metabolic profiles need to be determined in the cotyledonary tissues in order to confirm that the modified GA biosynthesis transcript profile increased the flux through to bioactive GA in the transgenic line. Ayele et al. (2006) suggested that GA biosynthesis in the cotyledons is controlled by a signal(s) from the embryo axis and it would be interesting to investigate how this relationship is affected in the *PsGA3ox1*-overexpressing cotyledons.

Shoots and roots of the pea seedlings exhibited different phenotypic responses for the *PsGA3ox1*-overexpression. Seedling shoots exhibited typical responses for increased bioactive GA levels (i.e. longer shoots), although the

transcription profile demonstrated the stimulation of feedback regulation mechanism as early as 3 DAI to maintain the GA homeostasis in rapidly growing shoots. Seedling roots exhibited a similar GA gene transcription profile, but transgenic roots were late in primary root extension and lateral root initiation. This could be due to the much higher levels of *PsGA3ox1* in roots than in shoots resulting in a shift in the GA: auxin ratio in the roots away from the optimum. The observations could also be due to the different nature of shoot and root responses to bioactive GA. A series of experiments based on exogenous application of bioactive GA or IAA in different concentrations as well as combined applications of these hormones would provide further insights to support this hypothesis.

GA biosynthesis and signaling link together to deliver the effect of GA on plant growth and development. DELLA proteins and the GA receptor (GID1) are key factors of the GA signaling pathway (Mauriat and Moritz, 2009). The investigation of the interactions and coordination of GA biosynthesis and signaling components is emerging as a novel branch of research in hormone biology. Overexpression of *PttGDI1* (codes for GA receptor GID1) in aspen resulted in decreased levels of bioactive gibberellins and it was suggested that an increase in GA signaling due to the overexpression of *GID1* induced the feedback mechanism that represses the GA biosynthesis pathway (Mauriat and Moritz, 2009). Conversely, studying *PsGA3ox1*-overexpressing transgenic pea plants would be useful to investigate how modifications in GA biosynthesis affect GA signaling.

The studies described in this thesis revealed for the first time that GA 3β-hydroxylation is a rate limiting step in GA biosynthesis in pea. These studies also uncovered a novel GA homeostasis mechanism in elongating pea stems of transgenic lines and provided evidence for possible sources that contribute to internodal GA pool. Furthermore, germination and seedling growth studies provided new information on the importance of hormone balance for the successful completion of the pea growth cycle, although there is still much that requires further study to provide a complete understanding of importance of plant hormone balance.

Literature Cited:

Ayele BT, Ozga JA, Reinecke DM (2006) Regulation of GA Biosynthesis Genes during Germination and Yong Seedling Growth of Pea (*Pisum sativum* L.). J Plant Growth Regul **25**: 219-232

Carrera E, Bou J, Gracia-Martinez JL, Prat S (2000) Changes in GA 20-oxidase gene expression strongly affects stem length, tuber induction and tuber yield of potato plants. Plant J **22**:247-256

Coles JP, Phillips AL, Croker SJ, Garcia-Lepe R, Lewis MJ, et al (1999) Modification of gibberellin production and plant development in *Arabidopsis* by sense and antisense expression of gibberellin 20-oxidase genes. Plant J **17**:547-556

Davidson SE, Swain SM, Reid JB (2005) Regulation of the early GA biosynthesis pathway in pea. Planta **222**: 1010-1019

Eriksson M, Israelsson M, Olsson O, Moritz T (2000) Increased gibberellin biosynthesis in transgenic trees promotes growth, biomass production and xylem fiber length. Nature Biotech **18**: 784-788

Fleet CM, Yamaguchi S, Hanada A, Kawaide H, David CJ, et al (2003) Overexpression of *AtCPS* and *AtKS* in *Arabidopsis* confers increased *ent*-kaurene production but no increase in bioactive gibberellins. Plant Physiol **132**: 830-839

Gallego-Giraldo L, Ubeda-Tomas S, Gisbert C, Garcia-Martinez JL, Moritz T, et al. (2008) Gibberellin homeostasis in tobacco is regulated by gibberellin metabolism genes with different gibberellin sensitivity. Plant Cell Physiol **49**: 679-690

Huang S, Raman AS, Ream JE, Fujiwara H, Cerny RE, et al. (1998) Overexpression of 20-oxidase confers a gibberellin-over production phenotype in *Arabidopsis*. Plant Physiol **118**:773-781

Mauriat M, Moritz T (2009) Analyses of GA20ox- and GID1-over-expressing aspen suggest that gibberellins play two distinct roles in wood formation. Plant J **58**: 989-1003

Radi A, Lange T, Tomoya N, Koshioka M, Pimienta LMP (2006) Ectopic expression of pumpkin gibberellin oxidases alters gibberellin biosynthesis and development of transgenic *Arabidopsis* plants. Plant Physiol **140**:528-536

Swain SM, Sing D P, Helliwell CA, Poole AT (2005) Plants with increased expression of ent-kaurene oxidase are resistant to chemical inhibitors of this gibberellin biosynthesis enzyme. Plant Cell Physiol **46**: 284-291

Vidal AM, Gisbert C, Talon M, Primo-Millo E, Lopez-Diaz I, et al. (2001) The ectopic over-expression of a citrus gibberellin 20-oxidase enhances the non 13-hydroxylation pathway of gibberellin biosynthesis and induces an extremely elongated phenotype in tobacco. Physiol Plant **112**:251-260

Appendix 1

Table A.1.1. Assessment of pea lines that were transformed with the *PsGA3ox1* sense vector construct (Figure 2.1) for the presence of reporter gene *NPTII* at the T_2 generation using primers to obtain the amplicon *NPTII-776.*

Transgenic lines	T_2 generation; Pot # (plant #)								
C3β$T6B(17-3T1)	+* 15(1)	+ 15(2)	+ 15(3)	+ 16(1)	+ 16(2)	+ 16(3)	+ 19(1)	+ 19(2)	+ 19(3)
C3β$T5D(6-3T1)	+ 1(2)	+ 1(3)	+ 2(1)	- 2(2)	+ 2(3)	- 3(1)	+ 4(1)	+ 4(2)	+ 5(1)
C3β$T5F(25-1T1)	+ 22(1)	+ 22(2)	+ 22(3)	+ 23(1)	+ 23(2)	+ 25(1)	+ 25(2)	+ 25(3)	+ 24(1)
C3β$T10B(12-1T1)	+ 8(1)	+ 8(2)	+ 8(3)	+ 9(1)	+ 9(2)	+ 9(3)	+ 10(1)	+ 10(2)	+ 10(3)
C3β$T10A(3-2T1)	+ 11(1)	+ 11(2)	+ 11(3)	+ 12(1)	+ 12(2)	- 12(3)	+ 13(1)	- 13(2)	+ 13(3)
C3β$T66B(20-3T1)	+ 36(1)	+ 36(2)	+ 36(3)	+ 37(1)	+ 37(2)	- 37(3)	+ 38(1)	+ 38(2)	+ 38(3)
Transgenic null lines	Plant number								
	1	2	3	4	5	6	7	8	9
C3β$T2A(11-3T1)	-	-	-	-	-	-	-	-	-
C3β$T5D(1-3T1)	-	-	-	-	-	-	-	-	-

*(+) presence or (-) absence of band at approximately 776 bp after separating PCR product by agarose gel electrophoresis.

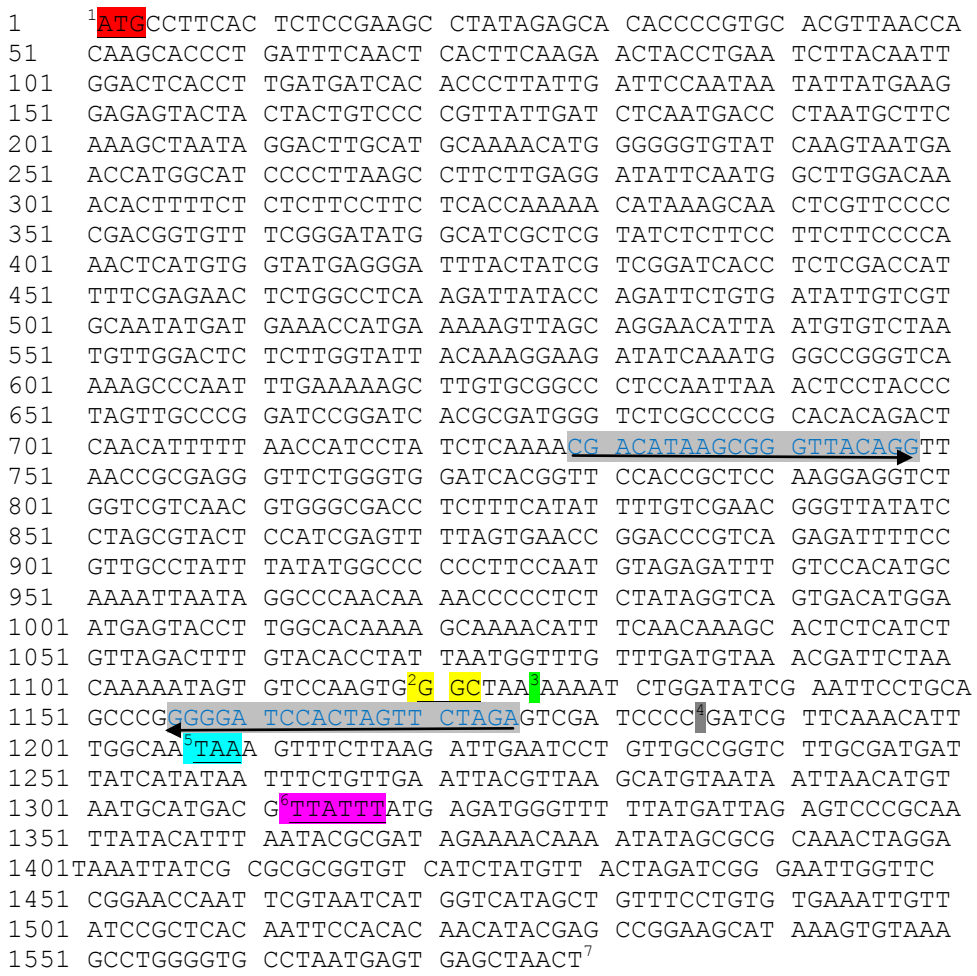

Figure A.1.1. Nucleotide sequence of *PsGA3ox1* mRNA (GenBank accession number AF001219, Martin et al., 1997) and NOS terminator sequence as found in the pCGN1559 plasmid vector used for plant transformation. The primers used to obtain the amplicon *TPsGA3ox1*-447 to confirm the presence of transgene in DNA extracts of the transformed plants are designated with arrows.

1- Start codon of *PsGA3ox1*
2- Last nucleotide of coding sequence
3- Residual cloning vector sequence
4- Start of NOS terminator
5- Stop codon for NOS termination

6- Polyadenylation signal

Table A.1.2. Amount of tissues used for RNA extractions (for expression study)

Tissue	Amounts used (mg FW)
Internodes	50-80
Stipules (stage 1)	30-50
Stipules (stage 2)	100-120
Stipules (stages 3 and 4)	180-200
Tendrils (stage 1)	20-30
Tendrils (stage 2)	80-100
Tendrils (stages 3 and 4)	180-200

Table A.1.3. Amount of tissues used for RNA extractions (for confirmation of *TPsGA3ox1* expression and for confirmation of specificity of the quantifying *TPsGA3ox1-130* amplicon)

Tissue	Amounts used (mg FW)
Internodes	100-120
Tendrils	150-190
Stipules	100-125
Pods (3 DAA)	150-200
Pericarps (10 DAA)	800-1000

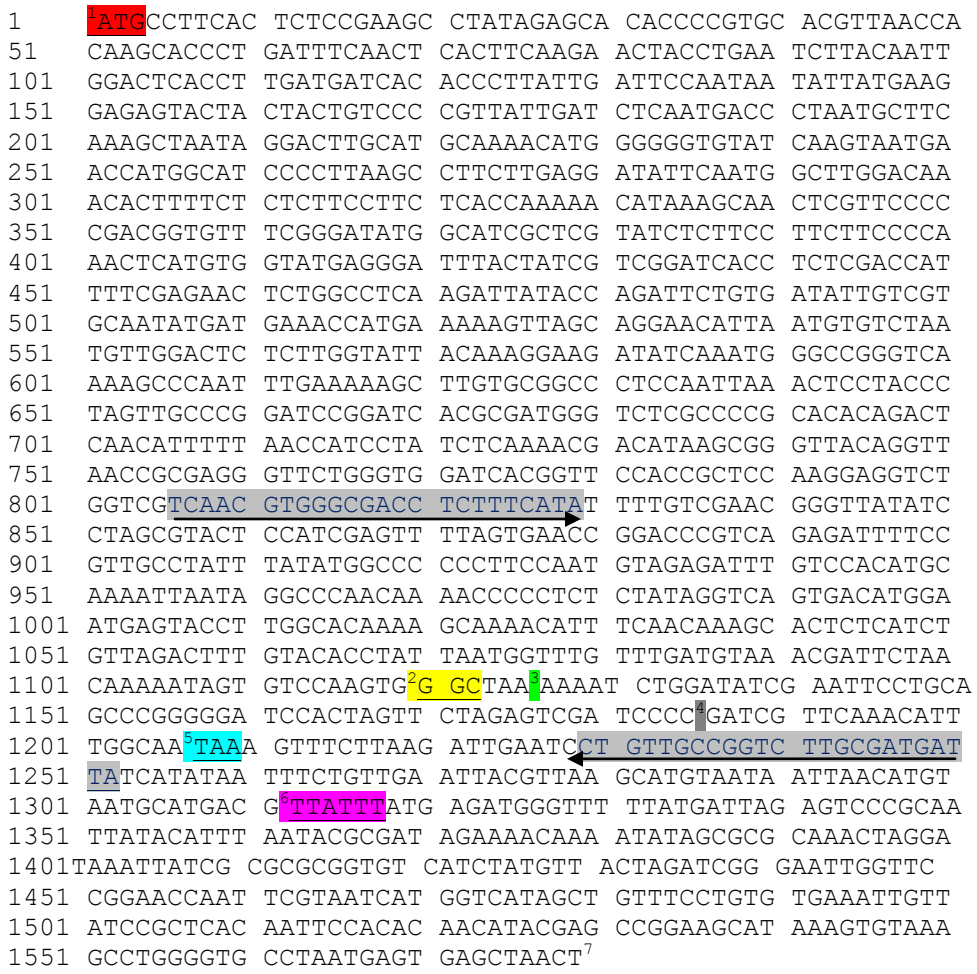

Figure A.1.2. Nucleotide sequence of *PsGA3ox1* mRNA (GenBank accession number AF001219, Martin et al., 1997) and NOS terminator sequence as found in the pCGN1559 plasmid vector used for plant transformation. The primers used to obtain the amplicon *TPsGA3ox1*-445 and confirm the expression of the transgene by RT-PCR in the T_3 generation are designated with arrows

1- Start codon of *PsGA3ox1*
2- Last nucleotide of coding sequence
3- Residual vector sequence
4- Start of NOS terminator

5- Stop codon in NOS termination
6- Polyadenylation signal

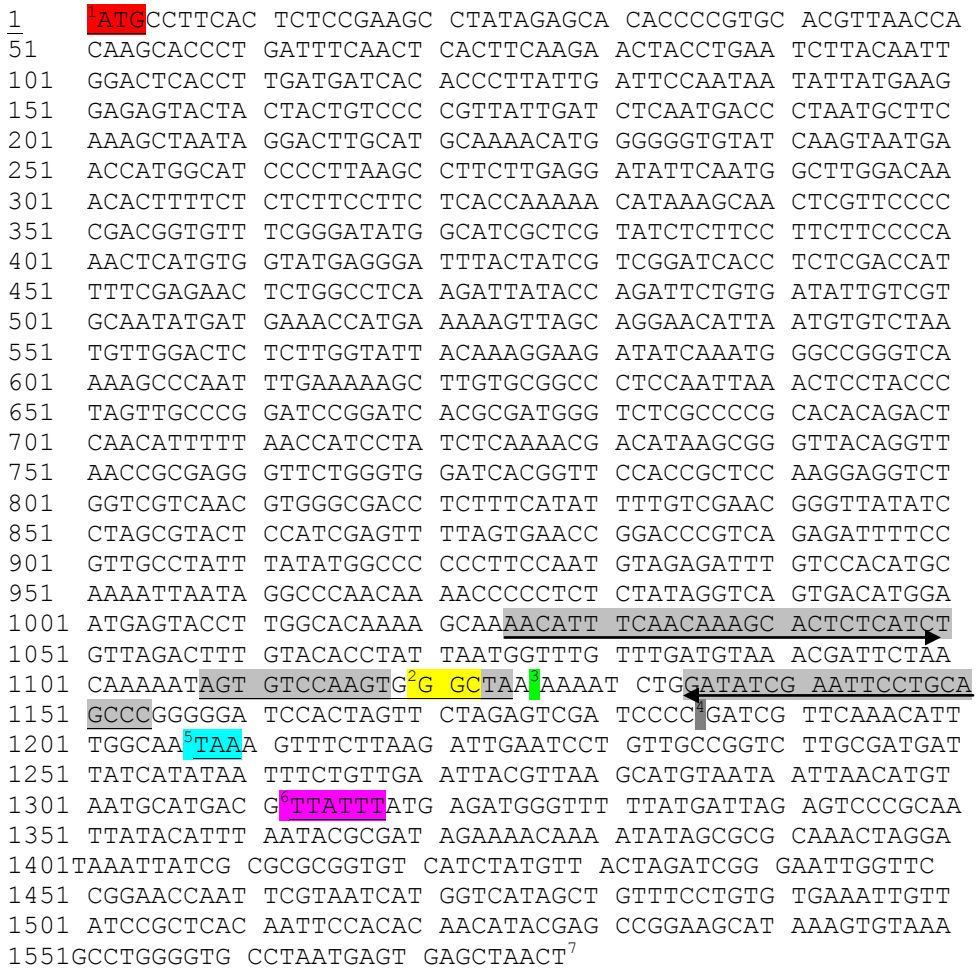

Figure A.1.3. Nucleotide sequence of *PsGA3ox1* mRNA (GenBank accession number AF001219, Martin et al., 1997) and NOS terminator sequence as found in the pCGN1559 plasmid vector used for plant transformation. The primers (shaded and underlined with arrows) and the probe (shaded and underlined) used to obtain the quantifying amplicon *TPsGA3ox1-130* using qRT-PCR are highlighted in the sequence.

1- Start codon of *PsGA3ox1*
2- Last nucleotide of coding sequence

3- Residual cloning vector sequence
4- Start of NOS terminator
5- Stop codon in NOS termination
6- Polyadenylation signal

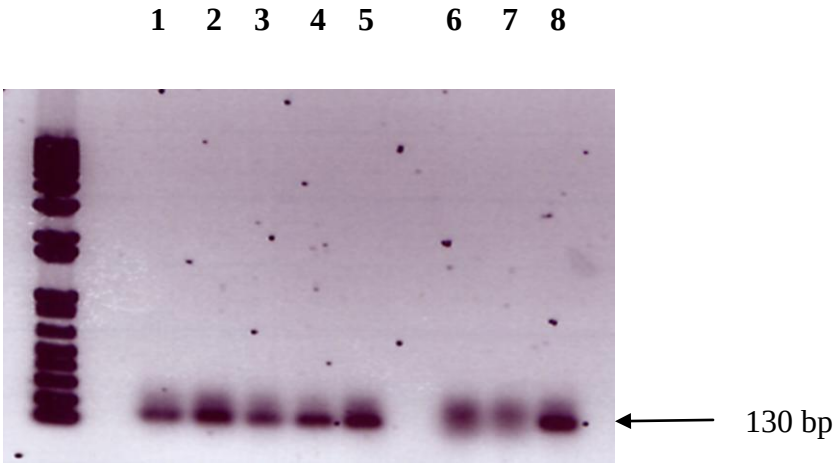

Figure A.1.4. Agrose gel electrophoresis of PCR products produced using primers to obtain the quantifying amplicon *TPsGA3ox1-130*. Total RNA isolated from TG2 pods (1), TG1 pericarps (2), TG1 internodes (3), TG1 stipules (4), TG1 internodes (5), C1 pods (6), C1 internodes (7), TG3 internodes (8),

```
Vector[1]1020     GCAAAACATTTCAACAAAGCACTCTCATCTGTTAGACTTTGTACACCTATTAATGGTTTG 1080
Amplicon[2]       ----AACATTTCAACAAAGCACTCTCATCTGTTAGACTTTGTACACCTATTAATGGTTTG
                      **********************************************************

vector             TTTGATGTAAACGATTCTAACAAAAATAGTGTCCAAGTGGGCTAAAAAATCTGGATATCG 1140
amplicon           TTTGATGTAAACGATTCTAACAAAAATAGTGTCCAAGTGGGCTAAAAAATCTGGATATCG
                   ************************************************************


vector             AATTCCTGCAGCCCGGGGGATCCACTAGTTCTAGAGTCGATCCCCGATCGTTCAAACATT 1200
amplicon           AATTCCTGCAGCCC----------------------------------------------
                   **************
```

Figure A.1.5. Sequence of amplicon obtained by PCR from primers for *TPsGA3ox1-130*.

Vector[1]: partial nucleotide sequence as found in the pCGN1559 plasmid vector used for plant transformation from the 1020 bp position of the nucleotide sequence of *PsGA3ox1* (GenBank accession number AF001219, Martin et al., 1997) through the NOS terminator sequence.
Amplicon[2]: composite sequence obtained by sequencing the PCR amplicon using forward and reverse primers for *TPsGA3ox1-130.*

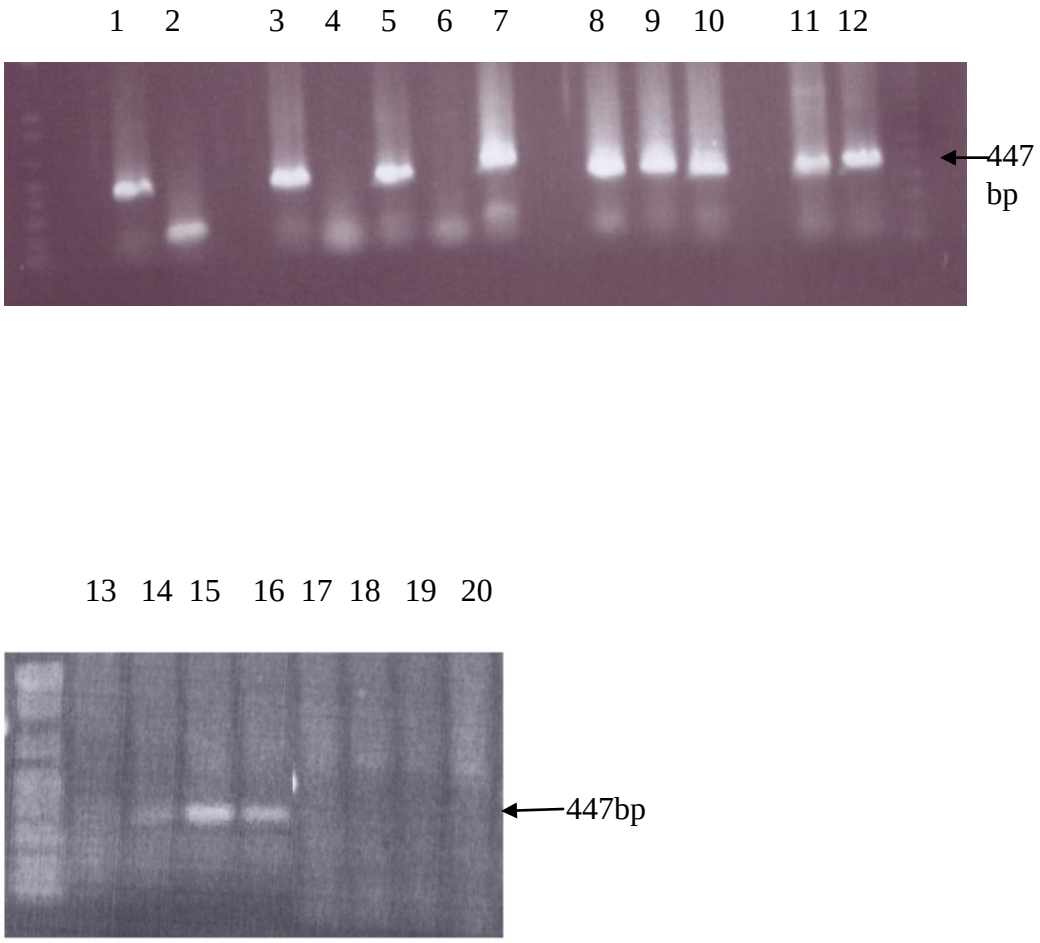

Figure A.1.6. Confirmation of the stable integration of transgenic *PsGA3ox1* into plant DNA. DNA was isolated from plasmid containing the *PsGA3ox1* construct (1), or from young stipules of TG2 (3, 5, and 7), TG1 (8, 9, 10, 11 and 12), C1 (4 and 6), TG3 (14, 15, and 16), and C3 (17, 18, 19, 20) lines, and tested for the

presence of the inserted *PsGA3ox1* gene using transgene specific primers for *TPsGA3ox1*-447.

Figure A.1.7. Sequence of transgenic *PsGA3ox1* PCR amplicon obtained using the forward and reverse primers for *TPsGA3ox1*-445.

Vector[1]: partial nucleotide sequence of *PsGA3ox1* mRNA (GenBank accession number AF001219, Martin et al., 1997) and NOS terminator sequence as found in the pCGN1559 plasmid vector used for plant transformation.

Amplicon[2]: composite sequence obtained by sequencing the PCR amplicon obtained using forward and reverse primers for *TPsGA3ox1*-445.

Table A.1.4. PCR efficiencies of quantifying amplicons used in qRT-PCR assays.

Amplicon	Efficiency	r^2
TPsGA3ox1-130	100.0%	0.967
PsGA3ox1-87	94.8%	0.999
PsGA3ox2-104	100.0%	0.973
PsGA20ox1-104	96.4%	0.994
PsGA20ox2-88	92.5%	0.997
PsGA2ox1-73	84.9%	0.984
PsGA2ox2-83	96.4%	0.999

Appendix 2

Figure A. 2.1. Nucleotide sequence of *PsPIN1* mRNA (GenBank accession number AY 222857) with forward and reverse primers (shaded and underlines with arrows) and probe (shaded and underline) sequences used for qRT-PCR.

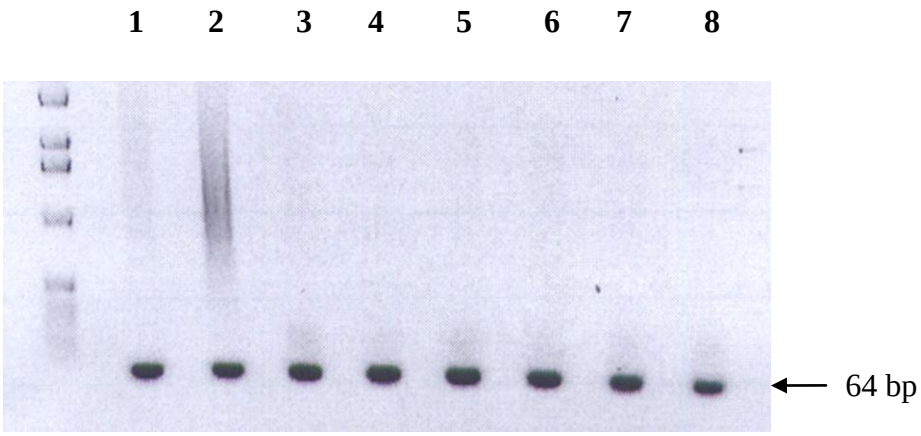

Figure A. 2. 2. Agarose gel electrophoresis of qRT-PCR products produced using primers to obtain the *PsPIN1-64* amplicon. Total RNA isolated from C1 internodes (1), WT internodes (2), TG2 internodes (3), TG1 internodes (4), TG3 internodes (5), TG2 pericarps (6), TG1 pods (7), TG3 tendrils (8).

```
PsPIN1[1]          GGTTTATCGGCCTCGCGAGGTGTTACTCCGAGGCCGTCTAATTACGAAGAAGATGCTTCG 900
Amplicon[2]        ---------------------------------GGCCGTCTAATTACGAAGAAGATGCTTCG
                                                    ****************************

PsPIN1             AATGCGAAGAAGTTGAAACATTATCCGGCTCCTAATCCGGGAATGTTTTCTCCTACTAAT 960
amplicon           AATGCGAAGAAGTTGAAACATTATCCGGCTC-----------------------------
                   *******************************
```

Figure A.2. 3. Sequence of amplicon obtained by PCR from primers for *PsPIN1-64*.

PsPIN1[1]: partial mRNA nucleotide sequence (GenBank accession number AY222857)

Amplicon[2]: composite sequence obtained by sequencing the *PsPIN1-64* amplicon.

```
   1 atgattacat tcaaagatct atacactgtc ttaacagcag tcgttccatt atatgttgct
  61 atgatcttag cctacggttc tgtccgttgg tggaagattt tctcacccga tcaatgctcc
 121 ggcataaacc gtttcgtcgc ggtttttcgcc gtccctctcc tctctttcca tttcatctca
 181 tccaacaatc cataccaaat gaacttcaga ttcatagcgg cagacacact gcaaaaaatc
 241 atcatgcttt tcgcgctttc gctatggact aagttcacta aaaacggcaa tttagaatgg
 301 atgataacca ttttctcctt gtccacgctt ccaaacactt tggttatggg aattcctctt
 361 ctaattgcta tgtatggtga ttattcagga accttaatgg ttcaagttgt ggttcttcag
 421 tgtatcattt ggtacactct tttgctcttt ctttttgagt accgtggtgc taagctttta
 481 atcatggaac agtttcctga aaccgcggct tcgatcgttt cgtttaaagt tgattcggac
 541 gttgtttcgc tcgacggaag agattttctt gaaacggatg cttctgttgg tgatgatggg
 601 aagttacatg ttactgtgag aaaatctaac gcgtcgcgga ggtcgtttat gatgactact
 661 ccgcgaccgt cgaatttgac tggagctgag atttatagtc tcagctccac gccaagaggg
 721 tctaatttca accacgccga gttttactcc atgatgggtt atcaacccag acattccaat
 781 tttggtacta ctgatctcta ttctgttgag tcttctagag gacccactcc tagaccttcg
 841 aatttcgaag aaaacggcgc aacttcgcct agattcgggt tttatccggc gcagaccgtg
 901 cctgcttcgt atcctgcgcc gaatcctgaa ttctcttcta ctgcgaaaac tgtgaagaat
 961 caaaatttga tgcagcagcc acaacagcaa caggtttcat tgcagacaaa gggctctcag
1021 gatgctaagg aattgcacat gtttgtgtgg agctcaagtc gttcgccggt gtcggaaagt
1081 gccggtctca acgccttccg aaattcggaa caatcagaag agggtgctaa agagatcaga
1141 atggtggttg ctgatgaaca taatcaaaat ggtgaaatca ataacaaagg ggaagttggt
1201 ggggaagaag atttcaagtt cattggagtg aaggggggaag aacaagttgg agaagggctc
1261 aatgggtcta acaaactgag ctccaatgca acaccagaga tccaccctaa agccaccgga
1321 gtggccgatt ccggtgtcgg aaaactcatg cctccggcga gtgtcatgac tcgtctcata
1381 ctcattatgg tttggagaaa acttatccga aatcccaaca cttattcaag tcttattggt
1441 ctcatttggt cccttgttgc atttaggtgg ggtgttcata tgcctaaaat agtagagaaa
1501 tcaatttcca tactctctga tgctgggctt ggaatggcta tgtttagctt aggtttattt
1561 atggctcttc aacctaagat aattgcatgt ggaaattcgg ttgcctcatt tgccatggct
1621 attagatttg tcactggtcc ggcagttatg gcagctgctt ctatcgctgt cggcctccgt
1681 ggtaccctcc ttcatgtagc aattgttcag gccgcacttc cacaagggat tgttccgttt
1741 gtgtttgcaa aagaatataa tgttcatcct gccattctta gtactgcggt tatatttggg
1801 atgttgatag ctcttccaat tactctactc tactacattc tccttggttt gtaa
```

Figure A. 2. 4. Nucleotide sequence of *PsPIN2* (GenBank accession number AB112364) with forward and reverse primers (shaded and underlines with arrows) and probe (shaded and underline) sequences used for qRT-PCR.

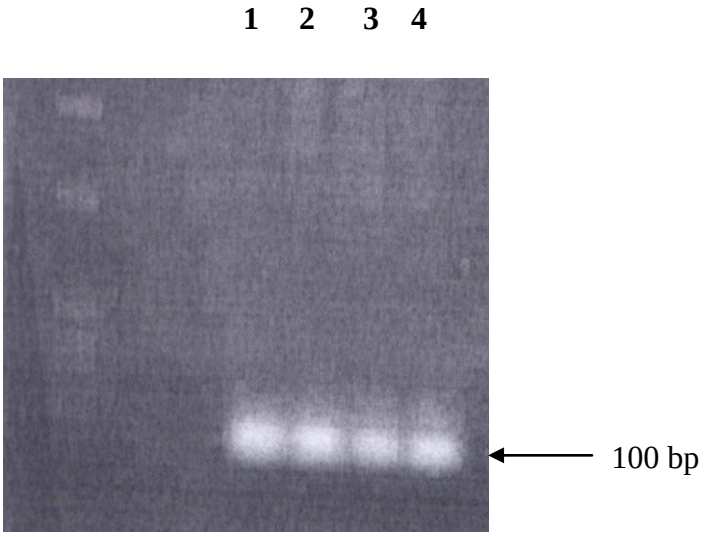

Figure A. 2. 5. Agrose gel electrophoresis of qRT-PCR products produced using primers to obtain the *PsPIN2-100* amplicon. Total RNA isolated from TG2 (1), TG1 (2), C1 (3), and TG3 (4).

```
PsPIN2[1]          GGAGCTGAGATTTATAGTCTCAGCTCCACGCCAAGAGGGTCTAATTTCAACCACGCCGAG 960
Amplicon[2]        ----------------------------------------------------CCACGCCGAG
                                                                       **********

PsPIN2             TTTTACTCCATGATGGGTTATCAACCCAGACATTCCAATTTTGGTACTACTGATCTCTAT 1020
amplicon           TTTTACTCCATGATGGGTTATCAACCCAGACATTCCAATTTTGGTACTACTGATCTCTAT
                   ************************************************************

PsPIN2             TCTGTTCAGTCTTCTAGAGGACCCACTCCTAGACCTTCGAATTTCGAAGAAAACGGCGCA 1080
amplicon           TCTGTTCAGTCTTCTAGAGGACCCACT-------------------------------
                   ***************************
```

Figure A. 2. 6. Sequence of amplicon obtained by PCR from primers for *PsPIN2-100.*

PsPIN2[1]: partial mRNA nucleotide sequence (GenBank accession number AB112364)

Amplicon[2]: composite sequence obtained by sequencing the PCR amplicon *PsPIN2-100*

```
PsPIN1          ------------------------------------------------------------
PsPIN2          ACATTTGTACTCTAGAATTACAAAACTCACTCTCACTTTCTCTGACACCTTCTCTTTCCG 60

PsPIN1          ------------------------------------------------------------
PsPIN2          AACCTCATTCTAATCTCACAAGCCAGTACTCCTACAAGTACAGTACCCACCAGACAATCA 120

PsPIN1          ------------------------------------------------------------
PsPIN2          CTGAAACACATCTCCTTCCTACTCCTACTTAACTAACTATAACCGTTTTCTTCCATTAAC 180

PsPIN1          ----------------------------------------ATGATAACTCTAATAGATTTC21
PsPIN2          TCCTCTTTCTCACATGCCACTCAACCTTCACTACCAAAAATGATTACATTCAAAGATCTA240
                                                        ***** **  * * **** *

PsPIN1          TACCATGTCATGACAGCAATGGTGCCACTTTATGTTGCTATGATCTTAGCTTATGGATCA81
PsPIN2          TACACTGTCTTAACAGCAGTCGTTCCATTATATGTTGCTATGATCTTAGCCTACGGTTCT300
                ***  **** * ****** * ** *** * ******************** ** ** **

PsPIN1          GTGAAATGGTGGAAGATATTCTCACCTGATCAATGTTCAGGAATCAACCGTTTTGTAGCA141
PsPIN2          GTCCGTTGGTGGAAGATTTTCTCACCCGATCAATGCTCCGGCATAAACCGTTTCGTCGCG360
                **    *********** ******** ******** ** ** ** ******** ** **

PsPIN1          CTTTTCGCTGTTCCACTTCTCTCATTCCATTTCATAGCCTCAAACAATCCTTACAAAATG201
PsPIN2          GTTTTCGCCGTCCCTCTCCTCTCTTTCCATTTCATCTCATCCAACAATCCATACCAAATG420
                 ******* ** ** ** ***** ***********  * ** ******** *** *****

PsPIN1          AACCTAAGATTCTTAGCTGCAGACACACTTCAAAAAATCATGATCCTAACCCTTCTCTTC261
PsPIN2          AACTTCAGATTCATAGCGGCAGACACACTGCAAAAAATCATCATGCTTTTCGCGCTTTCG480
                *** * ****** **** ********** ********** ** **   *   ** *

PsPIN1          ATTTGGAGCAATTTCTCCAAAAGGGGTTCTCTAGAATGGACAATAACACTCTTTTCACTC321
PsPIN2          CTATGGACTAAGTTCACTAAAAACGGCAATTTAGAATGGATGATAACCATTTTCTCCTTG540
                 * ****  ** *** * ****  **   * *********  *****  * ** **  *

PsPIN1          TCAACTTTGCCAAACACTTTGGTCATGGGAATCCCTTTACTCAAAGGAATGTACGGCGAT381
PsPIN2          TCCACGCTTCCAAACACTTTGGTTATGGGAATTCCTCTTCTAATTGCTATGTATGGTGAT600
                ** **  * ************** ******** *** * ** *  *  ***** ** ***

PsPIN1          TTCTCAGGTAGTTTAATGGTGCAAATCGTTGTTCTTCAATGTATTATCTGGTATACTATG441
PsPIN2          TATTCAGGAACCTTAATGGTTCAAGTTGTGGTTCTTCAGTGTATCATTTGGTACACTCTT660
                *  ***** *  ******** *** * ** ******** ***** ** ***** *** *

PsPIN1          ATGCTTTTCATGTTTGAGTTTAGAGGAGCAAGGTTGTTGATTTCTGAACAGTTTCCCGAC501
PsPIN2          TTGCTCTTTCTTTTTGAGTACCGTGGTGCTAAGCTTTTAATCATGGAACAGTTTCCTGAA720
                 **** **  * *******   * ** ** * * * ** **    *********** **

PsPIN1          ACTGCTGGTTCCATTGTTTCAATCCATGTTGATTCTGATGTCATGTCGTTAGACGGTAGA561
PsPIN2          ACCGCGGCTTCGATCGTTTCGTTTAAAGTTGATTCGGACGTTGTTTCGCTCGACGGAAGA780
                ** ** * *** ** *****  *  * ******** ** **  * *** * ***** ***
```

```
PsPIN1          ACACCATTGGAAACCGATGCTGAAATCAAACAAGATGGTAAACTTCATGTTACTGTTAGA621
PsPIN2          GATTTTCTTGAAACGGATGCTTCTGTTGGTGATGATGGGAAGTTACATGTTACTGTGAGA840
                       * ***** ******    *     * ***** **  * ********** ***

PsPIN1          AAATCAAACGCTTCAAGATCAGATATTTACTCAAGAAGATCACAGGGTCTTTCTTCCAAC681
PsPIN2          AAATCTAACGCGTCG----CGGAGGTC-GTTTATGATGACTAC-----------------878
                ***** ***** **     * **  *    * * ** **  **

PsPIN1          ACTCCTAGGCCTTCTAATCTTACTAACGCCGAGATTTACTCGTTGCAATCATCGCGAAAT741
PsPIN2          --TCCGCGACCGTCGAATTTGACTGGAGCTGAGATTTA----------TAGTCTC--AGC924
                  ***  * ** ** *** * ***   ** ********          *  ** *  *
PsPIN1          CCTACGCCAAGAGGGTCTAGTTTTAATCATACTGATTTTTATTCTATGATGGGTGGTGGA801
PsPIN2          TCCACGCCAAGAGGGTCTAATTTCAACCACGCCGAGTTTTACTCCATGATGGGTTATCAA984
                 * ***************** *** ** **  * ** ***** ** *********  *  *

PsPIN1          ---AGAAACTCTAACTTTAATGCTTCTGATGTTAATAACTACGGTTTATCGGCCTCGCGA858
PsPIN2          CCCAGACATTCCAATTTTGGTACTACTGATCTCTA----TTCTGTTCA-GTCTTCTAGA 1038
                   *** * ** ** ***  * ** ***** *  *    * * *** *  * * **  **

PsPIN1          GGTGTTACTCCGAGGCCGTCTAATTACGAAGAAGATGCTTCGAATGCGAAGAAGTTGAAA 918
PsPIN2          GGACCCACTCCTAGACCTTCGAATTTCGAAGAAAACGGCGCAACTTCGCCTAGATTCGGG 1098
                **    ***** ** ** ** **** ******* * *   * * * **   *  **

PsPIN1          CATTATCCGGCTC---CTAATCCGGGAATGTTTTCTCCTACTAATAAAAATCTTGGTTCT 975
PsPIN2          TTTTATCCGGCGCAGACCGTGCCTGCTTCGTATCCTGCGCCGAATCCTGAATTCTCTTCT 1158
                  ********* *   *    ** *    ** * ** *  * ***    *  *   ****

PsPIN1          AATGTCAA---TGTTAAGA----------GAAGTAATGGTCAGAACCAGGATCAGAATCA 1022
PsPIN2          ACTGCGAAAACTGTGAAGAATCAAAATTTGATGCAGCAGCCACAACAGCAACAGGTTTCA 1218
                * **  **   *** ****          ** * *   * ** ***    *   *  ***

PsPIN1          GAATCAACAGAAA-----CAAGATGAT------CTTCATATGTTTGTTTGGAGTTCAAGT 1071
PsPIN2          TTGCAGACAAAGGGCTCTCAGGATGCTAAGGAATTGCACATGTTTGTGTGGAGCTCAAGT 1278
                      *** *       ** **** *       * ** ******** ***** ******

PsPIN1          GCTTCACCTGTTTCTGATGTGTTTGGTGGACATGAATTTGGTTCTC----ATGATCAGAA 1127
PsPIN2          CGTTCGCCGGTGTCGGAAAGTGCCGGTCTCAACGCCTTCCGAAATTCGGAACAATCAGAA 1338
                  *** ** ** ** **       ***    * *  **  *   *     *  *******

PsPIN1          AGAAGT--TAAATTGAAC------GTGTCTCCAGGAAAAGTGGACGGTCATAGAGAAACT 1179
PsPIN2          GAGGGTGCTAAAGAGATCAGAATGGTGGTTGCTGATGAACATAATCAAAATGGTGAAATC 1398
                    **  ****  ** *      ***  * * *   **    *     ** * ****

PsPIN1          CA----AGAGGATTATTTGG--AGAAAGATGAATTCAGCTT--------TGGAAATAGAG 1225
PsPIN2          AATAACAAAGGGGAAGTTGGTGGGGAAGAAGATTTCAAGTTCATTGGAGTGAAGGGGAA 1458
                 *    * ***   * ****   * **** ** ****  **        ** *    **

PsPIN1          GAA-----TGGAAAGGGA---GATGAAT--AATCAAC-------------AACATGAAGG 1262
PsPIN2          GAACAAGTTGGAGAAGGGCTCAATGGGTCTAACAAACTGAGCTCCAATGCAACACCAGAG 1518
                ***     **** * **     ***  *  **  ***             ****  *  *

PsPIN1          --------TGAAAAAATTGGAGATGGAAAATC---------AAAAGTTATGCCACCAGCT 1305
PsPIN2          ATCCACCCTAAAGCCACCGGAGTGGCCGATTCCGGTGTCGGAAAACTCATGCCTCCGGCG 1578
                        * **   *  ****  *   * **         **** * ***** ** **

PsPIN1          AGTGTCATGACCCGCCTTATTCTTATTATGGTTTGGAGAAAACTTATCAGAAACCCAAAC 1365
PsPIN2          AGTGTCATGACTCGTCTCATACTCATTATGGTTTGGAGAAAACTTATCCGAAATCCCAAC 1638
                *********** ** ** ** ** ************************ **** ** ***

PsPIN1          ACTTATTCAAGCTTAATAGGTCTAGTTTGGTCTCTAGTTTCATTCAGATGGAATATTGAA 1425
PsPIN2          ACTTATTCAAGTCTTATTGGTCTCATTTGGTCCCTTGTTGCATTTAGGTGGGGTGTTCAT 1698
                ***********  * ** *****  ******* ** *** **** ** ***  * ** *

PsPIN1          ATGCCTGCTATAATAGCAAAATCTATATCTATATTGTCGGACGCAGGACTTGGCATGGCC 1485
PsPIN2          ATGCCTAAAATAGTAGAGAAATCAATTTCCATACTCTCTGATGCTGGGCTTGGAATGGCT 1758
                ******   *** ***  ***** ** ** *** * ** ** ** ** ***** *****

PsPIN1          ATGTTCAGTCTCGGTTTATTCATGGCATTGCAACCAAAAATCATAGCATGTGGAAATTCC 1545
PsPIN2          ATGTTTAGCTTAGGTTTATTTATGGCTCTTCAACCTAAGATAATTGCATGTGGAAATTCG 1818
                ***** **  * ******** *****  * ***** ** ** ** **************
```

```
PsPIN1          ATAGCAGCTTTTGCAATGGCTGTGAGATTCCTTACAGGTCCAGCTGTGATGGCAGCTGCT 1605
PsPIN2          GTTGCCTCATTTGCCATGGCTATTAGATTTGTCACTGGTCCGGCAGTTATGGCAGCTGCT 1878
                 * **  * ***** ****** * *****  * ** ***** ** ** ************

PsPIN1          TCATTTGCTGTTGGACTCAAAGGTGTTCTTTTTCATGTTGCAATTGTGCAGGCAGCTCTT 1665
PsPIN2          TCTATCGCTGTCGGCCTCCGTGGTACCCTCCTTCATGTAGCAATTGTTCAGGCCGCACTT 1938
                **  * ***** ** ***   ***   **  ******* ******** ***** ** ***

PsPIN1          CCCCAAGGAATTGTCCCATTTGTCTTTGCTAAAGAATATAATGTACATCCTGATATTTTA 1725
PsPIN2          CCACAAGGGATTGTTCCGTTTGTGTTTGCAAAAGAATATAATGTTCATCCTGCCATTCTT 1998
                ** ***** ***** ** ***** ***** ************** *******  *** *

PsPIN1          AGCACAGGTGTCATTTTTGGAATGTTGATTGCATTGCCCATTACTCTTGTGTACTACATT 1785
PsPIN2          AGTACTGCGGTTATATTTGGGATGTTGATAGCTCTTCCAATTACTCTACTCTACTACATT 2058
                ** ** *  ** ** ***** ******** **  * ** ********  * *********

PsPIN1          TTAATGGGACTATGA---------------------------------------------- 1800
PsPIN2          CTCCTTGGTTTGTAAAAAAAAAAAGAAAAATACATATTCATAGTTTGGAGTTGGAAGATA 2118
                 *  * **  * * *

PsPIN1          ------------------------------------------------------------
PsPIN2          GTAAACATGGATGGAGATGATTACAAGTGGAGTATTCTGTTATCACAAGGAGGAATATTT 2178


PsPIN1          ------------------------------------------------------------
PsPIN2          TTTTAATAAATCTCTTATTTGAAAAGTGTCACTACTAACTAGTTTTTCAACAACAGAAAT 2238


PsPIN1          ------------------------------------------------------------
PsPIN2          TGTCATTCCAAGTCTCAAAAAAGAAGAAGAGGGAATTTGAGAATATTTGAAGATTAAAAT 2298


PsPIN1          ------------------------------------------------------------
PsPIN2          GTTACATTCCTTGTTTCCAAGATGATGTAACTTTCAAAAGAGAGAATGTAACATTGTATG 2358


PsPIN1          ------------------------------------------------------------
PsPIN2          GGAGACATAAAAGAGGAAAACAAGGGAAAACTAGAATATGAAATTGTTCCTTTTCTATCA 2418


PsPIN1          ------------------------------------------------------------
PsPIN2          ACCATTTGTATACTTTTATGAGAAAAATATGTTTGGGTAGTAATTGTGTAGATGAAAGAA 2478


PsPIN1          ---------------------------------------------
PsPIN2          ATTGGAAATGACAATGAAGCCTTTTTACCTAAAAAAAAAAAAAA 2522
```

Figure A. 2.7. Sequence alignments of *PsPIN1* and *PsPIN2*. Primers and probes used for qRT-PCR for each gene are highlighted.

Appendix 3

Effect of crossing *PsGA3ox1*-overexpressing lines on plant phenotype and GA gene expression

The following crosses of *PsGA3ox1*-overexpressing transgenic lines were made to generate F1 progeny to determine the effect of *PsGA3ox1* gene insertion at different chromosomal positions in each parental haploid genome on phenotype of the F1 progeny, transgene expression, and late GA biosynthesis and catabolism gene expression.

1. TG1FxTG2M
2. TG2FxTG1M
3. TG1FxTG3M
4. TG3FxTG1M
5. TG3FxTG2M

The parent lines, TG1, TG2 and TG3 along with the F1 progeny of the above crosses and control line C1 were grown in a completely randomized design in a 2.5 × 1.4 m Conviron growth chamber environment as described in Chapter

2. For the morphological characterization studies, the plants were watered every three days and fertilized thrice 25, 45 and 62 days after planting with a fertilizer mix of N:P:K (15:30:15). Lateral shoots were removed as they emerged to facilitate the maximum extension of the main stem.

The total number of internodes (the first internode was defined as the one between the cotyledon attachment and the first stem node) and the length of each internode from position 1 to 20 were determined at plant maturity. The number of nodes to first flower and the number of fruits aborted before the first fruit set were also recorded. The area of the larger stipule of each pair at specific nodes was measured at maturity using a leaf area meter (LI-3100 Area Meter, LI-COR, inc. Lincoln, Nebraska, USA). The petiole length of tendrils at selected nodes was measured at maturity from the point of attachment to the main stem to the first tendril branching point. Pod length and the number of seeds per pod were also recorded. The morphological data were analyzed using the General Linear Model of SAS 9.1 statistical software (SAS Institute Inc., Cary, NC, USA) following a completely randomized design, and mean separation was by LSD at $P \leq 0.05$.

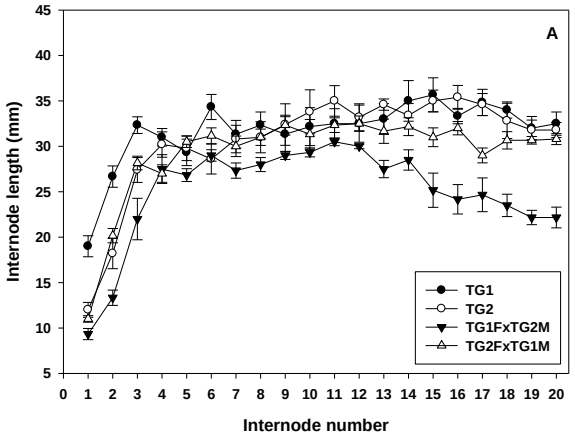
A
Internode length (mm)
Internode number
TG1
TG2
TG1FxTG2M
TG2FxTG1M

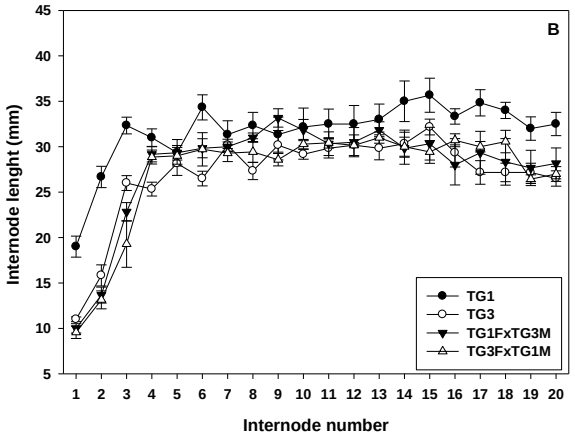
B
Internode lenght (mm)
Internode number
TG1
TG3
TG1FxTG3M
TG3FxTG1M

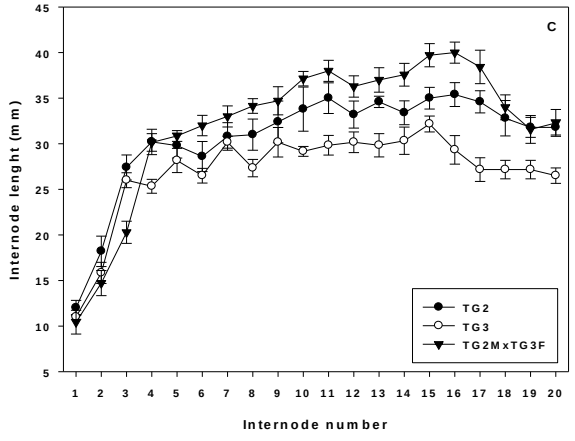
C
Internode lenght (mm)
Internode number
TG2
TG3
TG2MxTG3F

Figure A.3.1. Internode length at positions 1 to 20 of transgenic parents (TG1, TG2 and TG3) and F1 progeny of their crosses at plant maturity. Data are means ± SE, n= 6-11.

Table A.3.1. Tendril petiole lengths at maturity of transgenic parents (TG1, TG2 and TG3), F1 progeny of their crosses, and the control line at different nodal positions.

Line	Tendril petiole length (mm)[x]					
	Node 6	Node 8	Node 10	Node 16	Node 18	Node 20
TG1	70.3±2.7[y]abcd[z]	82.6±0.9ab	89.9±1.6bc	97.3±2.9a	91.1±3.3ab	82.6±3.8abc
TG2	76.7±2.2a	85.3±2.0a	93.6±1.3ab	96.1±2.6ab	93.4±1.1a	84.7±3.0ab
TG3	67.6±2.5bcd	77.7±2.9bc	92.3±2.3ab	90.0±3.1b	89.6±1.9abc	71.3±2.8e
TG1FxTG2M	71.8±2.4ab	85.1±2.5a	93.8±2.0ab	96.9±2.4ab	84.6±2.6bcd	85.1±2.3ab
TG2FxTG1M	71.3±2.0abc	81.3±3.1ab	85.5±2.2c	82.7±3.3c	81.3±4.0d	73.5±1.7de
TG1FxTG3M	75.1±2.7a	81.6±2.1ab	92.4±1.3ab	94.1±1.4ab	89.9±2.5abc	82.4±2.8abc
TG3FxTG1M	65.1±2.0cd	81.3±1.6ab	95.0±1.3a	90.4±2.2ab	82.4±2.9cd	79.6±3.6bcd
TG3FxTG2M	66.1±2.4cd	81.3±1.6ab	93.8±1.8ab	95.8±3.2ab	96.4±1.6a	88.1±2.2a
C1	64.4±1.8d	72.7±1.9c	86.0±1.7c	91.0±2.6ab	83.2±2.3bcd	76.2±1.8cde

[x] Petiole length was measured from the point of attachment to the stem to the first tendril branchlet.

[y] Data are means ± SE, n= 9 to 10.

[z] Means followed by different letters (a, b, c, d, e) indicate significant differences among lines within nodal position by LSD at $P<0.05$.

Tendril petiole length data were analyzed using the General Linear Model of SAS 9.1 statistical software (SAS Institute Inc., Cary, NC, USA) following a completely randomized design, and mean separation was by LSD at $p \leq 0.05$.

Table A.3.2. Stipule area at maturity of transgenic parents (TG1, TG2 and TG3), F1 progeny of their crosses, and the control line at different nodal positions.

Line	Stipule area (cm^2)[x]		
	Node 6	Node 8	Node 10
TG1	7.87±0.26[y]ab[z]	9.65±0.45ab	10.63±0.48def
TG2	7.24±0.35bc	9.84±0.35a	10.31±0.50ef
TG3	7.96±0.30ab	9.88±0.44a	12.13±0.32a
TG1FxTG2M	8.00±0.32ab	9.92±0.47a	11.18±0.29bcde
TG2FxTG1M	7.90±0.27ab	9.39±0.41ab	11.41±0.36abcd
TG1FxTG3M	8.51±0.26a	10.35±0.40a	12.02±0.36ab
TG3FxTG1M	7.68±0.19ab	9.82±0.43a	11.06±0.37cde
TG3FxTG2M	7.47±0.20bc	8.66±0.33bc	11.77±0.25abc
C1	6.74±0.35c	8.09±0.48c	9.74±0.32f

[x] Leaf area of the larger stipule

[y] Data are means ± SE, n= 9 to 10.

[z] Means followed by different letters (a, b, c, d, e) indicate significant differences among lines within nodal position by LSD at P<0.05.

Stipule area data were analyzed using the General Linear Model of SAS 9.1

Line	Total number of internodes	Nodes to first flower	Number of fruits aborted before first fruit set
TG1	45.7±2.6[x]a[y]	29.2±0.3a	6.0±1.2a

statistical software (SAS Institute Inc., Cary, NC, USA) following a completely randomized design, and mean separation was by LSD at $p \leq 0.05$.

Table A.3.3. Number of internodes per plant, nodes to first flower, and number of fruits aborted before first fruit set in transgenic parents (TG1, TG2 and TG3), the F1 progeny of their crosses, and the control line.

TG2	35.2±1.8cd	24.3±0.3bc	3.8±0.9bc
TG3	33.4±1.0de	23.1±0.4cd	1.6±0.3d
TG1FxTG2M	26.1±0.8fg	21.1±0.4e	1.1±0.3d
TG2FxTG1M (group 1)[z]	35.8±1.7cd	21.2±0.4e	4.2±0.9ab
TG2FxTG1M (group 2)[z]	25.6±0.7g	21.0±0.4e	1.8±0.8dc
TG1FxTG3M (group 1)[z]	44.5±3.0ab	24.8±0.8b	5.5±0.7ab
TG1FxTG3M (group 2)[z]	29.6±1.2efg	22.0±0.4de	0.6±0.4d
TG3FxTG1M(group 1) [z]	39.8±2.0bc	23.3±0.7c	4.4±0.9ab
TG3FxTG1M (group 2)[z]	26.6±0.7fg	21.0±0.5e	1.4±0.7d
TG3FxTG2M	40.0±1.4bc	23.4±0.4c	4.2±0.8ab
C1	31.0±1.7ef	23.2±0.2cd	11.4±0.5d

[x] Data are means ±SE, n= 6 to11.

[y] Means followed by different letters (a, b, c, d, e, f) indicate significant difference among lines by LSD, P<0.05.

[z] These lines exhibited two population means for each characteristic evaluated. Morhological data were analyzed using the General Linear Model of SAS 9.1 statistical software (SAS Institute Inc., Cary, NC, USA) following a completely randomized design, and mean separation was by LSD at p≤ 0.05.

Table A.3.4. Length of pericarps (pods) of transgenic parents (TG1, TG2 and TG3), F1 progeny of their crosses, and the control line at maturity.

Line	Pericarp length at maturity (mm)				
	3 seeds[x]	4 seeds	5 seeds	6 seeds	7 seeds
TG1	61.5±1.0[y]a[z]	62.0±1.4a	68.4±1.4a	75.7±1.7a	80.8±2.1a

TG2	49.6±2.5b	54.5±1.9c	62.1±3.8bc	68.58±1.5bc	75.0±3.5b
TG3	51.3±2.8b	55.9±1.8c	58.7±1.0c	61.6±1.6d	No pods
TG1FxTG2M	47.5±1.5b	55.7±1.2c	61.3±1.4bc	67.5±1.7bc	No pods
TG2FxTG1M	50.7±2.2b	55.1±0.9c	64.2±1.5ab	69.3±1.2bc	70.0±1.0bc
TG1FxTG3M	51.8±1.9b	57.3±0.9abc	63.3±1.1b	70.0±1.1b	73.7±1.1bc
TG3FxTG1M	52.6±2.9b	60.8±2.1ab	68.7±0.9a	69.6±1.7bc	74.5±1.0b
TG3FxTG2M	53.2±1.9b	56.5±1.3bc	64.4±1.2ab	70.7±1.0b	74.3±1.0b
C1	47.5±2.1b	57.5±2.3c	60.6±2.3bc	65.6±1.3cd	68.9±1.4c

[x] Number of seeds per fruit

[y] Data are means ±SE, n=4 to 21 (from 7 to 10 individual plants)

[z] Means followed by different letters (x, y, z) indicate significant difference among lines by LSD, $P<0.05$.

Pericarp length data were analyzed using the General Linear Model of SAS 9.1 statistical software (SAS Institute Inc., Cary, NC, USA) following a completely randomized design, and mean separation was by LSD at $p \leq 0.05$.

Expression analysis of GA genes in developing tendrils

The parent lines, TG1, TG2 and TG3 along with the F1 progeny of the above crosses and control line C1 were grown in a completely randomized design in a 2.5 × 1.4 m Conviron growth chamber environment as described before (Chapter 2). The developing tendrils were harvested (approximately 20-30% of

final length) from the 15th nodal position for total RNA extraction. Total RNA was extracted as described in Chapter 2. The relative transcript abundance of transgenic *PsGA3ox1*, total *PsGA3ox1*, *PsGA20ox1*, *PsGA20ox2*, *PsGA2ox1* and *PsGA2ox2* was determined by qRT-PCR as described in Chapter 4.

Table A.3.5. Relative transcript abundance of late GA biosynthesis and catabolism genes in elongating tendrils of the transgenic parents, TG1, TG2 and TG3 and their F1 progeny[a].

	Transgenic *PsGA3ox1*	Total *PsGA3ox1*	*PsGA20ox1*	*PsGA20ox2*	*PsGA2ox1*	*PsGA2ox2*
TG1	137.3±17.0[b]	1576.5±8.2	14480.5±1846.7	n.d.[c]	621.8±53.7	23.4±2.5
TG2	38.4±5.5	699.7±73.7	13110.8±907.3	n.d.	201.2±4.5	18.5±7.8

TG3	22.7±2.0	658.5±96.3	12826±998.2	n.d.	195.5±13.9	17.9±7.3
TG1FxTG2M	78.0±0.8	206.2±14.3	16108.7±446.5	n.d.	248.8±58.8	60.4±23.7
TG2FxTG1M	105.7±40.8	495.6±43.7	22458.7±1863.8	n.d	257.8±69.7	35.4±9.4
TG1FxTG3M	67.2±3.6	448.9±9.3	22951.6±2141.4	n.d.	223.0±30.3	17.9±2.5
TG3FxTG1M	27.821.8±7.2	132.3±3.9	6395.3±761.0	n.d.	373.3±112.8	217.9±21.8
TG3FxTG2M	21.8±6.7	441.9±57.9	13352.8±762.7	n.d.	332.0±33.8	79.6±25.8
C1	n.d.	226.8±60.2	9571.2±1464.6	n.d.	166.0±36.2	20.7±2.0

[a] Transcript levels were standardized across genes using the tendril stage 2 *PsGA20ox2* (Ct=37.96) sample of the TG1 line (Chapter 2) as the reference for normalization.

[b] Data are means ± SE, n= 2 to 3.

[c] no transcript was detected.